Investigating the functions of Polycomb Group proteins in potato development

A Thesis

Submitted in partial fulfillment of the requirements

for the degree of

Doctor of Philosophy

By

Amit Kumar

20133249

INDIAN INSTITUTE OF SCIENCE EDUCATION AND RESEARCH, PUNE

2019

CERTIFICATE

It is certified that the work incorporated in the thesis entitled **"Investigating the functions of Polycomb Group proteins in potato development"** submitted by Mr. Amit Kumar was carried out by the candidate, under my supervision. The work presented here or any part of it has not been included in any other thesis submitted previously for the award of any degree or diploma from any other university or institution.

Prof. Anjan K. Banerjee,
Supervisor

Date: 18th October 2019

DECLARATION

I declare that this written submission represents my ideas in my own words and where others' ideas have been included; I have adequately cited and referenced the original sources. I also declare that I have adhered to all principles of academic honesty and integrity and have not misrepresented or fabricated or falsified any idea/data/fact/source in my submission. I understand that violation of the above will be cause for disciplinary action by the Institute and can also evoke penal action from the sources which have thus not been properly cited or from whom proper permission has not been taken when needed.

Amit Kumar

Reg. No. 20133249

Date: 18th Oct. 2019

Acknowledgements

I thank my supervisor, Dr. Anjan. K. Banerjee for his constant help and guidance throughout my PhD. His insights and valuable suggestions helped me to see the fruition of my PhD. His tireless passion for plant science will be an inspiration for all who had the opportunity to work with him. I thank my RAC members Prof. Sanjeev Galande, Dr.Krishanpal Karmodia, and Dr. Mukesh Lodha, for their regular and timely suggestions.

My sincere thanks to The Council of Scientific & Industrial Research (CSIR, Gov. of India) for providing the fellowship. I thank IISER Pune for providing financial assistance and infrastructure as well as the Department of Biotechnology (DBT, Govt. of India) and Infosys Foundation for providing me international travel grants.

I especially thank Kirtikumar and Pallavi, for their contributions in my projects. I further thank all present and past AKB lab members for their help and useful suggestions. Lab members of Sanjeev, Krishanpal, and Sagar's lab are also thanked for their help and maintaining the friendly ambiance. I thank biology division support staff for their timely help in reagents procurement. Big thanks to Mr. Nitish Lahigude, for taking care of the plants throughout my Ph.D.

I sincerely thank Prof. (Sir) David Baulcombe for providing us PVX-VIGS vectors. I would also like to acknowledge the help received from Dr. Krishanpal Karmodiya (IISER Pune) and his lab members (Mr. Abhishek Kanyal and Mr. Mukul Rawat) for ChIP-sequencing.

Very special thanks to Kirtikumar, Sheeba, Ravi, and Mahesh for always helping me and getting me through my PhD days with love, joy, and fun. I also thank my former teachers Dr. Uma Pillai and Dr. Kailash Choudhary, for their excellent teaching and helping me to develop my interest in plant science.

Most importantly, I thank my parents, Ramkishor and Rajendra Kumari, my brother and his wife, Aneet and Rashmi, my niece and nephew Swaranaxi and Aviral for loving me unconditionally and standing by me in all the ebbs and flows of my life, for which I am greatly indebted. Love you all.

Amit

18th October 2019

Table of Contents

Contents **Page no.**

Chapter 2: Investigating the role of StMSI1 (a PRC2 member) and StBMI1-1 (a PRC1 member) in potato and target genes identification

Chapter 3: Functional characterization of StE(z)2 (a H3K27 methyltransferase) as a potential epigenetic regulator in potato

List of Figures

List of Tables

Abbreviations

PRC	Polycomb Repressive Complex
PcG	Polycomb Group
TrxG	Trithorax Group
E(z)	Enhancer of zeste
Su(z)	Suppressor of zeste
CLF	CURLY LEAF
MSI1	MULTICOPY SUPPRESSOR OF IRA 1
BMI	B CELL-SPECIFIC Mo-MLV INTEGRATION SITE 1
EMF	EMBRYONIC FLOWER
FIS	FERTILISATION INDEPENDENT SEED
FIE	FERTILIZATION INDEPENDENT ENDOSPERM
ABA	Abscisic Acid
CK	Cytokinin
ARF	Auxin Response Factors
GA	Gibberellic Acid
IAA	Indole Acetic Acid
JA	Jasmonic Acid
CO	CONSTANS
FT	FLOWERING LOCUS T
SP	SELF-PRUNING
GI	GIGANTIA
DOF	DNA-binding with one finger
RAP	Related to APETELLA

SPL	Squamosa Promoter binding-Like
TALE	Three Amino Loop Extension
LOG1	LONELY GUY 1
ChIP	Chromatin Immunoprecipitation
FPKM	Fragments per kb per million reads
GO	Gene ontology
NGS	Next-generation sequencing
PCA	Principal Component Analysis
PTGS	Post-Transcriptional Gene Silencing
RdRp	RNA-dependent RNA polymerase
RIN	RNA integrity number
RISC	RNA-Induced Silencing Complex
PVX	Potato Virus-X
VIGS	Virus Induced Gene Silencing
RISC	RNA Induced Silencing Complex

Synopsis

Investigating the functions of Polycomb Group proteins in potato development

Name: Amit Kumar

Roll number: 20133249

Name of supervisor: Prof. Anjan K. Banerjee

Department: Biology, IISER Pune

Date of registration: 1st August 2013

Chapter 1: Introduction

Phenotypic plasticity is the crucial survival strategy of plants against the odds of ever-changing environmental conditions. This often involves regulated gene expression mediated by chromatin modifications, such as histone acetylation, ubiquitination, or methylation. Polycomb group (PcG) proteins are important epigenetic regulators of development across all eukaryotic organisms. PcG proteins were first identified in *Drosophila melanogaster* as repressors of homeotic genes (Simon and Tamkun, 2002) and majorly divided into two categories, i.e., Polycomb Repressive Complex 1 (PRC1), and PRC2. PRC1 consists of four subunits: Polycomb (Pc), Posterior sex combs (Psc), Polyhomeotic (Ph), and Sex combs extra (Sce, or dRing1) (Cao et al., 2005). BMI1, a PRC1 like a member in plants, represses the target genes through H2A ubiquitination. The core subunits constituting the PRC2 are the Enhancer of zeste [E(z)], Suppressor of zeste 12 [Su(z)12], Extra sex combs (Esc) and nucleosome remodeling factor (Nurf55 or p55). Arabidopsis has three homologs of E(z), named as CURLY LEAF (CLF), SWINGER (SWN), and MEDEA (MEA). In addition to this, five p55 like proteins have been identified in Arabidopsis (MSI1-MSI5). The E(z) homologs in plants repress the target genes through H3K27 trimethylation, whereas MSI1 (a p55 homolog) helps in complex formation and its recruitment over histones through its WD40 repeat domain (Müller et al., 2002). Both E(z) and MSI1 like proteins in Arabidopsis are part of three PRC2 complexes: (i) FERTILIZATION INDEPENDENT SEED (FIS) complex that regulates seed development (Kohler et al., 2003), (ii) EMBRYONIC FLOWER (EMF) complex that suppresses flowering during juvenile stage (Yoshida et al., 2001), and (iii) VERNALIZATION (VRN) complex, that is essential for the onset of flowering after vernalization (De Lucia et al., 2008). Although the function of different histone modifiers has

been characterized in Arabidopsis, their role in other important crop species remains poorly understood. The focus of this investigation was to understand the role of StMSI1, StBMI1, and StE(z)2 proteins in photoperiod-dependent tuberization (potato development).

A potato tuber is a specialized stem that arises from the belowground organ known as the stolon. Wild Andean varieties like *Solanum tuberosum* ssp. *andigena* are adapted to short-day (SD) photoperiodic conditions and are unable to tuberize under long days (LD) (day lengths > 12 hours). This potato subspecies thus provides the researchers a unique opportunity to understand how environmental signals, such as light, temperature, and photoperiod, affect the potato development. Previous studies have revealed a number of common factors involved in flowering and tuberization. These includes StSP6A (a homolog of key florigen molecular FT) (Navarro et al., 2011) CONSTANS (CO) (Gonzalez-Schain et al., 2012), hormones like gibberellic acid (Xu et al,. 1998) as well as microRNAs such as miR156 (Bhogale et. al., 2014) and miR172 (Martin et al., 2009).

Based on the close similarities between flowering and tuberization pathways (Abelenda et al., 2014) and regulation of flowering related genes by PRC members, we hypothesized that PRC proteins might be playing a crucial role in governing the photoperiod dependent tuber development. We set the following objectives to validate our hypothesis-

1- To investigate the role of StMSI1 and StBMI1 in potato and identify their target genes through RNA-seq analysis.
2- To characterize the role of StE(z)2 (a H3K27 methyltransferase) in potato development through overexpression and knockdown strategies.
3- Identification of the direct targets of StE(z)2 and the genome-wide occupancy of histone modifications during stolon-to-tuber development in potato.

Chapter 2: Investigating the role of StMSI1 (a PRC2 member) and StBMI1-1 (a PRC1 member) in potato and target genes identification

BMI1 has been shown as the major regulator of miR156 in Arabidopsis (Pico et al. 2015) whereas, MSI1 regulates photoperiod dependent flowering by controlling the expression of flowering responsive genes, such as CONSTANS (CO) (Steinbach and Hennig, 2014). A previous study from our group demonstrated that the expression of miR156 changes in stolon tissues with respect to LD/SD photoperiod and miR156 overexpression affects the tuber yield (Bhogale et al., 2014). However, what leads to the differential expression of miR156 in a

photoperiod-dependent manner was not clear. Based on the role of PcG proteins in the regulation of miR156 in Arabidopsis (Pico et al., 2015) and similarities between flowering and tuberization pathways, we hypothesized that PRC1 and PRC2 members might be playing a crucial role in governing potato development. Besides this, we were also interested to know the target genes that are being regulated by these PRC proteins.

Here, we investigated the role of two PRC proteins, StMSI1 and StBMI1-1, in potato development. In wild-type *andigena* plants, *StMSI1* and miRNA156 levels increased in stolon, whereas *StBMI1-1* decreased under short-day conditions. *StMSI1-OE* and *StBMI1-1*-antisense lines produced pleiotropic effects, including altered leaf architecture/compounding and reduced below-ground tuber yield. Notably, these lines showed enhanced miRNA156 accumulation accompanied by aerial stolons and tubers from axillary-nodes, similar to miRNA156-OE lines, as demonstrated earlier. RNA-sequencing of axillary-nodes from *StMSI1*-OE and *StBMI1-1-antisense* lines revealed downregulation of auxin and brassinosteroid genes, and upregulation of cytokinin transport/signaling genes in both the lines. Moreover, we observed the downregulation of genes encoding H2A-ubiquitin ligase and StBMI1-1/3 and upregulation of the Trithorax group H3K4-methyl-transferases in *StMSI1*-OE line. ChIP-qPCR confirmed H3K27me3-mediated suppression of *StBMI1-1*/*3*, and H3K4me3-mediated activation of miRNA156 in *StMSI1-OE* plants. In summary, we establish that crosstalk between histone modifiers regulates miRNA156 and alters hormonal responses during aerial tuber formation in potato under short-day photoperiodic conditions.

Chapter 3: Functional characterization of StE(z)2 (a H3K27 methyltransferase) as a potential epigenetic regulator in potato

Potato E(z)2 is a PRC2 group histone methyl transferase orthologous to CURLY LEAF (CLF) in Arabidopsis. PRC2 performs trimethylation of H3K27, leading to the repression of target genes. Although the role of PRC proteins has been characterized in Arabidopsis (Goodrich et al., 1997) and some other crops, such as rice (Liu et al., 2014) and tomato (Boureau et al., 2016), their role in potato development is yet unexplored. A study by Jiang et al. (2010) had shown that CLF directly binds and deposits H3K27me3 mark to repress FT expression in Arabidopsis. Another interesting study by Navarro et al. (2011) proved that FT homolog in potato StSP6A is an important tuberization regulator. Based on these findings, we decided to investigate the effect of CLF homolog in tuber development.

Here, we have characterized the role of *StE(z)2* using overexpression and VIGS mediated knockdown strategies.

The *StE(z)2*-OE lines had a similar phenotype to *StMSI1*-OE lines (Kumar et al., 2019). Since MSI1 and E(z)2 are part of the same PRC2 complex, we anticipated similar mechanistic regulation behind both phenotypes. The OE lines had smaller leaf sizes and fewer leaflet numbers per leaf compared to the wild-type plants. Also, they had larger trichomes compared to WT leaves. The cross-sections through leaf mid-vain revealed vascular architecture alteration. To analyze the effect of *StE(z)2*-OE, plants were shifted to soil and maintained under LD condition for two months before transferred to SD photoperiodic condition for one month. We noticed a reduction in the belowground tuber yield as well as root biomass in OE plants compared to WT, post SD induction.

To check the effect of E(z)2 knockdown, we used the VIGS approach. Interestingly, the *StE(z)2* silenced plants that showed increased tuber yield, had higher levels of *StSP6A, StBEL5,* and *GA2ox1*. During inductive short-day conditions, a key TALE family protein member StBEL5 and its KNOX partner POTH1 (Chen et al., 2004), are induced, and they stimulate the expression of another important tuber inducing protein StSP6A (Sharma et al., 2016). StBEL5, StSP6A, and its biding partners St14-3-3 and StFD2 are transported to stolon (Banerjee et al., 2006; Navarro et al., 2011; Teo et al., 2017) and activate the expression of GA catabolic gene *GA2ox1* resulting in lower GA biosynthesis (Chen et al., 2004). This changes the pattern of cell division from longitudinal to radial plane resulting in stolon swelling that finally leads to tuber development (Xu et al., 1998). In line with this, we noticed low levels of *StSP6A* and *StBEL5* in *StE(z)2*-OE lines, possibly explains the reduced below ground tuber yield in these plants. In summary, we show that StE(z)2 plays a crucial role in tuber development.

Chapter 4: Identification of the direct targets of StE(z)2 and the genome-wide occupancy of histone modifications during stolon-to-tuber development in potato

Short-day photoperiod triggers the differential expression of numerous genes in potato development. However, the gene regulatory network that controls the expression of these genes in a Spatio-temporal manner during tuber development is not well understood. In this study, we explored if chromatin modifiers have any role in the activation or repression of the tuberization-associated genes. Since PRC2 protein regulates the genes by H3K27me3 modification that is counteracted by TrxG mediated H3K4me3 modification, we performed

ChIP-seq analysis from SD-induced stolon tissues to identify the tuberization related genes regulated by StE(z)2 as well as H3K27me3 and H3K4me3 modifications.

ChIP-seq analysis revealed >12,000 genes harboring active H3K4me3 modification. This list includes several genes involved in the tuber development pathway. For example, *BEL* and KNOX family transcription factors, *StGA2ox1*, *St14-3-3*, *StFD2*, *StMSI1*, *patatin*, *sucrose synthase,* and *transporters*. Consistently, through RT-qPCR analysis, we observed a significant upregulation of *StBEL5, St14-3-3*, *StMSI1*, *StZF2*, *StSDG4*, *purine transporter three* and *StGA2ox1* in stolon under SD compared to LD photoperiodic conditions. We found several other PRC members, such as *StMSI1*, *ubiquitin ligase* encoding genes as well as *histone deacetylases* as targets of H3K4me3 modifications. On the other hand, we observed an enrichment of H3K27me3 peaks over 2,300 sites; out of them, 89 were on the gene bodies. Several genes (*glutamine synthetase*, *cytochrome P450*, *cytochrome C oxidase subunit2,* and *multidrug-resistant (MDR) ABC transporter, glutaredoxin,* and *pyruvate kinase*) related to metabolic pathways were found as targets of H3K27me3 modifications. The accumulation of the repressive H3K27me3 mark on many of these genes was associated with their reduced transcript levels in SD stolons compared to LD conditions. Notably, ChIP-qPCR analysis detected a 70-80% reduction in deposition of H3K27me3 modification over the *StSP6A* locus in WT leaves under SD conditions compared to LD. Our analysis further revealed that approximately 7,600 genes lost the H3K4me3 modification mark in StE(z)2-OE lines compared to WT stolon. These include several auxin, brassinosteroid (BR), and cytokinin-related genes. Moreover, the overexpression of FLAG-tagged StE(z)2 increased the H3K27me3 modification over 226 genes compared to 88 genes in WT condition. In addition to this, overexpression also resulted in the gain of H3K27me3 marks over cytokinin biosynthesis/transport genes. In summary, our analysis revealed that a number of important genes involved in tuberization are controlled epigenetically by H3K27me3 and H3K4me3 modifications in potato.

List of author's publications during PhD work

1. **Kumar, A**., Kondhare, K. R & Banerjee, A. K. Polycomb and trithorax group proteins regulate potato tuberization in a photoperiod-dependent pathway 2019 (Under review, Journal of Exp. Bot.).

2. **Kumar, A**., Kondhare, K. R., Vetal, P. V. & Banerjee, A. K.(2019) Polycomb group proteins StMSI1 and StBMI1 regulate microRNA156 during aerial tuber formation in potato under short-day photoperiod (Plant Physiology, DOI:10.1104/pp.19.00416).

3. Kondhare, K. R., **Kumar, A**., Hannapel, D. J. & Banerjee, A. K. (2018) Conservation of polypyrimidine tract binding proteins and their putative target RNAs in several storage root crops. BMC Genomics 19, 124.

4. Mahajan, A. S., Kondhare, K. R., Rajabhoj, M. P., **Kumar, A**., Ghate, T., Ravindran, N., Habib, F., Siddappa, S. & Banerjee, A. K. (2016) Regulation, over-expression, and target gene identification of Potato Homeobox 15 (POTH15) - a class-I KNOX gene in potato. J. Exp. Bot. 67 (14), 4255-4272.

5. Kondhare, K. R., **Kumar, A**. & Banerjee, A. K (2018) Photoperiod-mediated regulation of tuberization in potato (S. tuberosum spp. andigena). Trends in Frontal Areas of Plant Science Research. ISBN: 978-81-8487-605-5. Narosa Publishing Group. (Book Chapter)

References

Bhogale, S., Mahajan, A.S., Natarajan, B., Rajabhoj, M., Thulasiram, H.V., and Banerjee, A.K. (2014). MicroRNA156: A potential graft-transmissible microRNA that modulates plant architecture and tuberization in *Solanum tuberosum* ssp. andigena. Plant Physiol. 164: 1011-1027.

Boureau L, How-Kit A, Teyssier E, et al. (2016). A CURLY LEAF homolog controls both vegetative and reproductive development of tomato plants. Plant Molecular Biology 90, 485–501.

Cao R. Tsukada Y. Zhang Y. Role of Bmi-1 and Ring1A in H2A ubiquitylation and Hox gene silencing. Mol Cell. (2005) ;20:845–854

Chen H, Banerjee AK, and Hannapel DJ. (2004) The tandem complex of BEL and KNOX partners is required for transcriptional repression of ga20ox1. The Plant Journal, 38:276–284.

De Lucia F, Crevillen P, Jones AM, Greb T, Dean C (2008) A PhD-polycomb repressive complex 2 triggers the epigenetic silencing of FLC during vernalization. Proc Natl Acad Sci U S A. Nov 4; 105(44):16831-6.

Gonzalez-Schain, N. D., Diaz-Mendoza, M., Zurczak, M., and Suarez-Lopez, P. (2012). Potato CONSTANS is involved in photoperiodic tuberization in a graft-transmissible manner. Plant J. 70, 678–690.

Goodrich, J., Puangsomlee, P., Martin, M., Long, D., Meyerowitz, E.M., and Coupland, G. (1997). A Polycomb-group gene regulates homeotic gene expression in Arabidopsis. Nat. 386: 44-51

J.A. Simon, J.W. Tamkun (2002), Programming off and on states in chromatin: mechanisms of Polycomb and trithorax group complexes Curr. Opin. Genet. Dev., 12 pp. 210-218

J.A. Abelenda, C. Navarro, S. Prat ,(2014), Flowering and tuberization: a tale of two nightshades Trends Plant Sci., 19 pp. 115-122

Köhler C, Hennig L, Bouveret R, Gheyselinck J, Grossniklaus U, Gruissem W. (2003a) Arabidopsis MSI1 is a component of the MEA/FIE Polycomb group complex and required for seed development. EMBO J 22: 4804–4814

Kumar A, Kondhare KR, Vetal PV, Banerjee AK. (2019). PcG proteins MSI1 and BMI1 function upstream of miR156 to regulate aerial tuber formation in potato. Plant Physiology, pp.00416.2019.

Liu X, Zhou C, Zhao Y, Zhou S, Wang W, Zhou D. (2014). The rice enhancer of zeste [E (z)] genes SDG711 and SDG718 are respectively involved in long day and short day signaling to mediate the accurate photoperiod control of flowering time. 5, 1–9.

Martin, A., Adam, H., Díaz-Mendoza, M., Zurczak, M., González-Schain, N.D., and Suárez-López, P. (2009). Graft-transmissible induction of potato tuberization by the microRNA miR172. Dev. 136: 2873-2881.

Müller J, Hart CM, Francis NJ, Vargas ML, Sengupta A, Wild B, Miller EL, O'Connor MB, Kingston RE, Simon J a. (2002). Histone methyltransferase activity of a Drosophila Polycomb group repressor complex. Cell 111, 197–208.

N. Yoshida, Y. Yanai, L. Chen, Y. Kato, J. Hiratsuka, T. Miwa, Z.R. Sung, S. Takahashi (2001) EMBRYONIC FLOWER2, a novel polycomb group protein homolog, mediates shoot development and flowering in Arabidopsis Plant Cell., 13 pp. 2471-2481

Navarro, C., Abelenda, J.A., Cruz-Oró, E., Cuéllar, C.A., Tamaki, S., Silva, J., Shimamoto, K., and Prat, S. (2011). Control of flowering and storage organ formation in potato by FLOWERING LOCUS T. Nat. 478: 119-122

Picó, S., Ortiz-Marchena, M.I., Merini, W., and Calonje, M. (2015). Deciphering the role of POLYCOMB REPRESSIVE COMPLEX1 variants in regulating the acquisition of flowering competence in Arabidopsis. Plant Physiol. 168: 1286-1297.

Sharma P, Lin T, Hannapel DJ. (2016). Targets of the StBEL5 transcription factor include the FT ortholog StSP6A. Plant Physiology 170, 310-324

Steinbach, Y., and Hennig, L. (2014). Arabidopsis MSI1 functions in photoperiodic flowering 1162 time control. Front. Plant Sci. 5: 77.

Teo, C.J., Takahashi, K., Shimizu, K., Shimamoto, K., and Taoka, K.I. (2017). Potato tuber induction is regulated by interactions between components of a tuberigen complex. Plant Cell Physiol. 58(2): 365-374

Xu, X., van Lammeren AA, Vermeer, E., & Vreugdenhil, D. (1998). The role of gibberellin, abscisic acid, and sucrose in the regulation of potato tuber formation in vitro. Plant physiology, 117(2), 575–584. doi:10.1104/pp.117.2.575

Chapter 1

Introduction

1.1 Background

Conrad Waddington, the first time in 1942, used the term "epigenetic" to describe "The interactions of genes with their environment that bring the phenotype into being" (Waddington, 1942). Epi is a Greek term meaning "over, above or outer." Hence, epigenetics means above than or beyond genetics. The most widely accepted definition of epigenetics was given by Berger as ''An epigenetic trait is a stably heritable phenotype resulting from changes in a chromosome without alterations in the DNA sequence'' (Berger et al., 2009). Several events, such as paramutation, imprinting, gene silencing, position effect variegation, reprogramming, maternal conditioning, RNA interference, long and small non-coding RNAs, DNA methylation, and chromatin modifications are now considered under epigenetic regulation. Epigenetic modifications involve covalent attachment of a functional group over the chromatin, affecting the electrostatic attraction between the histones and DNA that results in a change in the chromatin architecture. These changes either lead to the creation of a new site for the recruitment of transcription regulators or disrupt the previously set interaction, leading to expression or repression of target gene activity. In the eukaryotic cell, DNA is arranged inside the nucleus in a highly organized nucleoprotein complex termed as chromatin. The nucleosome is the fundamental unit of chromatin, made up of histone octamer (two copies of each of the histones H2A, H2B, H3, and H4) that is wrapped around by ~147 base pairs of DNA (Figure 1-1). Nucleosomes are dynamic entities that can be reconfigured at particular genome locations upon a perception of developmental cues or specific environmental signals. Inside the cell, not all the genes are active at a given time, the change in nucleosome and chromatin architecture modulates DNA accessibility and gene expression. Phenotypic variability brought by epigenetic modifications cannot be explained by the classical Mendelian Genetics Model, as they do not alter nucleotide sequences. Hence, it is necessary to understand the role of other factors bringing the phenotypic differentiation despite having the same genotype in each cell of an organism.

In this chapter, I have thoroughly reviewed the literature regarding the different epigenetic modifications and their role in diverse plant developmental processes.

1.2 Epigenetic regulation through DNA and histone modification

In eukaryotes, governance of chromatin structure chromatin and gene expression is regulated by several epigenetic mechanisms. Besides DNA methylation, chromatin-based gene regulations include replacement of histones, covalent posttranslational modifications (PTMs) of histones, and ATP-dependent chromatin remodeling. The histone modification and their effect in gene regulation are carried over by three class of proteins that can be classified as histone writers, erasers, and readers that adds removes, or recognizes these modifications, respectively. In the next section, the different types of DNA and histone modification and their effect on gene expression are described.

1.2.1 DNA methylation

DNA methylation is a heritable modification (Kato et al., 2003). It regulates gene expression mainly in two ways, first by directly binding to a gene promoter or gene body and converting it to the condensed heterochromatin form that cannot be accessed by the transcriptional machinery. Another mode of repression through DNA methylation involves the recruitment of histone modifiers, such as H3K9-methyltransferases (Woo et al., 2008) that bind at the methylated site and carry out the repression of target genes. DNA methylation is mostly done on cytosine at the fifth carbon position. However, sometimes, it occurs at other sites also, e.g., N-6 (Wion and Casadesús, 2006) position. In mammals, DNA methylation mostly happens in CG sites, but in plants, it also extends to CHH and CHG, where H represents A, T, or C (Cokus et al., 2008). Methylation at CG sites is carried out by METHYLTRANSFERASE 1 (MET1), while methylation at CHG and CHH sites is carried out by CHROMOMETHYLASE 3 (CMT3), and DOMAINS REARRANGED METHYLTRANSFERASE 2 (DRM2), respectively (Cao et al., 2003).

During semi-conservative DNA replication, the newly synthesized DNA strand is methylated by copying the modification pattern of the parent strand by DNA methyltransferases. DNA methylation is mostly done on repetitive sequences (Simon et al., 2005) present at the centromere and in the transposable element at CG and non-CG sites by MET1 and CMT3, respectively. Small non-coding RNAs play an important role in guiding the methylation machinery to a particular gene sequence through RNA dependent DNA methylation (RdDM).

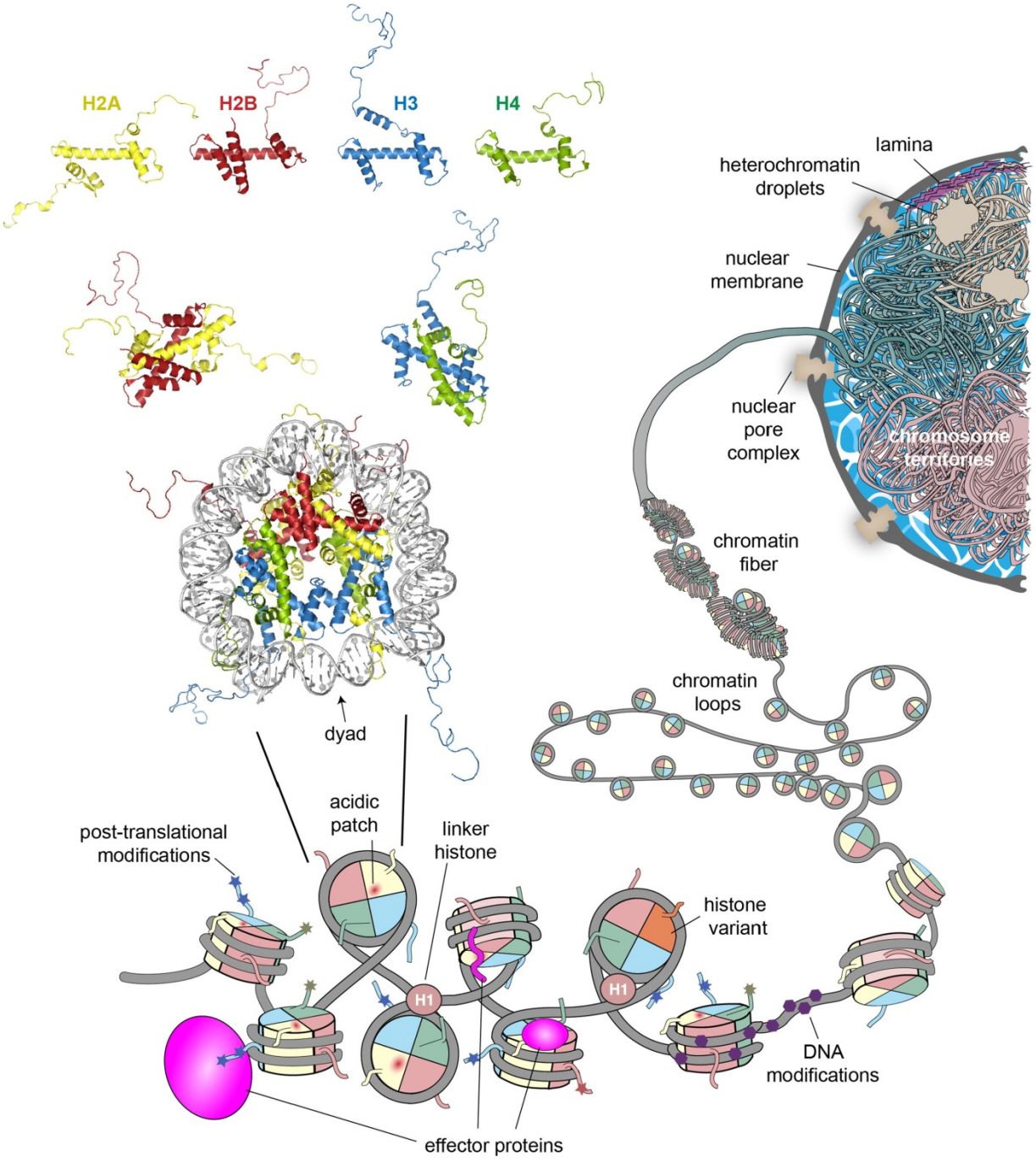

Figure 1.1. **Schematic representation of nucleosome and chromatin organization**. DNA is wrapped around histone octamer to form nucleosome that further compacts to form chromatin fiber and chromosome (Emmerik, and Ingen 2019, reproduced with permission from Elsevier).

This process consists of two steps. The first step is the generation of small interfering RNA (siRNA), and the second step involves guiding the methylation on target DNA with the help of

siRNA. Generation of siRNA involves plant-specific RNA dependent RNA polymerase 2 (RdR2) and Pol IV (Onodera et al., 2005). By interaction of these two polymerases, a double-stranded RNA (dsRNA) is produced (Huettel et al., 2007). This dsRNA is cleaved into 21-24 nucleotide siRNAs by a DICER-LIKE 3 (DCL3) endonuclease (Xie et al., 2004). After that, siRNAs undergo maturation that involves the addition of a methyl group to their 3' end. Matured siRNA associate with ARGONAUTE 4 (AGO4) to form the RNA-Induced Silencing Complex (RISC) (Henderson and Jacobsen, 2007). Another polymerase Pol-V present at the target site helps in binding of the RISC complex. The interaction between Pol V, AGO4, and KTF1, recruits the DOMAINS REARRANGED METHYLTRANSFERASE 2 (DRM2) that methylates the target DNA site (Cao et al., 2003). Maintenance of DNA methylation patterns over the next cell division provides epigenetic memory to plants. Epigenetic memory helps the plants to give a long-term response to environmental stimuli or stress conditions.

1.2.2 Nucleosome remodeling

In eukaryotes, DNA is packed in condensed form with the help of histone proteins forming a bead-like structure called nucleosome. Core nucleosome has approximately 147 bp of DNA wrapped around a histone protein octamer containing two copies each of the H2A, H2B, H3, and H4 histones (Luger et al., 1997). Assembly of nucleosome octamer begins by (H3–H4)2 tetramer formation, followed by the addition of two H2A–H2B dimers. Genes coding for canonical histones are present in multiple copies, whereas the variant histones are generally present in a single copy. Forty histone coding genes have been identified in Arabidopsis so far, among which, thirteen genes encode for H2A, eleven for H2B, thirteen for H3, eight for H4, whereas five genes encode for H1 histone. Histone variants are shown to be involved in regulating multiple functions in a cell, including transcription initiation and termination, DNA repair, meiotic recombination, chromosome condensation, chromosome segregation, etc. (Deal RB, Henikoff S. 2011). All the histone families, except H4, have variant forms (Talbert and Henikoff, 2010; Talbert et al., 2012). For example, H2A and H3 histones have two variants, each named H2A.Z, H2A.X and H3.1, H3.3, respectively. H2A variant H2A.Z is recruited by ATP dependent chromatin remodeling enzyme SWR1c (Mizuguchi et al., 2004). H2A.Z occupies nucleosome at a lower temperature around 17 °C and removed at a higher temperature above 27

°C. The H2A replacement mediated gene regulation mechanism plays a role in the vernalization-mediated flowering response in plants.

1.2.3 Histone modifications

Histones are evolutionarily conserved proteins in eukaryotes that can be subjected to post-translational modifications (PTMs) on the N-terminal tail of histones protruding outside of nucleosome core (Vaillant and Paszkowski, 2007). Different types of covalent histone modifications affect the chromatin state and, ultimately, expression of target genes (Figure 1-2). Some histone modifications, like acetylation, makes the chromatin more accessible for transcription factors, whereas methylation or ubiquitination at selective sites makes the chromatin inaccessible for the transcriptional machinery. The following section describes the various kind of histone modifications involved in gene regulation.

1.2.4 Histone acetylation/deacetylation

Histone acetylation is associated with transcriptional activation. The N terminal tails of histones have positively charged lysine and arginine amino acids. The addition of a negatively charged acetyl group (CH3COO-) on histone lysine (K) residues modifies the DNA and the histone interaction. It neutralizes the positive charge of lysines and decreases the affinity for negatively charged DNA, which facilitates the access of transcription factors to the genomic sequence. In Arabidopsis, Histone acetyltransferases (HATs) catalyze the addition of an acetyl group on the various lysine residues of histone 3 and -4 from a donor acetyl-CoA (Lee et al., 2007). Based on their distribution in a cell, HATs have been divided into two categories. Type A HATs are located in the cell nucleus and acetylate nucleosomal core histones to regulate gene expression, whereas Type B catalyzes the acetylation of free histones in the cytoplasm (Roth et al., 2001).

The effect of HATs is controlled by the antagonistic action of histone deacetylases (HDACs). In Arabidopsis, HDACs are classified into three groups: SIR2 family, HD2-like family, and RPD3-like superfamily (Pandey et al., 2002).

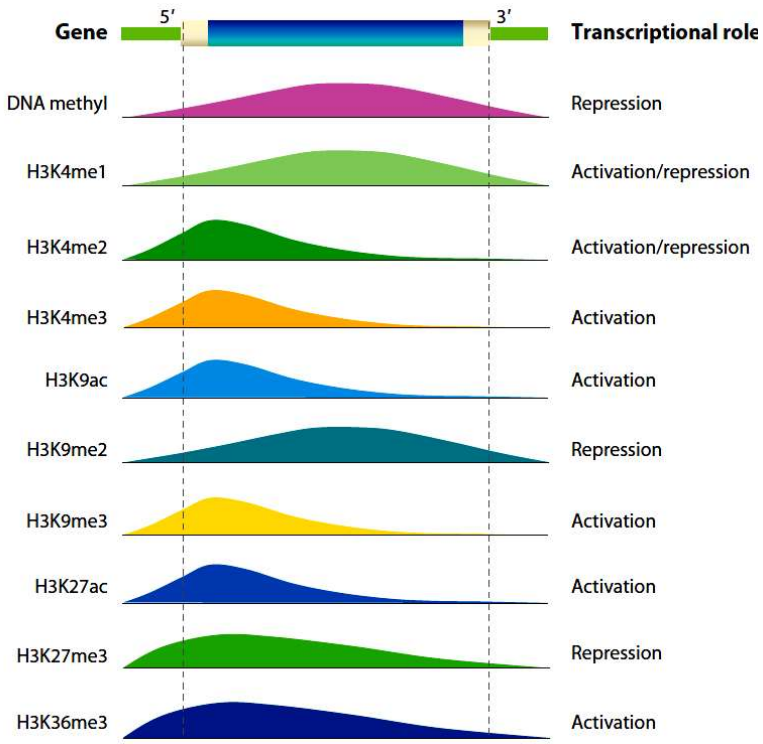

Figure 1.2. DNA and histone modifications distribution patterns and their effect in gene expression. The distribution of different histone modifications along a schematic gene in the transcribed region as well as 5′ and 3′ flanking regions are based on the genome-wide analysis. (He et al., 2011, reproduced with permission from Annual Reviews, Inc).

Among the four Arabidopsis RPD3-like HDACs, in vitro acetylation activity has been demonstrated for AtHDA19, and its overexpression or downregulation affects H3 acetylation levels, whereas the other RPD3 member AtHDA6 deacetylates the H3 and H4 lysines and regulates the expression of rRNA genes (Probst et al., 2004). The HD2-like HATs represses the gene expression during seed development (Dangl et al., 2001) while SIR2-like deacetylases suppress the salicylic biosynthesis pathway and negatively regulate plant defense response (Wang et al., 2010).

1.2.5 Histone ubiquitination/de-ubiquitination

Histone ubiquitination is performed by covalent attachment of a 76 amino acids long ubiquitin protein to the target site. The complete process of ubiquitination requires the serial activities of ubiquitin-activating enzyme E1, the ubiquitin-conjugating enzyme E2 (Ubc), and the ubiquitin-protein ligase E3 enzyme (Pickart et al., 2001). The poly-ubiquitination modification on the

target protein leads to its degradation by the 26S proteasome-mediated pathway (Smalle et al., 2004), whereas mono-ubiquitination does not lead to protein degradation, but affects the biochemical activity of the target protein (Hicke 2001, Zhang 2003). Nucleosomal core histones, specifically H2A, H2B, and other variant histones, are reported to be mono-ubiquitinated (Hicke, 2001). Interestingly, the mono-ubiquitination (H2Aub1) modification is associated with gene silencing, while H2Bub1 leads to transcriptional activation; however, it needs to be removed later for transcription progression (Zhang, 2003). The action of ubiquitin ligases is counter acted by another class of proteins, called ubiquitin proteases (UBPs) or Deubiquitinating enzymes. UBPs remove modification over the substrate by cleaving the peptide bond between ubiquitin and substrate protein. In Arabidopsis, over 27 putative UBP's have been identified (Lue et al. 2008). However, the majority of them are still uncharacterized, except few studies, like Luo et al. (2006) that describes the role UBP26 during endosperm development.

1.2.6 Histone methylation/demethylation

Similar to acetylation, methylation of histone is another very important epigenetic modification that regulates gene expression. Histone methyltransferases (HMT) catalyze the covalent addition of one, two, or three methyl groups on H3 or H4 histone lysine residues. Depending on the lysine residue at which the methyl group is added, histone methylation can act as a repressor or activator mark for gene regulation (Cloos et al., 2008). H3K27me3, H3K9me2, and H3K9me3 modifications repress the gene expression, whereas modifications like H3K4me3, H3K4me2, H3K4me1, H3K36me3, and H3K36me2 activate the gene expression (Zhou, 2009). The HMTs involved in different lysine methylation generally possess a conserved sequence of 130-150 amino acids coding for SET (Su(var)3-9), Enhancer of Zeste (E(z)) and Trithorax (TRX)] domain. A study by Pontvianne et al. (2010) described 49 SET domain proteins in the Arabidopsis genome, categorized into four conserved families: E(Z), ASH1, TRX, and SU(VAR)3-9-related proteins. The SET domain proteins belong to the trithorax group (TrxG), and ASH1 are involved in gene activation, while E(Z) family protein represses the gene during plant development, respectively (Grossniklaus and Paro, 2014).

The histone methyl groups are removed by two classes of demethylase (i) lysine-specific histone demethylase-LIKE (LDL) and (ii) JUMONJI-C-DOMAIN (JmjC) proteins. Arabidopsis

has four LDL demethylases that remove methyl group *via* amine oxidation while the 21 genes codes for JmjC proteins that perform demethylation via hydroxylation (Shi and Tsukada, 2013). Both of the LDL proteins and some JmjC proteins target a specific sets of genes and regulate various developmental activities, such as flowering time control in Arabidopsis.

1.3 Plants as model systems to study epigenetics

Being anchored throughout its life, plants have adapted a crucial survival strategy of fine-tuning their responses to adjust themselves ia a dynamic environment. Unlike mammals, in which organ development is already specified during embryonic establishment, plants throughout their life keep developing new organs from meristematic regions. Epigenetic modifications are important for plants to integrate the environmental signals and regulate the gene expression response accordingly, which results in phenotypic plasticity. The ability to reversibly alter their phenotype helps the plant to adapt according to external environmental conditions. The heritable epigenetic modifications provide a stable memory to the plant by which it can remember the previous environmental signals such as vernalization, throughout its life and perform the developmental transitions. The ease of mutagenesis and identification of homozygous mutants in plants has made them an ideal system to study epigenetics. Screening for mutations in epigenetic regulators is generally done by generating a transgenic plant with an engineered transgene that results in the recovery of expression of the mutated gene. The ability to conduct forward and reverse genetics approaches to identify gene functions has greatly helped to understand the epigenetic regulators in plants. Also, increased ploidy levels in plants compared to mammals results in functional redundancy between genes making it easy to generate and study different gene modifier mutants, which would be otherwise lethal in the absence of polyploidy. Moreover, considering legal and moral issues that arise is generating the mutant animals, it is easy in plants to study the function of epigenetic mutants with morphological defects. Additionally, a large number of plants can be easily screened to characterize a transgenic trait. Recent advances in genome sequencing and availability of enormous mutant lines covering almost every gene in the model plant (i.e., Arabidopsis), has made it an excellent system to pursue epigenetics research. A table given below (Table 1.1) summarizes the important histone modifiers, whose functions have been characterized in Arabidopsis so far.

Table 1.1 – List of important DNA, histone modifiers and their functions described in Arabidopsis (Modified from Pikaard and Scheid, 2014)

Gene Acronym	Complete name	Biochemical activity	Biological function	Reference
Histone Acetyl transferases				
HAC1	Histone acetyltransferase CBP-like	Histone acetyltransferase	Flowering onset and root development	Deng et al., 2007
HAG1	Histone acetyltransferase GCN5-like	Histone acetyltransferase (H3K14ac)	leaf and floral organogenesis	Servet et al., 2010
HAM1	Histone acetyltransferase Myst-like	Histone acetyltransferase	FLC mediated flowering time regulation	Xiao et al., 2013
Histone deacetylases				
HDT1	Histone deacetylase	A typical histone deacetylase	Root growth	Li et al., 2017
HDA6	Histone deacetylase-6	Histone deacetylase	Leaf development	Luo et al., 2012
HDA19	Histone deacetylase-19	Histone deacetylase	repression of embryonic properties	Tanaka et al., 2008
Histone ubiquitin ligases				
HUB1	E3 ubiquitin ligase	H2B monoubiquitination	Seed dormancy	Liu et al., 2007
UBC1	E2 ubiquitin-conjugating enzyme	H2B monoubiquitination	Female gametophyte development	Wang et al., 2016
BMI1 A/B	B cell-specific Mo-MLV integration site 1	H2A monoubiquitination	Regulate plant embryonic and stem cell development	Bratzel et al., 2010
BMI1 C	B cell-specific Mo-MLV integration site 1	H2A monoubiquitination	Regulates flowering onset	Li et al., 2011
AtRING1a/b	RING finger protein	H2A monoubiquitination	Regulate the Vegetative Phase Transition in	Li et al., 2017

			Arabidopsis	
Histone deubiquitinase				
OTLD1	Otubain-like deubiquitinase	H2B deubiquitination	Stimulates plant growth	Keren et al., 2016
SUP32/UBP26	Suppressor of ros, ubiquitin protease	H2B deubiquitination	Required for heterochromatic histone H3 methylation	Sridhar et al., 2007
Histone methyltransferase				
ATX1	Arabidopsis homolog of trithorax	Histone methyltransferase	Floral organ development	Alvarez-Venegas et al., 2003
ATXR3/SDG2	Arabidopsis homolog of trithorax, SET domain group	Histone methyltransferase	Regulates onset of Flowering	Yun et al. 2012
ATXR5,-6	Arabidopsis trithorax-related proteins	Arabidopsis trithorax -related proteins (ATXR5,-6: H3K27me1)	Leaf development	Jacob et al., 2009
ATXR7	Arabidopsis trithorax-related proteins	Histone methyltransferase	FLC mediated flowering regulation	Tamada et al., 2009
EFS/SDG8/ASHH2	Early flowering in short days, SET domain group, ASH1 homolog	Histone methyltransferase	Seed development	Cheng et al., 2018
ULT1/2	Ultrapetala	Regulator of histone methylation, ATX1 interactor	restrict shoot and floral stem cell activity	Carles et al., 2009
CLF	Curly leaf	H3K27 trimethylation	Leaf and floral organ development	Goodrich et al., 1997
MEA, FIS1	Medea, fertilization-independent seeds	H3K27 trimethylation	Maternal imprinting of seed development genes	Kohler et al., 2005

SWN	Swinger	H3K27 trimethylation	Act redundantly with CLF to regulate plant development	Chanvivattana et al., 2004
MSI1	Multicopy suppressor of IRA homolog	Polycomb-group protein (p55)	Regulates flowering time onset	Bouveret, et al., (2006)
MSI4/FVE	Multicopy suppressor of IRA homolog	Polycomb-group protein (p55), Cul4-DDB1 and PCR2 interactor	Promotes flowering	Pazhouhandeh et al., 2011
MSI5	Multicopy suppressor of IRA homolog	Polycomb-group protein (p55), an interactor of HDA6, FLC silencing	Regulates FLC mediated flowering pathway	Gu et al., 2011
EMF1/2	Embryonic flower	Polycomb-group protein (Su(z)12)	Repression of flower homeotic genes	Kim et al., 2010
FIE, FIS3	Fertilization-independent endosperm, fertilization-independent seeds	Polycomb-group protein (Esc)	Seed development	Ohad et al. (1999)
Histone demethylases				
ELF6	Early flowering	Histone demethylase (H3K4me1,-2,-3)	Regulates onset of Flowering	Jeong et al., 2009
FLD, LDL1,-2	Flowering locus D, LDS1-like	Histone demethylases	Regulates the Transition to Flowering	He et al., 2005

1.4 Polycomb Repressive Complex (PRC) proteins in plants

Polycomb group genes (PRCs) were first time identified in Drosophila through a genetic screen of different homeotic mutants. This study led to the identification of 13 polycomb genes in Drosophila (Simon et al., 1995). PRCs in Drosophila are mainly categorized into two groups PRC-2 and PRC-1. PRC-2 complex consists of ENHANCER OF ZESTE(E(z)), SUPPRESSOR OF ZESTE (Su(z)), EXTRA SEX COMB (ESC) and WD40 domain-containing p55 (Tie et al., 2001). Whereas, the PRC1 complex consists of Polycomb (Pc), Posterior sex combs (Psc),

RING, and Polyhomeotic (PH) proteins (Franke et al., 1992, Poux et al., 2001, Shao et al., 1999). Arabidopsis PRC2 complex contains 3 homologs of E(z), i.e. Curly leaf (CLF), MEDEA (MEA), SWINGER (SWR), five homologs of P55, i.e. MULTICOPY SUPPRESSOR OF IRA (MSI1-5), one ESC homolog FERTILIZATION INDEPENDENT ENDOSPERM (FIE) and three Su(z)12 homologues, i.e. EMBRYONICFLOWER2 (EMF2), FERTILIZATION INDEPENDENT SEED2 (FIS2)], and VERNALIZATION2 (VRN2) (Goodrich et al., 1997, Grossniklaus et al., 1999; Chanvivattana et al., 2004; Hennig et al., 2005) CLF, MEA, and SWR are the SET domain-containing methyltransferases that catalyze H3K27 trimethylation (Figure 1-3).

In plants, although homologs of Drosophila PRC1 complex proteins are absent, however, they have some proteins with a similar function. PRC1 like member in Arabidopsis includes -Like Heterochromatin Protein (LHP1) (Turck et al., 2007), also known as Terminal Flower 2 (TFL2), EMF1 (Calonje et al., 2008) AtRING1 A and -B, AtBMI1A, AtBMI1B, AtBMI1C, and VRN1 are other members of PRC1-like complex in Arabidopsis (Turck et al., 2007; Zhang et al., 2007). LHP works similarly to heterochromatin protein (HP) in animals. LHP1 binds to the H3K27me3 mark placed by PRC2 and also helps in retention and spreading of repressor tri-methyl group over other histones, which keeps chromatin in heterochromatic form and keep it repressed. LHP1 also associates with a DNA methyltransferase CHROMOMETHYLASE3 (CMT3) (Jackson et al., 2002), converting the DNA to heterochromatin form.

1.4.1 Role of PRC2 proteins in plant development-

As described previously, PRC2 contains four core members; out of them Enhancer of Zeste-2 (E(z)2) is the main catalytic subunit involved in the histone modification, whereas MSI1 helps in the complex formation and its recruitment. In the next section, the role of E(z)2 and MSI1-like proteins is described in detail.

1.4.1.1 Role of Enhancer of Zeste-2 (E(z)2) like proteins in plant development-

E(z) is the core subunit of PRC2 complex catalyzing the H3K27 tri-methylation that acts as a repressor mark for gene expression. E(z) protein contains a Cys-rich region and the SET (Su(var)3-9, Enhancer-of-zeste, Trithorax) domain near their C terminus. The SET domain of E(z) has methyl transferase activity (Müller et al., 2002). In addition to this domain, plant E(z)

protein also contains a SANT (SWI3, ADA2, N-CoR, and TFIIIB DNA-binding domains), EZD1 and EZD2 domains (Springer et al., 2014). Arabidopsis has three homologs of E(z) named as CURLY LEAF (CLF), SWINGER (SWN), and MEDEA (MEA). They play a role during different transition stages of plant development. They are component of three types of PRC complexes named as the FERTILIZATION INDEPENDENT SEED (FIS) complex involved in early endosperm development, VERNALISATION (VRN) complex involved in onset of flowering after the cold treatment, and EMBRYONIC FLOWER (EMF) complex, which inhibits flowering during early plant development stages (Hennig and Derkacheva, 2009).

Homeotic genes in animals are well-known targets of Polycomb repressor proteins. Plant development is also regulated by homeobox-containing Class-I *KNOX* genes. Recent studies have shown that the repressors of *KNOX*, such as AS1 and AS2, recruit PRCs over *KNOX* genes (Lodha et al., 2013*a*) and regulates their spatiotemporal expression. Repression of CLF leads to ectopic expression of *KNOX* genes that result in abnormal plant development (Goodrich et al., 1997). In rice, the role of two orthologs of E(z) gene, *OsSDG711,* and Os*SDG718,* have been characterized in flowering during LD and SD photoperiods. These two genes are related to Arabidopsis E(z) homologs, CLF, and SWN, respectively (Liu et al., 2014). In Arabidopsis, these two genes act redundantly, but they don't seem to be working together in rice, suggesting that the regulatory mechanism of flowering is distinct in LD vs. SD plants.

1.4.1.2 Role of MSI-1 like proteins in plant development

The name, MULTICOPY SUPPRESSOR OF IRA1 (MSI-1), is based on the identification of this gene from yeast mutant. MSI-like proteins are present in all eukaryotes. Its homolog in drosophila, named as P55, is the core subunit of Polycomb Repressor Complex 2 (PRC-2), Histone Deacetylase complex, and Chromatin Assembly factor (CAF). MSI1-like (MSIL) proteins are the members of the WD40 repeat-containing protein family. MSI like proteins have seven WD40 repeats with small four-stranded β-sheets forming a β-propeller fold, which allows the protein to form a closed circular structure that assists their binding to histone and making the interaction with other proteins (Hennig et al., 2005). MSI-like proteins seem to have diversified multiple times independently, as indicated by the monophyletic origin of MSI-like proteins. Arabidopsis has five MSI-like proteins. Although most of them show a similar expression pattern, their functions are not redundant (Ach et al., 1997).

MSI1, the core subunit of FERTILISATION INDEPENDENT SEED (FIS)-PRC2 repressor complex, is involved in the regulation of seed development. It is also one of the components of the EMF complex that inhibits flowering during the early vegetative phase by repressing key florigen, FLOWERING LOCUS T (FT) (Steinbach and Hennig, 2014). Interestingly, MSI1 also works with the vernalization complex and helps in promoting flowering after the long cold treatment by repressing the Flowering Repressor C (FLC) (Steinbach and Hennig, 2014).

Arabidopsis complex	Arabidopsis protein	Protein domain	Biochemical activity	Drosophila homolog
EMF 	EMF2	Zn finger		Su(z)12
	FIS2	Zn finger		Su(z)12
	VRN2	Zn finger		Su(z)12
FIS 	CLF	SET	H3K27 trimethylation	E(z)
	SWN	SET	H3K27 trimethylation	E(z)
	MEA	SET	H3K27 trimethylation	E(z)
VRN 	MSI1	WD 40		p55
	FIE	WD 40		Esc
PRC1 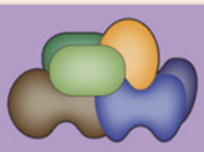	LHP1/TFL2	Chromodomain	bind. to methylated H3K27	SCE (RING)
	AtRING1a-b	RING		
	AtBMI1A-C	RING	H2A monoubiquitination	
	EMF1	LXXLL motif		
	VRN1	2 B3 domains		

Figure 1.3. Details of different PRC complex members in Arabidopsis. (Holec et al., 2012, reproduced with permission from American Society of Plant Biologists).

1.4.1.3 Role of different Polycomb complexes in regulating the developmental transitions in plants

Various members of PRC2 complex make mainly- three types of complexes that govern plant developmental phase transitions from seed development till the onset of flowering (Figure 1-4). Detailed functions of these complexes are provided in the following sections.

1.4.1.4 Fertilization Independent Seed (FIS) complex

The FIS complex functions in the female gametophyte and inhibits the initiation of endosperm as well as seed development before fertilization (Kohler et al., 2003). The components of the FIS complex include MEA or SWN, FIE, FIS2, and MSI1 (Leroy et al., 2007). In plants, from pollen grain, two sperm nuclei develop, one of them fertilizes with the egg, while the other fuses with the central cell to form endosperm. This process is called double fertilization, which is the unique feature of plants. After this, eight cycles of syncytial nuclear division occur without cellularization, following which cellularization starts. However, in plants, in which Fertilization Independent Seed (FIS) was mutated, no cellularisation happened after the eighth division of the nucleus and embryo (Chaudhury and Peacock, 1997). Notably, loss of PRC2 subunits in rice did not result in autonomous seed development, suggesting that PRC2 activity is required for the overall seed development and not just limited to prevent apomixes (Luo et al., 2009).

1.4.1.5 Embryonic Flower (EMF) complex

EMBRYONIC FLOWER genes (EMF1 and EMF2) play an important role in the repression of flowering during embryonic stages (Yoshida et al., 2001). Plants in which EMF1 or EMF2 genes are mutated, escape the vegetative shoot growth, and initiate flowering from a very early stage. The EMF complex promotes vegetative development by repressing the expression of genes associated with floral induction, such as *FT* and *AGAMOUS-LIKE 19 (AGL19)*. EMF2 is a structural homolog of Drosophila Suppressor of zeste 12 [Su(z)12] and encodes for a zinc finger protein, similar to FERTILIZATION-INDEPENDENT SEED2 (FIS) and VERNALIZATION2 (VRN) of Arabidopsis PRC2 members. EMF2 is found to be expressed in embryos, organ primordia and in shoot meristems (Yoshida et al., 2001)

1.4.1.6 Vernalization (VRN) complex

Plants sense environmental conditions, such as photoperiod and temperature, to synchronize their developmental programs for better adaptation. Plants grown in temperate climate zones initiate flowering during the spring season. To ensure this, they require longer periods of low temperature (vernalization) before being shifted to the reproductive phase. The important regulator of vernalization is a MADS-box gene FLOWERING LOCUS C (FLC), which delays flowering by repressing the FT protein, a major flowering inducer. The VRN

complex is required to repress FLC after vernalization (De Lucia et al., 2008). The VRN complex is composed of VRN2, CLF/SWN, FIE, and MSI1 (wood et al., 2006). Subsequent studies showed that during prolonged cold conditions, VRN complex associates with VERNALIZATION INSENSITIVE 3 (VIN3), VRN5, and VEL1 to repress flowering repressor FLC through H3K27me3 modification, leading to flowering induction.

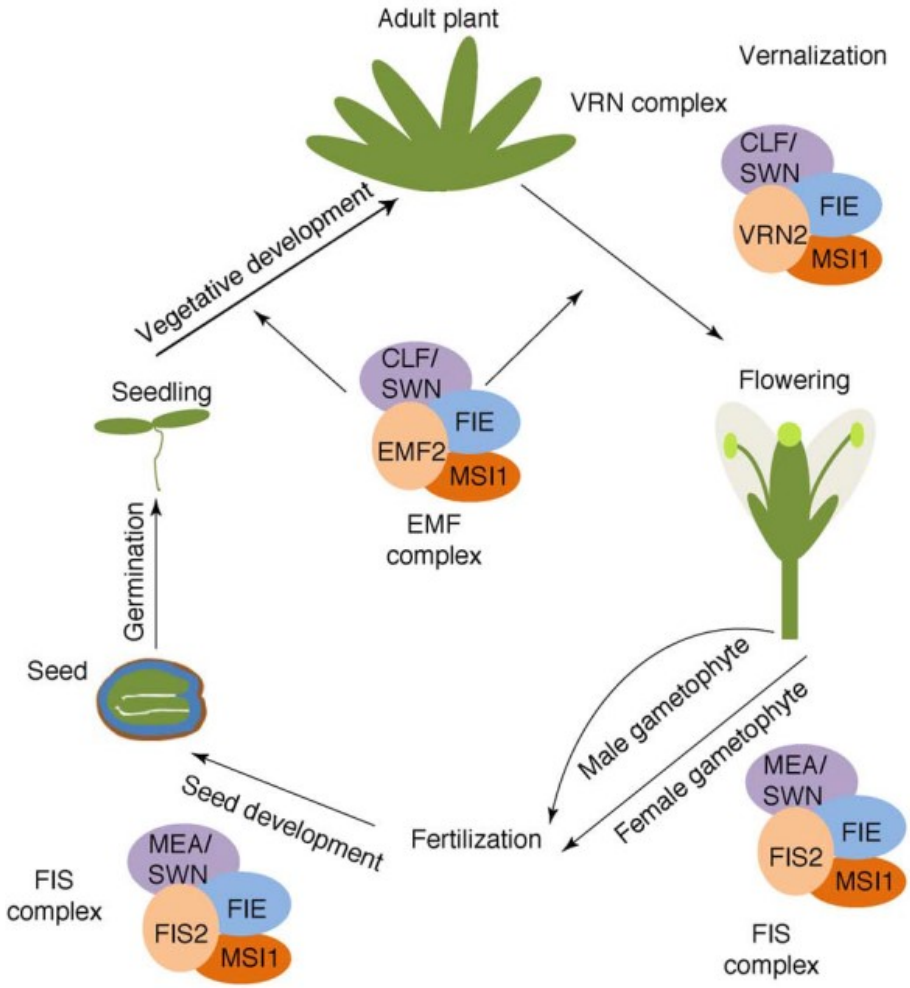

Figure 1.4. PRC2 like complexes regulate important developmental transitions in plants. The FIS complex prevents seed development in the absence of fertilization, The EMF complex promotes vegetative development and delays reproduction, The VRN complex establishes epigenetic silencing of FLC after vernalization and enables flowering (Hennig et al., 2009, reproduced with permission from Elsevier).

1.4.2 Role of PRC1 members in plant development

The PRC1 complex in Drosophila contains four members, namely Polycomb (Pc), Polyhomeotic (Ph), Posterior sex comb (Psc), and dRING1 proteins (Shao et al., 1999; Peterson et al., 2004). They repress target chromatin by H2A mono-ubiquitination (Cao et al., 2005). Arabidopsis has three homologs of Psc (AtBMI1A, AtBMI1B, and AtBMI1C) and two homologs of dRING1 (AtRING1A, and AtRING1B; Sanchez-Pulido et al., 2008; Xu and Shen, 2008; Bratzel et al., 2010, 2012; Chen et al., 2010; Yang et al., 2013; Calonje, 2014). Additionally, LIKE-HETEROCHROMATIN PROTEIN1 (LHP1), also known as TERMINAL FLOWER2 (TFL2), is identified in Arabidopsis, which recruits PRC1 complex over H3K27me3 mark on the targets (Turck et al., 2007). Another plant-specific protein in the PRC1 group is EMBRYONIC FLOWER1 (EMF1), which maintains the juvenile stage of the plant through interaction with PRC2 members such as MSI1 and EMF2 (Calonje et al., 2008). BMI1 (B cell-specific Mo-MLV integration site 1) acts as E3 ubiquitin ligases and represses the target gene through ubiquitination of histone H2A at lysine 119 position. A recent study in Arabidopsis has shown that BMI1 regulates meristem maintenance and cell differentiation by repressing *PLETHORA (PLT)* and *WUS homeobox-containing (WOX)* genes (Merini et al., 2017). Further, BMI1 mutants show down-regulation of important flowering genes, like *SQUAMOSA PROMOTER BINDING PROTEIN-LIKE (SPL)* and *FT*, indicating its role in the flowering response. To avoid precocious flowering, *SPLs* are suppressed by miR156 during the juvenile phase of plants. However, during adult and reproductive phases, miR156 levels are brought down by BMI1-mediated suppression to allow the expression of *SPLs*. Interestingly, many of the upregulated genes in *BMI1* mutants that govern meristematic maintenance and flowering response show H3K27me3 modification in their gene bodies (Merini et al., 2017), suggesting that both PRC complexes (PRC1 and PRC2) regulate these developmental events.

In a landmark experiment, Chailakhya et al. (1981) observed that hetero-grafting between flowering tobacco and non-induced potato plant leads to the initiation of tuber development from non-induced potato stock. Later on, Navarro et al. (2011) demonstrated that StSP6A is a tuberization signal and is a homolog of well-known flowering inducer FT protein in arabidopsis.

Based on these findings, it is clear that flowering and tuberization inducing signals are similar. The following section describes in detail the similarities between flowering and tuberization networks.

1.5.1 CDF-CO-FT module controls photoperiod dependent flowering and tuberization

Light and temperature are crucial cues for plants to sense the change in the environment. In Arabidopsis, the photoreceptors group includes five phytochromes (phyA- phyE), two cryptochromes (CRY1 and CRY2), and two phototropins (PHOT1 and -2) (Briggs et al., 1999; Cashmore et al., 1999). Phytochrome B represses the flowering, whereas phytochrome A, cryptochrome, and flavin-binding kelch repeat F box protein (FKF1; a blue light receptor) induces flowering by controlling the CONSTANS (CO) levels (Imaizumi et al., 2003). CO is a B box zinc finger containing protein (Putterill et al., 1995). It has two B boxes at the N terminal end and a CCT domain (Wenkel et al., 2006) at the C terminal end. During the night and early morning, an E3 ubiquitin ligase COP1 forms complex with SPA1 and leads to 26S proteasome-mediated degradation of CO (Liu et al., 2008). Another transcriptional repressor CYCLING DOF FACTOR (CDF) and an E3 ubiquitin ligase HOS1 also inhibit CO expression (Lazaro et al., 2012) in the morning period (Valverde et al., 2004). During the latter half of the day, when far-red availability is more, phytochrome A and cryptochrome bind with the COP1-SPA1 dimer and inhibit their function. Moreover, COP1 also moves out of the nucleus with the help of phytochrome-A and cryptochrome (Zuo et al., 2011). At the same time, the levels of circadian clock protein GIGANTIA (GI) increases, and it forms a complex with blue light photoreceptor FKF1 having ubiquitin ligase activity (Imaizumi et al., 2005). GI-FKF1 complex degrades the CDF1 and relive the CO from its repression (Park et al., 1999). Once CO is free to work, its CCT domain-containing C terminus interacts with Nuclear factor Y protein (NF-Y) (Ben-Naim et al., 2006), which helps it to bind at the CCAAT element or CO responsive element (CORE) over FT promoter and activates its expression (Adrian et al., 2010 ,Tiwari et al., 2010) (Figure 1-5).

Recently, Kloosterman et al. (2013) noticed that late tuberizing potato lines had fully intact CDF1 allele, whereas early tuberizing lines had truncated CDF1.2 and CDF1.3 alleles. Also, it was noticed that CDF1.1 has an intact C domain involved in its interaction with StGI and StFKF1. The truncated version lacks the region involved in FKF1 binding, leading to its constitutive expression. Moreover, overexpression of truncated StCDF1.2 variant resulted in

early tuber formation as well as produced tubers in non-inductive LD conditions in photoperiod-dependent potato subspecies andigena. Under tuber inducing conditions, the enhanced StCDF1 levels result in CO repression. Unlike the stimulatory effect of CO in flowering, its overexpression in potato represses tuberization, whereas its silencing promotes tuberization (González-Schain et al., 2012). It was further shown that StCO inhibitory effect is graft transmissible and is involved in long-distance signaling to control tuberization in potato. The negative effect of CO on tuberization is mainly mediated by different FT homologs, as described in the next section.

1.5.2 FT protein homologs regulate the onset of flowering and tuberization

FT protein (175 amino acids) (Ho and Weigel, 2014) is synthesized in the vascular tissue of leaves. It belongs to the CETS (CENTRORADIALIS, TERMINAL FLOWER 1, and SELF PRUNING) Family (Kobayashi et al., 1999). Arabidopsis has six close members belonging to this family, named as FT, TSF, BFT, ATC, MFT, and TFL1. Terminal Flower1 (TFL1) acts as an inhibitor of flowering (Ohshima et al., 1997). FT can be converted to TFL like protein just by one amino acid substitution, i.e Tyrosine with Histidine at 85^{th} base, while TFL can function as FT by replacing Histidine with Tyrosine at 88^{th} base position (Hanzawa et al., 2005). FT protein forms heterodimer with a bZIP transcription factor Flowering Locus D (FD) (Wigge et al., 2005) and reaches to shoot apical meristem (Corbesier et al., 2007); where they activate MADS BOX genes, like SUPPRESSOR OF OVEREXPRESSION OF CONSTANS 1 (SOC1) (Immink et al. 2012), which regulates *LEAFY* (*LFY*) gene. LFY regulate various Floral Meristem Identity Genes like AGAMOUS (AG), APETALA1 and APTELA3, SEPALLATA4 (SP4) (Moyroud et al., 2011), which form different floral organs (sepal, petals, anther, and stigma).

In *Solanum tuberosum* ssp. andigena, three paralogues of FT protein (StSP3D, StSP6A, and StSP5G) play important roles in controlling flowering and tuberization (Figure 1-6). Among them StSP3D is involved in flowering, StSP6A promote tuberization (Navarro et al., 2011), and

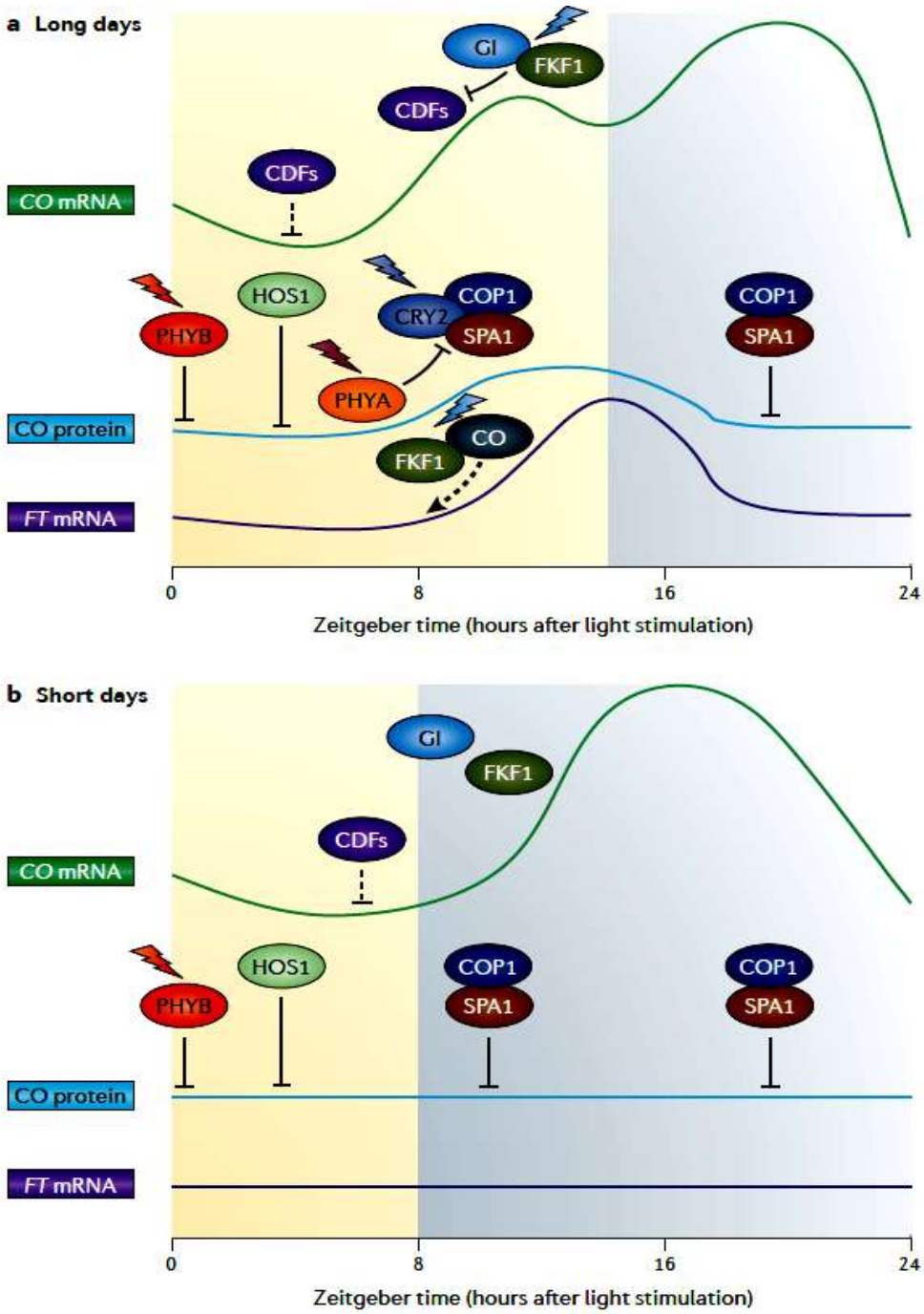

Figure 1.5. Photoperiod dependent regulation of key components of the flowering pathway. GIGANTEA (GI), FLAVIN KELCH F BOX 1 (FKF1), CONSTANS (CO), and FLOWERING LOCUS T (FT) are a major regulator of the flowering pathway. Their differential availability under SD vs. LD conditions regulate the photoperiodic flowering of *Arabidopsis thaliana* (Andres and Coupland, 2012, Reproduced with permission from Springer Nature).

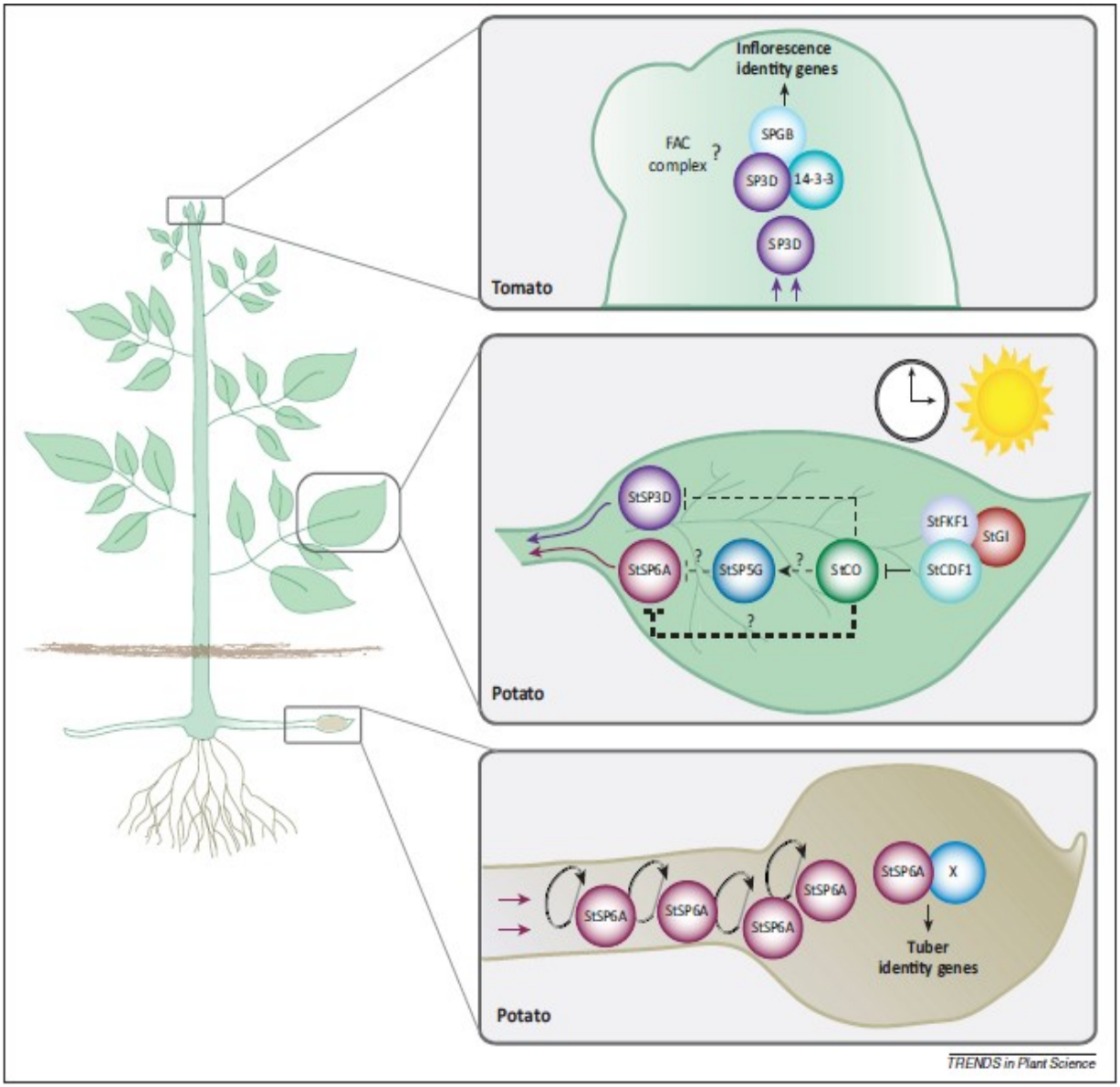

Figure 1-6. Model for flowering and tuberization. Photoperiod signal is perceived in the leaves and integrated with the endogenous clock to regulate expression of the CO factor that controls activation of the *StSP6A* gene. Under SD conditions, induced *StSP6A* expression promotes tuberization (Abelenda et al., 2014, Reproduced with permission from Elsevier)

the third member, StSP5G, inhibits tuberization indirectly by inhibiting StSP6A (Kloosterman et al., 2013). Potato lines in which the *StSP6A* gene is silenced show delayed tuberization. Overexpression of StSP3D and StSP6A induced flowering; however, down-

regulation of StSP6A affects only tuberization, but not flowering. Moreover, StSP6A overexpression induced tuberization even under non-inducing LD conditions. In Arabidopsis, expression of *StSP6A* in FT mutated background, initiated flowering, suggesting the functional similarity between StSP6A and FT proteins (Navarro et al., 2011). Under SD condition, there is an increase in levels of StSP6A, whereas StSP5G expression drastically reduces. StSP6A leads to a drop in the level of phytohormone Gibberellin (GA) by inducing the expression of GA catabolism enzyme StGA2ox1. GA affects the plane of cell division in stolon by regulating the cortical microtubule orientation. Microtubules are made up of α- and β-tubulin heterodimer, their dimerization is assisted by a chaperon (named as prefoldin) that assists in the folding of tubulin in the cytoplasm. The GA signaling repressor (DELLA) binds and adversely affects the function of prefoldin by bringing them to the nucleus, leading to a drop in the α/β-tubulin heterodimer availability (Locascio et al., 2013). Thus, the directional pattern of cell division is disturbed. The StSP6A-mediated reduction in GA levels changes the microtubule orientation, thus randomizing the plane of cell division, leading to a swollen stolon.

1.5.3 Role of microRNAs in flowering and tuberization control

MicroRNAs (miRNAs) are small (21-24 nucleotides), endogenous, non-coding RNAs that down-regulate expression of their target genes by transcriptional cleavage and/or translational inhibition. Various plant developmental pathways, like leaf development (Palatnik et al., 2003), floral development (Aukerman and Sakai, 2003), and root development, are regulated through miRNAs. In the subsequent section, the role of two important miRNAs (miR156 and -172) in flowering and tuberization pathways is explained.

1.5.3.1 Role of microRNA156 and -172 in flowering

miR172 regulates the onset of flowering in plants. Its expression is very low during germination, but it increases as the plant progresses towards the flowering stage (Aukerman and Sakai, 2003). Moreover, overexpression of miR172 leads to early flowering in plants. miR172 promotes flowering by targeting the flowering repressor gene *APETALA2 (AP2)* and five other AP2-like flowering repressor genes *TARGET OF EAT1 (TOE1), TOE2, TOE3, SCHLAFMUTZE (SMZ),* and *SCHNARCHZAPFEN (SNZ)* (Teotia and Tang, 2015). A study by Zhang et al. (2015) has shown that TOE1 indirectly represses *FT* expression by targeting CO. Additionally, in maize,

miR172 is shown to target the *APETALA2-like gene, glossy15 (gl15),* controlling the flowering phenotype (Lauter et al., 2005). miR172 plays an important role in the juvenile-to-adult phase transition by repressing the flowering inhibitors.

miR156 plays a crucial role during the juvenile-to-adult phase transition in plants. It targets the *SQUAMOSA PROMOTER BINDING LIKE (SPL)* family of transcription factors (Wu et al. 2009) to control plant growth and development. One of the SPL members, SPL3, has been shown to mediate vegetative to adult phase change and promote the flowering onset in Arabidopsis (Wu and Poethig, 2006). In line with this, the expression of miR156 decreases, whereas the SPL3 levels increase as the plant grow towards maturity (Wang et al., 2009; Wu and Poethig, 2006). miR156 indirectly represses the expression of miR172 by targeting SPL9/10 that is known to induce the expression of miR172. Moreover, overexpression of miR156 shows a prolonged juvenile phase and delayed flowering. In contrast, the miR156 insensitive-SPL3 overexpression causes early flowering plants. In this way, the sequential action of the miR156-SPL9-miR172-TOE1/2 module controls the complete juvenile-to-adult phase transition in arabidopsis.

1.5.3.2 Role of microRNA156 and -172 in tuberization

A recent study has shown the role of miR156 in the regulation of potato development (Bhogale et al., 2014). Similar to Arabidopsis, the levels of miR156 steadily decrease as the potato plant grows from the juvenile-to-adult phase. The known targets of miR156 in potato are SPL family of transcription factors, namely *StSPL3, StSPL6, StSPL9, StSPL10*, and *LIGULELESS1 (StLG1)*. Among these targets, StSPL9 is known to promote the expression of miR172 by directly binding to its promoter. Thus, as the plant ages, the expression of *StSPL9* increases, leading to higher accumulation in miR172 and induction of tuberization. Consistently, overexpression of miR156 reduces levels of miR172 and decreases the below-ground tuber yield. Interestingly, miR156 overexpression lines show increased levels of cytokinin and decreased levels of strigolactone. This change in hormone levels was accompanied by aerial tuber development from axillary-nodes in miR156 overexpression lines, suggesting the positive role of miR156 in the tuberization pathway (Bhogale et al., 2014). In potato, expression of miR172 increases in all tissues types under tuber inducing SD conditions compared to LD. It has highest

expression in stem and swollen stolon (Martin et al., 2009). Notably, miR172 overexpression leads to early flowering and tuberization, suggesting its conserved function in Arabidopsis and potato. Moreover, miR172 overexpression plants could overcome the inhibitory effect of LD conditions, and exhibit tuber development under a non tuber-inducing LD photoperiod. In potato, miR172 is predicted to target the AP2-like gene *RELATED TO APETALA2 1 (RAP1)* similar to Arabidopsis (Figure 1-7). The expression of *RAP1* shows an inverse trend compared to miR172. Its expression reduces in swollen stolon, whereas levels of miR172 remain high. These findings suggest that miR172 is an important regulator of tuberization.

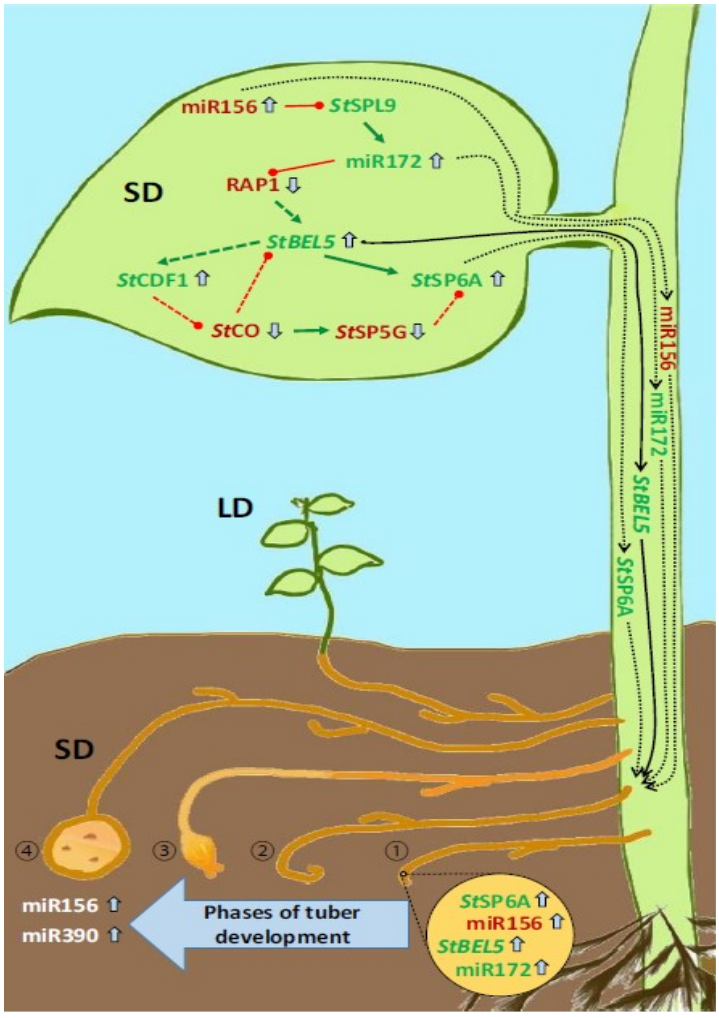

Figure1.7. **Model to describe the role of different factors in stolon to tuber transitions**. green and red color represents positive and negative regulation respectively (Natarajan et al. 2017, Reproduced with permission from Springer Nature)

1.5.4 PRC mediated control of flowering

Plants optimize their developmental programs according to environmental conditions. The transition from vegetative to reproductive phase is one such crucial event in plants that determine their rate of survival. Proper vegetative growth is necessary for the plant to fulfill the energy requirement during flowering and fruit development. Several studies have unraveled many factors that control floral transition in plants. In the following section, different ways through which PRC members can regulate the onset of flowering are described.

1.5.4.1 PRC mediated repression of genes involved in flowering

Repression of flowering during the vegetative stage is controlled by the FERTILIZATION INDEPENDENT ENDOSPERM (FIE) complex. The other members of the FIE complex include MEDEA, a methyl transferase homolog of E(z) in Drosophila, FERTILIZATION INDEPENDENT SEED (FIS), and EMBRYONIC FLOWER (EMF). FIE complex regulates the onset of flowering by repressing the homeotic genes, like *LEAFY (LFY), APETALA (AP), PISTILATA (PI),* and *AGAMOUS (AG)*. The loss-of-function of FIE leads to the formation of flower-like structure from the root and juvenile seedling (Kinoshita et al., 2001). Some winter annual accessions of Arabidopsis require a prolonged cold treatment before flowering. After exposure of the plant to cold treatment (vernalization), *FLC* mRNA level starts diminishing. *FLC* downregulation is mediated by the PRC2 variant termed as the vernalization complex through H3K27me3 repressive modification over the *FLC* locus (Jiang et al., 2008). The recruitment of PRC over the *FLC* locus is mediated by two long noncoding RNAs, COLDAIR and COOLAIR, synthesized from the intronic region of the *FLC* gene itself (Swiezewski et al., 2009). Besides this, another PRC2 complex, termed as EMF, checks the onset of flowering during embryonic and juvenile stages by repression of the *FT* expression.

1.5.4.2 PRC mediated regulation of flowering through miR156 and miR172 repression

A study by Lafos et al. (2016) revealed that approximately 50% of the miRNAs, including miR156 and miR172 loci, are regulated through H3K27me3 modification. Besides H3K27me3 mediated repression, miRNA156 and -172 are also shown to be regulated by PRC1 members. A study by Pico et al. (2015) revealed that in *atbmi1* mutant plants showed higher levels of miR156A/C expression at the adult stage of the plants compared to wild-type. Authors also found that PRC1 members assist in the function of PRC2 mediated H3K27me3 deposition.

In line with this, *atbmi1a/b* mutants had reduced levels of H3K27me3 deposition near the transcriptional start site (TSS) of miR156 locus contributing to its higher expression in the mutant background. Higher miR156 levels contribute to reduced SPLs and FT levels in leaves that, in turn, extend the juvenile phase and repress the onset of flowering. Besides miR156, another PRC1 member, AtEMF1, is required to check the precocious flowering during the juvenile stage of the plants. This is mediated by repression of SPL and miR172 through AtEMF1. Consistently, EMF1 mutation results in the upregulation of pri-MIR172 as well as SPL3/9 levels during the juvenile stage of the plants. This possibly triggers the upregulation of *FT* and acquisition of flowering competence even before the plant reaches the adult phase (Figure 1-8).

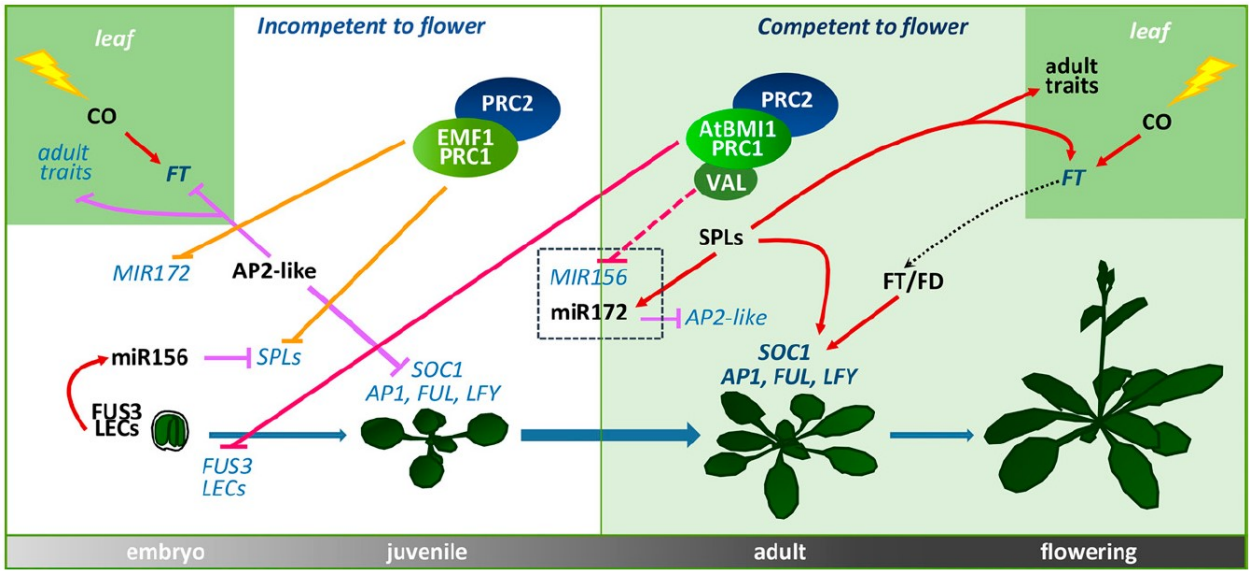

Figure 1.8. Model of PRC mediated regulation of juvenile-to-adult phase transition in Arabidopsis. EMF1-PRC1 represses MIR172 and SPLs to maintain the juvenile phase. On the other hand, AtBMI1-PRC1-mediated repression of miR156 allows the development of adult traits and the acquisition of flowering competence (Pico et al., 2015, reproduced with permission from the American Society of Plant Biologists)

1.6 Role of phytohormones in potato development

1.6.1 Gibberellin

Gibberellins (GA) are known to stimulate stem elongation. It was shown that the high GA level favors stolon initiation (Vreugdenhil et al., 1989). The initiation of stolon swelling leading to tuber development is accompanied by a decrease in GA levels (Xu et al., 1998). Moreover, the treatment with GA leads to retardation in tuberization, whereas tuber formation was stimulated by treating the plant with GA biosynthesis inhibitors (Simko 1994, Jackson et al., 1996). GA_1 and its precursor GA_{20} are the essential GA forms shown to be involved in tuberization (Berg et al., 1995). Although many enzymes are involved in the biosynthesis of active GA from its precursor diterpene trans-geranylgeranyl diphosphate, the key enzyme responsible for the synthesis of GA_{20} precursors as well as GA_{20} is GA_{20} oxidase. Besides this, another important enzyme GA3-oxidase converts inactive GA metabolite GA_{20} into bioactive GA form (GA_1). On the other hand, inactivation of bioactive GA_{20} and GA_1 is performed by GA2oxidase converting them to inactive forms, GA29 and GA8, respectively (Hedden and Phillips, 2000). Three genes coding for GA20oxidase were detected from *S. tuberosum* ssp. andigena plant. Out of them, *StGA20ox1* was found to be expressed exclusively in leaves, and its levels increase in the presence of light and decrease during the dark period. In line with this, the overexpression of *StGA2ox1* delays and reduces tuber formation, whereas its suppression accelerates tuberization (Jackson et al., 2000). Besides this, the experiments that aimed to characterize the role of *StGA3ox2* in tuberization revealed that it has tissue-specific effects on tuber development (Bou-Torrent et al., 2011). The tuber specific expression of *StGA3ox2* delayed tuberization, whereas it's overexpression in leaves prompted early tuberization (Bou-Torrent et al., 2011).

1.6.2 Auxin

Detailed transcriptome analysis of potato carried out by Kloosterman et al. (2008) provided crucial insights about the role of auxin-related genes in tuber development. These authors showed that several auxin transport-related genes (PINs) and repressors AUX/IAA showed differential expression during the stolon-to-tuber transition. Besides this, levels of IAA increases during tuber initiation (Roumeliotis et al., 2012). Based on the previous findings, Roumeliotis and co-workers proposed a model describing the role of auxin in tuber development.

According to their model, during the initial stolon growth phase, GA levels remain high, and auxin levels remain relatively low to support the stolon elongation. During tuber-inducing SD conditions, the levels of auxin peak and GA levels go down. This leads to a change in the plane of cell division, the longitudinal growth of stolon ceases, and the sub-apical region of the stolon starts to swell. Interestingly, Dhonukshe et al. (2012) have also shown that in Arabidopsis, the change of plane in cell division is governed by auxins. This reinforces the idea that auxins play an important role in tuber development by governing meristem cell identity and changing the plane of cell division required for stolon-to-tuber transition.

1.6.3 Cytokinin

During the initial stages of tuber growth, cytokinin (CK) levels increases but reduces during tuber growth. Addition of CK (kinetin or Benzyl Amino Purine [BAP]) to culture medium also reduced the size of tubers produced on stem explants under *in vitro* conditions (Sarkar et al., 2006). Based on these results, it is quite clear that CK is attributed to stimulate cell division during early stages of tuber initiation, (Ewing, 1995, Falcon et al., 2006). A study by Mokronosov et al. (1990) showed that incoming CK from nearby roots to the stolon greatly enhances its capacity as a sink, thus helping in tuber growth. Another study by Eviatar-Ribak et al. (2013) demonstrated that overexpression of cytokinin biosynthesis gene, LOG1 stimulates tuber development from axillary nodes of above-ground stem of a tomato plant. This experiment further validated the important role of CK in tuber development.

1.6.4 Role of other phytohormones in tuberization

Besides GA, auxin, and CK, other plant growth hormones are also shown to affect the tuberization process. Abscisic acid (ABA) is shown to work antagonistically to GA during tuberization. In line with this, the levels of ABA increases during SD induction in *S. tuberosum* ssp. andigena (Macháková et al., 1998). A study by Pelacho et al. (1991) showed that another hormone, Jasmonic acid (JA), induces tuberization by changing the microtubule orientation in stolon (Matsuki et al., 1992). The effect of JA treatment is similar to that of GA inhibitors. Moreover JA treatment reverses the inhibitory effect of GA_3 on tuber formation. Besides JA, two more growth hormones, ethylene and Strigolactone, have an inhibitory effect on tuber development (Vreugdenhil et al., 1989; Roumeliotis et al., 2012). It was also shown that knockdown of the strigolactone biosynthesis gene, *StCCD8*, induces tuber formation (Pasare et al., 2013).

1.6.5 PRC2 mediated regulation of phytohormone signaling

Chromatin modifiers and phytohormones crosstalk with each other to regulate various plant developmental phenomena. Chromatin modifiers can regulate the expression of genes encoding for enzymes involved in phytohormone biosynthesis. On the other hand, phytohormone signaling can affect the expression of genes coding for histone modifiers. In the third scenario, both phytohormones and chromatin modifiers act on developmental pathway-related genes. (Maury et al. 2019). Meristematic regions of the plants have been shown as the hotspot of epigenetic regulation. For example, the key meristematic identity gene *WUSCHEL (WUS)* is regulated by DNA methylation, H3K27me3 modification, and cytokinin signaling (Dodsworth, 2009; Cao et al., 2015; Liu H. et al., 2018). Besides this, the other important stem cell identity maintaining factors, such as PLT1, PLT2, WOX4 or WOX5, are regulated through the PRC2 complex (Oh et al., 2008; Lafos et al., 2011). Expression of these factors is ectopically induced in PRC2 mutants (Chanvivattana et al., 2004; Ikeuchi et al., 2015; Mozgová et al., 2017). Auxin biosynthesis and signaling genes in shoot apex and leaves are also repressed by PRC2 members (Lafos et al., 2011). Whereas in Root Apical Meristem (RAM), the expression of auxin transporters, such as (PIN) genes, is repressed by PRC2 but activated by BRAHMA, resulting to the expression of PLETHORA genes involved in RAM specification (Yang et al., 2015). Besides regulating the biosynthesis and transport of phytohormones, histone modifiers are also involved in controlling the expression of phytohormone response genes. In one such example, PRC2 member MSI1 recruits the HISTONE DEACETYLASE 19 (HDA19) to repress the ABA-responsive genes (Mehdi et al., 2016). In line with this, plants with reduced levels of MSI1 or HDA19 demonstrate ABA-dependent growth defects, but improved drought tolerance. Additionally, a report by Liu et al. (2016) has revealed that in rice H3K27me3 reduction alters the levels of auxin, GA, ABA, and other hormones. All these examples clearly infer the role of chromatin modifiers on phytohormone signaling. However, there are reports that suggest that phytohormones in turn also regulate the expression of several histone modifiers, e.g. BRASSINAZOLE-RESISTANT 1 (BZR1), a brassinosteroid (BR) signaling factor antagonize the activity of H3K27me3 repressive modification by recruiting a H3K27me3-demethylase EARLY FLOWERING-6 (ELF-6), over a flowering repressor *FLC* to prevent flowering during the juvenile stage of the plant (Li et al. 2018).

1.7 Homeobox group transcription factors in potato development and their regulation by PRC members

Similar to animals, plant growth and development are also affected by the homeobox domain-containing transcription factors. Based on the expression pattern and domain similarity, *Knotted1-like Homeobox* (*KNOX*) genes in plants are categorized into three groups: *KNOX-I*, *KNOX-II,* and *mini-KNOX* (Magnani and Hake, 2008) Among them, *Class-I KNOX* genes play a most important role in plant development by regulating meristematic activity zones. They form a heterodimer with BEL1-like (BEL) proteins to execute their function. Both BEL and KNOX belong to the Three Amino Acid Loop Extension (TALE) superfamily, consisting of Proline-Tyrosin-Proline, which extends between the first and second helices of the homeodomain and helps in DNA-protein interaction (Burglin, 1997). Overexpression of *KNOX* genes resulted in ectopic meristem initiation and lobed leaf phenotype in Arabidopsis (Scofield et al., 2008, Hake et al., 2004) and potato (Mahajan et al., 2015) Additionally, a *class-I KNOX* gene (*POTH1*) overexpression has been shown to induce tuberization in potato (Rosin et al., 2003) by forming heterodimer with StBEL5 (Chen et al., 2004). This heterodimer binds to the promoter of *StGA20oxidase* and downregulates its expression, resulting in reduced GA levels (Chen et al., 2004). Besides StBEL5, two other BEL1-like members (StBEL11 and -29) have been implicated in the tuberization pathway (Ghate et al., 2017). The study by Ghate et al. (2017) has shown that individual overexpression of StBEL11 or -29 decreases belowground tuber yield, whereas their knockdown results in increased tuber yield.

Through a genome-wide target analysis approach, Zhang et al. (2007a) identified several *KNOX* gene family members that are regulated by PcG mediated H3K27me3 modification in arabidopsis. PcG proteins mediated *KNOX* genes regulation maintains the balance between stem cell renewal and their differentiation (Hay and Tsiantis, 2010). KNOX activity is required at the growing shoot tip, but they need to be repressed for lateral organ differentiation. Several studies have shown that *SHOOTMERISTEMLESS (STM)* a class-I KNOX member is regulated by polycomb-mediated H3K27me3 modification (Schubert et al., 2006; Zhang et al., 2007b). Besides *STM*, other KNOX members *BREVIPEDICELLUS (BP)* and *KNAT2* are also targeted by PcG members in seedling and root, respectively (Xu and Shen, 2008). Further, it was shown that

two DNA binding proteins ASYMMETRIC LEAVES1 (AS1) and AS2 physically interact with core components of PRC2 and recruit them to *BP* and *KNAT2* loci (Lodha et al., 2013*b*).

1.8 Challenges and open questions

With the advancement in technologies, the epigenetic studies involving chromatin modification and their impact on gene expression have become quite easier. However, many times, Chromatin Immunoprecipitation (ChIP) studies are necessary for experiments aiming to characterize the histone modifiers. The suitable antibody against particular histone modification and histone modifiers is often a challenging aspect of such studies. Unlike animals, plants cells are protected by a cell wall that poses a challenge to carry-out chromatin immunoprecipitation and requires standardization for the plant to plant and even between different tissue types. Moreover, the high cost of sequencing services involved in ChIP-sequencing limits the number of samples a researcher can proceed with. The downstream bio-informatic analysis of ChIP-seq data alignment requires the availability of a reference genome sequences.

1.8.1 Open questions

A number of studies have revealed the role of histone modifications in plant development. Several studies on Arabidopsis mutants have unraveled the important histone modifiers involved in various developmental events in plants. However, we are still far from understanding how epigenetic modifiers are regulated. Identifying the upstream signaling pathway involved in the regulation of the chromatin modifications will be a fascinating part of epigenetic studies.

Studies have shown the effect of an environmental conditions, such as temperature and photoperiod on chromatin-based gene regulation. The role of polycomb genes in regulating the *FLC* based vernalization memory to control the onset of flowering in Arabidopsis suggests that similar regulation might be involved in other environmentally controlled developmental events in plants. It would be interesting to study the mechanisms through which environmental signals are integrated and converted to an epigenetic response. Moreover, the genetic diversity between different ecotypes of a species is a crucial factor for their adaption and survival in that particular habitat. However, the role of epigenetic modifications in this process is still not clear. It would

be interesting in the future to study the epigenetic variation between different ecotypes and their effect on plants' performance under varying environmental conditions.

The recent findings that DNA sequences, such as Polycomb Response Elements (PREs), helps in the recruitment of polycomb and trithorax members over the target sites, indicate the cross-talk between both processes (Xiao et al.2017, Roy et al. 2019). On the other hand, the changes in chromatin architecture through histone modification can affect the genetic rearrangements, such as DNA recombination events, causing permanent effect in the nucleotide sequence (Paszkowski and Grossniklaus, 2011). Understanding the relationship between genetic codes and their role in controlling the gene expression through the epigenetic modifiers is an open field to explore.

1.9 Potato *(Solanum tuberosum* ssp. *andigena)* as a model system

Potato, *Solanum tuberosum* L, is considered an important food crop in terms of calories generated per acre and holds strong promise to ensure food security for a rapidly growing human population. A potato tuber is formed from the below-ground modified stem, known as the stolon (Jackson, 1999). Potatoes were first originated in South America, where day-lengths are close to 12 hours (short days, SD) with low night temperatures. Wild Andean varieties are adapted to such conditions and are unable to tuberize under long days (LD) (day lengths > 12 hours). Under inductive SD conditions, the tuberization signals travel from leaf to stolon and orchestrate a series of developmental events beginning from swelling of stolon to the development of a mature tuber (Xu et al., 1998a) (Figure 1-9). With the availability of recently published genome sequence (Xu et al., 2011) and efficient transformation protocol (e.g., Banerjee et al. 2006b), it is now possible to conduct functional genetic studies and characterize the role(s) of the gene(s) of interest. Potato as a model system thus provides the researchers with a unique opportunity to understand how environmental signals, such as light, temperature, and photoperiod, affect the below-ground organ development. Although the role of PcG proteins is well studied in model plant species like Arabidopsis, their role in potato development is still unknown. Given the economic importance of potato as a food crop and having the characteristic photoperiod-dependent stolon-to-tuber fate transition, we choose *Solanum tuberosum* ssp. *andigena* as a model system to understand the role of PcG proteins in potato development in the photoperiod-dependent pathway.

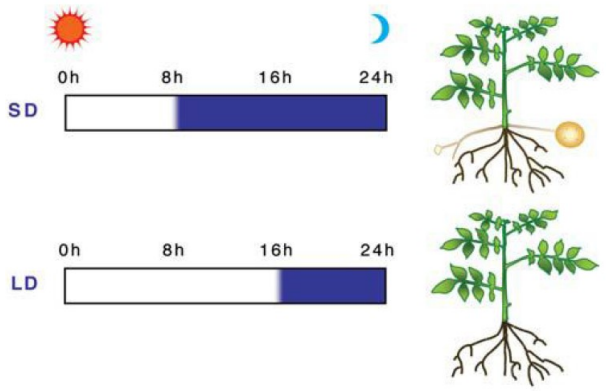

Figure 1.9. **Photoperiod-dependent tuberization in *Solanum tuberosum* ssp. andigena**. Long photoperiod inhibits tuberzation, whereas a short photoperiod promotes stolon to tuber transition. (Rodriguez-Falcon et al., 2006, reproduced with permission from Annual Reviews, Inc.)

1.10 Hypothesis and objectives

A literature survey suggested that the photoperiod-dependent flowering in Arabidopsis and tuberization pathways in potato share several common molecular components, such as FT homolog StSP6A and miR156. (Navarro et al., 2011, Bhogale et al., 2014). Moreover, both FT and miR156 coding loci are shown to be epigenetically regulated through PcG proteins during the flowering process (Jiang et al. 2008, Pico et al. 2015). Although, several studies in the past have identified a group of transcription factors, including full-length mobile mRNAs (Banerjee et al., 2006a; Mahajan et al. 2012), microRNAs (Martin et al., 2009; Bhogale et al., 2014 the role of epigenetic modifiers in tuberization mechanism in potato remains unexplored. Based on the role of PRC proteins in flowering pathways, we hypothesized that PRC1 and PRC2 members might be playing crucial roles in governing potato development. To validate the hypothesis, we set the following objectives:

1. To investigate the role of StMSI1 (a PRC2 member) and StBMI1-1 (a PRC1 member) in potato and identify their target genes (Chapter 2).

2. Functional characterization of StE(z)2 (a H3K27 methyltransferase) as a potential epigenetic regulator in potato (Chapter 3).

3. Identification of the direct targets of StE(z)2 and the genome-wide occupancy of histone modifications during stolon-to-tuber development in potato (Chapter 4).

Chapter 2

Investigating the role of StMSI1 (a PRC2 member) and StBMI1-1 (a PRC1 member) in potato and target genes identification

2.1 Introduction

Plants sense multiple environmental cues, such as temperature, light, and nutrient availability, and synchronize developmental programs accordingly. Photoperiod is one such environmental cue that plays an important role during tuber development (tuberization) in potato (*Solanum tuberosum* ssp. *andigena*). During tuberization, the stolon (a modified below-ground stem) passes through various developmental stages and matures into a potato under short-day (SD) condition. Apart from phytohormones (auxin, cytokinin, and gibberellin; Xu et al., 1998), phytochromes, flowering genes (CONSTANS [CO]; Martinez-Garcia et al., 2002), a number of mobile signals, including mRNAs (*StBEL5*, *-11*, *-29*, and *POTH1*; Banerjee et al., 2006a, Mahajan et al., 2012, Ghate et al., 2017), miRNAs (miR172 and miR156; Martin et al., 2009, Bhogale et al., 2014) and a Flowering Locus T (FT) orthologous protein StSP6A (Navarro et al., 2011) are now known to regulate tuberization. Earlier, we showed that miR156 levels increase in stolon under tuber-inducing SD photoperiodic conditions, and its overexpression led to aerial tuber formation in potato (Bhogale et al., 2014). However, the basis for aerial tuber formation and what regulates miR156 under short-day conditions is not known. Previous studies in Arabidopsis (*Arabidopsis thaliana*) revealed that Polycomb Group (PcG) proteins mediate the repression of several miRNAs (Lafos et al., 2011), including miR156 and miR172 (Pico et al., 2015).

PcG proteins are important regulators of growth and development across eukaryotic lineages. They were first identified in Drosophila as multiprotein complexes, termed as Polycomb Repressive Complex 1 (PRC1) and PRC2. The PRC1 complex in Drosophila contains four members, namely Polycomb (Pc), Polyhomeotic (Ph), Posterior sex comb (Psc), and dRING1 proteins (Shao et al., 1999; Peterson et al., 2004). They repress target chromatin by H2A mono-ubiquitination (Cao et al., 2005). Arabidopsis has three homologs of Psc (AtBMI1A, AtBMI1B, and AtBMI1C) and two homologs of dRING1 (AtRING1A, and AtRING1B; Calonje, 2014). BMI assists in activity of E3 ubiquitin ligases that monoubiquitylate histone H2A at lysine 119 position leading to the repression of target genes. A recent study in Arabidopsis has shown that BMI1 regulates meristem maintenance and cell differentiation by repressing *PLETHORA (PLT)* and *WUS homeobox-containing* (*WOX*) genes (Merini et al., 2017). Further, BMI1 mutants show downregulation of important flowering genes, like *SQUAMOSA PROMOTER BINDING PROTEIN-LIKE* (*SPL*) and *FT*, indicating an important role in the

flowering response. To avoid precocious flowering, *SPLs* are suppressed by miR156 during the juvenile phase of plants. However, during adult and reproductive phases, miR156 expression is suppressed by BMI1 to allow the expression of *SPLs* (Merini et al., 2017). The core PRC2 complex in Drosophila consists of four subunits, namely Enhancer of Zeste [E(z)], Suppressor of Zeste 12 [Su(z)12], Extra sex combs (Esc), and p55. The [E(z)] protein represses target genes by catalyzing H3K27me3 modification of these genes (Müller et al., 2002), whereas p55 helps in the recruitment of PRC2 complex to target chromatin. Arabidopsis has five p55 homologs named MSI1-5 (Henning et al., 2005). They belong to the WD-40 repeat-containing protein family and have seven Tryptophan Aspartate (WD) repeats with four antiparallel β-sheets at the C-terminal end that assists in its interaction with other proteins. A previous report on MSI1 in Arabidopsis showed that it regulates overall plant architecture and ovule development (Henning et al., 2003). Subsequent studies also revealed that MSI1 is a component of several histone modifier complexes that regulate different phases of plant development. It is a part of three PRC2 complexes, known as FERTILIZATION INDEPENDENT SEED (FIS) complex that regulates seed development (Kohler et al., 2003), EMBRYONIC FLOWER (EMF) complex that suppresses flowering during juvenile stage (Yoshida et al., 2001), and VERNALIZATION (VRN) complex, which is essential for the onset of flowering after vernalization (De Lucia et al., 2008). Additionally, MSI1 is also a part of CHROMATIN ASSEMBLY FACTOR1 (CAF-1; Exner et al., 2006), nucleosome-remodeling factor (NURF; Martinez-Balbas, 1998), and histone deacetylase (HDAC; Mehdi et al., 2016), indicating its diverse role in plant development. MSI1 also promotes flowering in Arabidopsis in a photoperiod-dependent manner by assisting in the expression of *CO* and *SUPPRESSOR OF CO* (*SOC1*) through H3K4 methylation and H3K9 acetylation over *SOC1* locus (Bouveret et al., 2006; Steinbach and Hennig, 2014).

Tuberization and flowering are two reproductive phenomena that share common molecular players and environmental cues (Martinez-Garcia et al., 2002). Considering the PcG proteins' role in flowering, we hypothesize that they might govern tuber development in potato. In an experiment, we observed that overexpression of *StMSI1* produced aerial stolons and tubers under SD photoperiodic conditions from axillary-nodes, a phenotype that was demonstrated earlier for miR156 overexpression in potato (Bhogale et al., 2014). This raised a number of interesting questions with respect to the function of PcG proteins in potato, such as (i) what is the cause of aerial stolon and tuber development from axillary-nodes? (ii) Do PcG proteins have any

role in photoperiod-mediated control of tuberization? and (iii) Is miR156 directly regulated by StMSI1, or there are other epigenetic modifiers that could regulate miR156? In this study, using several approaches, such as overexpression or knockdown of two PcG proteins StMSI1 and StBMI1-1, RNA-sequencing analysis of axillary-nodes of *StMSI1* overexpression and *StBMI1-1* knockdown lines, homo- and hetero-grafting and ChIP-qPCR method, we established that StMSI1 and StBMI1-1 function upstream of miR156 to regulate aerial tubers in potato under SD photoperiodic conditions.

2.2 Materials and Methods

2.2.1 Plant material and growth conditions

Potato cultivar (*Solanum tuberosum* ssp. *andigena* 7540), which tuberizes under short-day (SD) conditions (16 h dark/8 h light), but not under long-day (LD) conditions (16 h light/8 h dark), was used throughout this study. Wild-type (WT) *andigena* plants were propagated by sub-culturing nodal stem explants in Murashige and Skoog's basal medium (Murashige and Skoog, 1962) supplemented with 2% (w/v) sucrose. *In vitro* plants were maintained in a plant growth incubator (Percival Scientific) at 22 °C and light intensity of 300 μmol m^{-2} s^{-1} under LD conditions unless mentioned otherwise.

2.2.2 Phylogenetic analysis

A phylogenetic tree was constructed for putative MSI-like protein sequences from Arabidopsis, potato, tomato, rice, Selaginella, Physcomitrella, and Chlamydomonas using T-COFFEE (hRp://www.ch.embnet.org/soaware/TCoffee.html) and graphical representation was performed with TreeDyn (v198.3) (Dereeper et al., 2008). Similarly, a phylogenetic tree was also prepared for putative BMI1 orthologs from potato, tomato, and Arabidopsis. For both gene families, the full-length amino acid sequences were used to build the phylogenetic trees.

2.2.3 MSI1 and BMI1-like proteins in potato

StMSI1 protein structure, as well as the position of WD repeats in the protein sequence, were predicted using WD-repeat protein structure predictor (WDSP) tool developed by Wu et al. (2012). The binding partners of potato StMSI1 were predicted using the STRING database (Szklarczyk et al., 2017). Web CD Search Tool

(https://www.ncbi.nlm.nih.gov/Structure/bwrpsb/bwrpsb.cgi) was used to identify conserved domains in BMI1 proteins from Arabidopsis, tomato, and potato. Domain schematics were drawn using DOG2.0 software (Ren et al., 2009) and edited manually. Genomic location of putative MSI and BMI1 orthologs in potato were retrieved from Spud DB Genome Browser in the PGSC database (http://solanaceae.plantbiology.msu.edu/cgi-bin/gbrowse/potato). Gene Structure Display Server (GSDS) (http://gsds.cbi.pku.edu.cn) was used for visualization of gene features, e.g. position of introns, exons, and conserved domains in four potato BMI1 proteins.

2.2.4 Tissue-specific transcript abundance under SD and LD conditions

For investigating the influence of photoperiod on the tissue-specific expression of *StMSI1* and *StBMI1-1*, *in vitro* grown wild-type *andigena* plants were transferred to soil and maintained under LD photoperiod with 300 µmol m^{-2} s^{-1} light intensity for a period of ten weeks (until attained 10-12 leaf stages) in a growth chamber (Percival Scientific, Inc.). Later, half of the plants were transferred to tuber-inducing SD photoperiodic conditions for 14 days, while the remaining plants were maintained under LD conditions. Different tissues (shoot tip, leaf, stem, root, and the stages of stolon-to-tuber transitions) were harvested at 14 days post LD/SD induction in triplicates between Zeitgeber time ZT=2 to ZT=4. Total RNA was isolated using RNAiso Plus (DSS TAKARA) as per the manufacturer's instructions. cDNA synthesis was carried out using two µg of total RNA, Superscript IV Reverse Transcriptase (SSIV-RT, Invitrogen) and Oligo dT primers. qPCR reactions were performed on a CFX96 Real-Time System (BIO-RAD) with gene-specific primers (Supplemental Table S11). The reactions were carried out using TAKARA SYBR® green master mix (Takara-Clontech) and incubated at 95 °C for 30 s, followed by 40 cycles at 95 °C for 5 s, gene-specific annealing temperature for 15 s and extension for 72 °C for 15 s. PCR specificity was checked by melting curve analysis, and data were analyzed using the $2^{-\Delta\Delta Ct}$ method (Livak and Schmittgen, 2001).

2.2.5 Generation of constructs and potato transgenic lines

To generate constitutive overexpression (OE) constructs, full-length coding sequences (CDSs) of *StMSI1* (1368 bp) and *StBMI1-1* (1292 bp) were amplified by RT-PCR from *in vitro* grown *andigena* plants using primers listed in Supplemental Table S11. PCR amplified sequences were mobilized into binary vectors, pBI121 and pCB201 (respectively) downstream of

the CaMV 35S promoter (Xiang et al., 1999). A respective non-conserved sequence from the sense strand was used to design antisense (AS) constructs for both *StMSI1* and *StBMI1-1* genes. PCR amplified fragments (584 bp for *StMSI1*, whereas 357 bp for *StBMI1-1*) were cloned in antisense directions into the binary vectors pBI121 and pCB201 (respectively) driven by the CaMV 35S promoter. *StMSI1* and *StBMI1-1* overexpression constructs were referred as *35S::StMSI1-pBI121 (StMSI1-OE)* and *35S::StBMI1-1-pCB201 (StBMI1-1-OE)* respectively, whereas their antisense constructs were referred as *35S::StMSI1-AS-pBI121* (*StMSI1-AS*) and *35S::StBMI1-1-AS-pCB201* (*StBMI1-1-AS*). The *StMSI1* promoter sequence (1544 bp) was amplified from *andigena* genomic DNA (Supplemental Table S11) and cloned into a binary vector pBI121 upstream of the β-glucuronidase gene (uidA) to generate the *promStMSI1::GUS-pBI121* construct. MicroRNA156 overexpression construct (miR156-OE) is from the previous study from our lab (Bhogale et al., 2014). All six types of binary constructs were transformed into *Agrobacterium tumefaciens* strain GV2260 and transgenic potato lines were generated as per the method described in Banerjee et al. (2006b). Transgenic *andigena* line containing *35S::GUS* construct was used as a vector control (VC) in the study. Several phenotypic characters (plant height, internodal distance, leaf length, leaflet number per leaf, root length, tuber numbers, root and tuber biomass yields) were recorded after four weeks of LD/SD inductions.

2.2.6 Analysis of *StMSI1* promoter activity

StMSI1 promoter transgenic lines (*promStMSI1:: GUS-pBI121*) were grown *in vitro* under LD conditions for 20 days. Promoter lines were also transferred to soil and subjected to LD/SD induction for 15 days. Entire *in vitro* grown plantlets as well as stolon and tuber samples from LD/SD-induced soil-grown plants were used for GUS assay. The protocol described in Jefferson (1987) was followed. After overnight incubation at 37 °C, samples were bleached with a series of ethanol gradients (50 to 100%, v/v) and photographed under a Leica stereo microscope (S8APO).

2.2.7 Histology and scanning electron microscopy

For anatomical studies, a modified protocol of Cai and Lashbrook (2006) was followed on leaf and stem tissues of eight weeks old LD grown (*StMSI1-OE3* and WT) plants. Ten micrometers (10 μm) sections were obtained using Microtome (Leica), cleared with xylene, and

photographed under a Zeiss compound microscope. External leaf architecture of transgenic and WT plants was documented using a Quanta 200 3D eSEM apparatus (FEI), under environmental mode (eSEM).

2.2.8 *In vitro* tuberization

In vitro tuberization experiment was conducted as per the previous report of Prematilake and Mendis (1999) with minor modifications. Shoot apex (2-3 cm) of WT, VC, and five types of transgenic *andigena* lines - *StMSI1-OE* (OE3); *StMSI1*-AS (AS8), *StBMI1-1*-OE (#II-9), *StBMI1-1-AS* (#G9), and miR156-OE, were sub-cultured on MS medium containing 2% (w/v) sucrose and 0.2% (w/v) phytagel, and grown *in vitro* for four weeks under LD conditions. Single-node explants from the middle region of individual shoots were further cultured on MS medium with 8% (w/v) sucrose (induction medium) and incubated for four weeks. Twelve independent plants for each line were recorded for the number of tubers formed up to a period of 4 weeks.

2.2.9 RNA-seq analysis

For RNA-sequencing, *35S::StMSI1-OE* (OE3), *35S::StBMI1-1-AS* (#G9), and *35S::GUS* (VC) lines were grown in soil for 12-weeks under LD conditions and subjected to SD induction for another 3 weeks (until the aerial stolon initiation starts in OE3 and #G9 lines). Axillary-nodes (5 mm length) containing a part of the stem from either end of the node was harvested between ZT=2 to ZT=4 from six independent plants per line. All the nodes were harvested from the upper half of the plant. Samples were pooled from 2 to 3 plants, forming either two or three biological replicates per line. The total RNA was isolated using RNAiso Plus., RNA concentration and purity were measured using Qubit® RNA Assay Kit in Qubit®4.0 Flurometer (Life Technologies, CA, USA) and RNA Nano 6000 Assay Kit of the Bioanalyzer 2100 system (Agilent Technologies, CA, USA). Total RNA (3 μg per sample) was used as input material for the sample preparations. Sequencing libraries were generated using NEBNext® UltraTM RNA Library Prep Kit for Illumina® (NEB, USA), and index codes were added to attribute sequences to each sample. The library quality was assessed using an Agilent Bioanalyzer 2100 system. The clustering of the index-coded samples was performed on a cBot Cluster Generation System using TruSeq PE Cluster Kit v3-cBot-HS (Illumina). After cluster generation, the library preparations

were sequenced on an Illumina Hiseq platform, and 150 bp paired-end reads were generated.

The reads were aligned to the potato reference genome (PGSC_DM_v3.4_gene.fasta.zip) using alignment software - STAR (version 2.6.1c; Dobin et al., 2013). Downstream differential expression analysis of aligned reads was done using Tuxedo suite tools (Tarpnell et al., 2013), based on the protocol of Mahajan et al. (2016). Gene Ontology (GO) analysis was performed using Blast2GO software v1.3.3 for functional annotation of differentially expressed genes (Conesa et al., 2005; Götz et al., 2008), as described previously by Mahajan et al. (2016). Validation of select target genes identified in the RNA-seq analysis was done using qPCR as described above. The list of primers used is provided in Supplemental Table S11.

2.2.10 RLM-RACE assay

To map the cleavage site of miR156e/f-5p on *StSPL13* transcript, a modified 5' RLM-RACE (RNA Ligase-Mediated Rapid Amplification of Complementary DNA Ends) was carried out using the First Choice RLM-RACE kit (Ambion) as described previously (Bhogale et al., 2014).

2.2.11 ChIP-qPCR analysis

Chromatin immunoprecipitation (ChIP) was performed on potato leaves from *35S::GUS (VC)*, *StMSI1-OE3,* and *StBMI1-1-AS*#G9 plants using the reagents and protocol provided in Diagenode's universal plant ChIP-Seq kit **(**Cat. No. C01010152) as per the manufacturer's instructions. The sheared chromatin was immunoprecipitated using the DiaMag protein A-coated magnetic beads and one µg of either anti-H3K4me3 (Diagenode, Cat. No. C15410003), anti-H3K27me3 (Abcam, Cat. No ab6002) or anti-IgG antibody (Diagenode, Cat. No. C15410206), in each reaction. Finally, eluted DNA was used for subsequent qPCR analysis using gene-specific primers (Supplemental Table S11).

2.2.12 Identification of Light Regulatory Elements (LREs), Polycomb Response Elements (PREs), and BMI-binding sites

The 1.5 kb promoter sequences of *StMSI1*, all eleven miR156 members (miR156a-k), and three *StBMI1* genes (*StBMI1-2, -3* and *-4*) were searched for the presence of light regulatory elements (LREs) using PlantCARE tool (Lescot et al., 2002). Polycomb response elements (PREs; Xiao et

al., 2017) and BMI-binding sites (Merini et al., 2017) were also searched in the promoters of miR156 members using RSAT tool (van Helden 2003; Nguyen et al., 2018). PREs were also identified in the promoters and gene bodies of *StBMI1*. As the promoter sequence of the *StBMI1-1* gene is not annotated in potato, LREs and PREs were identified from the 5' UTR region (298 bp) of its transcript sequence.

2.2.13 Grafting

WT, *StMSI1-OE*, and *StBMI1-1-AS* lines were maintained *in vitro* on MS medium for one month under LD conditions. Three combinations of homo- (WT/WT; StMSI1-OE/StMSI1-OE, and StBMI1-1-AS/StBMI1-1-AS) and four types of hetero-grafts (StMSI1-OE/WT, StBMI1-1-AS/WT, WT/ StMSI1-OE, and WT/StBMI1-1-AS) were made under *in vitro* conditions as per the protocol described earlier with modifications (Banerjee et al., 2006a). After one week of *in vitro* incubation, successful grafts were again transferred to MS medium containing 2% (w/v) phytagel and cefotaxime (250 mg/L) and allowed to grow for additional two weeks under LD conditions. Three weeks after grafting, an average number of roots, root length (cm), and biomass (gram fresh weight) were recorded, and tissues were harvested for further evaluation.

2.2.14 Statistical Analysis

Throughout the experiments, Student's t-test was performed to check significance with one, two, three, and four asterisks indicating p-values of < 0.05, < 0.01, < 0.001, and < 0.0001, respectively. Error bars represent ± standard deviation (SD).

Accession Numbers

Accession numbers used in this study are listed in Supplemental Table S12, and also provided at the end of the Thesis.

2.3 Results

2.3.1 Phylogenetic analysis revealed conservation of MSI1- and BMI1-like proteins in potato

BLAST results revealed ~91% identity between potato MSI1-like protein (StMSI1; XP_006349413.1) and Arabidopsis MSI1 (AtMSI1; NP_200631.1) (Figure – 2.1). From the PGSC database, we observed that the *StMSI1* gene (~5.20 kb) resides on chromosome 1. Its longest open reading frame spans 1368 bp and encodes for 425 amino acid residues (48.36 kDa protein). Using WD-repeat protein structure predictor tool, we could identify seven WD repeats in StMSI1 protein, positioned between amino acids 33 and 403 (Figure – 2.1 C). Further analysis revealed the presence of 14 hotspot residues in the StMSI1 protein sequence that are likely to be involved in protein-protein interactions (Figure 2.1 B). Arabidopsis MSI2 and MSI3 proteins match with potato nucleosome/chromatin assembly factor (StMSI2) and share about 68% identity (Figure 2.1 A). Like StMSI1 protein, StMSI2 also has seven WD repeats, and it shares 57% sequence similarity with StMSI1.

In contrast, other MSI-like proteins from Arabidopsis showed less conservation with potato proteins (Figure 2.2A). STRING tool analysis predicted that StMSI1 could interact with a range of proteins, including other PRC proteins, Chromatin Assembly Factor (CAF), histone acetylases, and deacetylases (Figure 2.2B).

In potato, four BMI1 proteins (StBMI1-1, -2, -3, and -4) have been identified, and they share about 55, 50, 45, and 32% sequence identity with Arabidopsis BMI1a, respectively. When potato BMI1 proteins were analyzed for conserved domains, we found that a cysteine-rich RING domain involved in zinc binding and the ubiquitination process is present in StBMI1-1, -2, and -4 similar to Arabidopsis BMI1 proteins (AtBMI1a, -1b and -1c), but this domain was absent in StBMI1-3 (Figure 2.4).

Arabidopsis BMI1 proteins also have a RAWUL domain (ubiquitin-like domain likely to be involved in protein-protein interactions), however, this domain is absent in potato or tomato BMI1 homologous proteins. StBMI1-4 has an additional RAD18 domain, which is a putative nucleic acid binding domain (Figure 2.4). From the PGSC database, we found that the *StBMI1-1* gene was located on chromosome 9, *StBMI1-2,* and *-3* genes on chromosome 6, and the *StBMI1-4* gene is on chromosome 1 (Supplemental Table S1). Phylogenetic analysis indicated that

StBMI1-1, StBMI1-2, and StBMI1-3 displayed close conservation to respective tomato BMI1 proteins, whereas StBMI1-4 had close conservation to AtBMI1c (Figure 2.3).

(A)

```
AtMSI       MGKDEEEMRGEIEERLINEEYKIWKKNTPFLYDLVITHALEWPSLTVEWLPDREEPSGKD   60
StMSI1      MGKDEDEMRGEIEERLINEEYKIWKKNTPFLYDLVITHALEWPSLTVEWLPDREEPSGKD   60
StMSI2      MAEEEMEAAGET-EQEVEEEFAVWKKNTPLLYDLVVCHALEWPSLTVQWLPSPTIDD-GA   58
            *.::* *  **  *: ::**: :******:*****: **********:***.    .

AtMSI       YSVQKMILGTHTSESEPNYLMLAQVQLPLDDIESEARQYDDDRSEFGGFGCATGKVQIIQ   120
StMSI1      YSVQKMILGTHTSENEPNYLMLAQVQLPLEDAENDARHYDDDRSEFGGFGCANGKVQIIQ   120
StMSI2      FAVHKLILGTHTSDDCPNFLMVANVHLPRNPASGLEH---------NLMNPQIPKVEIVQ   109
            ::*:*:*******:. **:**:*:*:** : :..  :         . :.    **:*:*

AtMSI       QINHDGEVNRARYMPQNPFIIATKTVNAEVYVFDYSKHPSKPPLDGACNPDLKLRGHSSE   180
StMSI1      QINHDGEVNRARYMPQNPFIIATKTVSAEVYVFDYSKHPSKPPLDGACNPDLRLRGHSTE   180
StMSI2      KIHVDGEVNRARCMPQKPAVVAAKTSSSEVYVFDSAKQPLD-HEGGSCNPDVRLRGHDKE   168
            :*: ******** ***:* ::*:** .:****** :*:* .   .*:****::****..*

AtMSI       GYGLSWSKFKQGHLLSGSDDAQICLWDINATPKNKSLDAQQIFKAHEGVVEDVAWHLRHE   240
StMSI1      GYGLSWSQFKQGHLLSGSDDAHICLWDINATPKNKALEAMQIFKVHEGVVEDVAWHLRHE   240
StMSI2      GYGLSWSPFKEGFLLSGSNDQKICLWNVSALPQDKVLMAHHTYEEHEDVVEDVSWHPKNE   228
            ******* **:*.*****:* :****::.* *::* * * : :: **.*****:** ::*

AtMSI       YLFGSVGDDQYLLIWDLRSPSASKPVQSVVAHSMEVNCLAFNPFNEWVVATGSTDKTVKL   300
StMSI1      YLFGSVGDDQYLHVWDLRTPSVTKPIQSVVAHQSEVNCLAFNPFNEWVVATGSTDKTVKL   300
StMSI2      NLFGSVGDDCRLIIWDLRTNK---AQQSVLAHEKEVNYLSFNSYTEWVLATASSDSTVGL   285
             ********  * :****: .     ***:**. *** *:** :.***:**.*:*.** *

AtMSI       FDLRKLSTALHTFDSHKEEVFQVGWNPKNETILASCCLGRRLMVWDLSRIDEEQTVEDAE   360
StMSI1      FDLRKISTALHTLDCHKEEVFQVGWNPKNETILASCCLGRRLMVWDLSRIDEEQTPEDAE   360
StMSI2      FDMRKLSSPLHVFGSHTDEVFQVEWDPNHETVLASSGGDRRLMVWDLNRIGDEQLEGEAE   345
            **:**:*: **.:..*.:***** *:*::**:***.  .********.**.:**   :**

AtMSI       DGPPELLFIHGGHTSKISDFSWNPCEDWVISSVAEDNILQIWQMAENIYHDEDDAPGEEP   420
StMSI1      DGPPELLFIHGGHTSKISDFSWNPCEDWVVASVAEDNILQIWQMAENIYHDEDDLPGDDP   420
StMSI2      DGPSELLFSHGGHKAKISDFSWNKNEAWVISSVAEDNCVQVWQMAESIYREDNDNGNC*-   403
            *** **** ****.:********  * **::****** :*:*****.**::::*  .

AtMSI       SKAS-       424
StMSI1      PKGP*       424
StMSI2      -----       403
```

(B)

Repeats	Score	Start	End	Hotspots_on_the_top_face
WD1	34.18	33	116	L45
WD2	81.28	117	168	E127 N129
WD3	122.27	169	217	E180 Y182 D199
WD4	121.70	218	263	E231 D248
WD5	120.22	264	307	E275 N277
WD6	125.63	308	364	E319 F321
WD7	119.60	365	403	K376 E395

(C)

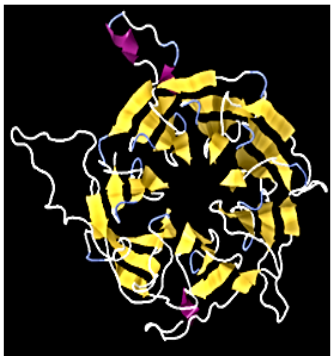

Figure 2.1. Conservation between Arabidopsis MSI1 and potato MSI proteins. (A) Amino acid alignment of Arabidopsis MSI1 (AtMSI1) with two potatoes MSI proteins (StMSI1 and StMSI2). Alignment was done using a Clustal Omega program. Two domains, such as histone-binding protein RBBP4 or subunit C of CAF1 complex (19-88 aa) and WD40 super family (124-404 aa), are highlighted in yellow and cyan, respectively. (B) List of WD repeats in AtMSI1, and StMSI1 proteins are shown as per the prediction by the WDSP tool along with the protein structure of StMSI1 (C) showing 14 hotspot residues on the top surface of the protein structure.

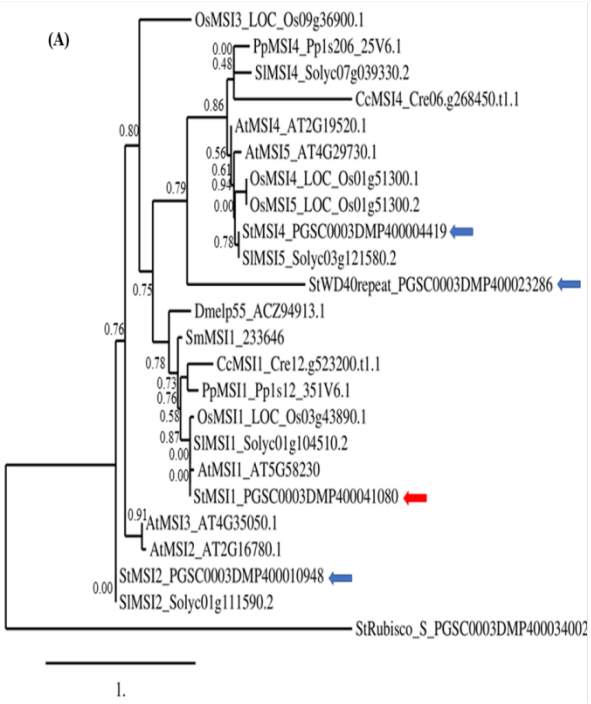

Nodes	Annotation
PGSC0003DMT400023342	EZ1
PGSC0003DMT400030280	Conserved gene of unknown function
PGSC0003DMT400046818	Histone deacetylase
PGSC0003DMT400049479	Fertilization-independent endosperm protein
PGSC0003DMT400061016	WD-40 repeat-containing protein MSI1
PGSC0003DMT400068240	Histone deacetylase
PGSC0003DMT400069419	HDA6 (HISTONE DEACETYLASE 6); histone deacetylase
PGSC0003DMT400073807	Chromatin assembly factor I P60 subunit
PGSC0003DMT400076252	Histone deacetylase
PGSC0003DMT400083511	Histone acetyltransferase type B catalytic subunit
PGSC0003DMT400084490	EZ2

Figure 2.2. Phylogenetic map and binding partners of StMSI1 protein. (A) Phylogenetic tree for MSI-like proteins. The deduced amino-acid sequences of MSI-like proteins from Arabidopsis, potato, tomato, rice, Selaginella, Physcomitrella, and Chlamydomonas were analyzed. Rubisco small subunit (a potato non-MSI related protein) amino-acid sequence was included to root the tree. Phylogenetic analysis was performed using T-COFFEE (hRp://www.ch.embnet.org/soaware/TCoffee.html), and graphical representation was performed with TreeDyn (v198.3). Accessions for protein sequences used are written after protein names in the phylogenetic tree. In the phylogenetic tree, the branch length is proportional to the number of substitutions per site, and the tree is rooted using midpoint rooting in TreeDyn. StMSI1 protein from potato is shown by the red arrow, whereas other potato MSI proteins are highlighted by blue arrows. (B) Prediction of binding partners of StMSI1 protein using the STRING program with transcript IDs. Abbreviations used: St, *Solanum tuberosum*; Sl, *Solanum lycopersicum*; At, *Arabidopsis thaliana*; Dmel, *Drosophila melanogaster*; Cc, *Chlamydomonas caudata*; Os, *Oryza sativa;* Sm, *Selaginella moellendorffii*

2.3.2 Short-day (SD) photoperiod influences *StMSI1* expression in stolon and root tissues

qPCR analysis showed a significant increase of *StMSI1* transcript abundance in stolons under short-day (SD) than long-day (LD) photoperiodic conditions (Figure 2.6A). However, its transcript level was significantly lower in roots (Figure 2.6A) and mature tubers (Figure 2.5A) under SD compared to LD. The expression of *StMSI1* remains unchanged in shoot tip, leaf, and stem under SD compared to LD conditions (Figure 2.6A). From the RNA-sequencing data available in the PGSC database (Xu et al., 2011), it was further evident that three *StMSI* genes

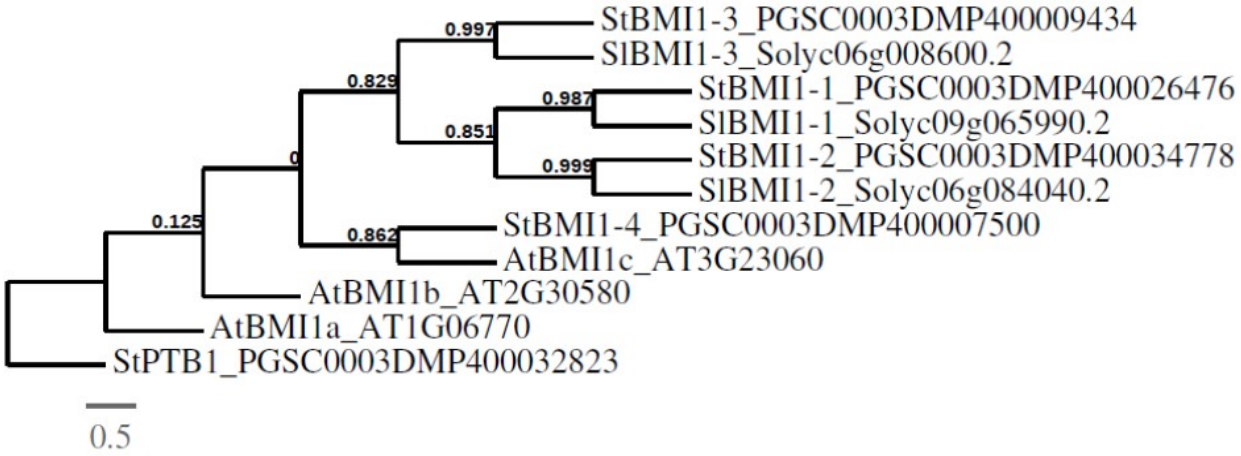

Figure 2.3. Phylogenetic relationship of BMI1 like proteins. The deduced amino-acid sequences of BMI1 proteins from potato, tomato, and Arabidopsis were analyzed. StPTB1 (a potato non-BMI1 related protein) amino-acid sequence was included to root the tree. Phylogenetic analysis was performed using T-COFFEE (hRp://www.ch.embnet.org/soaware/TCoffee.html), and graphical representation was performed with TreeDyn (v198.3) [41]. Accessions for protein sequences used are written after protein names in the phylogenetic tree. In the phylogenetic tree, the branch length is proportional to the number of substitutions per site, and the tree is rerooted using midpoint rooting in TreeDyn. St, *Solanum tuberosum*; Sl, *Solanum lycopersicum*; At, *Arabidopsis thaliana*.

(*StMSI1*, *StMSI2*, and *StMSI4*) are highly expressed in the stolons, but their expression is reduced in mature tubers and roots (Figure 2.5B). In order to characterize *StMSI1* promoter activity, we generated *promStMSI1::GUS-pBI121* potato transgenic lines. GUS assay on *in vitro* grown plantlets showed a ubiquitous *StMSI1* expression pattern. Promoter activity was observed in shoot tip, stem, leaf, shoot-root junction, and root (Figure – 2.6 B-H) with strong activity in meristematic regions (axillary-nodes and root tips) (Figure 2.6 C; 2.6E).

When promoter activity was assayed from soil-grown plants induced under LD/SD conditions for 14 days, it was observed that swollen stolon samples from the SD condition had strong GUS activity (Figure – 2.6 F; right) compared to stolons from LD conditions (Figure 2.6 F; left). GUS activity was also noticed in tuber peel and pith of SD-induced promoter transgenic plants (Figure 2.6D).

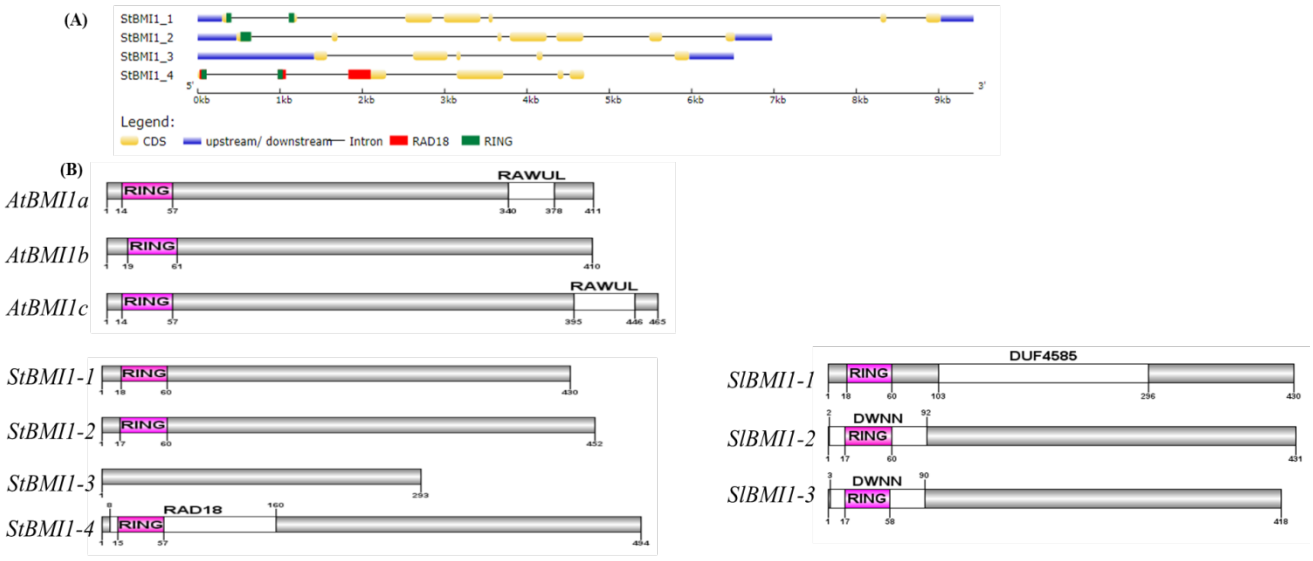

Figure 2.4. Potato and tomato orthologs of AtBMI1 contain the RING finer domain. Graphical representation of potato *StBMI1* gene structures (A) and the conserved domains in protein sequences (B). For visualization of gene features, e.g., position of introns, exons, and conserved domains in potato BMI1 proteins (StBMI1-1, StBMI1-2, StBMI1-3, and StBMI1-4), FASTA files containing coding and genomic sequences were given as an input to Gene Structure Display Server (GSDS) (http://gsds.cbi.pku.edu.cn). Arabidopsis BMI1 protein sequences (AtBMI1a, AtBMI1b and AtBMI1c) were obtained from TAIR database (https://www.arabidopsis.org). Tomato BMI1 orthologue sequences (SlBMI1-1, SlBMI1-2, and SlBMI1-3) were retrieved by NCBI BLAST (https://blast.ncbi.nlm.nih.gov/Blast.cgi) using respective Arabidopsis BMI1 protein sequences as queries. Potato orthologues (StBMI1-1, StBMI1-2, StBMI1-3 and StBMI1-4) were identified from PGSC database (http://solanaceae.plantbiology.msu.edu/pgsc). Conserved domains, such as RING, RAWUL, RAD18, DUF4585, and DWNN, were identified using Web CD Search Tool (https://www.ncbi.nlm.nih.gov/Structure/bwrpsb/bwrpsb.cgi). Domain schematic was drawn using DOG2.0 software (Ren et al. 2009) and edited manually. Protein IDs are as follows. StBMI1-1, PGSC0003DMP400026476; StBMI1-2, PGSC0003DMP400034778; StBMI1-4, PGSC0003DMP400007500; StBMI1-3, PGSC0003DMP400009434; AtBMI1a, AT1G06770; AtBMI1b, AT2G30580; AtBMI1c, AT3G23060; SlBMI1-1, Solyc09g065990.2; SlBMI1-2, Solyc06g084040.2; SlBMI1-3, Solyc06g008600.2. St, *Solanum tuberosum*; Sl, *Solanum lycopersicum*; At, *Arabidopsis thaliana*

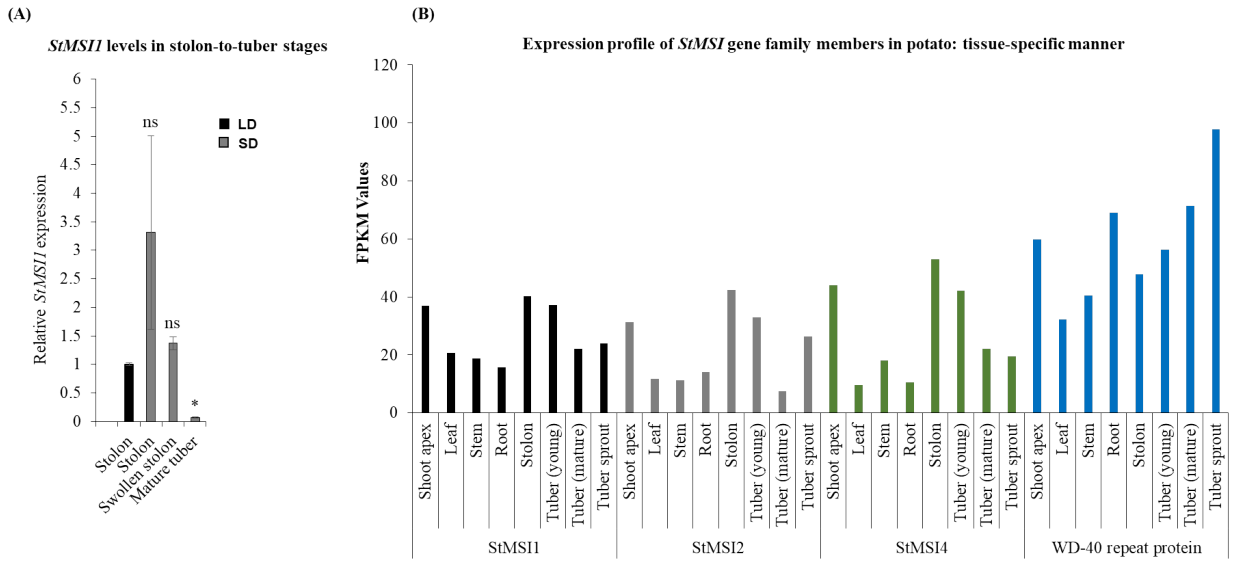

Figure 2.5. Expression profiles of *StMSI* gene family members. *StMSI1* expression in different stolon-to-tuber stages under LD and SD conditions (A). Expression analysis is from three biological replicates and three technical replicates. Transcript level in LD stolons was considered as 1 to calculate the relative fold change in other stolons and tuber tissues. Error bars = ± SD. In silico expression profiles of *StMSI* genes (B) were mined from the publically available RNA-seq database of *S. tuberosum* Group *Tuberosum* RH89-039-16 (RH; ERP000627) genotype (Xu et al. 2011). Four *StMSI* genes are presented with abundance values in FPKMs (fragments per kb per million mapped reads) in six organs (shoot apex, leaf, stem, root, stolon, and tubers).

2.3.3 Overexpression of *StMSI1* results pleiotropic effects in potato including aerial stolons/tubers

Several constitutive overexpression (OE) lines of *StMSI1* (*StMSI1-OE)* driven by 35S CaMV promoter were generated to characterize its role in potato development (Figure 2.8A). Of them, two independent OE lines (OE1 and OE3) with moderate levels of *StMSI1* overexpression were used for further analysis (Figure 2.7A). OE lines showed drastic changes in overall plant phenotype compared to wild-type (WT) plants (Figure 2.7B). OE plants exhibited decreased plant height (Figure 2.8B) and internodal distance (Figure 2.8C); they had a lesser number of leaflets per leaf (Figure 2.7C-D); leaf length was reduced (Figure 2.7E), whereas leaf thickness was increased (Figure 2.7F) compared to WT plants. OE lines also showed altered epidermal cells, bigger trichomes, increased stomatal number, and altered vascular bundle arrangement in stem compared to WT plants (Figure – 2.7 G-N). Moreover, the root length (Figure 2.7D) and

root biomass (Figure 2.7O) were decreased in OE lines compared to WT plants. To evaluate tuber yield potential, soil-grown *StMSI1-OE* lines maintained under LD conditions were subjected to SD inductions for six weeks. Interestingly, these lines produced numerous aerial stolons from axillary-nodes post three weeks of induction (Figure 2.9A-B). On further incubation of 2-3 weeks, the aerial stolons were noticed to branch profusely and to develop into mini-tubers in about 70-80% of the plants (Figure 2.9C-D). The mini-tubers were purple in colour and had characteristic tuber-eyes' with 100% sprouting efficiency when attempted for germination. Neither *StMSI1-OE* (this study) nor miR156-OE (Bhogale et al., 2014) showed aerial tuber phenotype in potato under LD conditions. Throughout our experiments, vector control (VC) plants behaved like wild-type (WT) plants.

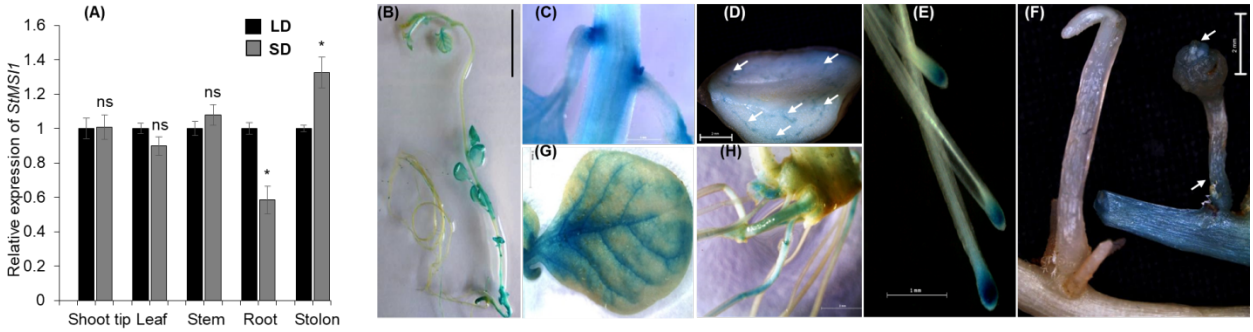

Figure 2.6. *StMSI1* promoter has ubiquitous expression but induced in stolon under the SD photoperiod. Effect of long-day (LD) and short-day (SD) photoperiod on transcript accumulation of *StMSI1* in different tissues (shoot tip, leaf, stem, root and stolon) of a wild-type (WT) andigena (7540) potato plants grown under LD/SD conditions for 14 days post 8-weeks of LD induction in soil (A). Fold-change of *StMSI1* across different tissues is compared between SD vs. LD in a tissue-specific manner. Data are mean ± SD for three biological and three technical replicates. *EIF3e* was used as a reference gene for expression analysis. The student's t-test was performed to check the level of significance at $p<0.05$. Promoter activity of *StMSI1* in *promStMSI1:: GUS* transgenic lines (B). GUS activity in 3-weeks old entire plant grown *in vitro* (B), stem and nodes (C), tuber pith (D), root tip (E), LD stolon (F; left), SD swollen stolon (F; Right), leaf (G) and the shoot-root junction (H). Stolon and tuber samples are from soil-grown plants incubated under LD/SD conditions for 14 days. Scale bars: panel (B)= 2 cm and panels (C-H)= 2 mm. Arrows in panel (D) and (F) represent GUS activity.

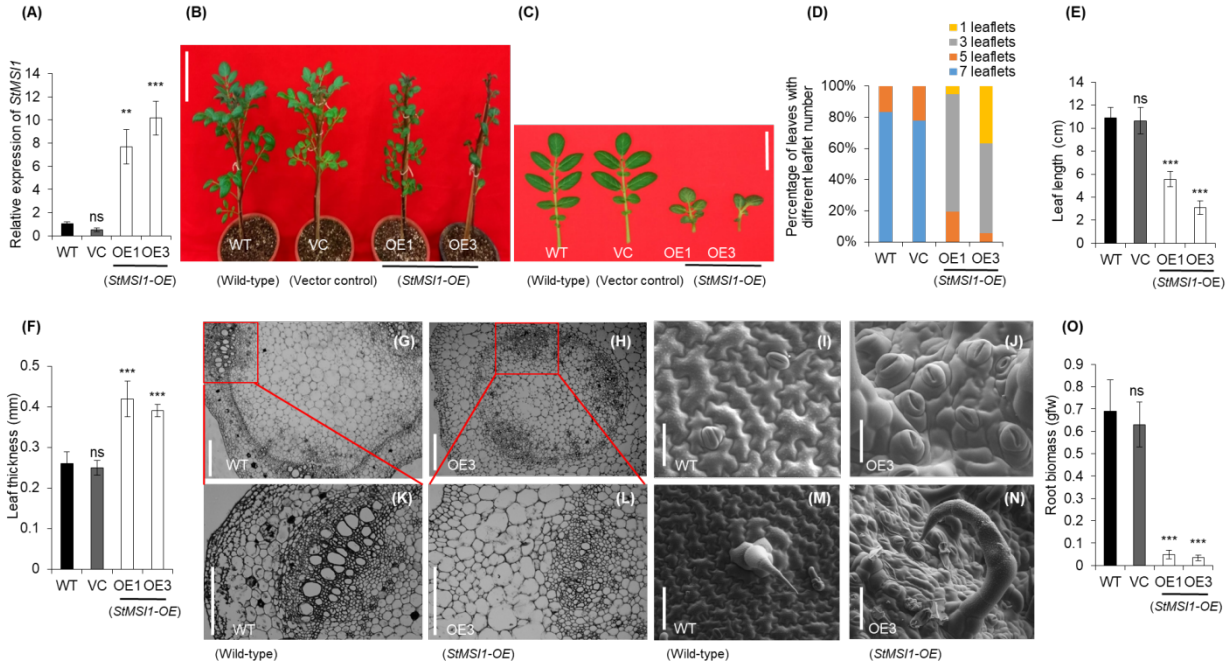

Figure 2.7. *StMSI1* over-expression affects plant architecture in potato. Transcript levels of *StMSI1* in leaves of OE lines (OE1 and OE3) compared to wild-type (WT) (A). Data are mean ± SD for three biological replicates. *EIF3e* was used as a reference gene for expression analysis. Plant architecture of *StMSI1* over-expression potato lines (OE1 and OE3) along with WT and vector control (VC) plants (B). The leaf size (C), the number of leaflets per leaf (D), the leaf length (E), and thickness (F) in *StMSI1* over-expression potato lines (OE1 and OE3) are shown along with WT and VC plants. Six individual plants per line were considered for phenotypic data analysis. Student's t-test was performed to check significance with one, two, three and four asterisks indicating p-values of < 0.05, < 0.01, < 0.001 and < 0.0001, respectively. ns = not significant. Error bars represent ± SD. Transverse cross-section of the stem of WT plant (G) and *StMSI1* over-expression line OE3 (H). Panels (K) and (L) shows the magnified images of vascular bundles in WT and over-expression line, respectively. SEM images showing the leaf epidermis cells, number of stomata (J), and trichomes (N) in OE lines compared to WT (I and M), respectively. Root biomass (O) in *StMSI1* over-expression potato lines (OE1 and OE3) are shown along with WT and VC plants. Scale bar in panel (B)= 10 cm, panel (C)= 5 cm, panels G, H, K and L= 300 µm, and panels I, J, M and N= 50 µm.

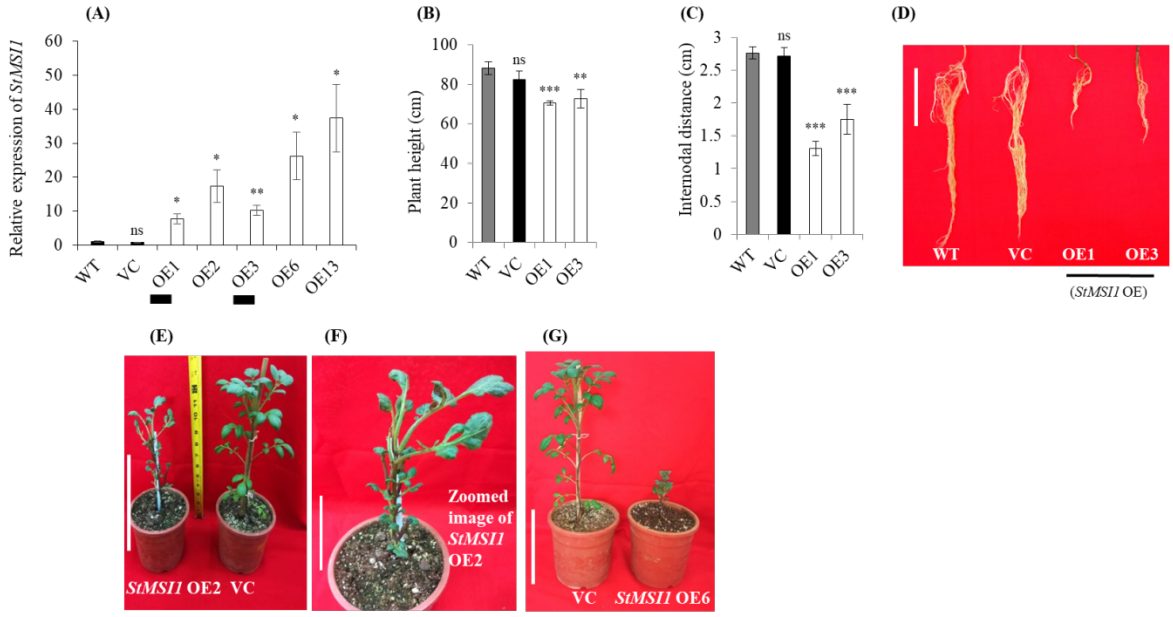

Figure 2.8. Phenotypes of *StMSI1* overexpression lines. *StMSI1* transcript levels in OE lines (A). Plant height (B), internodal distance (C), root biomass (D), and belowground tuber yield (E) in *StMSI1* OE lines (OE1 and OE2) compared to wild-type (WT) and vector control (VC). Error bars are ± SD from 6 independent plants per line. Student's t-test was performed to check significance with one, two, three and four asterisks indicating p-values of < 0.05, < 0.01, < 0.001 and < 0.0001, respectively. ns = not significant. *StMSI1* OE lines, OE1, and OE3, were taken forward for further characterization. *StMSI1* OE potato (andigena) lines, OE2, and OE6 (F-G), which were not used in later experiments. Scale bars in panels D and E= 5 cm; F-G= 10 cm.

2.3.4 *StMSI1-OE* line showed an altered expression of miR156 and *StBMI1*

To analyze if miR156 levels were affected in *StMSI1-OE* lines, miR156a/b/c expression was measured in leaf tissues of SD-induced plants. Interestingly, miR156a/b/c expression was nearly 5-fold higher in the OE line (OE3) compared to VC (Figure 2.9E). Earlier, a PRC1 member, AtBMI1, has been shown to repress miR156 during reproductive phase maintenance in Arabidopsis (Pico et al., 2015). Anticipating crosstalk between StMSI1, StBMI1, and miR156 in potato, the relative transcript levels of all four *StBMI1* genes (*StBMI1-1*, *-2*, *-3*, and *-4*) were quantified in the *StMSI1-OE* line (OE3) using primers from non-conserved regions of each variant. The transcript levels of *StBMI1-1*, *-3*, and *-4* were low in the *StMSI1-OE* line compared to VC (Figure 2.9F). Due to the close conservation of mRNA sequences between *StBMI1-1* and *-2* transcript variants, we could not validate the *StBMI1-2* variant. The transcript levels of a cytokinin biosynthesis gene, *StLOG3*, and a GA catabolism gene, *StGA2ox1*, were significantly

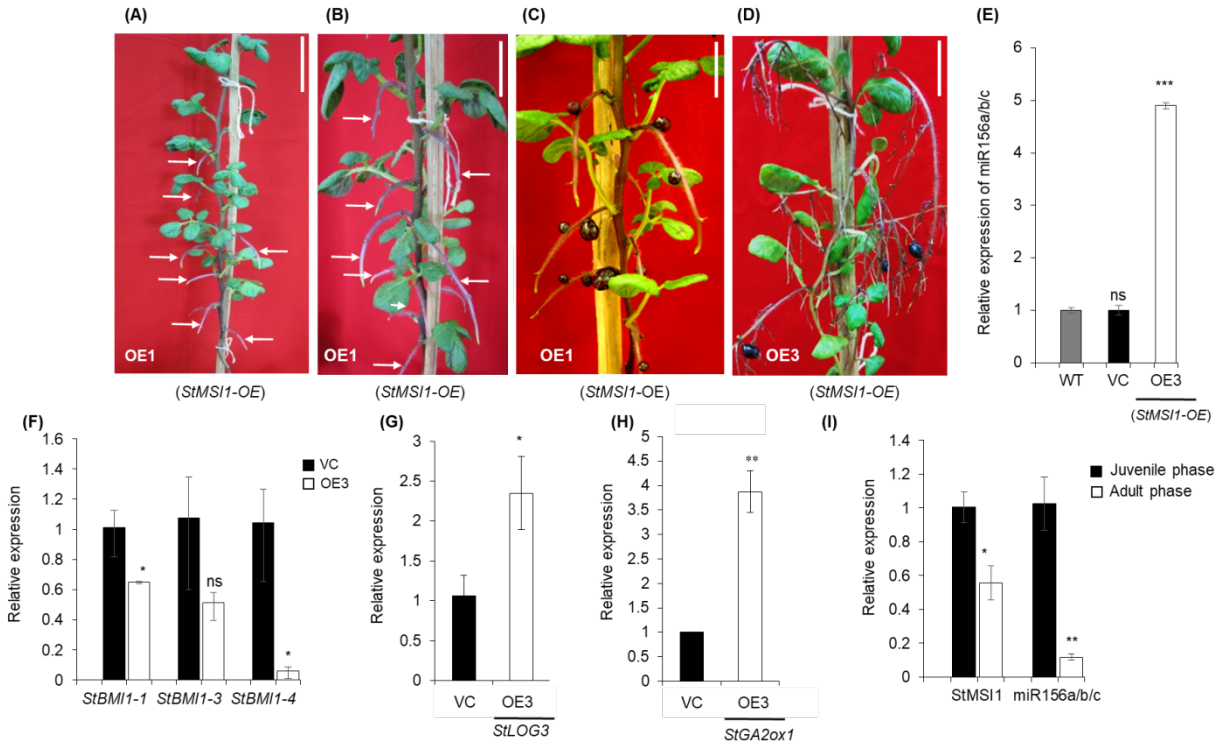

Figure 2.9. *StMSI1* over-expression lines produce aerial stolons and tubers. Aerial stolons (A and B; white arrows) and tubers from axillary nodes under short-day induction (C and D) in *StMSI1* over-expression lines, OE1 and OE3, respectively. Relative miR156a/b/c levels in leaves of *StMSI1* over-expression line OE3 compared to wild-type (WT) plant (E). As miR156a, -b and -c sequences in potato cannot be distinguished at the mature miRNA level, we have referred them as miR156a/b/c throughout the text. Relative transcript levels of *StBMI1-1*, *StBMI1-3,* and *StBMI1-4* in leaves of *StMSI1-OE* line (OE3) compared to vector control (VC) line (F). Relative levels of *StLOG3* (G) and *StGA2ox1* (H) in the *StMSI1-OE* line (OE3) are shown in comparison to VC plants. Relative levels of *StMSI1* and miR156a/b/c in leaves during the juvenile vs. adult phase in WT potato plants (I). For panels, E, F, H, and I, data are mean of three biological and three technical replicates with ± SD. *U6* was used as *a* reference gene for miRNAs, whereas *EIF3e* for gene expression analysis. Relative level in WT was considered as 1 with ± SD for panels E, F, H and I, whereas relative levels in juvenile phase was considered as 1 with ± SD for panel J. Student's t-test was performed to check significance with one, two, three and four asterisks indicating p-values of < 0.05, < 0.01, < 0.001 and < 0.0001, respectively. ns = not significant. Scale bars in panel (A)= 7 cm and panels (B-D)= 5 cm.

higher in leaves of the *StMSI1-OE* line compared to VC plants (Figure 2.9G-H). Moreover, *StMSI1* and miR156 levels in leaves were high in the juvenile phase of wild-type *andigena* plants, whereas their levels were significantly lower in the adult phase of the plant (Figure 2.9I).

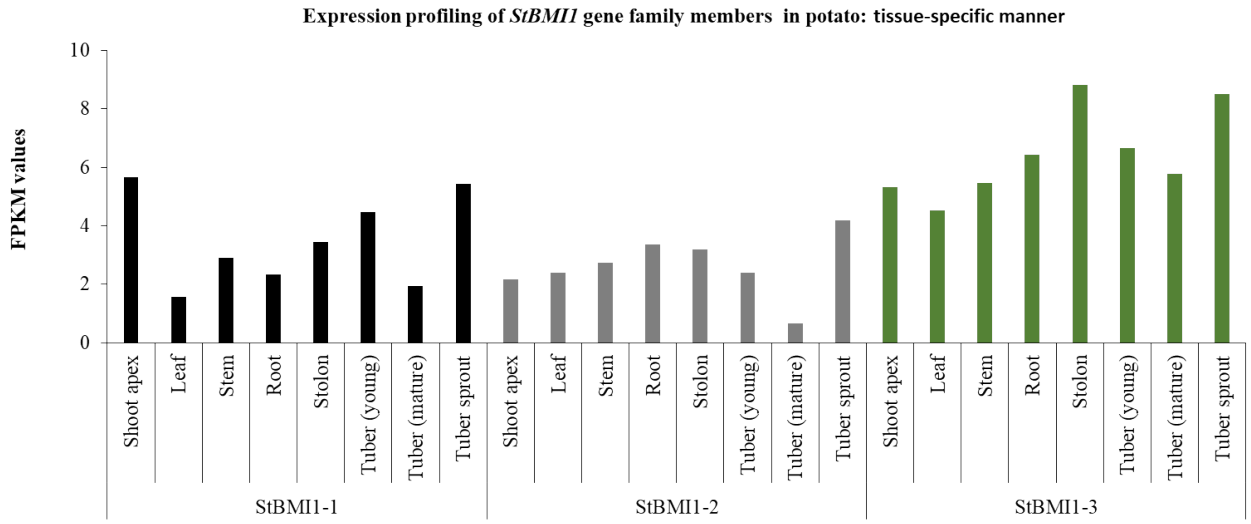

Figure 2.10 Expression profiles of *StBMI1* gene family members. Data were mined from the publically available RNA-seq database of *S. tuberosum* Group *Tuberosum* RH89-039-16 (RH; ERP000627) genotype (Xu et al. 2011). Three *StBMI1* genes are presented with abundance values in FPKMs (fragments per kb per million mapped reads) in six organs (shoot apex, leaf, stem, root, stolon, and tubers).

2.3.5 SD photoperiod affects *StBMI1-1* and miR156 expression in shoot tip and stolons

The StBMI1-1 level was quantified by qPCR in different tissues, and the stages of stolon-to-tuber transitions in *andigena* plants grown under LD/SD conditions for 14 days (Figure 2.12A-B). Our analysis demonstrated that *StBMI1-1* transcript levels were significantly low under the SD photoperiod in shoot tip, stem, and stolon tissues compared to LD conditions (Figure 2.12A). However, the transcript levels remained unchanged in leaf and root tissues under LD and SD photoperiodic conditions (Figure 2.2A). Further, *StBMI1-1* transcript levels were significantly low in stolon, swollen stolon, and mini-tuber, but high in tubers under SD conditions compared to the stolons from LD (Figure 2.12B). Moreover, miR156 levels were quantified in shoot tip and stolon tissues under LD/SD conditions. We noticed about 2.5- and 2-fold increase of miR156 expression in shoot tip and stolon (respectively) under SD conditions

compared to LD (Figure 2.12C). From the PGSC resources (Xu et al., 2011), it was evident that *StBMI1-4* is expressed only in floral organs and not in any other tissue types (i.e. shoot apex, leaf, stem, root, stolon, young/mature tuber, sprouted tuber) in potato. Since *StBMI1-1* is expressed more abundantly than *StBMI1-2* (Figure 2.10), and the absence of RING domain in StBMI1-3 protein, we chose *StBMI1-1* for its functional characterization in the current study.

2.3.6 *StBMI1-1* knockdown affects leaf and root development but induces aerial tuber formation

To investigate if StBMI1-1 functions upstream of miR156 in potato, its antisense (*StBMI1-1-AS*) lines were generated (Figure 2.11). Of the two lines (#G9 and #G12), #G9 had about 35% downregulation, whereas #G12 had about 30% downregulation of *StBMI1-1* (Figure 2.12D). The overall architecture of the plant was weak in *StBMI1-AS* line (#G9) when compared to WT or VC plants (Figure 2.12E). Shoot biomass was significantly lower in *StBMI1-1-AS* lines #G9 and #G12 (Figure 2.11D). The expression of *StLOG3* remained unchanged, whereas, that of *StGA2ox1* was upregulated in *StBMI1-1-AS* line (Figure 2.11C). *StBMI1-1-AS* line (#G9) showed a reduction in leaf size as well as leaf compounding post 2-3 weeks of incubation under LD conditions in soil (Figure 2.12F).

The leaf phenotypes were similar to miR156-OE lines #K1 and #K6 (Figure 2.12G) as well as *StMSI1-OE* lines (Figure 2.7C). On an average, WT or VC plants had 7 leaflets per leaf in mature plants, whereas *StBMI1-1-AS* lines (#G9 and #G12) always had less than 5 leaflets per leaf (Figure 2.12H). Root biomass was also significantly lower in *StBMI1-1-AS* line (#G9) compared to WT plants (Figure 2.12 I). qPCR analysis demonstrated that *StBMI1-1-AS* line (#G9) had >2-fold increase of miR156a/b/c levels in leaves compared to WT or VC plants (Figure 2.12J). Similar to *StMSI1-OE* lines, an extended incubation of *StBMI1-1-AS* line (#G9) under SD conditions resulted in formation of aerial tubers in approximately 50% of the plants (Figure 2.12K); however, no such phenotype was observed in #G9 line under LD conditions (Figure 2.12E).

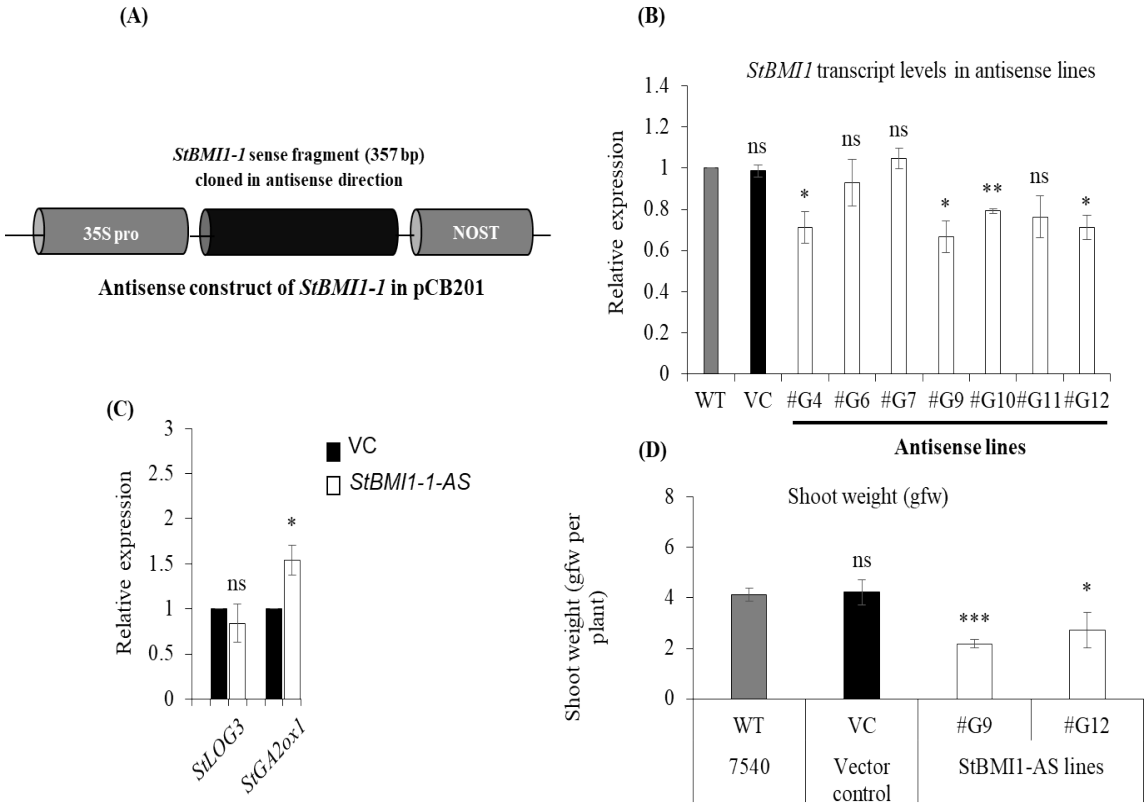

Figure 2.11. *StBMI1-1-AS* line screening and phenotype. Diagrammatic illustration of *StBMI1-1* antisense construct in a binary vector pCB201 (A). Screening of *StBMI1-1* antisense transgenic lines by qPCR analysis (B). Shoot weight in WT and *StBMI1-1* antisense lines #G9 and #G12 (C). Nine independent plants per line were used in this analysis. SD= Standard deviation. Expression analysis of *StLOG3* and *StGA2ox1* in *StBMI1-1-AS* line #G9 (D). For panels B and D, RNA was isolated from leaves of six independent transgenic plants per line along with wild-type (WT) and vector control lines (VC). Leaf samples were pooled from two plants forming three biological replicates per line and qPCR was performed using *StBMI1-1* specific primers with three technical replicates. Relative expression in each transgenic line is with respect to WT or VC *andigena* plants. Antisense lines (#G9 and #G12) were used in subsequent experiments. *EIF3e* was used as a reference gene for *StBMI1-1* for expression analysis. Student's t-test was performed to check significance with one, two, three and four asterisks indicating p-values of < 0.05, < 0.01, < 0.001 and < 0.0001, respectively. ns= Not significant. SD= Standard deviation.

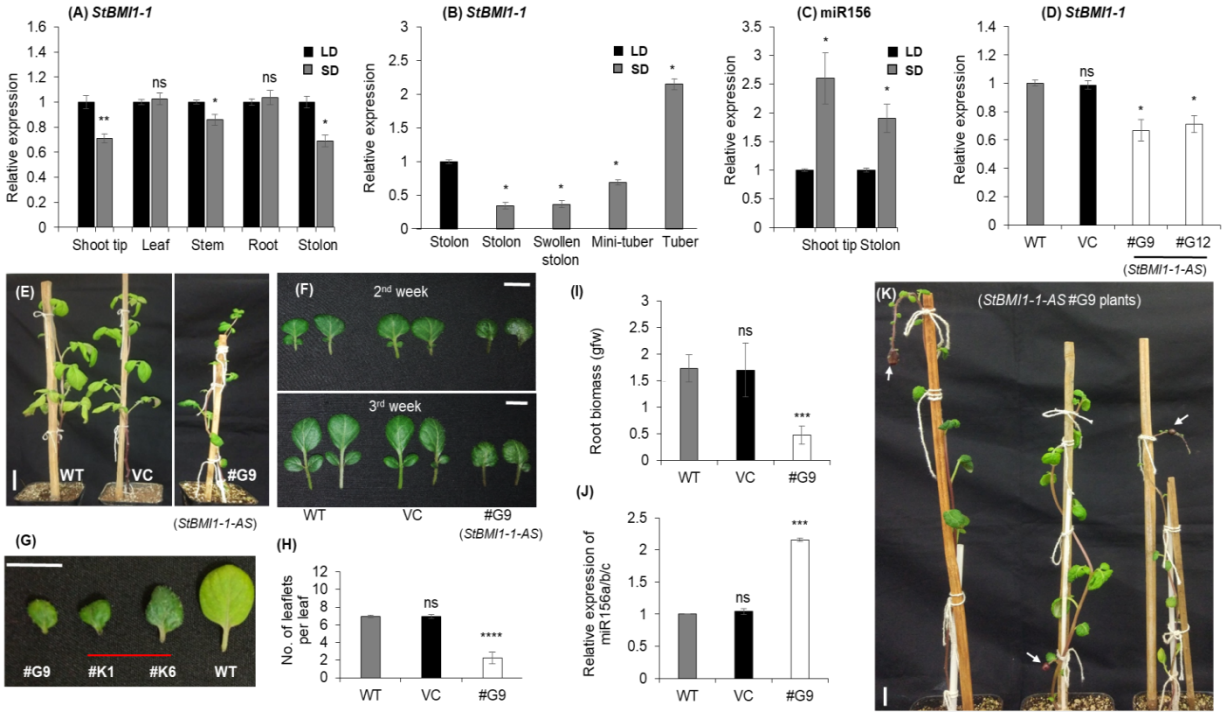

Figure 2.12. Phenotypic characterization of *StBMI1-1* antisense lines. Effect of LD and SD photoperiod on the expression of *StBMI1-1* in different tissue types - shoot tip, leaf, stem, and root (A) and in various stages of stolon-to-tuber transitions (B). Wild-type (WT) potato plants were grown under LD/SD conditions for 14 days, post 8-weeks of growth in soil under LD conditions. The relative levels of miR156a/b/c in shoot-tip and stolon tissues at 14 days under LD/SD conditions (C). The relative transcript levels of *StBMI1-1* or miR156a/b/c in different tissues under SD conditions is calculated considering its levels under LD condition as 1 with ±SD. *EIF3e* and *U6* were used as reference genes for *StBMI1* and miR156a/b/c expression analysis, respectively. The transcript levels of *StBMI1-1* in leaves of antisense transgenic lines, #G9, and #G12 (D) compared to WT and vector control (VC) line. The analysis was performed with three biological replicates per line. RT-qPCR was performed using *StBMI1-1* specific primers. *StBMI1-1-AS* transgenic lines, along with WT and VC (E). Leaf phenotype of *StBMI1-1-AS* line #G9 along with WT and VC plants at 2nd and 3rd week in soil (F) and the leaf phenotype of miR156-OE lines (#K1 and #K6) after the first week in soil (G). A number of leaflets per leaf (H) and root biomass (I) in *StBMI1-1-AS* transgenic line (#G9) and VC are presented with respect to WT. Data is represented from 9 independent plants per line. Relative miR156a/b/c levels in antisense line #G9 and VC with respect to WT (J). Formation of aerial tubers in the *StBMI1-1* antisense line (#G9) after four weeks of SD incubation (K). White arrows indicate aerial tubers. *U6* was used as a reference gene. Student's t-test was performed to check significance with one, two, three and four asterisks indicating p-values of < 0.05, < 0.01, < 0.001 and < 0.0001, respectively. ns = not significant. Error bars represent ± SD. Scale bars in panel E, F, G, and K= 1 cm.

2.3.7 Knockdown of *StMSI1* and overexpression of *StBMI1-1* affects leaf development

To assess the effect of *StMSI1* knockdown on potato phenotype, two independent *StMSI1-AS* lines (AS8 and AS9) displaying up to 50% reduction of *StMSI1* transcript levels were selected for phenotypic analysis (Fig 2.13A). *StMSI1-AS* lines exhibited reduced plant height (Figure 2.13b), internodal distance (Figure 2.13C), and leaf length (2.13D-E) compared to WT or VC plants. Unlike *StMSI1-OE* lines, there was no effect on the root biomass of *StMSI1-AS* lines (Figure 2.13F-G). The levels of miR156a/b/c were significantly decreased in the *StMSI1-AS* line (AS8) compared to VC plants (Figure 2.13H). Two independent *StBMI1-1-OE* lines (#II-9 and #II-10) (Figure 2.14A-B) showed an increase in leaf size and number of leaflets per leaf compared to WT plants (Figure 2.14C). In mature plants, the average number of leaflets per leaf increased to nine or more in OE lines in comparison to seven in WT or VC (Figure 2.14D). However, root biomass was not affected in *StBMI1-1-OE* lines (Figure 5I). Shoot and root biomass did not show any changes in *StBMI1-1-OE* lines (#II-9 and #II-10) compared to VC plants (Figure 2.14E-F).

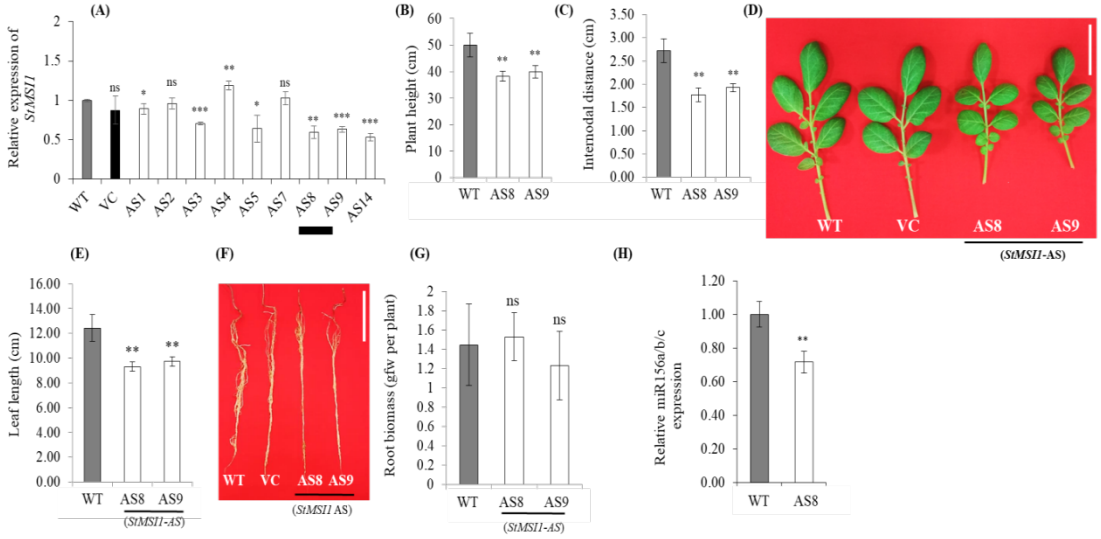

Figure 2.13. Phenotypes of *StMSI1-AS* (AS8 and AS9) lines. Relative levels of *StMSI1* in leaves of antisense lines compared to wild-type (WT) (A). RNA was isolated from leaves of six independent transgenic plants per line. Data are mean ± SD for three biological replicates and three technical replicates. *EIF3e* was used as a reference gene. *StMSI1* level in WT leaves was considered 1 to calculate relative fold-change in respective lines. AS8 and AS9 were taken forward for further characterization. Plant height (B), internodal distance (C), leaf size (D), length (E), root length (F) and biomass (G) in AS8 and AS9 lines and vector control (VC) is shown along with WT plants after one month of SD induction. Six individual plants per line were considered for phenotypic data analysis. Student's t-test was performed to check

significance with one, two, three and four asterisks indicating p-values of < 0.05, < 0.01, < 0.001 and < 0.0001, respectively. ns = not significant. Errors bars for panels E and G= ± SD. miR156 levels in *StMSI1-AS* line AS8 compared to WT (H). For miR156 analysis, mean ± SD for three biological replicates and three technical replicates were used. Scale bars: panel (D)= 3 cm and panel (F)= 5 cm

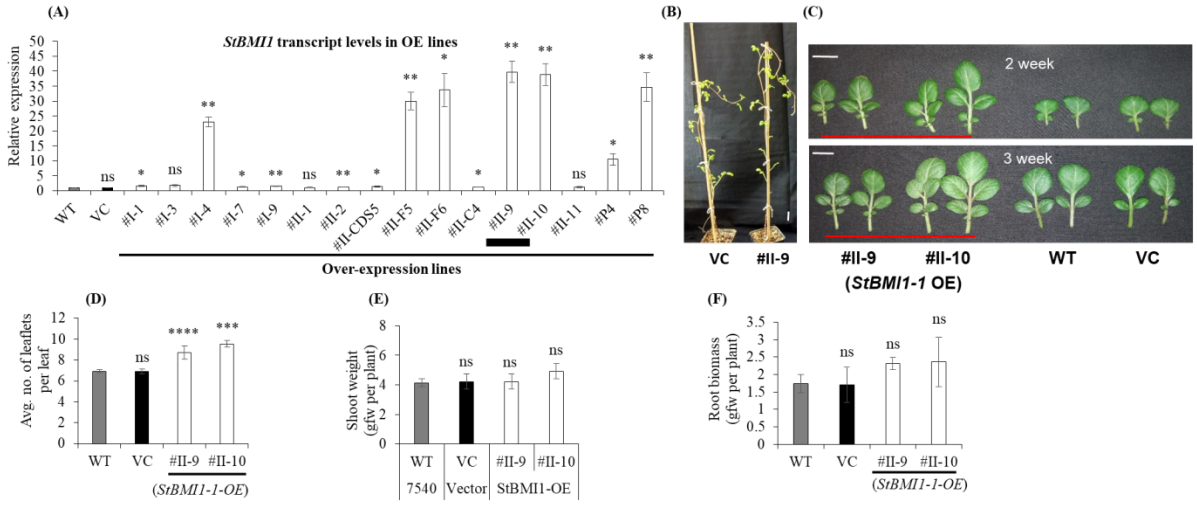

Figure 2.14. **Phenotypes of *StBMI1-1-OE* (II-9 and II-10) lines**. Screening of *StBMI1-1* over-expression transgenic lines (A). RNA was isolated from leaves of six independent transgenic plants per line along with wild-type (WT) and vector control lines (VC). Data are mean ± SD for three biological replicates and three technical replicates. Relative expression in each transgenic line is with respect to WT. Over-expression lines (#II-9 and #II-10) were used in subsequent experiments. *EIF3e* was used as a reference gene for expression analysis. The overall architecture of *StBMI1-1-OE* line (#II-9) compared to WT and VC plants (B). Leaf phenotype of *StBMI1-1-OE* (#II-9 and #II-10), VC, and WT plants at 2nd and 3rd-week post growth in soil (C). A number of leaflets per leaf (D), shoot (E), and root biomass (F) in *StBMI1-1-OE* and VC lines are presented with WT. Data are shown from 9 independent plants per line. Student's t-test was performed to check significance with one, two, three and four asterisks indicating p-values of < 0.05, < 0.01, < 0.001 and < 0.0001, respectively. ns = not significant. Errors bars= ± SD. Scale bar in panel (B and C)= 1 cm.

2.3.8 Overexpression or knockdown of *StMSI1* or *StBMI1-1* influences tuberization

Tuber yield potential was assessed both in *in vitro* and in soil-grown plants of *StMSI1-OE/AS*, miR156-OE, and *StBMI1-1-OE/AS* lines. Under tuber-inducing *in vitro* conditions, *StMSI1-OE* (OE3) *StMSI1-AS* (AS8), *StBMI1-1-AS* line (#G9), and miR156-OE lines exhibited delayed tuberization and reduced tuber yield compared to WT, whereas *StBMI1-1-OE* line (#II-9) showed an earliness for *in vitro* tuberization as well as increased tuber yield (Figure 2.15A).

The expression of tuber marker genes, such as miR172 (Martin et al., 2009), *StBEL5* (Banerjee et al., 2006a), and *StSP6A* (Navarro et al., 2011) were significantly reduced in leaves of *StMSI1-OE* and *StBMI1-1-AS* lines (Figure 2.15B). In contrast, the expression of StSP6A repressors, such as *StCO2, StCO-like 9*, and *StSP5G* was significantly higher in leaves of *StMSI1-OE* and *StBMI1-1-AS* lines (Figure 2.15B), which is consistent with the reduced tuber yield phenotype in these lines. Although there was no effect on tuber numbers in *StMSI1-OE* or *-AS* lines in soil-grown plants (Figure 2.15C), both showed about 3- to 5-fold reduction in tuber yield compared to WT (Figure 2.15D; Figure 2.16A-B). *StBMI1-1-OE* lines showed no difference in tuber numbers, but they had increased tuber yield (Figure 2.15E-F). However, *StBMI1-1-AS* lines showed a reduction in tuber numbers as well as in tuber yield (Figure 2.15E-F).

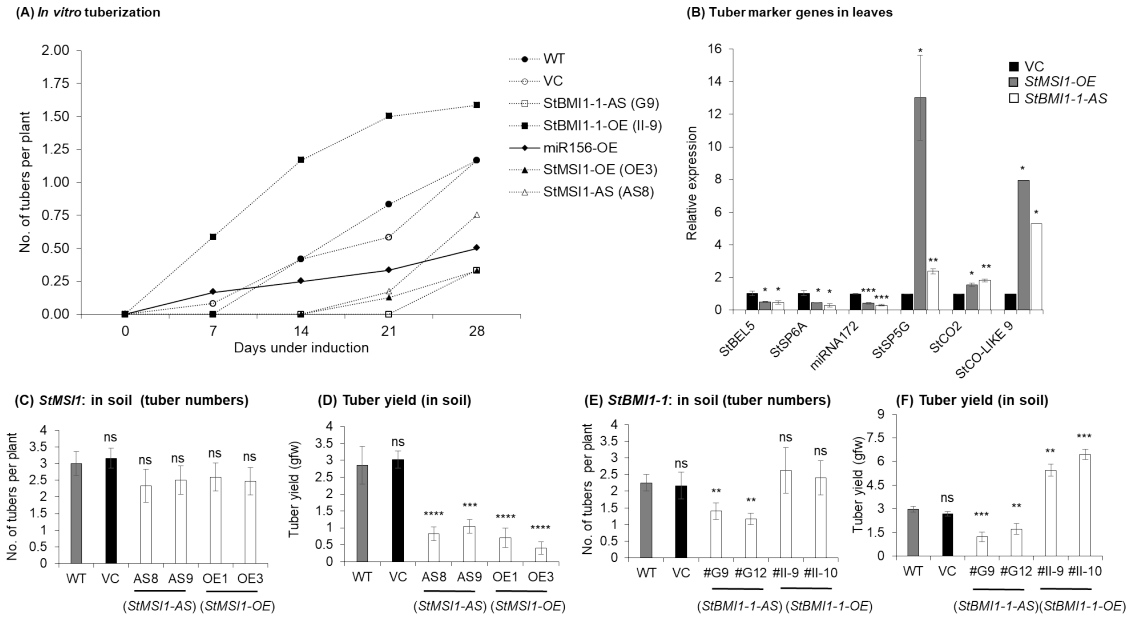

Figure 2.15. Over-expression or knock-down of *StMSI1* or *StBMI1-1* influences tuberization. The number of tubers produced by over-expression and antisense lines of *StMSI1* and *StBMI1-1* on 8% sucrose in the dark under *in vitro* conditions over a period of 28 days. Data is plotted at seven days interval along with miR156a/b/c over-expression, wild-type (WT) and vector control (VC) lines. For better representation, one representative line per transgenic construct was plotted (A). The relative transcript levels of *StBEL5*, *StSP6, miRNA172, StSP5G, StCO2,* and *StC0-like 9* in leaves of *StMSI1-OE* (OE3) and *StBMI1-1-AS* (#G9) lines incubated under SD for 20 days are shown with respect to VC plants (B). Three biological and three technical replicates were used in the analysis. *EIF3e* was used as a reference for genes, whereas *U6* for miRNA. Number of tubers and tuber yield (C-F) was calculated from soil-grown plants after 1 month of SD induction in all four types of transgenic lines- *StMSI1-OE* (OE1 and OE3), *StMSI1-AS* (AS8 and AS9), *StBMI1-1-OE* (#II-9 and #II-10) and *StBMI1-1-AS* (#G9 and #G12) lines, compared to WT and VC plants. Data is plotted from 6 individual plants per line for *StMSI1-OE/AS* lines, whereas nine individual plants per line for *StBMI1-1-OE/AS* lines.

Student's t-test was performed to check significance with one, two, three and four asterisks indicating p-values of < 0.05, < 0.01, < 0.001 and < 0.0001, respectively. ns = not significant. Error bars represent ± SD.

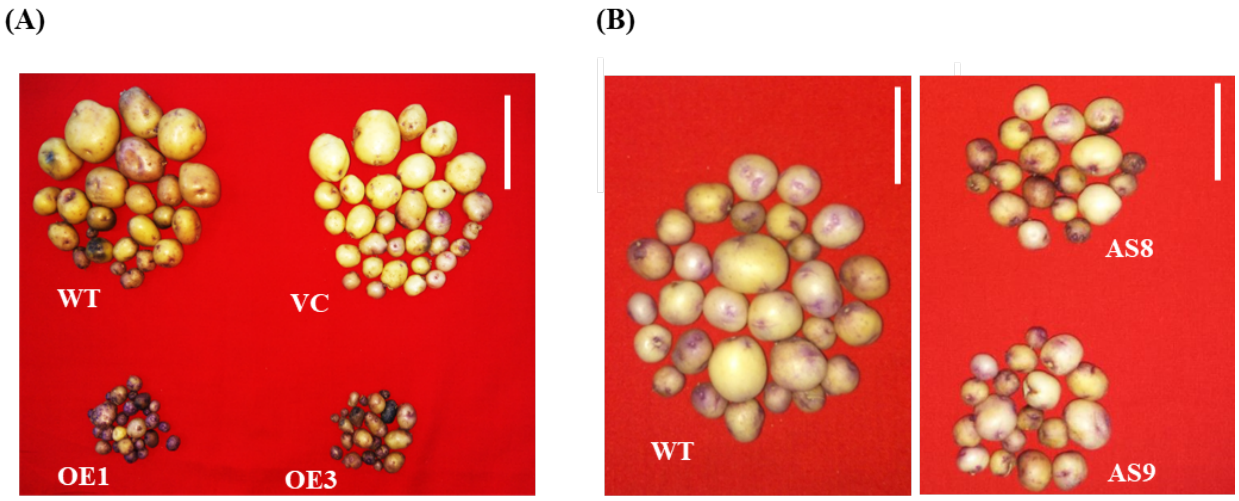

Figure 2.16 Tuber yield (below-ground) in *StMSI1-OE* and *-AS* lines. Photographs of belowground tubers in *StMSI1-OE* lines (OE1 and OE3; A) and *StMSI1-AS* lines (AS8 and AS9; B) are shown along with WT or VC plants. Tubers from 6 independent plants are pooled for each line — scale bars: A and B= 3 cm.

2.3.9 RNA-seq analysis revealed common DE genes between *StMSI1-OE* and *StBMI1-1-AS* lines

In order to understand the cause for aerial tuber formation, we performed paired-end RNA-sequencing from axillary-nodes of SD-induced *StMSI1-OE* and *StBMI1-1-AS* lines along with VC plants. Overall, 172 million final clean reads were obtained from 181 million raw reads after quality filtering and adapter trimming. Of them, 88.86% read pairs uniquely mapped to the potato genome (Table 1). Downstream processing of RNA-seq data revealed that about 7386 and 1690 genes were differentially expressed (DE) in *StMSI1-OE* and *StBMI1-1-AS* lines, respectively, compared to VC plants (Figure 2.17A). Among the DE genes in *StMSI1-OE* line, about 3360 and 4026 genes were up- and downregulated, respectively. Whereas 921 genes were up- and 769 were downregulated in the *StBMI1-1-AS* line. Approximately 6363 DE genes were unique only to the *StMSI1-OE* line, whereas about 667 genes were specific to the *StBMI1-1-AS* line (Figure 2.17A). Interestingly, we observed that out of 1690 DE genes identified in the

StBMI1-1-AS line, 1023 genes (~60%) were common between both the lines (*StMSI1-OE* and *StBMI1-1-AS*). When common DE genes were analyzed.

Further, we found that 345 genes were upregulated, and 371 were downregulated in both lines. However, 307 DE genes from the common pool showed opposite expression patterns in *StMSI1-OE* and *StBMI1-1-AS* lines; where 123 genes were upregulated in *StMSI1*-OE, but downregulated in *StBMI1-1-AS* line, and 184 genes were downregulated in *StMSI1-OE,* but upregulated in *StBMI1-1-AS* line (Figure 2.17A). Amongst the common DE genes, a large number related to auxin and brassinosteroid (BR) biosynthesis, transport, and signaling were downregulated, whereas the genes involved in cytokinin (CK) transport and signaling were upregulated.

Table 2.1 Summary of read counts and alignment statistics after RNA-sequencing.

Sample Name	**Raw reads**	**Cleaned reads**	**% read pairs uniquely mapped to the genome**
Vector control line replicate 1	26,452,575	25,414,994	89.06%
Vector control line replicate 2	21,156,895	20,288,178	86.84%
Vector control line replicate 3	19,426,628	18,589,972	85.46%
StMSI1 over-expression line OE3 replicate 1	23,727,153	22,661,717	90.78%
StMSI1 over-expression line OE3 replicate 2	19,741,392	18,514,718	92.89%
StMSI1 over-expression line OE3 replicate 3	28,251,381	26,807,328	86.92%
StBMI1-1 antisense line G9 replicate 1	25,269,133	24,046,116	87.22%
StBMI1-1 antisense line G9 replicate 2	16,943,329	16,239,229	91.72%

2.3.10 RNA-seq and qPCR analysis revealed altered expression of histone modifiers, tuber marker, and development related genes in *StMSI1-OE* and *StBMI1-1-AS* lines

RNA-seq analysis also revealed downregulation of *StBMIs* (*StBMI1-1* and *StBMI1-3)*, LHP1 (which recruits PRC1 complex over H3K27me3 modified target genes; Turck et al., 2007), and HDA19 (that catalyzes the removal of acetylation marks on target genes), in the *StMSI1-OE* line compared to VC (Supplemental Table S2). Further, we could identify that

trithorax members, such as SDG4 and a member of SET7/9 family (SET7/9) having histone H3K4 methyltransferase activity, were significantly upregulated in these lines (Figure 2.17B). The expression of SDG4 and SET7/9 genes were upregulated, whereas that of LHP1 was downregulated in the StMSI1-OE line (Figure 2.17B). ABA signaling gene PYL4, and auxin-responsive genes like SAUR and ARF16,

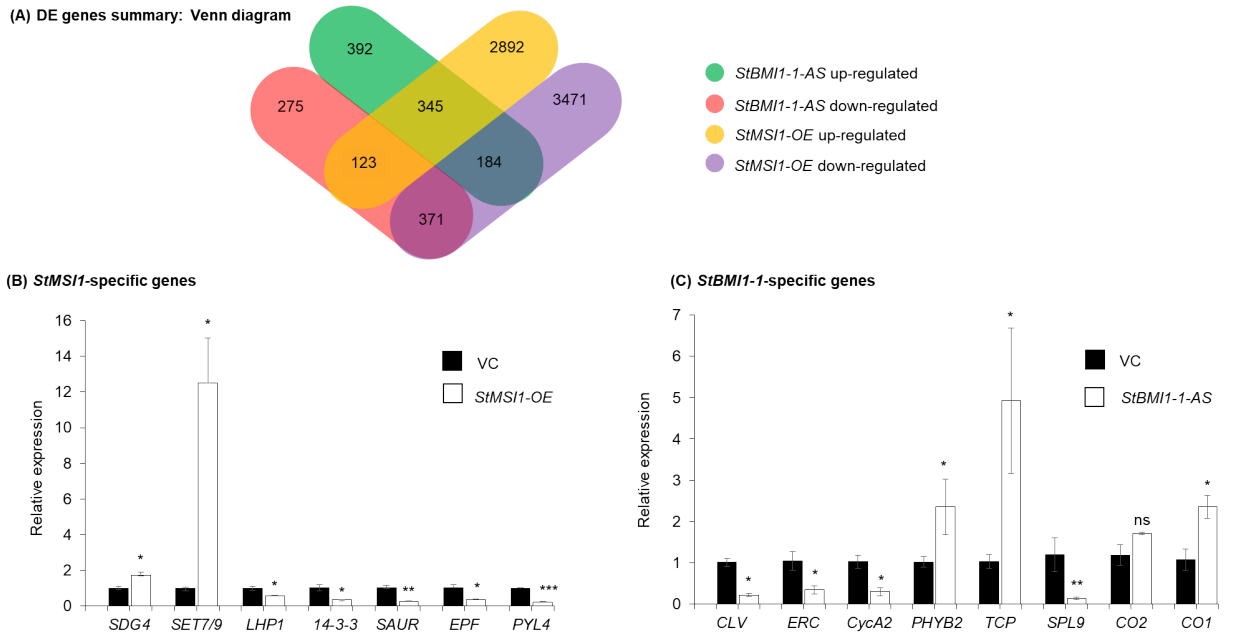

Figure 2.17. RNA-seq. analysis and validation of DE genes specific to the *StMSI1-OE* or *StBMI1-1-AS* line. Venn diagram shows the summary of differentially expressed (DE) genes in *StMSI1-OE* and *StBMI1-AS* lines compared to vector control (VC) line (A). Validation of selective *StMSI1*-specific (B) and *StBMI1-1*-specific genes (C) compared to VC. The relative fold-change of respective gene expression in *StMSI1-OE* or *StBMI1-1-AS* lines was calculated with respect to its transcript level in the VC plant. Student's t-test was performed to check significance with one, two, three and four asterisks indicating p-values of < 0.05, < 0.01, < 0.001 and < 0.0001, respectively. ns = not significant. Error bars represent ± SD from three biological and three technical replicates. *EIF3e* was used as a reference gene.

and epidermal patterning factor (EPF) was downregulated in the StMSI1-OE line (Figure 6B; Supplemental Table S2). The expression of SDG4 and SET7/9 genes were upregulated, whereas that of LHP1 was downregulated in the StMSI1-OE line (Figure 2.17B). ABA signaling gene PYL4, and auxin-responsive genes like SAUR and ARF16, and epidermal patterning factor (EPF) were downregulated in StMSI1-OE line (Figure 6B; Supplemental Table S2). The transcript levels of a gene which induces tuber formation, StSP6A (Navarro et al., 2011) and a

member of the tuberigen activation complex (TAC), St 14-3-3 (Teo et al., 2016), were significantly reduced in the StMSI1-OE line (Figure 2.17B; Supplemental Table S2). On the other hand, genes involved in cell division (cyclin A2, CycA2), shoot-apical meristem formation and maintenance (CLAVATA1, CLV, and ERECTA, ERC), and leaf development (TCP TF and SPL9) were altered in the StBMI1-

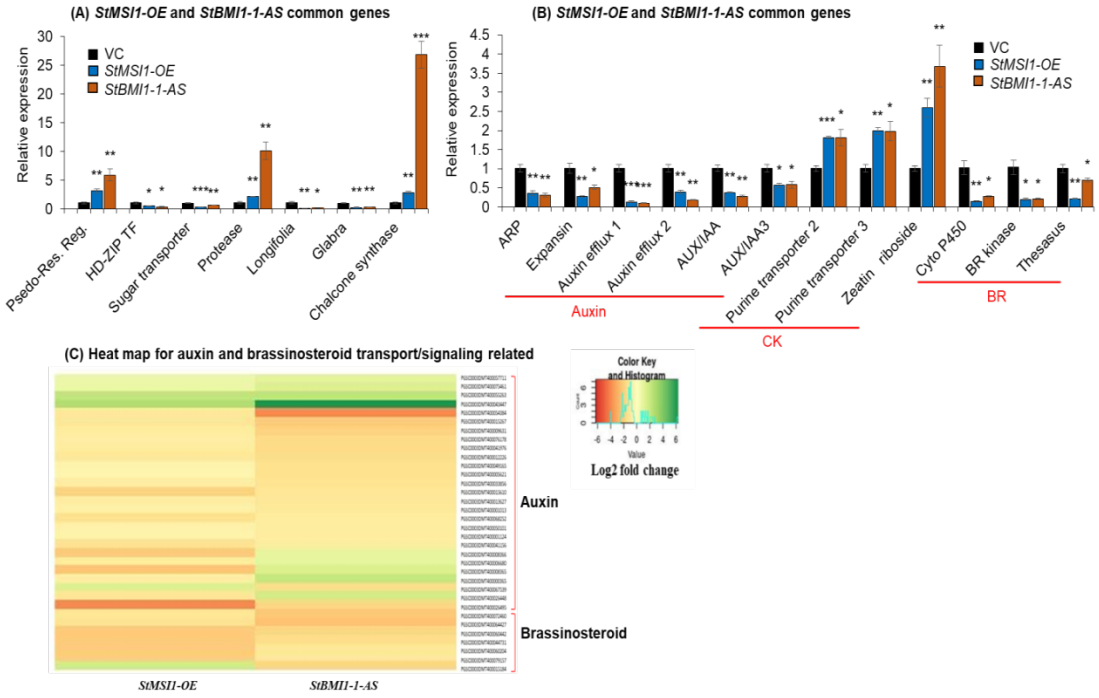

Figure 2.18. Expression analysis of phytohormone signaling related genes in transgenic lines. Auxin and BR related genes were down-regulated, whereas CK related genes were upregulated in *StMSI1-OE* and *StBMI1-1-AS* lines. Validation of selective DE genes common between *StMSI1-OE* and *StBMI1-1-AS* lines compared to vector control (VC) line (A-B). The relative fold-change of respective gene expression in the *StMSI1-OE* or *StBMI1-1-AS* line was calculated with respect to its transcript level in VC plant. Student's t-test was performed to check significance with one, two, three and four asterisks indicating p-values of < 0.05, < 0.01, < 0.001 and < 0.0001, respectively. ns = not significant. Error bars represent ± SD from three biological and three technical replicates. *EIF3e* was used as a reference gene. In panel A, red underlines represent the genes related to auxin, CK, and BR metabolism and/or transport. The heat map was plotted for all auxin and BR transport/signaling related genes from a pool of DE genes common between *StMSI1-OE* and *StBMI1-AS* lines (C).

1-AS line compared to VC (Figure 2.17C). Moreover, the transcript levels of tuberization repressors, such as *PHYB2* and *CONSTANS* (CO1 and CO2), were significantly increased in

StBMI1-1-AS lines (Figure 2.17C; Supplemental Table S3). Validation of common DE genes between *StMSI1-OE* and *StBMI1-1-AS* lines showed that three genes, such as *pseudo-response regulator* (governs circadian rhythm and plant fitness), *protease* (associated with leaf senescence), and *chalcone synthase* (involved in flavonoid biosynthesis) were upregulated, whereas several other genes, such as *HD-ZIP* TF (required for vascular development), *longifolia* (involved in leaf morphology), and *glabra* (associated with trichome branching), were downregulated in *StMSI1-OE* and *StBMI1-1-AS* lines (Figure 2.18A; Supplemental Table S4). Among the common DE genes between *StMSI1-OE* and *StBMI1-1-AS* lines, we found 22 genes (of 1023) were associated with sugar transport or sugar/starch metabolism (Supplemental Table S4).

2.3.11 Phytohormone-related genes were affected in *StMSI1-OE* and *StBMI1-1-AS* lines

Analysis of common DE genes between *StMSI1-OE* and *StBMI1-1-AS* lines showed the genes encoding auxin transport proteins (*auxin efflux 1* and *-2*), and auxin response proteins (*ARP*, *expansin*, *AUX/IAA*, and *AUX-IAA3*) were downregulated in *StMSI1-OE* and *StBMI1-1-AS* lines compared to VC (Figure 2.18B;). Additionally, genes related to brassinosteroid (BR) biosynthesis (*cytoP450*) and signaling (*BR kinase, thesasus* and *Phi-1 protein*) were downregulated (Figure 2.18B;). The transcript of a gene (sigma factor sign regulation protein rsbq), which acts as a negative regulator of strigolactone (STL) signaling, was high, whereas an STL responsive gene (PGSC0003DMT400043632) was downregulated in the axillary-nodes of *StMSI1-OE* and *StBMI1-1-AS* lines. Further, *StMSI1-OE* lines had reduced levels of GA biosynthesis genes, *GA20ox* and *GA3ox*, and increased expression of a GA catabolic gene, *GA2ox*, in axillary-nodes. Genes encoding CK transporters, such as *purine transporter 2* and *-3*, as well as a responsive gene (*zeatin riboside*), were upregulated in *StMSI1-OE* and *StBMI1-1-AS* lines in comparison to VC (Figure 2.18B). Further, the heat map (Figure 2.18 C;) showed that among the 28 auxin-related genes, 23 were downregulated in the *StMSI1-OE* line, and 19 were downregulated in the *StBMI1-1-AS* line. The remaining five genes were upregulated in the *StMSI1-OE* line, and nine were downregulated in the *StBMI1-1-AS* line compared to VC (Figure 2.18C;). Of the seven BR related genes, six were downregulated in the *StMSI1-OE* line, whereas all seven were downregulated in the *StBMI1-1-AS* line compared to VC (Figure 2.18C). Gene

ontology (GO) analysis for DE genes categorized GO terms into different biological processes (BP), molecular functions (MF), and cellular components (CC) (Figure 2.19).

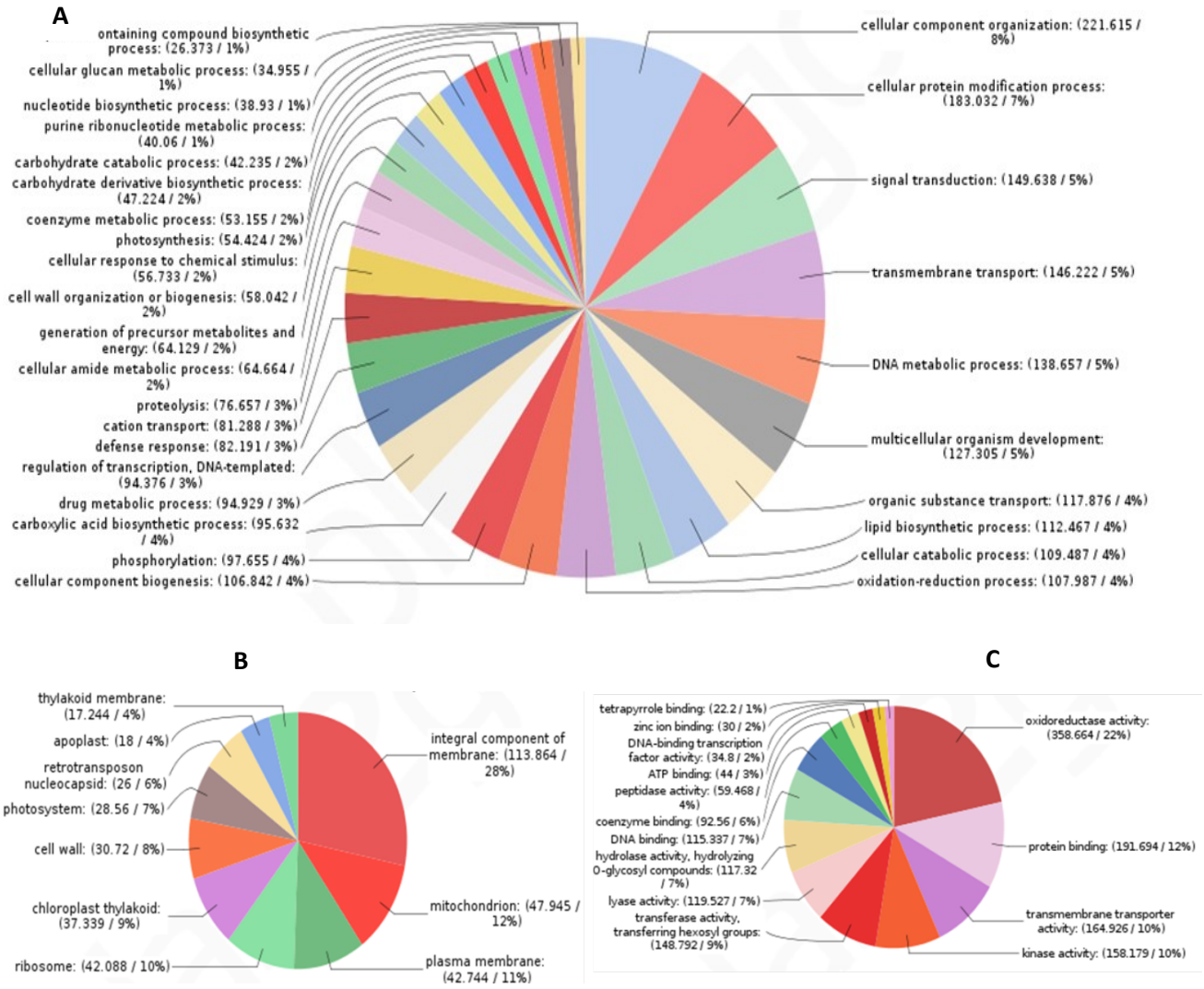

Figure 2.19. GO classification for differentially expressed genes common between *StMSI1-OE* and *StBMI1-1-AS* lines. GO terms were categorized into biological process (A), cellular components (B), and molecular functions (C).

2.3.12 Grafting of *StMSI1-OE* or *StBMI1-1-AS* on WT influenced miR156 accumulation and reduced root biomass in WT stock

Considering the mobile nature of tuberization signals, to investigate if overexpression of *StMSI1-OE* or *StBMI1-1* knockdown has any effect on miR156 expression, different combinations of

homo- and hetero-grafts were made under *in vitro* conditions (Figure 2.20A). Overall, we produced about 70-80% successful grafts and 3-weeks after grafting, several root growth parameters were measured. As expected, homo-grafts of *StMSI1-OE* or *StBMI1-1-AS* showed a reduction in a number of roots, root length, and biomass compared to WT homo-grafts. Interestingly, we noticed that root growth was affected in hetero-grafts containing *StMSI1-OE* or *StBMI1-1-AS* as scion and WT as stock as well as in reverse grafts (Figure 2.20A-D).

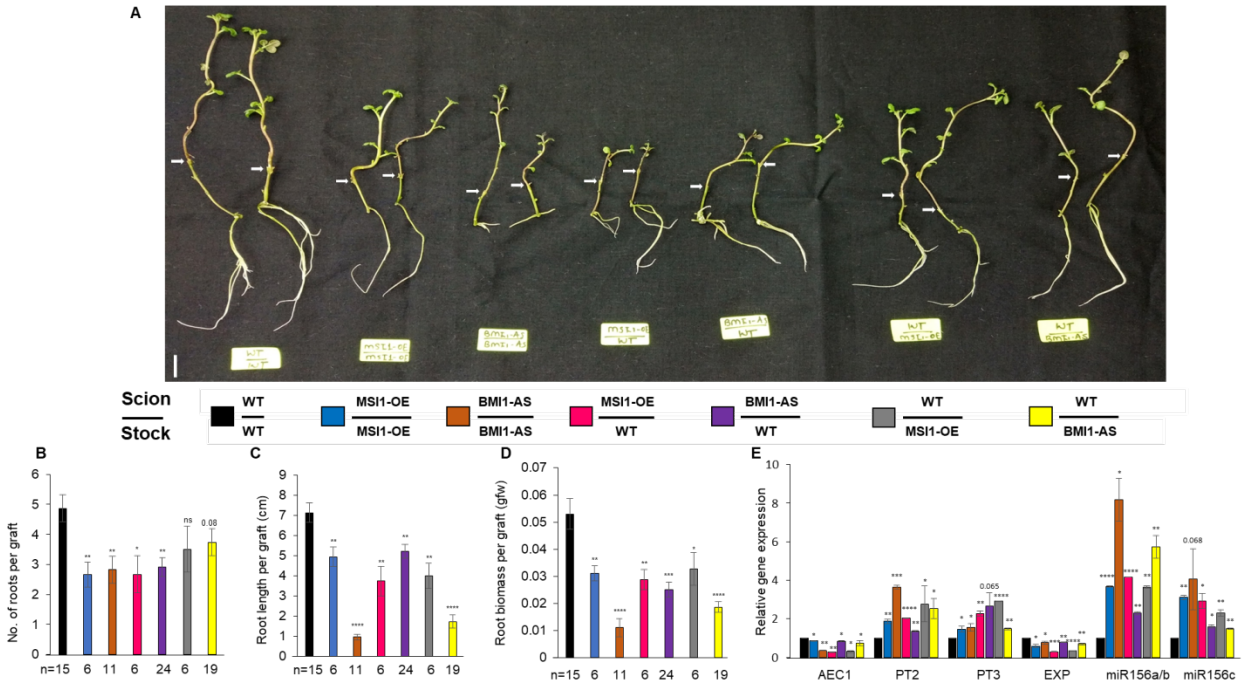

Figure 2.20. **Hetero-grafts of StMSI1-OE or StBMI1-AS line with wild-type (WT) plants**. Two representative images of *in vitro* grown plants are shown for each combination of homo- and hetero-grafts after 3-weeks of graft-initiation (A). An average number of roots (B), root length (C), and root biomass (D) per homo- or heterograft are presented. Statistical analysis was performed using t-test assuming unequal variances. Number of biological replicates (n) per each homo- or hetero-graft combination are shown below graphs. Statistical significance with one, two, three and four asterisks indicating p-values of < 0.05, < 0.01, < 0.001 and < 0.0001, respectively. ns = not significant. Comparison for each homo- or hetero-graft was performed with respect to WT/WT homograft. Scale bar in (A) is 1 cm. Arrows (white) indicate the graft unions. Relative transcript levels of auxin and cytokinin transport/signaling genes as well as pre-miR156a/b and pre-miR156c levels in roots of different homo- and hetero-grafts after 21 days (E). In panel E, the mean values of two biological replicates per graft combination were plotted. *EIF3e was* used as a reference gene for qRT-PCR analysis. Error bars represent ±SD. AEC1, Auxin efflux carrier 1; PT, Purine transporter; EXP, Expansin, miR156a/b, pre-miR156a/b; miR156c, pre-miR156c

To analyze the cause of reduced root growth, the expression of auxin and CK transport/signaling genes was quantified in roots of all homo- and hetero-grafts (Figure 2.20E). The expression levels of *auxin efflux carrier 1* and *expansin* were reduced, whereas, those of CK transporters (purine transporter 2 and -3) were increased in all homo- and hetero-grafts compared to WT homo-grafts (Figure 2.20E), Additionally, we found that the precursor levels of miR156a/b and miR156c were also high in roots of all homo- and hetero-grafts compared to WT homo-grafts (Figure 2.20E).

2.3.13 ChIP-qPCR shows enrichment of H3K27me3 and H3K4me3 over *StBMI1-1* and miR156 genes respectively

We noted the upregulation of miR156a/b/c (Figure 2.9E) and suppression of *StBMI1-1* and *StBMI1-3* (Figure 2.9F) in the *StMSI1-OE* line. To understand the possible crosstalk between these regulators, ChIP-qPCR analysis was performed to quantify the level of the repressive mark (H3K27me3) at the first intron of *StBMI1-1* and *StBMI1-3* genes. Our analysis found that the levels of H3K27me3 on *StBMI1-1* and *StBMI1-3* genes were significantly increased in the *StMSI1-OE* line (Figure 2.21 A). Apart from increased levels of miR156a/b/c (Figure 2.9E), the expression of miR156e was also high in leaves of *StMSI1-OE* and *StBMI1-1-AS* lines (Figure 2.21B). Moreover, the miR156f level was high in the *StMSI1-OE* line; however, it was surprisingly low in the *StBMI1-1-AS* line (Figure 2.21B). The transcript level of trithorax members having histone H3K4 methyltransferase activity (*SET7/9* and *SDG4*) was significantly higher in both *StMSI1-OE* and *StBMI1-1-AS* lines compared to VC (Figure 2.21B). Hence, we tested the possibility of miR156 activation by quantifying the levels of H3K4me3 marks made by trithorax members. We observed that H3K4me3 marks were increased in the upstream regions of different miR156 family members (miR156b, miR156e, miR156f, and miR156g) in *StMSI1-OE* and *StBMI1-1-AS* lines (Figure 2.21C).

2.3.14 RLM-RACE confirms miR156-mediated cleavage of *StSPL13*

From RNA-seq data, three *SPL* genes, including *StSPL8*, *StSPL9,* and *StSPL13,* were differentially downregulated in *StMSI1-OE* or *StBMI1-1-AS* lines (Supplemental Tables S2-3). Of these, *StSPL9* and *StSPL13* are predicted to be cleaved by different miRNA156 members. Through a degradome analysis, Seo et al. (2018) recently showed that *StSPL13* is cleaved by miR156 in potato. In our analysis, we observed that the transcript levels of *StSPL6* and *-13* were

significantly reduced in both *StMSI1-OE* and *StBMI1-1-AS* lines compared to VC (Figure 2.21D). However, *StSPL3* and *-8* transcript levels remain unchanged in the *StMSI1-OE* line, but both were significantly reduced in the *StBMI1-1-AS* line (Figure 2.21D). Further, psRNATarget analysis predicted that miR156e/f-5p/g-5p can also cleave *StSPL13* with an expectancy-value of E=1.0, followed by miR156a/b/c members. Through a modified 5' RLM-RACE assay, we confirmed that the *StSPL13* transcript is cleaved by miR156 members with 100% cleavage efficiency (7 out of 7) at the $11^{th}/12^{th}$ nucleotide position (Figure 2.21E). However, it may be noted that the cleavage site confirmed here on *StSPL13* transcript is different than that reported in Bhogale et al. (2014),

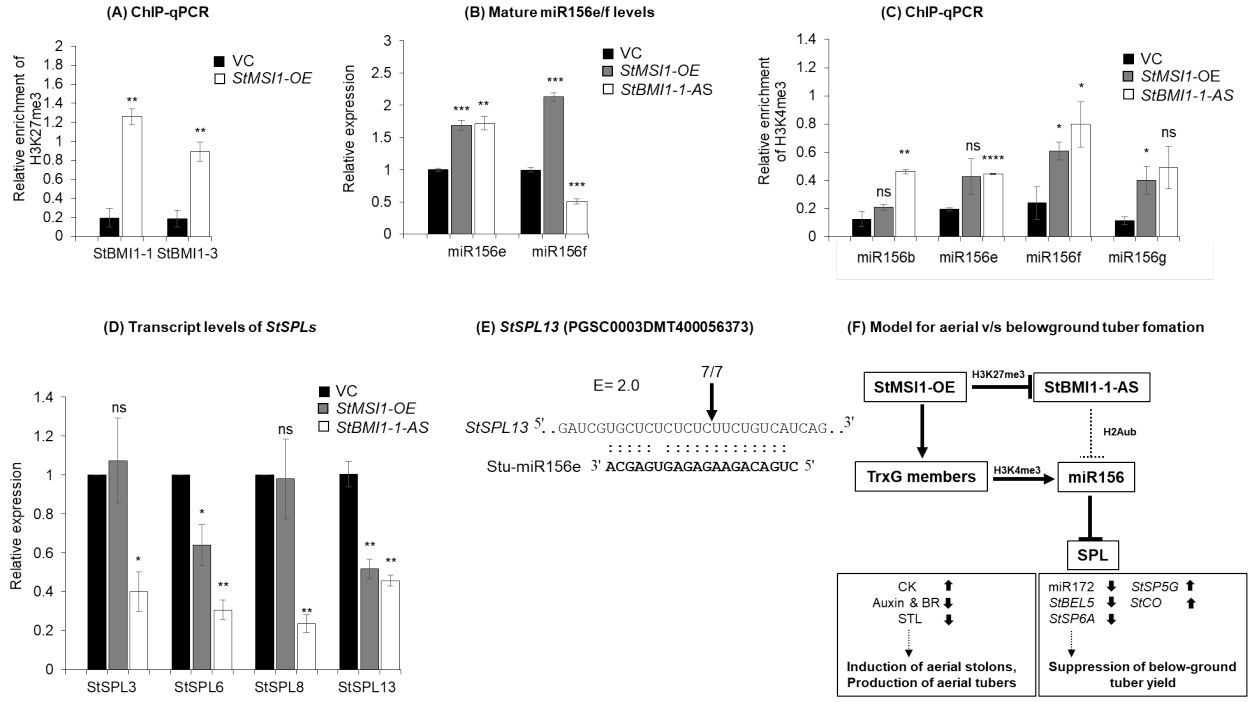

Figure 2.21. ChIP-qPCR validates H3K27me3-mediated repression of *StBMI1* and H3K4me3-mediated activation of miR156. The enrichment of H3K27me3 repressive marks on the promoters of *StBMI1-1* and *-3* in the *StMSI1-OE* line (OE3) compared to VC (A). The relative levels of miR156e and miR156f in *StMSI1-OE* and *StBMI1-AS* lines compared to vector control (VC) (B). The enrichment of H3K4me3 activation marks over the promoters of miR156 members in the transgenic lines - *StMSI1-OE* and *StBMI1-AS* compared to VC (C). The relative levels of *StSPLs (StSPL3, -6, -8, and -13)* in *StMSI1-OE* and *StBMI1-AS* lines compared to VC (D). Alignment of *StSPL13* transcript and miR156f-5p is shown with the predicted efficiency of cleavage (E=2). '7/7' represents the actual cleavage frequency after RLM-RACE analysis (E). The relative enrichment of respective marks in *StMSI1-OE* and *StBMI1*-AS lines was calculated with respect to the VC sample. Student's t-test was performed to check significance with one, two, three and four asterisks indicating p-values of < 0.05, < 0.01, < 0.001 and < 0.0001, respectively. ns = not significant. Error bars represent ± SD from three biological and three

technical replicates. *EIF3e* or *U6* was used as a reference gene. The proposed model considering the cross-talk between StMSI1, StBMI1-1, and miR156 during aerial and below-ground tuber formation in potato under SD photoperiodic conditions (F).

suggesting a different member of the miR156 family is cleaving the *StSPL13* transcript rather than miR156a/b/c. Additionally, psRNATarget analysis (Dai and Zhao, 2011) of 1023 common DE genes unveiled that many of these genes could be targets of different miRNAs (Supplemental Table S8).

2.3.15 Promoters of *StMSI1*, *StBMI1,* and miR156 members have numerous LREs

When the promoter sequence of *StMSI1* (~1.5 kb) was analyzed by PlantCARE tool, we could identify several light regulatory motifs (LREs), e.g. Box4 motifs (2), GT1 motifs (4), GA motif (1), TCT motifs (2), and one ATCT motif (Supplemental Table S9). In addition, two CAT-box motifs related to meristem expression were identified in its promoter sequence (Supplemental Table S9). Similarly, several LREs were found in the 1.5 kb promoters of all eleven miR156 members in potato (miR156a-k) and three *StBMI* genes (*StBMI1-2, -3*, and *-4*) (Supplemental Table S9) Additionally, numerous PREs were identified in the promoters of miR156 members and *StBMI1* genes (*StBMI1-2, -3* and *-4*) (Supplemental Table S10).

2.4 Discussion

PcG proteins are important regulators of plant development and control the expression of homeotic genes involved in the meristematic activity and organ differentiation (Goodrich et al., 1997). Previous studies in Arabidopsis have shown that a large number of miRNAs involved in phytohormone regulation and other key developmental processes are also regulated by PcG proteins (Lafos et al., 2011; Teotia and Tang, 2015). Although much progress has been made to understand the role of PcG proteins in Arabidopsis, their role in potato development remains to be explored. Here, we have shown that two PRC members, StMSI1 and StBMI1-1, regulate tuber development in potato by controlling the expression of miR156 and hormonal response in a photoperiod-dependent manner.

2.4.1 Short-day photoperiod influences expression of *StMSI1*, *StBMI1-1* and miR156 in stolon

MSI1 is a crucial component of several histone modifier complexes that are involved in meristem maintenance, branching, flowering, and leaf and ovule development (Hennig et al., 2003; 2005). Previous studies (Hennig et al., 2003; Liu et al., 2016) showed ubiquitous expression of *MSI1* in Arabidopsis and tomato. Similarly, we noticed a ubiquitous expression pattern of GUS in the *promStMSI1::GUS-pBI121* potato lines, with the highest expression in axillary-nodes and root tips (Figure 2.6C; F). Additionally, when these promoter lines were subjected to LD/SD induction, GUS expression was higher in swollen stolon under the SD photoperiod compared to stolon from LD (Figure 2.6G-H). qPCR analysis further validated the higher expression of *StMSI1* in stolon under SD conditions (Figure 2.6A). These observations indicate that the photoperiod could regulate *StMSI1* expression in potato. In potato, miR156 has been shown to play an important role in controlling tuber development, and its expression increases in stolons under the SD photoperiod (Bhogale et al., 2014). Additionally, both in potato and Arabidopsis, miR156 has been shown to control juvenile-to-adult phase transition by targeting SPL proteins; miR156 is highly expressed during the juvenile phase but remains suppressed during adult phase of the plant (Wu et al., 2009; Bhogale et al., 2014). Interestingly, in our study, the expression pattern of both *StMSI1* and miR156 was similar in stolon during SD induction as well as in leaves during juvenile and adult phases in the potato plant (Figure 2.9I). Apart from the factors reported in several studies (Hsieh et al., 2009; Lee et al., 2010; Xin et al., 2010; Yu et al., 2012; 2013; Yang et al., 2013), recently, a PRC1 member (AtBMI1) has been shown to control miR156 expression in Arabidopsis (Pico et al., 2015). We found that *StBMI1-1* expression was significantly low, whereas that of miR156 was high in shoot tip and stolon under the SD photoperiod compared to LD conditions (Figure 2.12A). Further, the presence of numerous LREs in the promoters of *StMSI1* and *StBMI1* genes and eleven miR156 members in potato (miR156a-j) (Supplemental Table S9) suggest that photoperiod could regulate the expression of these genes. The identification of PREs in the promoters of all miR156 members (Supplemental Table S10), suggests a possible role of PcG proteins in photoperiod-mediated regulation of miR156 during the stolon-to-tuber transition in potato. In the present report, *StMSI1* overexpression and *StBMI1* knockdown lines had an increased level of miR156 (Figure 2.9E; 2.12J) and both showed phenotypes similar to miR156 overexpression, including aerial tubers

(Figure 2.9C-D; 2.12K) and reduced below-ground tuber yield (Figure 2.15D; F), suggesting that StMSI1 and StBMI1-1 function upstream of miR156 in potato.

2.4.2 *StMSI1-OE* and *StBMI1-1-AS* lines exhibit altered plant architecture and reduced tuber yield

Both *StMSI1-OE* and *StBMI1-AS* lines had drastic changes in overall plant architecture (Figure 2B; 4E), including reduced leaf compounding, lamina size, petiole length (Figure 2.9B-C; 2.12E-F), root biomass (Figure 2.8G; 2.12I), and tuber yield (Figure 2.15D; F). The *StMSI1-OE* line also showed increased numbers of leaf stomata, trichome length, and altered stem vascular bundles (Figure 2.7 G-N). We demonstrated earlier that miR156 overexpression leads to reduced leaf size, compounding, and tuber yield in potato (Bhogale et al., 2014). We observed that *StMSI1-OE* and *StBMI1-AS* lines had a five- and two-fold increase of miR156 expression, respectively (Figure 2.9E; Figure 2.12J). SPLs, the targets of miR156 work antagonistically to TCP (TEOSINTE BRANCHED1/CYCLOIDEA/PCF) transcription factors belonging to class-II CINCINNATA subgroup during leaf development (Rubio-Somoza et al., 2014). The reduced transcript levels of several SPLs, including *StSPL6* and *-13* in both lines (*StMSI1-OE* and *StBMI1-AS*) (Figure 9D) and RLM-RACE mediated validation of *StSPL13* cleavage by miR156 (Figure 2.21E), further justifies the reduced leaf size and compounding phenotype in both transgenic lines. A number of reports (Uchida et al., 2007; Hay and Tsiantis, 2010, Mahajan et al., 2016) have demonstrated that class-I *KNOX* genes regulate meristem activity, leaf architecture, and compounding. The high level of *POTH15* (a class-I *KNOX* gene in potato) transcript in the *StMSI1-OE* line and the presence of approximately 800 common DE genes between *POTH15*-OE and *StMSI1*-OE line could also be the cause of altered leaf architecture. In *StMSI1-OE* and *StBMI1-AS* lines, we noticed downregulation of several genes coding for auxin efflux carriers (PIN proteins), HD- ZIP TFs, and BR signalling pathway genes (Figure 2.18A-B), which have been shown to affect vascular bundle formation (Mattsson et al., 1999; Sieburth, 1999; Lee et al., 2018).

PcG proteins control the development of primary and lateral roots through regulating stem cell activity (Aichinger et al., 2011) and auxin transporter PIN1 expression (Gu et al., 2014). Auxin and BR stimulate, whereas CK inhibits lateral root development (Mussig et al., 2003; Aloni et al., 2005). Our RNA-seq data showed high expression of CK and low expression

of auxin and BR signaling related genes (Figure 2.18B;). A number of genes, such as *PINs*, *PLETHORA (PLT)*, *SCARECROW*, and *ARFs* that are involved in root development (Blilou et al., 2005, Aida et al., 2004, Sabatini et al., 2003, Wang et al., 2005) were affected in *StMSI1-OE* or *StBMI1-1-AS* line, possibly explaining the reduced root growth phenotype. Similar to miR156-OE lines (Bhogale et al., 2014), *StMSI1-OE* and *StBMI1-1-AS* lines showed a significant reduction in below-ground tuber yield than WT plants (Figure 2.15D; F). In contrast, *StBMI1-1-OE* lines showed increased tuber yield (Figure 2.15F). We further noticed *StMSI1-AS* lines had comparatively reduced plant architecture and tuber yield (Figure 2.15D). Considering MSI1 functions as a component of both activator and repressor complexes, we assume that its moderate levels are essential for tuber development. Similar results were also observed in the *in vitro* tuberization experiment (Figure 2.15A). One of the reasons for the reduction in the below-ground tuber yield could be due to the weaker plant architecture of these lines than WT. Further, the downregulation of crucial tuber marker genes downstream of miR156 in the tuberization pathway, for example miR172 (Martin et al., 2009), *StBEL5* (Banerjee et al., 2006a), and *StSP6A* (Navarro et al., 2011), and the upregulation of tuber growth repressors (*StPHYB*, *StCO* and *StSP5G*; Jackson et al., 1996; Navarro et al. 2011; Kloosterman et al., 2013), could be another reason for reduced tuber yield in these lines (Figure 2.15B; Supplemental Tables S2-3). Moreover, we observed an increase in miR156 (Figure- 2.9E, 2.12 C), but a reduction in miR172 expression (Figure 2.15B) in *StMSI1-OE* and *StBMI1-1-AS* lines. psRNATarget analysis unveiled numerous common DE genes as targets of different miRNAs, including miR156 and -172. About 247 common DE genes (of 1023) related to plant growth and development were predicted to be cleaved by miR156 and miR172 family members (Supplemental Table S8), suggesting that altered levels of miR156 and miR172 and their potential downstream target genes could have also contributed to the low tuber yield phenotype. Interestingly, grafting of *StMSI1-OE* or *StBMI1-1-AS* on wild-type stock resulted in reduced root biomass (Figure 2.20A-D) and showed increased accumulation of miRNA156a/b and -c precursors in the roots of wild-type stocks (Figure 2.20E), suggesting that PRC proteins could have influenced the accumulation of miR156 in roots. The reduced root biomass in these hetero-grafts could possibly be due to altered expression of genes encoding auxin and CK transport/signaling proteins in roots of these hetero-grafts (Figure 2.20 E). These findings are consistent with the earlier report of Bhogale et

al. (2014), where the authors demonstrated that miR156 functions as a potential mobile signal in potato.

2.4.3 Crosstalk of histone modifiers regulates miR156 and alters hormonal response during aerial tuber formation in *StMSI1-OE* and *StBMI1-1-AS* lines under SD photoperiod

In potato plant, every axillary meristem possesses the ability to form a stolon/tuber, however, this potential remains suppressed in all meristems except the below-ground one (Ewing and Struik, 1992). In this study, *StMSI1-OE* and *StBMI1-1-AS* lines produced aerial stolons/tubers from axillary-nodes (Figure 2.9A-D; Figure 2.12K), a phenotype that matched with our previous demonstration of miR156 overexpression in potato (Bhogale et al., 2014). Both of these lines showed high levels of miR156 expression (Figure – 2.9E, 2.12 C), indicating a possible regulation of miR156 either through StMSI1 or StBMI1-1. *StBMI1-1-AS* lines show a weaker phenotype of aerial tuber development than either *StMSI1-OE* or *miR156-OE* lines. It could be because of a lower level of RNA suppression (which was about 35%) in the *StBMI1-1-AS* line (#G9). Also, it is possible that the function of four potato BMI proteins could be redundant. Hence, silencing only *StBMI1-1* might not result in a more robust phenotype. Recent studies have demonstrated BMI-mediated suppression of miR156 (Pico et al., 2015) triggers onset of the adult phase in Arabidopsis, which is consistent with our observation of increased miR156 levels in *StBMI1-1-AS* line in potato (Figure 2.12J). Moreover, the presence of multiple BMI1-binding motifs (Merini et al., 2017) in the promoter and precursor sequences of miR156 further supports the notion. However, the reason behind the increased level of miR156 in the *StMSI1-OE* line (Figure 2.9E) and the aerial tuber phenotype (Figure 2.9C-D) was not clear. RNA-sequencing of axillary-nodes from both of these lines provided crucial insights into StMSI1-mediated regulation of miR156.

The *StMSI1*-OE line exhibited altered expression of several genes encoding histone modifiers (Supplemental Table S2). For example, the expression of PRC1 members, such as *StBMIs* (*StBMI1-1*, *1-3* and *1-4*) and *StLHP1*, was reduced in the *StMSI1-OE* line. BMI1 and LHP1 maintain repressed states of target genes through assisting H2A ubiquitination and maintaining H3K27me3 modification, respectively (Derkacheva et al., 2013). Additionally, genes encoding *Histone Deacetylase 19* (*HDAC19*; Supplemental Table S2), ring finger proteins, and E3 ubiquitin ligase PUB14, involved in suppression of target genes, were downregulated

(Supplemental Table S4; common down sheet). Enrichment of the repressive mark (H3K27me3) on the first introns of *StBMI1-1* and *-3* genes in *StMSI1-OE* line (Figure – 2.21A), as well as the presence of several PREs in *StBMI* (*StBMI1-2, StBMI1-3* and *StBMI1-4*) promoters), further supports the regulation of *StBMI1* genes by PRC2 complex. In the *StMSI1-OE* line, we further observed upregulation of genes encoding JMJC domain-containing H3K9 demethylase (Sun et al., 2008) and trithorax members (*SDG4* and *SET7/9*; Figure 2.17B), which are involved in catalyzing H3K4 methylation of target genes (Cartagena et al., 2008). Moreover, ChIP assay confirmed the increased enrichment of H3K4me3 modification of the miR156 promoter (Figure 2.21 C). On the basis of the above findings, we assume that the combined effect of reduction in repressive histone ubiquitination and the increase in expressive methyl modification of the miR156 locus might have resulted in its enhanced expression in both *StMSI1-OE* and *StBMI1-1-AS* lines. Additionally, the presence of PREs and BMI1-binding motifs in the promoters of miR156 members, suggests that PcG proteins can regulate miR156 expression in potato.

From the RNA-seq analysis, we observed that 1023 differentially expressed genes were common between *StMSI1-OE* and *StBMI1-1-AS* lines. Subsequent analysis of these common DE genes hinted at the cause of aerial stolon/tuber formation from axillary-nodes of these lines. Bhogale et al. (2014) showed that *miR156-OE* lines had higher levels of CK as well as increased expression of CK biosynthesis gene (*LONELY GUY1; LOG1)* and a responsive gene (*StCyclin D3.1*). In tomato, Eviatar-Ribak et al. (2013) demonstrated that overexpression of *SlLOG1* causes development of mini-tubers from axillary-nodes in tomato. Interestingly, in both *StMSI1-OE* and *StBMI-1-AS* lines, we also found increased expression of CK transport and response genes in axillary-nodes (Figure – 2.18). Although we could not find CK biosynthesis genes to be differentially expressed in *StMSI1-OE* and *StBMI1-AS* lines in the RNA-seq data, we observed that the expression of *StLOG3* was high in leaves of the *StMSI1-OE* line (Figure 2.9H). Besides this, both of the transgenic lines shared a number of common DE genes with that of *SlLOG1* overexpression lines as described in Eviatar-Ribak et al. (2013), indicating that common downstream effectors of PcG and/or *LOG* genes could be involved in aerial tuber development. These results are consistent with the role of CK as a branching stimulator (Domagalska and Leyser, 2011) and a tuber inducer (Palmer and Smith, 1969). Two previous studies (Eviatar-Ribak et al., 2013; Bhogale et al., 2014) emphasized the potential role of CK during aerial tuber development. Although the role of auxin in developmental phase transition of stolon-to-tuber

(Roumeliotis et al., 2012) is well established, its role in aerial stolon/tuber development was not known. In our RNA-seq analysis, we noted a reduced expression of several auxin transport and signaling genes in *StMSI1-OE* and *StBMI1-1-AS* lines (Figure 2.18B-C), suggesting the involvement of auxin in aerial stolon formation from axillary-nodes.

To summarize, we propose a model to explain PcG protein mediated regulation of tuber development in potato. StBMI1-1 suppresses miR156 expression, whereas StMSI1-OE induces miR156 expression by downregulating *StBMI1-1*. Further, StMSI1-OE increases the expression of miR156 through Trithorax members involved in H3K4me3 modification. Increased miR156 causes downregulation of key tuberization genes (miR172, *StBEL5, StCO, StSP5G*, and *StSP6A*), which results in reduced below-ground tuber yield in *StMSI1-OE* and *StBMI1-1-AS* lines. Additionally, reduced expression of auxin, BR, and STL (Pasare et al., 2013) related genes and increased expression of CK transport/signaling genes in the axillary-nodes of both transgenic lines inhibit the apical dominance effect and stimulate the induction of axillary stolons. Finally, the reduced expression of GA biosynthesis and signaling genes could support the development of aerial tubers from axillary stolons under SD photoperiod (Figure 2.21F).

2.5 Availability of supplementary information and raw sequencing data

All the supplementary tables (S1 – S13) mentioned in this chapter are available online at plant physiology website and can be accessed using the following link –
http://www.plantphysiol.org/content/early/2019/08/16/pp.19.00416/tab-figures-data

The raw sequencing data were deposited in the NCBI Short Read Archive (SRA) database (http://www.ncbi.nlm.nih.gov/sra/) and can be retrieved using the accession number PRJNA546591

Findings of this chapter have been published in the following research article:

Kumar, A., Kondhare, K. R., Vetal, P. V. & Banerjee, A. K.(2019) Polycomb group proteins StMSI1 and StBMI1 regulate microRNA156 during aerial tuber formation in potato under short-day photoperiod (**Plant Physiology**, DOI:10.1104/pp.19.00416).

Chapter 3

Functional characterization of StE(z)2 (a H3K27 methyltransferase) as a potential epigenetic regulator in potato

3.1 Introduction

Flowering in Arabidopsis and tuberization in potato are both reproductive phenomena and known to be governed by a set of common molecular regulators and various environmental cues, such as temperature and duration of light (photoperiod) (Martinez-Garcia *et al.,* 2002). A number of mobile signals, including full-length mRNAs (Banerjee *et al.,* 2006a; Mahajan *et al.* 2012), microRNAs (Martin *et al.,* 2009; Bhogale *et al.,* 2014) and the Flowering Locus T (FT) orthologous protein StSP6A (Navarro *et al.,* 2011) have been shown to regulate tuberization in potato. Upon perception of the tuberization signals in stolons under short-day (SD) conditions, dynamic changes orchestrate the pattern and fate of cell division at the sub-apical region of stolon (belowground modified stem). The cell division pattern changes from longitudinal to transverse plane leading to a radial swelling of the stolon sub-apex (Xu *et al.,* 1998a), accompanied by the synchronized process of photosynthate on-loading in veins of leaves and off-loading into the swelling stolon that ultimately transitions into a mature tuber. Auxin, cytokinin (CK), and gibberellin (GA) play a critical role in initiating the stolon-to-tuber transition stages in potato (Palmer and Smith, 1969; Aksenova *et al.,* 2012; Roumeliotis *et al.*, 2012). Another distinct change that happens at the stolon tip is the reduction of bioactive GA levels, which is mediated through the interaction of BEL-KNOX (StBEL5-POTH1) heterodimer and the StSP6A protein with the promoters of GA metabolism genes, such as *StGA20ox1* (Chen *et al.,* 2004) and *StGA2ox1* (Navarro *et al.*, 2011), respectively. At the onset of tuberization, the expression of StSP6A protein (Navarro *et al.*, 2011) as well as the mRNAs of *StBEL5* (Banerjee *et al.,* 2006a) and *POTH1* (Mahajan *et al.*, 2012) increase in stolon under SD conditions. Additionally, the expression of genes encoding *starch synthase* (Nazarian-Firouzabadi and Visser, 2017), *sucrose transporter* (Chincinska *et al.*, 2008; Abelenda *et al.*, 2019) and a storage protein *patatin* (Sonnewald *et al.*, 1989; Ewing and Struik, 1992) increase in stolon to coordinate the tuber development process. Moreover, StBEL5 targets ~ 10,000 genes in stolon, suggesting the complexity of the tuberization mechanism (Sharma *et al.*, 2016). In spite of the knowledge of numerous tuberization related genes, the regulatory mechanisms that control the differential expression of many of these genes during tuber development are not well understood.

Chromatin-remodeling through histone modification leads to Spatio-temporal regulation of genes that regulate developmental programs in response to environmental signals (Pikaard and Scheid, 2014). Polycomb Repressive Complex (PRC) and Trithorax Group (TrxG) proteins are important chromatin modifiers that antagonistically regulate target genes to ensure developmental transitions in plants (Pien and Grossniklaus, 2007). Several PRC proteins are shown to regulate flowering and hormonal pathways in Arabidopsis (Goodrich *et al.,* 1997; Jiang *et al.,* 2008; Shafiq *et al.,* 2014; Steinbach and Hennig, 2014; Gu *et al.,* 2014). The E(z) is the main catalytic subunit of PRC2 that adds H3K27me3 repressive modification on the target chromatin through the SET domain (Su(var)3-9, E(z), Trx) (Müller *et al.,* 2002). Previous studies demonstrated that PRC2 proteins are involved in diverse processes in plants, including regulation of hormonal pathways (Lafos *et al.*, 2011; Teotia and Tang, 2015), meristematic activity and organ differentiation (Goodrich *et al.*, 1997), vernalization (De Lucia *et al.*, 2008), flowering (Bouveret *et al.*, 2006; Steinbach and Hennig, 2014), and development of ovule, fruit and seed (Hennig *et al.*, 2003; 2005).

Based on the striking similarities between the flowering and tuberization pathways (Martinez-Garcia *et al.*, 2002), we hypothesized that PRC members could regulate tuber development. Recently, we showed that two PRC members *StMSI1* and *StBMI1-1,* are differentially expressed in stolons under the SD photoperiod and play a significant role in tuberization (Chapter 2; Kumar *et al.*, 2019). Notably, through RNA-sequencing of the StMSI1 over-expression (OE) line, we identified key genes involved in hormonal metabolism and tuber development potentially regulated by PRC proteins (Chapter 2). In the absence of any catalytic activity of StMSI1, it was unclear to us how these tuberization related genes were differentially regulated in the StMSI1-OE line. We speculated that this could be because of the chromatin modifications made by H3K27 methyltransferase StE(z)2, a CURLY LEAF (CLF) homolog belonging to the PRC2 clade. Earlier, Liu *et al.* (2014) showed that two E(z)2 homologs in a SD plant rice, OsSDG711, and OsSDG718, regulate the onset of flowering by controlling the expression of FT homologs in long-day (LD) and SD photoperiodic conditions, respectively. Since FT homolog (StSP6A) has a crucial role in the tuber initiation process (Navarro *et al.*, 2011), we decided to dissect the role of StE(z)2 in the photoperiod-dependent tuberization pathway using overexpression and knock-down strategies.

3.2 Materials and Methods

3.2.1 Plant material and growth conditions

Throughout this study, a photoperiod sensitive cultivar of potato (*Solanum tuberosum* ssp. andigena 7540) was used. Wild-type (WT) potato plants were multiplied *in vitro* by sub-culturing stem cuttings in basal Murashige, and Skoog's medium (Murashige and Skoog, 1962) supplemented with 2% sucrose. *In vitro* plants were maintained in plant growth incubator (Percival Scientific) at 22 °C with a light intensity of 300 μmol $m^{-2}s^{-1}$ under long-day (LD) photoperiodic conditions (16 h light/8 h dark). Fifteen days old *in vitro* grown plants were transferred to soil and maintained in plant growth chambers (Percival Scientific) at 22 °C under LD photoperiodic conditions.

3.2.2 Phylogenetic analysis and conserved domain identification of E(z)2-like proteins in potato

Full-length transcript and protein sequences of E(z)1, E(z)2- and CLF-like genes from Arabidopsis (*Arabidopsis thaliana*), tomato (*Solanum lycopersicum*), and potato were fetched from TAIR (https://www.arabidopsis.org/), NCBI (https://www.ncbi.nlm.nih.gov/), and Potato Genome Sequence Consortium (PGSC) databases (http://solanaceae.plantbiology.msu.edu/pgsc_download.shtml), respectively. The phylogenetic tree was prepared for E(z)2- or SDG4-like (a TrxG member) proteins from the plant mentioned above species using T-COFFEE (hRp://www.ch.embnet.org/soaware/TCoffee.html) and graphical representation was performed with TreeDyn (v198.3) (Dereeper *et al.,* 2008; http://www.phylogeny.fr/simple_phylogeny.cgi). The TreeDyn program uses MUSCLE programming (neighbor-joining) for alignment, Gblocks for curation, and PhyML for phylogeny analysis. Conserved domains from these proteins were identified using NCBI CD Search Tool (https://www.ncbi.nlm.nih.gov/Structure/cdd/wrpsb.cgi). DOG2.0 software (Ren *et al.,* 2009) was used to draw domain schematics. Genomic location and transcript variants of *StE(z)2* and *StSDG4* were retrieved through the PGSC database.

3.2.3 Tissue-specific gene expression analysis under SD and LD photoperiodic conditions

To investigate if SD/LD photoperiods have any influence on the expression of *E(z)2-like (StE[z]1* and *StE[z]2)* members in potato, *in vitro* grown WT andigena plants were transferred to soil and maintained under LD conditions for eight weeks. Later, half of the plants (having 8-10 leaves) were shifted to SD conditions (8 h light/16 h dark), whereas, the remaining plants were maintained under LD conditions at 22 °C in plant growth chambers. Different tissues, such as shoot tip, leaf, stem, root, and stolon, were harvested after 14 days post SD/LD induction. The total RNA was isolated using RNAiso Plus reagent (DSS-Takara) as per the manufacturer's instructions. Complementary DNA (cDNA) synthesis was performed using two µg of the total RNA, Superscript IV Reverse Transcriptase (Invitrogen) and oligo(dT) primers. Quantitative Reverse Transcription PCR (RT-qPCR) reactions were carried out on the CFX96 Real-Time System (BIO-RAD) with gene-specific primers (Supplementary Table S1) and TAKARA SYBR® green master mix (Takara-Clontech) by incubating at 95 °C for 3 min, followed by 40 cycles at 95 °C for 5 s, 60 °C for 30 s. Data were analyzed using the $2^{-\Delta\Delta Ct}$ relative fold-change method (Livak and Schmittgen, 2001). Moreover, the presence of different *cis*-regulatory elements in the *StE(z)2* promoter (1.9 kb) was identified using the PlantCare tool (http://bioinformatics.psb.ugent.be/webtools/plantcare/html/). The binding partners of potato StE(z)2, StMSI1, StLHP1 (LIKE-HETEROCHROMATIN PROTEIN 1), StZF2 and StTRB3 (Telomere Repeat Binding protein 3) were predicted using the STRING database (Szklarczyk *et al.,* 2017; https://string-db.org/).

3.2.4 Vector construction and transgenic lines generation

To generate constitutive over-expression (OE) construct of *StE(z)2* (*35S:StE(z)2-pBI121*), its full-length coding sequence (CDS; ~2.7 kb) was amplified by reverse transcriptase PCR using *in vitro* grown andigena plants with gene-specific primers (Supplementary Table S1). PCR amplified sequence was cloned into a sub-cloning vector pGEM-T Easy (Promega), sequence confirmed and further mobilized into the binary vector pBI121 downstream of Cauliflower Mosaic Virus (CaMV) 35S promoter (Xiang *et al.,* 1999). The *StE(z)2* promoter sequence (~1.9

kb) was amplified from andigena genomic DNA and cloned into a binary vector pBI121 upstream to *β-glucuronidase* gene (*uidA*) to generate the *promStE(z)2::GUS-pBI121* construct. *35S:StE(z)2-pBI121* and *promStE(z)2:GUS-pBI121* constructs were individually transformed into the *Agrobacterium tumefaciens* strain GV2260 and stable potato transgenic lines were generated as per the method described in Banerjee *et al.* (2006b). Transgenic andigena line containing the *35S:GUS-pBI121* construct was used as a vector control (VC) in all the subsequent experiments. A number of parameters, like leaf length (cm), a number of leaflets per leaf, root, and tuber biomass (gram fresh weight) were recorded at the end of 4 weeks of SD induction from WT, VC and *StE(z)2*-OE lines.

3.2.5 Analysis of *StE(z)2* promoter activity

To analyze the promoter activity, *promStE(z)2:GUS-pBI121* transgenic lines were grown *in vitro* under LD conditions for 20 days. These lines were also grown in soil for eight weeks in plant growth chambers, followed by LD/SD induction for 15 days. *In vitro* grown plantlets, as well as stolon and tuber samples from these lines, were subjected for GUS assay (Jefferson, 1987). After overnight incubation at 37 °C, samples were bleached with a series of ethanol gradient (50 to 100%), and photographed under a Leica Stereo Microscope (S8APO).

3.2.6 Histology and Scanning Electron Microscopy

For anatomical studies, a modified protocol of Cai and Lashbrook (2006) was followed on leaf and stem tissues of eight-weeks old LD grown (*StE(z)2-OE1* and WT) plants. Ten micrometer (10 μm) sections were obtained using Microtome (Leica) and photographed under the Zeiss Compound Microscope. External leaf architecture of *StE(z)2-OE1* and WT plants were documented using the Quanta 200 3D eSEM apparatus (FEI) under environmental mode (eSEM).

3.2.7 Virus-induced gene silencing (VIGS)

To study StE(z)2's function in potato development, Virus-Induced Gene Silencing (VIGS) method was employed to knockdown *StE(z)2* levels in WT andigena plants. For the VIGS construct preparation, the 721 bp region from *StE(z)2* CDS was amplified from the leaf cDNA using gene-specific primers (Supplementary Table S1). The amplified product was cloned

into a binary vector pGR106 using *ClaI* and *SalI* restriction sites. After sequence confirmation, the vector construct was transformed into the *Agrobacterium tumefaciens* strain GV3101 harboring helper plasmid pJIC SA_Rep. *Agrobacterium* culture containing the *StE(z)2-pGR106* construct was infiltrated into the leaves of 4-weeks old soil-grown plants as per the protocol described in Du *et al.* (2014). Three leaves from 10 individual plants were infiltrated with the *StE(z)2-pGR106* VIGS construct, whereas another set of plants were infiltrated with *Agrobacterium tumefaciens* containing the empty pGR106 vector (VC). To validate the suitability of the VIGS mechanism in andigena, the *phytoene desaturase* VIGS construct (*StPDS-pGR106*) was also infiltrated into the leaves as a positive control. WT and infiltrated plants were maintained under controlled environmental conditions in plant growth chambers (Percival Scientific) for 20 days at 22 °C and light intensity of 300 μmol $m^{-2}s^{-1}$. Post 20 days of infiltration, leaves of *StPDS-pGR106* showed the initiation of bleaching phenotype that persisted for almost two months. Hence, after 20 days of infiltration, half of the *StE(z)2-pGR106* infiltrated and VC plants were shifted to other chamber and maintained under SD condition for the downstream analysis. Silencing of *StPDS* and *StE(z)2* transcripts were checked from leaves using RT-qPCR analysis. After one month of SD treatment, plants were scored for belowground tuber yield.

3.3 Results

3.3.1 Potato E(z)2 is a homolog of Arabidopsis CLF protein

We identified three CLF-like proteins in potato; namely StE(z)1 (PGSC0003DMP400015912; XP_006349182.1), StE(z)2 (PGSC0003DMP400056358; XP_006361736.1) and PHCLF2 (PGSC0003DMP400007142; XP_015168875.1) (Figure 3.1A). BLAST analysis also revealed StE(z)2 has ~58% identity with Arabidopsis CLF (Goodrich *et al.,* 1997; Kim *et al.,* 1998), whereas it has 93% identity with tomato E(z)2-like protein. The sequence identity of StE(z)2 with the other two CLF homologs in Arabidopsis, MEDEA (MEA), and SWINGER (SWN) were 37 and 39%, respectively. The identity of StE(z)2 protein with two homologs of CLF in potato, is ~57% for StPHCLF2, and 48% for StE(z)1. Using the NCBI and PGSC databases, we observed that *StE(z)2* gene (~9.68 kb) resides on chromosome 3 (Figure 3.2) and has two transcript variants (XM_006361673.2 and XM_006361674.2) encoding for 922 and 890 amino acid (aa) (XP_006361735.1 and XP_006361736.1) respectively. Conserved

domain analysis and the amino-acid sequence alignment of AtCLF and StE(z)2 revealed close conservation of the SET domain (741 to 857 aa) with histone methyl transferase activity (Figure 3.1 B-C).

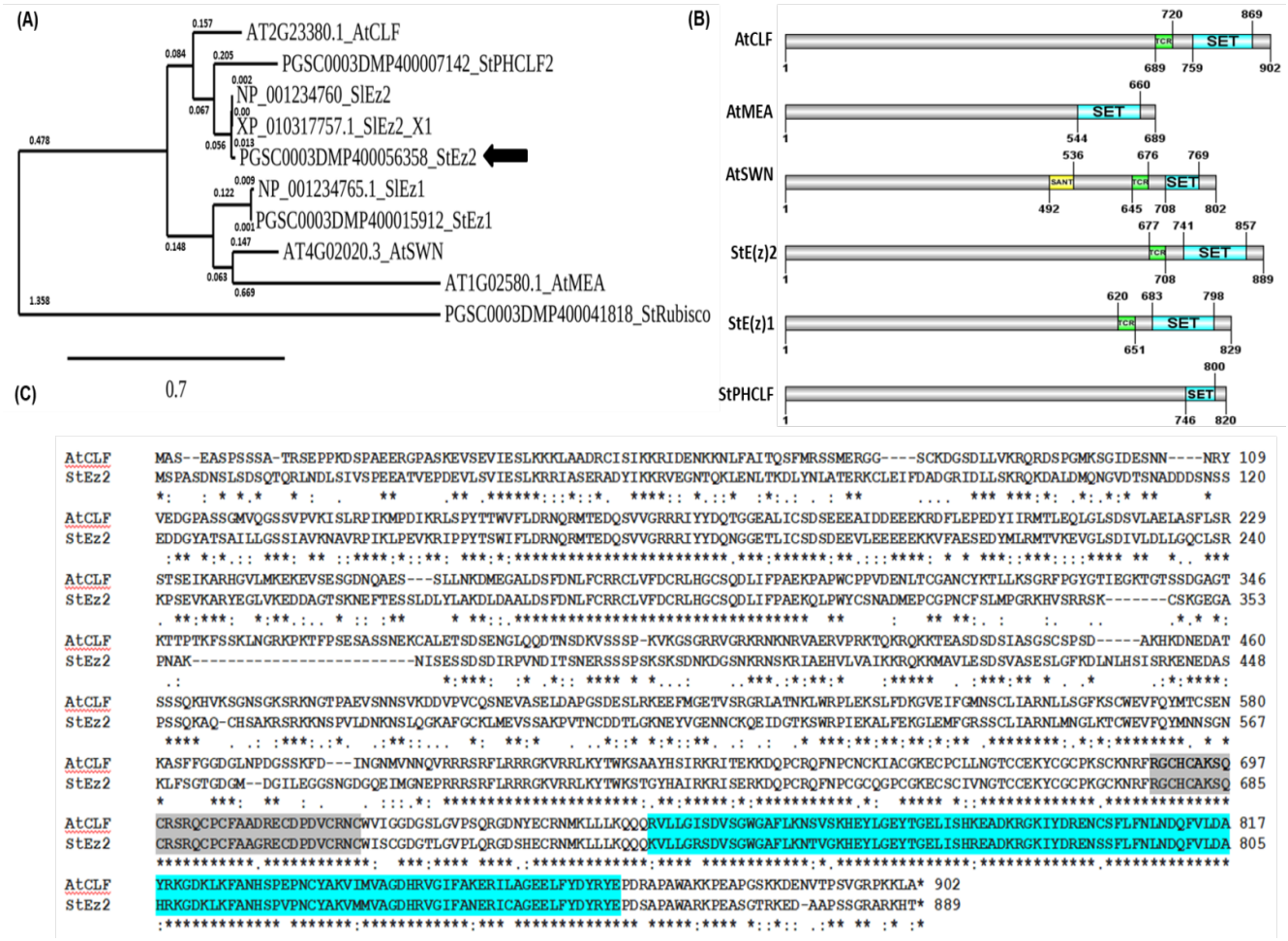

Figure 3.1. Phylogenetic analysis and amino acid sequence alignment of E(z)2-like proteins Phylogenetic analysis reveals a close conservation of potato E(z)2 with tomato E(z)2 and Arabidopsis CURLY LEAF (CLF). Phylogenetic analysis of E(z)2-like proteins from potato (StE(z)1, StE(z)2) and StPHCLF2), tomato (SlE(z)1, SlE(z)2 and SlE(z)2_X1 variant) and Arabidopsis (CLF, MEDEA [MEA] and SWINGER (SWN) (A). Accessions for protein sequences are mentioned in the phylogenetic tree along with the gene names. The branch length is proportional to the number of substitutions per site and the tree is re-rooted using midpoint rooting in TreeDyn. For rooting the tree, potato rubisco protein (a non-E(z)2 related protein) was used. *StE(z)2* gene (highlighted by arrow) was characterized in this study. Graphical representation of conserved domains in CLF homologs of Arabidopsis and potato (B). Amino acid alignment between Arabidopsis CLF and potato E(z)2 protein (C). The conserved SET domain (115 amino acids) catalyzing H3K27 trimethylation is highlighted in cyan, whereas the TCR domain (31 amino acids) having cysteine-rich motifs is highlighted in gray. At, *Arabidopsis thaliana*; St, *Solanum tuberosum;* Sl, *Solanum lycopersicum*.

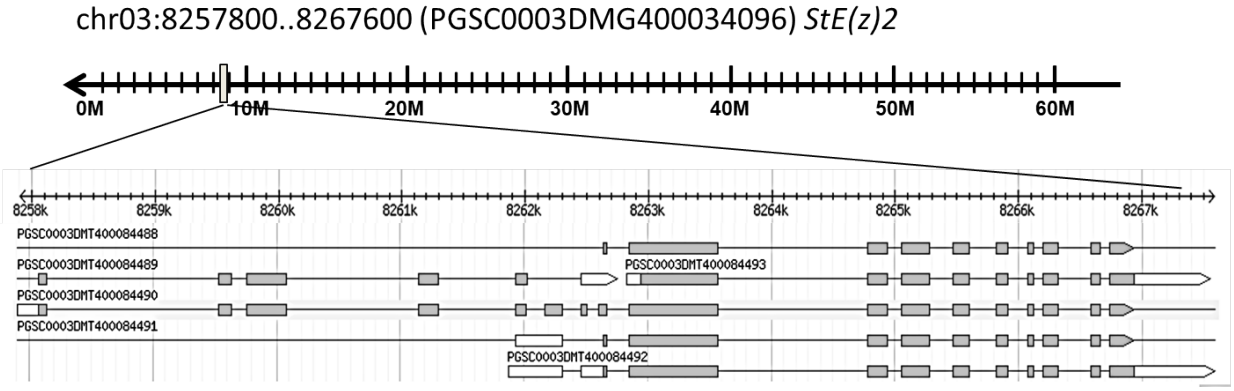

Figure 3.2. Locations of *StE(z)2* gene in the potato genome. Genomic locations were retrieved from the PGSC database for Phureja cultivar. Zoomed region shows the genome coordinates, and different transcripts coded by *StE(z)2* gene.

3.3.2 PRC2 members (StE(z)1 and -2) exhibit differential expression in stolon under SD/LD photoperiod

To see if photoperiod (LD or SD) has any influence on the expression of these genes, we studied the effect of LD/SD induction in 5 different tissue types of a photoperiod-sensitive potato variety (*S. tuberosum* ssp. andigena). Although PRC2 members (*StE(z)1* and *StE(z)2*) had varied gene expression patterns in all tissue types (Figure 3.3) in stolon, however, *StE(z)1* and *StE(z)2* had significantly reduced (40-50%) transcript abundance (Figure 3.3A-B) expression under SD conditions. Considering the fact that StE(z)2 has the highest identity with the AtCLF protein, we focused on *StE(z)2* variant (XM_006361674.2) in this investigation.

StE(z)2 promoter transgenic andigena lines (*StE(z)2::GUS-pBI121*) displayed GUS activity across different tissue types (Figure 3.3C-F). Interestingly, the reporter lines showed localized GUS activity in shoot apex (Figure 3.3E) and root-tips (Figure 3.3F). Moreover, *StE(z)2* promoter was also found to be active in the apical regions of LD- and SD-induced stolons as well as in tubers (Figure 3.3G-K). Consistently, seven light-responsive motifs were identified in the *StE(z)2* promoter (2 kb) (Supplementary Table S2).

3.3.3 PRC proteins could interact with telobox and GAGA binding proteins in potato

STRING analysis predicts that StE(z)2 could possibly interact with 200 different proteins, including StMSI1, StLHP1, and zinc finger protein, StZF2, involved in the PRC2

recruitment over the telobox motif at the target sites (Xiao *et al.* 2017). Similarly, StTRB3 involved in the recruitment of PRC (Zhou *et al.* 2015; 2018) and TrxG complexes over the GAGA rich sites at the target chromatins (Roy *et al.,* 2019) was predicted to interact with LHP1 (Supplementary Table S3). Moreover, TRB proteins were also predicted to interact with BEL1-like proteins (StBEL5 and -29), important regulators of the tuberization pathway (Supplementary Table S3).

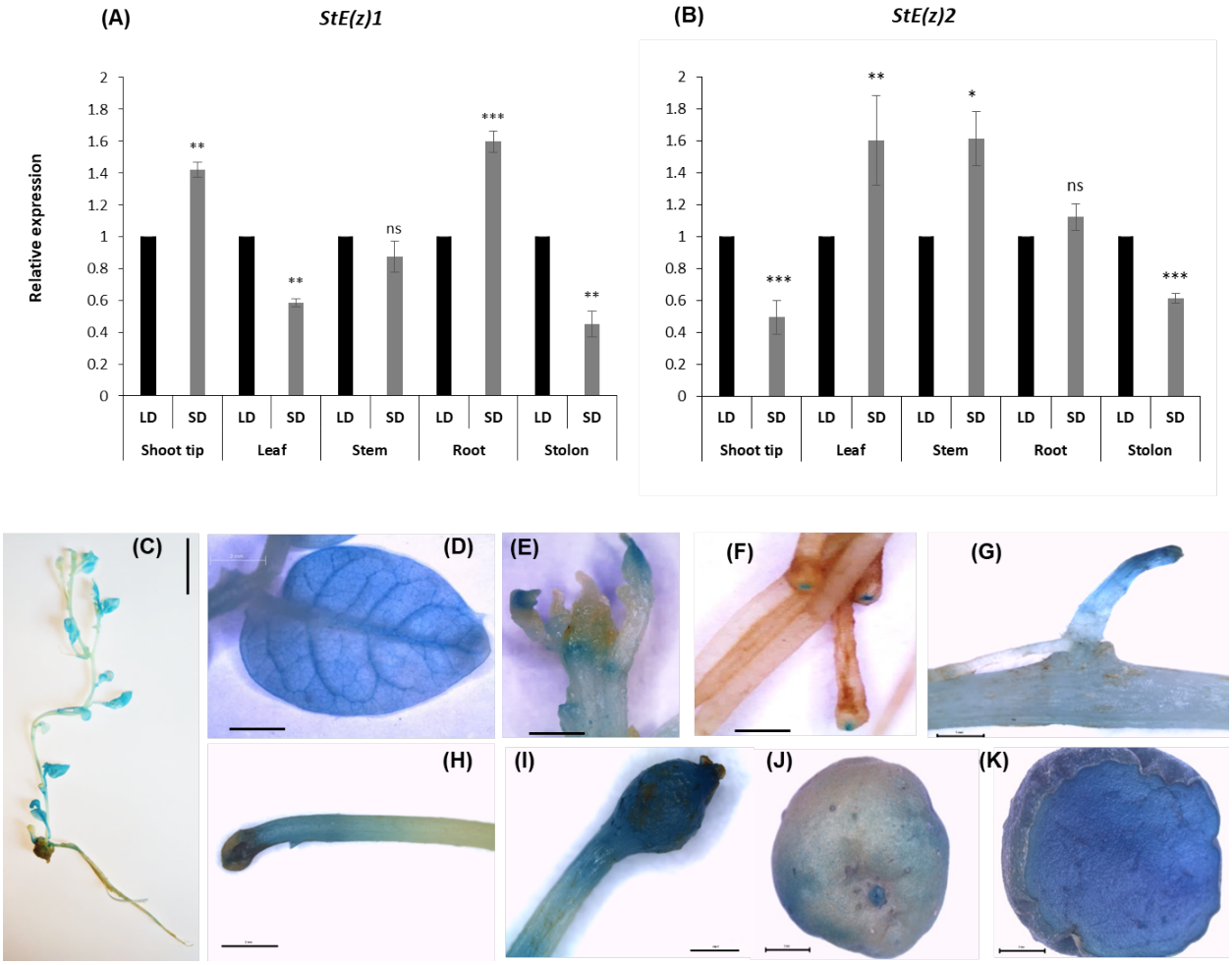

Figure 3.3. Short-day (SD) photoperiod influences the transcript accumulation of *StE(z)1*, *StE(z)2* in a tissue-specific manner. Effect of long-day (LD) and SD photoperiod on gene expression of *StE(z)1* (A), *StE(z)2* (B) and in different tissues (shoot tip, leaf, stem, root and stolon) of wild-type (WT) andigena (7540) potato plants grown under LD/SD conditions for 14 days, following 8-weeks of LD induction in soil (A). Relative fold-change of gene expression under SD conditions was calculated with respect to LD levels for each tissue type. Data are mean ±SD for three biological replicates. Each biological replicate had three technical replicates. *EIF3e* was used as a reference gene for RT-qPCR analysis. *StE(z)2* promoter andigena (7540)

line was grown for 3-weeks *in vitro* under LD conditions, and plantlets were incubated in GUS assay buffer (C). GUS activity in leaf (D), shoot apex (E), root tip (F), LD stolon (G), LD shooty stolon (H), SD swollen stolon (I), SD young tuber (J) and tuber-pith (K). Stolon and tuber samples are from soil-grown plants (2 months under LD conditions), which were further incubated under LD/SD conditions for 14 days before the GUS assay. Student's t-test was performed to check the level of significance. Asterisks (*, ** and ***) indicate significance at $p<0.05$, $p<0.01$ and $p<0.001$, respectively. ns=not significant. Scale bars: panel D-E = 2 cm, Panel F = 5 mm and panels H-L= 2 mm.

3.3.4 Overexpression of *StE(z)2* affects plant architecture in potato

To understand the function of *StE(z), 2* in potato (andigena), *StE(z)2* overexpression (OE) lines (OE1 and OE2) were generated (Figure 3.4A-C). *StE(z)2* overexpression affected the shoot architecture (Figure 3.4B), particularly leaf size (Figure 3.4D) and leaflet numbers (Figure 3.4E). Mature WT plants had the highest number of leaves with an average of 5 or 7 leaflets per leaf, whereas OE plants had either 5, 3 or 1 leaflet(s) per leaf (Figure 3.4E). Moreover, the leaves of the OE lines were smaller compared to WT plants (Figure 3.4D). Further analysis revealed that OE lines had bigger trichomes compared to WT leaves (Figure 3.4F-G). Additionally, the transverse leaf sections showed that the size of the vascular bundle was reduced in the OE line compared to the WT plant (Figure 3.4H-I). *StE(z)2*-OE lines also had a higher accumulation of miRNA156a/b/c precursor and mature miRNA166 levels in leaves, and altered expression of auxin (*AUX/IAA3*) and brassinosteroid (BR) (*Theseus kinase 1*) signaling related genes (Figure 3.4J). Interestingly, when two-months-old soil-grown plants (WT, VC, and *StE(z)2-OE*) having about 7-8 leaves were subjected for SD photoperiodic induction, they produced ectopic stolons and tubers from some of the axillary nodes (Figure 3.6A-C). Besides this, OE lines had reduced root length and biomass compared to WT plants (Figure 3.6D, F).

3.3.5 Over-expression or knockdown of *StE(z)2* influence belowground tuber yield

To check the effect of *StE(z)2* on tuber yield, OE lines were grown in soil for two months (LD), and after four weeks of SD photoperiod induction, they were scored for tuber yield. OE lines resulted in a significant reduction in tuber yield compared to WT plants (Figure 3.6E-F). *Agrobacterium*-mediated infiltration of the *StE(z)2-VIGS* constructs resulted in the silencing of *StE(z)2* transcript by 30 to 90% (Figure 3.6G). No change in the shoot or root architecture of *StE(z)2-* was observed in VIGS knockdown lines (Figure 3.6H-I). In contrast, *StE(z)2*-VIGS

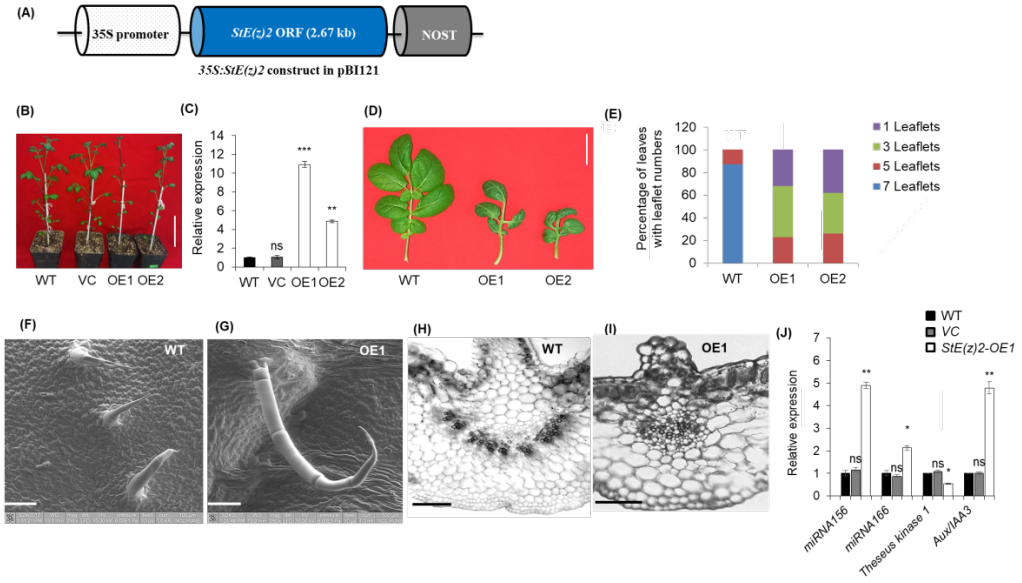

Figure 3.4. *StE(z)2* overexpression influenced the overall architecture of the potato plant. The schematic representation of the *35S:StE(z)2* construct (A). The phenotype of *StE(z)2* overexpression (OE) lines, OE1 and OE2 (B), and the relative transcript levels of *StE(z)2* in OE and vector control (VC) plants (C) compared to wild-type (WT). Leaf phenotypes, such as leaf size (D) and a number of leaflets per leaf (E) in WT and *StE(z)2* OE plants, are represented. For phenotypic comparisons, WT, VC, and *StE(z)2*-OE lines were maintained under long-day (LD) conditions for eight weeks. Data were collected from six biological replicates for each line. SEM images showing the trichome length in leaves of WT (F) and *StE(z)2*-OE line OE1 (G). Transverse cross-sections through the leaf mid-vein of WT (H) and *StE(z)2*-OE line OE1 (I). The levels of miRNA156a/b/c, miRNA166, *Theseus kinase 1,* and *AUX/IAA3* in leaves of *StE(z)2*-OE line and VC plants are shown in comparison to WT plants (J). Data are mean ±SD for three biological replicates. Each biological replicate had three technical replicates. *EIF3e* and *U6* were used as reference genes for mRNAs and miRNAs, respectively. The transcript level in WT was considered as 1 to calculate the relative fold-change. Student's t-test was performed to check the level of significance. Asterisks (* and **) indicate significance at $p<0.05$ and $p<0.01$, respectively. ns=not significant. Scale bars in panel B = 8 cm, D = 3 cm, F-I= 100 µm.

Silenced plants showed a variable increase in tuber yield (Figure 3.6J). As a positive control for the VIGS experiments, we silenced the *phytoene desaturase (StPDS)* gene in potato, and all the *PDS*-VIGS infiltrated plants showed leaf photobleaching phenotype (Figure 3.5). Interestingly, *StE(z)2*-OE lines had lower levels of key tuberization genes, such as *StBEL5*, *StSP6A,* and *StGA2ox1*; whereas their transcript levels were significantly higher in *StE(z)2*-VIGS infiltrated plant (Figure 3.6K).

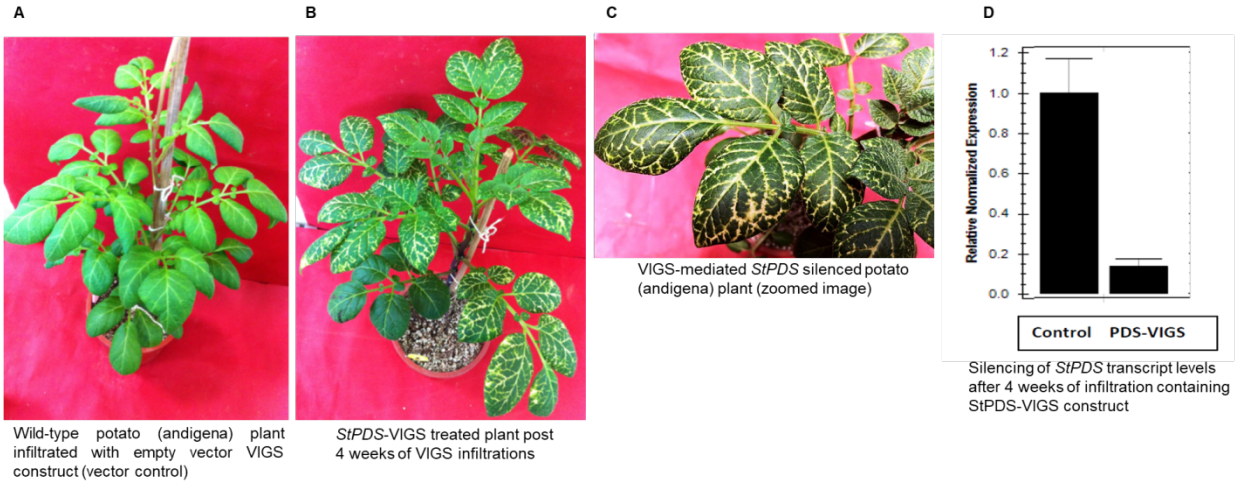

Figure 3.5. VIGS mediated silencing of potato *phytoene desaturase* (*StPDS*) gene in andigena (7540) plants. The *StPDS*-VIGS construct was used as a positive control for the optimization of VIGS infiltrations in the subsequent StE(z)2-VIGS experiments. Yellow-colored photobleaching phenotype in the *StPDS*-VIGS treated plants (B-C) and reduced transcript levels of *StPDS* (D), shows the functionality of the *StPDS*-VIGS construct. Vector control (VC) plants don't show any photobleaching phenotype (A). Panel C is a zoomed image of panel B. *EIF3e* was used as a reference gene for normalization in the qRT-PCR analysis.

3.4 Discussion

Potato E(z)2 is a PRC2 group histone methyl transferase orthologous to CURLY LEAF (CLF) in Arabidopsis. PRC2 performs trimethylation of H3K27, leading to the repression of target genes. Although the role of PRC proteins has been characterized in Arabidopsis (Goodrich et al., 1997) and in some other crops such as rice (Liu *et al.*, 2014) and tomato (Boureau *et al.*, 2016), their role in potato development is yet unexplored. Studies by Jiang et al. (2010) have shown that CLF directly binds and deposits H3K27me3 mark to repress FT expression in Arabidopsis. Another interesting study by Navarro et al. (2011) proved that FT homolog in potato, StSP6A is an important tuberization regulator. Based on these findings, we decided to investigate the effect of CLF homolog in tuber development in potato. Here, we have characterized the role of *StE(z)2* using overexpression and VIGS-mediated knock-down strategies. In addition to this, we have identified the genes that are being targeted by *StE(z)2* in stolon during tuber development. In order to analyze the effect of *StE(z)2* overexpression on histone modifications, we have performed genome-wide ChIP-seq against H3K27me3 and H3K4me3 marks in SD-induced stolon samples from WT and as well StE(z)2 overexpression

lines. Our study has revealed important genes related to potato development that are epigenetically regulated in response to SD photoperiod.

3.4.1 Photoperiod affects the *StE(z)2* expression in stolon tissues -

qPCR analysis revealed that *StE(z)1* and *StE(z)2* expression is reduced in SD induced stolon, indicating their role in regulating the onset of tuberization in a photoperiod dependent manner. Moreover, we noticed several light regulatory elements in the promoter of *StE(z)2* indicating its regulation by photoperiod . To validate this, we generated prom*StE(z)2*::GUS lines harboring approx. 2 kb *E(z)2* promoter fused upstream to GUS reporter gene. GUS assay from in vitro grown plantlet revealed expression of *StE(z)2* in diverse tissue types, however in shoot tip, it shows high expression at leaf primordial, and in roots, its expression was restricted to root tips, suggesting its role in regulating the meristematic activity and organ differentiation. Moreover to check the *StE(z)2* expression in stolons, we transferred *prom(z)2*::GUS lines to soil and after two months distributed equally to SD and LD photoperiods. Its promoter showed high activity towards the apical region compared to the basal region under both LD as well as SD induced stolon, indicating its role in stolon fate differentiation.

3.4.2 StE(z)2 overexpression affects overall plant architecture

For the functional characterization of *StE(z)2*, we generated its overexpression construct by putting *StE(z)2* coding ORF under constitutive 35S promoter. The *StE(z)2*-OE lines had a strikingly similar phenotype to *StMSI1*-OE lines described in our previous paper (Kumar *et al.*, 2019; Chapter 2). Since StMSI1 and *StE(z)2* are part of the same PRC2 complex, we are expecting similar mechanistic regulation behind both the phenotypes. The *StE(z)2*-OE lines had smaller leaf size and less leaflet number per leaf compared to the WT plant. Also, they had larger trichomes compared to WT leaves. The cross-section through mid-vain reveled altered vascular architecture in leaf. To analyze the effect of *StE(z)2*-OE, these plants were shifted to the soil, and after two months, they were transferred to SD photoperiodic conditions. After harvesting the OE and WT plants after one month of SD treatment, we noticed reduced root biomass in OE plants compared to WT plants (Figure 3.6D). Interestingly, some of these plants developed aerial tubers from axillary nodes. These phenotypes are consistent with our previous findings, where we report that overexpression of another PRC2 member StMSI1, alters overall plant architecture, and develops aerial tubers (Kumar et al. 2019; Chapter 2).

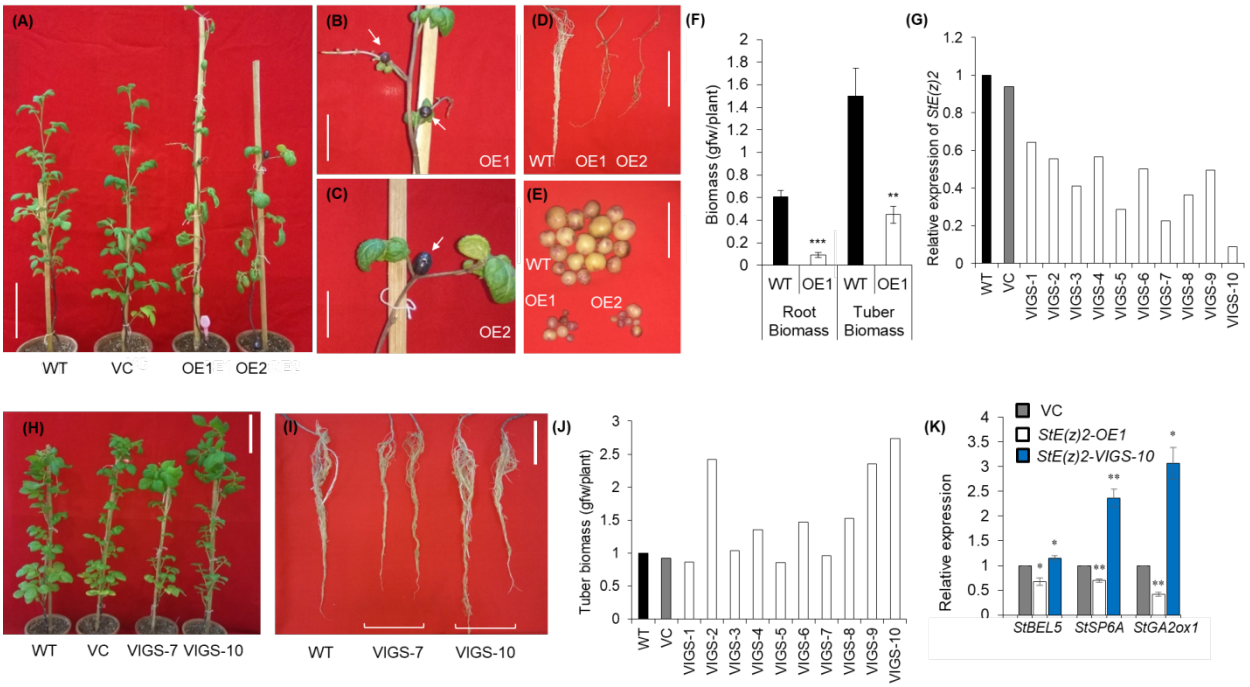

Figure 3.6. Phenotypic characterization of *StE(z)2* over-expression (OE) lines. *StE(z)2* over-expression resulted in reduced belowground tuber yield accompanied by the formation of aerial tubers, whereas *StE(z)2*-VIGS plants exhibited improved tuber yield under SD photoperiodic conditions. Phenotype of WT, VC, and *StE(z)2*-OE lines (OE1, OE2) grown under SD photoperiod for six weeks, following 8-weeks under LD conditions in soil (A). VC plants show a phenotype similar to WT plants; however, *StE(z)2*-OE lines produce aerial tubers (B and C; white arrows), had reduced root length, biomass and belowground tuber yield (D-F). Data is collected from six biological replicates for each line. Relative levels of *StE(z)2* transcript in WT, VC, and *StE(z)2*-VIGS treated plants (G). *StE(z)2*-VIGS infiltrated plants show similar shoot and root phenotype to VC plants (H and I), but the belowground tuber yield was increased in selective VIGS infiltrated plants (J). Expression profile of key tuberization genes (*StBEL5*, *StSP6A,* and *StGA2ox1*) in *StE(z)2-OE* and *StEz2-VIGS* infiltrated plants compared to VC (K). *EIF3e* was used as a reference gene for expression analysis. For WT and VC, mean values from three biological replicates are plotted for RT-qPCR analysis, whereas six independent plants were considered for tuber yield measurements. Individual values were plotted for VIGS plants for both expression analysis as well as tuber yield measurement. Ten independent plants were treated with the *StE(z)2*-VIGS construct. Student's t-test was performed to check the level of significance. Asterisks (*, ** and ***) indicate significance at $p<0.05$, $p<0.01$ and $p<0.001$, respectively. ns=not significant. Scale bars in panel A and H = 10 cm, I = 5 cm and B-E= 4 cm.

Similar to StMSI1-OE lines, we found reduced levels of receptor Theasus kinase 1 and high levels of auxin signaling inhibitor AUX/IAA. Indicating the defects in brassinosteroid and auxin signaling pathway. Since auxin and brassinosteroid play an important role in xylem differentiation as well as cell division(Mattsson et al., 1999; Sieburth, 1999; Lee et al., 2018), this might be a possible cause for reduced root and shoot architecture as well as perturbed vascular architecture in these plants.

3.4.3 Overexpression of *StE(z)2* reduced belowground tuber yield whereas its knockdown results in increased yield

To check the effect of *StE(z)2* knockdown, we used the VIGS approach. We generated a number of plants with differing levels of *StE(z)2* silencing. VIGS silenced plant did not display any remarkable effects in the shoot or root architecture, possibly because of inconsistent silencing in overplant as happens in case of VIGS mediated knockdown. However, they demonstrated the trend of increased tuber yield (Figure 3.6J), contrary to reduced tuber yield in *StE(z)2*-OE line (Figure 3.6E). The tuber yield differed from plant to plant, possibly because of different levels of silencing in leaves and stolons from *StE(z)2* VIGS infiltrated plants. Interestingly, the *StE(z)2* VIGS silenced plant that showed increased tuber yield and had higher levels of tuberization marker genes (*StSP6A* and *StBEL5* and *GA2ox1)* (Fig 3.6K). During inductive SD conditions, a key TALE family protein member StBEL5 and its KNOX partner POTH1 (Chen et al. 2004) get induced, and they induce expression of another very important tuber inducing protein StSP6A (Sharma et al. 2016). StBEL5-POTH1 complex and the tuberization activation complex members (StSP6A and its biding partners, St14-3-3 and StFD2) are transported to stolon (Banerjee et al. 2006, Navarro et al. 2011, Teo et al. 2017) and affect the expression of GA metabolic genes, *StGA20ox* and *GA2ox1* (Chen et al., 2004). Both these pathways ensure reduced bioactive GA levels in the stolon, an essential step for the onset of stolon-to-tuber transition in potato (Xu *et al.*, 1998b). Consistent with this model, we noticed that expression of candidate tuber marker genes (*StBEL5*, *StSP6A,* and *StGA2ox1*) was reduced in *StE(z)2*-OE lines, but increased in *StE(z)2*-silenced plants (Figure 4K). This justifies the observed tuber yield phenotypes in *StE(z)2*-OE and -silenced lines.

In summary, our results reveal that *StE(z)2* regulated tuber development in potato by controlling the expression of important genes related to the tuberization pathway.

3.5 Availability of supplementary information

All the supplementary tables (S1 – S10) mentioned in this chapter are available online and can be accessed using the following link –
https://drive.google.com/drive/u/0/folders/1UbVk8Y0W3DsLfgU90FNGF0gw_tVm6V2V

Chapter 4

Identification of the direct targets of StE(z)2 and the genome-wide occupancy of histone modifications during stolon-to-tuber development in potato

4.1 Introduction

Polycomb group (PcG) proteins are important regulators of development in all eukaryotic organisms. They were first identified in *Drosophila melanogaster* as repressors of homeotic genes (Simon et al., 2002) and majorly divided into two categories, i.e., PRC1 (Polycomb Repressive Complex 1), and PRC2 (Polycomb Repressive Complex 2). PRC1 consists of four subunits; Polycomb (Pc), Posterior sex combs (Psc), Polyhomeotic (Ph), and Sex combs extra (Sce, or dRing1) (Cao et al., 2005). A detailed description of PRC1 and its members are provided in chapter-1 & 2, whereas, in this chapter, I describe PRC2 and its member proteins.

The core subunits constituting PRC2 are the Enhancer of zeste [E(z)], Suppressor of zeste 12 [Su(z)12], Extra sex combs (Esc) and Nucleosome remodeling factor (Nurf55 or p55). The E(z) catalyzes H3K27 trimethylation through the SET domain (Müller et al., 2002). Su(z)12 is a zinc finger protein with VEFS [VRN2-EMF2-FIS2-Su(z)12]– a domain that interacts with E(z) and assists in its activity through an allosteric interaction. Esc and p55 are WD40-repeat proteins and involved in the complex formation and the recruitment of PRC2 complex over H3 and H4 histones. Subsequent studies (Goodrich, et al. 1997, Chanvivattana, Y. et al. 2004, Mosquna, A. et al. 2009), identified homologs of PcG complex members in a diverse range of plants, starting from unicellular algae *Chlamydomonas reinhardtii* to higher plants, suggesting that in eukaryotic evolution PcG proteins appeared early before diversification of major plant lineages (Shaver et al., 2010). In plants, 10–15% of genes are regulated through the H3K27me3 modification laid by PRC2 (Zhang et al. 2007). Arabidopsis have three E(z) homologs, CURLY LEAF (CLF), MEDEA (MEA), and SWINGER(SWI), three Su(z)12 homologs, EMBRYONIC FLOWER2 (EMF2), VERNALIZATION2 (VRN2), and FERTILIZATION INDEPENDENT SEED2 (FIS2), one homolog of Esc, FERTILIZATION INDEPENDENT ENDOSPERM (FIE) and five homologs of p55 termed as MULTIPLE SUPPRESSOR OF IRA1-5 (MSI1-5). Studies in Arabidopsis have further revealed three types of PRC2 complexes (EMF, VRN, and FIS) involved in the regulation of different developmental stages. The EMF complex represses the floral activators, thus maintaining the juvenile stage of the plants (Yoshida et al., 2001), The VRN complex enables Arabidopsis plants to flower after sensing vernalization by repressing the floral repressor gene FLOWERING LOCUS C (FLC) (De Lucia et al., 2008). The third PRC2 complex, known as the FIS complex, is functional in female gametophyte and keeps a check on

seed development before fertilization (Guitton et al., 2004). EMF and VRN complexes contain either CLF or SWN, whereas the FIS complex contains MEA, which is conserved in the Brassicaceae family only. In addition to this, all PRC2 complexes are accompanied by Esc homolog FIE and one of the p55 homologs MSI1 (Henning et al., 2005).

On the other hand, the Trithorax group (TrxG) complexes perform H3K4 and H3K36 methylation over the genes being actively transcribed (Saleh et al., 2008). They also harbor the histone methyl transferase SET domain and counteract the activity of PcG members. TrxG family in Arabidopsis has five TRX homologs (ATX1- ATX5), seven ATX related (ATXR1 – ATXR7) (Tamada et al., 2009), four ASH1 (SDG8, SDG7, SDG24 and SDG26), and three ASH1 related homologs (SDG4, SDG37 and SDG39), (Baumbusch et al., 2001) (Shen *et al.*, 2009). ATX1 and ATX3 have pleiotropic effect in Arabidopsis development (Alvarez-Venegas et al., 2003), and their loss of functions in *clf* mutant background can recover the flowering and leaf developmental aberrations ((Saleh et al. 2008). ASH1 or SET Domain Group 8 (SDG8) is involved in H3K4me3 as well as H3K36me2/me3 and H3K9me3 modifications. It has an important role in flowering time regulation in a photoperiod-dependent pathway (Kim et al., 2005; Zhao et al., 2005). Besides these, Ultrapetala-1 and 2 work with TrxG members to regulate flowering (Monfared *et al.*, 2013). Interestingly, they compete with PcG members for recruitment over the same target genes. Arabidopsis plants with *sdg* loss of function have low levels of H3K4 and H3K36 methylation and exhibit late flowering (Berr et al. 2009).

Several reports have described the role of histone modifiers in flowering in Arabidopsis and other developmental phenomena (Jiang et al. 2008) in many plants (tomato, rice). However, there is no report if histone modifications can play any role in tuber development/ tuberization in potato. Very recently, Zeng. et al. (2019) reported the role of H3K27me3 and H3K4me3 modifications in the context of cold-stress during tuber dormancy. These authors showed that cold stress induces enhanced chromatin accessibility and bivalent histone modifications of active genes. Here, we have performed ChIP-seq analysis from stolon tissues (SD induced) to identify the genes targeted by the StE(z)2. Also, we have performed the genome-wide target identification of H3K4me3 activator and H3K27me3 repressive modifications from short-day

induced stolon tissues to investigate if these modifications could have any role in regulating key tuberization genes in potato.

4.2 Materials and Methods

4.2.1 Plant material and growth conditions

Throughout this study, a photoperiod sensitive cultivar of potato (*Solanum tuberosum* ssp. andigena 7540) was used. Wild-type (WT) potato plants were multiplied *in vitro* by sub-culturing stem cuttings in basal Murashige, and Skoog's medium (Murashige and Skoog, 1962) supplemented with 2% sucrose. *In vitro* plants were maintained in plant growth incubator (Percival Scientific) at 22 °C with a light intensity of 300 μmol $m^{-2}s^{-1}$ under long-day (LD) photoperiodic conditions (16 h light/8 h dark). Fifteen days old *in vitro* grown plants were transferred to soil and maintained in plant growth chambers (Percival Scientific) at 22 °C under LD photoperiodic conditions.

4.2.2 Vector construction and transgenic lines generation

To generate N-terminal FLAG-tagged *StE(z)2*-OE construct (*35S:FLAG-StE(z)2-pBI121*), its full-length coding sequence (CDS; ~2.7 kb) was amplified by reverse transcriptase PCR using *in vitro* grown andigena plants with gene-specific primers (Supplementary Table S1). The forward primer contained the N terminal FLAG tag. PCR amplified product was then cloned into a sub-cloning vector pGEM-T Easy (Promega), sequence confirmed and further mobilized into the binary vector pBI121 downstream of Cauliflower Mosaic Virus (CaMV) 35S promoter (Xiang *et al.,* 1999). The *35S:FLAG-StE(z)2-pBI121* construct was transformed into the *Agrobacterium tumefaciens* strain GV2260 and stable potato transgenic lines were generated as per the method described in Banerjee *et al.* (2006b).

4.2.3 Chromatin immunoprecipitation protocol

Chromatin immunoprecipitation was performed on stolons of WT and FLAG-tagged StE(z)2-OE potato lines that were incubated for 15 days under SD conditions. The Diagenode's Universal Plant ChIP-seq kit (Cat. No. C01010152) was used as described in the next section.

4.2.3.1 Crosslinking of stolon tissues

Fifteen days short-day-induced stolon tissues (1 gram) were harvested and washed properly before being used for the experiment. The tissues were chopped into fine pieces and kept inside a crosslinking bag. The samples were transferred to a 50 ml falcon tube containing 30 ml of crosslinking buffer (having a 1% formaldehyde solution. The tube (without cap) containing samples was put inside desiccator filled with ice. The crosslinking was performed by applying the vacuum (~ 950 Millibars) for 10 minutes. Crosslinking was stopped by replacing the 2.5 ml of the crosslinking buffer with an equal volume of glycine. After 5 minutes, the crosslinking solution was discarded, and samples were washed thoroughly with cold deionized water. After this, samples were transferred to a new tube and snap froze using liquid nitrogen.

4.2.3.2 Chromatin extraction and shearing

Prefixed samples were homogenized and dissolved in 30 ml of cold extraction buffer one and incubated for 30 minutes at 4°C. After this, the suspension was filtered using Miracloth, and flow-through was collected in a pre-chilled 50 ml falcon tube. The solution was centrifuged for 20 min at 4 °C at 1900 x g, and the supernatant was discarded. The pellet was washed and centrifuged for five times with extraction buffer 2. Finally, the nucleus containing pellet was washed with 5 ml of extraction buffer three and centrifuged for 5 min at 4 °C at 1900 x g. The supernatant was discarded, and the pellet was resuspended in 600 µl of and transferred to a pre-chilled 1.5 ml tube. The homogenized solution was further distributed into three tubes and incubated at 4°C in a rotating wheel for 15 minutes. Following this, the chromatin was sonicated with the Diagenode twin Bioruptor® at high mode with the 30 seconds ON / OFF at 4 ° C, for 45 cycles. The sonicated solution was centrifuged for 5 min at 18000g at 4 °C and supernatant were collected. One aliquot out of these tubes was used to check the shearing efficiency of the chromatin before proceeding for the immuno-precipitation step.

4.2.3.3 Immunoprecipitation

The sheared chromatin was immunoprecipitated using one µg of either anti-H3K4me3 (Diagenode, Cat. No. C15410003), anti-H3K27me3 (Abcam, Cat. No. ab6002), anti-FLAG (Sigma, Cat. No. F3165) or anti-IgG antibody (Diagenode, Cat. No. C15410206), in individual reaction. Two biological replicates were used for each ChIP reaction (WT input, WT anti-

H3K4me3, WT anti-H3K27me3, 35S:FLAG-StE(z)2 input, 35S:FLAG-StE(z)2 anti-FLAG, 35S:FLAG-StE(z)2 anti-H3K4me3, and 35S:FLAG-StE(z)2 anti-H3K27me3).

DiaMag protein A-coated magnetic beads (20 µl per ChIP reaction) were washed and re-suspended in (21 µl per ChIP reaction) ChIP Dilution Buffer. After this, one µl of (anti FLAG, anti H3K4me3, anti H3K27me3, anti IgG) antibody was added separately to different tubes containing the magnetic beads and incubated overnight on a rotating wheel at 4°C. On the next day, antibody-coated beads were washed three times with 200 µl 1x ChIP dilution buffer. After the last wash, beads were resuspended in ChIP Dilution Buffer (21 µl) and kept on ice till further use.

The sheared chromatin (40 µl) from the second step was diluted by adding 160 µl of cold 1x ChIP Dilution Buffer. Two microliters of the diluted chromatin was kept aside (-20 °C) to be used as input control. Antibody coated magnetic beads (20 µl) were added to the diluted chromatin for each ChIP reaction and incubated at 4 °C overnight in a rotating wheel. After the incubation, beads were washed with 200 µl of wash buffer by replacing the supernatant with wash buffer 1, 2, 3, and 4 each time using a magnetic stand.

4.2.3.4 De-crosslinking and DNA isolation

Beads pellet from the previous step was resuspended in 100 µl of Elution Buffer-1 and transferred to a clean 200 µl strip tubes. Samples were incubated for 30 min at room temperature on a rotating wheel. Meanwhile, the Input control sample was thawed on ice and made up to a final volume of 100 µl by adding 98 µl of Elution buffer 1. After 30 minutes of incubation, samples were kept on a DiaMag02 magnetic rack, and supernatant was transferred into a new 200 µl strip tubes. For DNA de-crosslinking, four µl of elution buffer-2 was mixed with all samples and incubated at 65 °C for overnight. After overnight incubation, samples were mixed with two µl of carrier and 100 µl of 100% isopropanol and resuspended with ten µl of IPure Magnetic beads and incubated for 10 minutes at room temperature on a rotating wheel (40 rpm). Following incubation, beads were washed with 100 µl of wash buffer 1 and 2, and supernatant was discarded. The bead pellet was resuspended in 40 µl of buffer C and incubated for 15 minutes at room temperature on a rotating wheel. Post incubation, the supernatant was

transferred carefully to a new tube using the magnetic stand. Recovered DNA was used finally for library preparation.

4.2.4 DNA library preparation protocol

The library preparation was carried out as per the protocol described in NEBNext® Ultra™ II DNA Library Prep Kit for Illumina (NEB; # E7645S/L)

4.2.4.1 End repair and adapter ligation into Immunoprecipitated DNA fragments

Five nanograms of fragmented DNA was dissolved with 1X TE to make up the final volume to 50 µl. It was mixed with three µl of End Prep Enzyme Mix and seven µl of End Prep Reaction Buffer, respectively. The tubes were kept in a thermocycler at 20°C followed by 65°C for 20 minutes each. For ligation of adapters to the DNA library, the NEB Next Adaptor provided with Illumina kit was diluted with Tris/NaCl to a working concentration of 1.5 µM. The 30 µl end-repaired DNA from the previous step was mixed with one µl of Ligation Enhancer and 2.5 µl of diluted adapters. The samples were incubated at 20°C for 15 minutes with the heated lid off. Following this, three µl of USER Enzyme was mixed to the ligation mixture and incubated at 37°C for 15 minutes with a heated lid set to ≥ 47°C.

4.2.4.2 Size Selection, cleanup of adaptor-ligated DNA

Before proceeding DNA library for size selection, the Agencourt AMPure XP beads (Beckman Coulter, Cat. No. A63882) were resuspended and incubated at room temperature for 10 minutes. 40 µl of resuspended beads were mixed with 96.5 µl of ligation reaction and incubated at room temperature for 5 minutes. The supernatant containing the desired DNA was transferred to a new tube using the magnetic stand. Following this, 20 µl of resuspended the Agencourt AMPure XP beads were again mixed with the supernatant and incubated samples on the bench top for 5 minutes at room temperature. At this state, the supernatant was discarded, and beads containing the desired size of the DNA library (200 bp) were washed twice with 200 µl of 80% freshly prepared ethanol. Following this, the ethanol was removed, and beads were air-dried. The DNA library was eluted by mixing the beads with 17 µl of 10 mM Tris-HCl. The elute transferred to a fresh tube using a magnetic stand.

4.2.4.3 Indexing and PCR amplification of DNA library

Because of the low amount of DNA recovered from a ChIP experiment, it is often required to amplify the DNA library. The indexing primers are also added to the library to distinguish the DNA sequences belonging to the different samples after ChIP-seq. The 15 µl adaptor-ligated DNA fragments were mixed with 25 µl of Q5 master mix and five µl each of index primer (i7) and universal PCR primer (i5). PCR amplification was performed using the initial denaturation cycle of 98°C for 30 seconds and 14 cycles of denaturation and extension at 98°C and 65°C for 10 seconds and 75 seconds, respectively. The samples were incubated for a final extension of 5 minutes and stored at 4°C.

4.2.4.4 Cleanup of PCR Reaction

Before proceeding for the cleanup step, the Agencourt AMPure XP beads were homogenized and warmed at room temperature for 10 minutes. The resuspended beads (45 µl) were mixed with 50 µl of PCR reaction at room temperature for 5 minutes. Afterward the tubes were kept on a magnetic stand, and supernatant was discarded. Beads were washed twice with 200 µl of 80% freshly prepared ethanol. Following this, the ethanol was removed, and beads were air-dried. The DNA Sample was eluted by adding the 33 µl of 0.1X TE to the beads. Before proceeding for ChIP-sequencing, the size distribution and DNA library quality were assessed using the Agilent Bioanalyzer high sensitivity DNA chip. All samples were diluted to make equimolar concentration (4 nM) before proceeding for ChIP-sequencing, as given below (Table 4.1).

In summary, fourteen (14) ChIP-sequencing libraries were prepared using five ng of each DNA sample with the NEB Next Ultra II DNA Library Prep kit (New England Biolabs, Cat. No. E7103S). Immunoprecipitated DNA samples were end-repaired. Adapters were ligated and fragments were PCR amplified using indexing primers, followed by the size selection (200 bp) and purification using the Agencourt AMPure XP beads (Beckman Coulter, Cat. No. A63882). The library quality was assessed on the Agilent Bioanalyzer 2100 (Agilent Technologies, Inc.). Libraries were pooled in equimolar concentrations (Table 4.1). Subsequently, 76 bp reads were subjected to paired-end sequencing using Illumina Next Sequencer 550 (IISER Pune, India).

Table 4.1. DNA library dilution table

S. No.	Sample details	Initial Conc (ng/ul)	Template Length. (bp)	Template Conc. (nM)	Template vol. to be added (ul)	Buffer vol. To be added (ul)
1	WT input rep 1	15.2	280	82.25	1.95	38.05
2	WT input rep 2	16.4	280	88.74	1.8	38.2
3	WT H3K4me3 rep 1	14.7	280	79.55	2.01	37.99
4	WT H3K4me3 rep 2	27.7	280	149.89	1.07	38.93
5	WT H3K27me3 rep 1	8.2	280	44.37	3.61	36.39
6	WT H3K27me3 rep 2	27.2	280	147.19	1.09	38.91
7	StE(z)2-OE input rep 1	15.4	280	83.33	1.92	38.08
8	StE(z)2-OE input rep 2	17.5	280	94.7	1.69	38.31
9	StE(z)2-OE H3K4me3 rep 1	19	280	102.81	1.56	38.44
10	StE(z)2-OE H3K4me3 rep 2	15.55	280	84.15	1.9	38.1
11	StE(z)2-OE H3K27me3 rep 1	24.25	280	131.22	1.22	38.78
12	StE(z)2-OE H3K27me3 rep 2	15.3	280	82.79	1.93	38.07
13	FLAG:StE(z)2-OE rep 1	17	280	91.99	1.74	38.26
14	FLAG:StE(z)2-OE rep 2	13.4	280	72.51	2.21	37.79

4.2.5 Enriched DNA motif identification

To identify the motifs enriched on StE(z)2 target sites as well as H3K27me3 and H3K4me3 modifications on the global target genes in LD/SD stolon samples, the DNA sequences corresponding to the respective peak regions were extracted using the RSAT retrieve sequence program (http://rsat.eead.csic.es/plants/retrieve-seq-bed_form.cgi). Corresponding peak co-ordinates from MACS2 peak-calling were used. The significantly enriched DNA motifs in target regions of respective histone modification were searched using RSAT peak-motifs tools (Thomas-Chollier *et al.,* 2012; http://rsat.eead.csic.es/plants/peak-motifs_form.cgi).

4.3 Results

4.3.1 Genome-wide identification of StE(z)2, H3K27me3 and H3K4me3 targets in stolon

To identify the targets of StE(z)2 and the effect of two important histone modifications (H3K4me3 and H3K27me3) on tuberization, we performed ChIP-seq experiment on 15 days SD-induced stolon from WT as well as FLAG-tagged StE(z)2-OE line. Two biological replicates were used for each type of sample. Principal Component Analysis and correlation matrix showed that there was a significant correlation between the ChIP-seq output data of both biological replicates for each category (Figure 4.1 A-B), suggesting the reliability of our ChIP experiment. Bowtie alignment matched ~ 88% paired-end reads to the potato genome (Table 4.2). MACS2 peak calling tool unraveled 20,860 peaks of H3K4me3 and 2,309 peaks of H3K27me3 in WT stolon. However, in FLAG-tagged StE(z)2-OE line, we could identify 2,035 peaks of E(z)2, 10,306 of H3K4me3, and 4,682 of H3K27me3 modifications from SD-induced stolon (). Out of these peaks, we could associate 12409 genes having H3K4me3 modification and 89 genes having H3K27me3 modification in WT stolon. In contrast, in the *StE(z)2-OE* line, the number of genes associated with H3K4me3 modification decreased to 5,175, and the genes associated with H3K27me3 modification increased to 226. Additionally, we found 67 genes as direct targets of FLAG-tagged StE(z)2.

The plot profile of peaks over the target genes showed that H3K4me3 modification was mostly located towards the Transcription Start Site (TSS) (Figure 4.2 A-B, F), whereas StE(z)2 and H3K27me3 target regions were spread across all over the gene bodies (Figure 4.2 C-E, G-H). GO analysis for the target genes harboring H3K4me3, H3K27me3 or StE(z)2-FLAG histone modifications showed that GO terms related to the binding and catalytic activity were most enriched in the category of molecular function, whereas GO terms related to metabolic activity were enriched in the biological process category (Figure 4.4 to Figure 4.6).

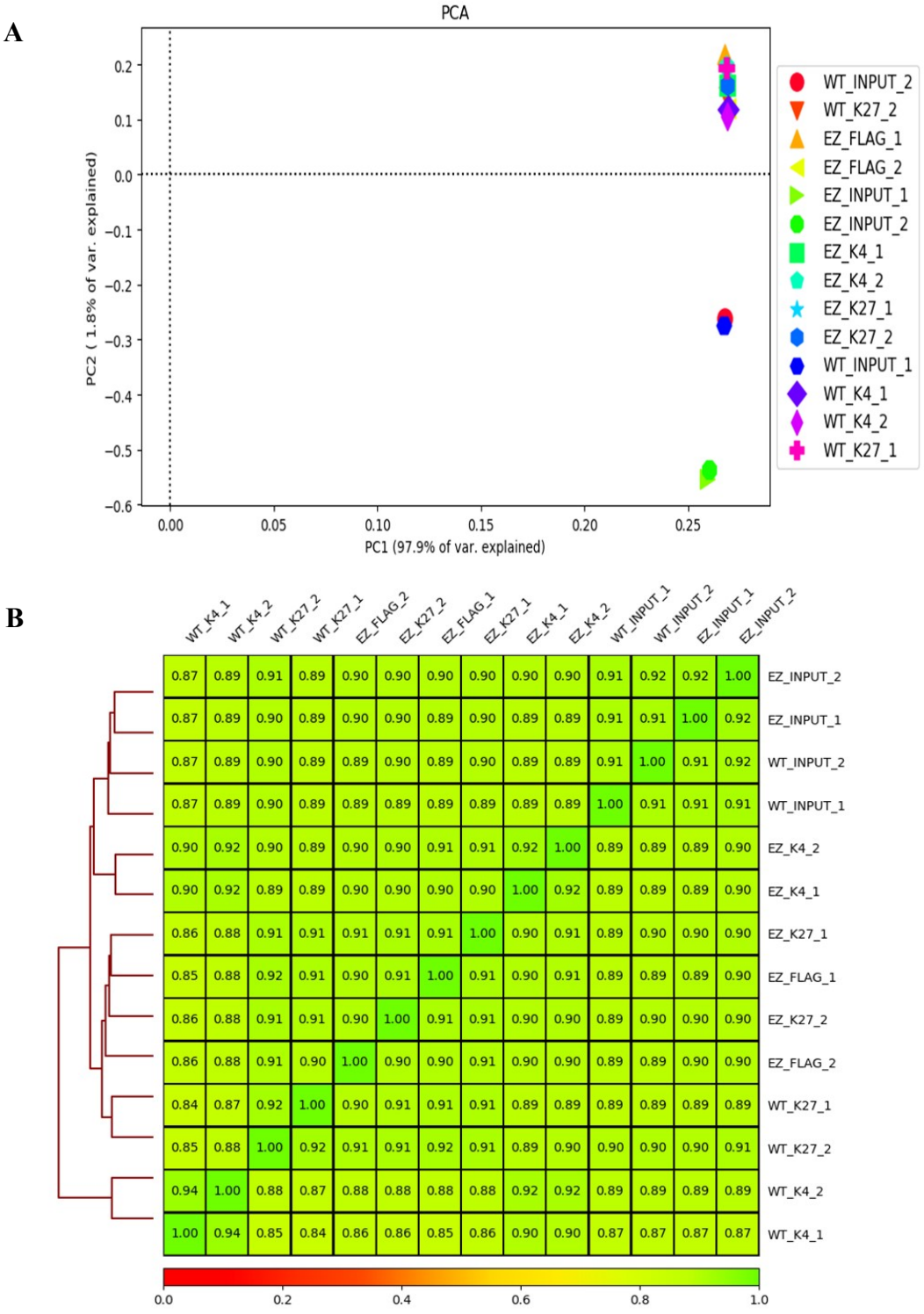

Figure 4.1. Correlation analyses showing the relationship between samples and biological replicates. Principal Component Analysis (A) and correlation matrix (B) showing the relationship between all the samples as well as biological replicates. In contrast, in the *StE(z)2-OE* line, the number of genes associated with H3K4me3 modification.

Table 4.2 Summary of read counts and Bowtie2 alignment statistics after ChIP-sequencing

Sr. No.	Sample	Total raw reads	Total cleaned reads	% of mapped paired
1	Wild-type input rep 1	1,28,08,442	1,25,65,396	87.88%
2	Wild-type input rep 2	1,39,23,940	1,36,55,890	86.07%
3	Wild-type anti-H3K4me3 rep 1	1,75,21,404	1,71,27,022	87.70%
4	Wild-type anti-H3K4me3 rep 2	2,04,58,900	2,00,39,450	88.15%
5	Wild-type anti-H3K27me3 rep 1	1,29,52,894	1,26,86,592	81.24%
6	Wild-type anti-H3K27me3 rep 2	1,68,21,570	1,64,76,048	88.77%
7	StE(z)2-OE input rep 1	1,53,10,480	1,50,24,062	88.26%
8	StE(z)2-OE input rep 2	1,85,59,912	1,82,18,734	88.46%
9	StE(z)2-OE anti-H3K4me3 rep 1	1,48,10,392	1,44,93,752	89.00%
10	StE(z)2-OE anti-H3K4me3 rep 2	1,56,29,458	1,53,09,706	89.46%
11	StE(z)2-OE anti-H3K27me3 rep 1	1,36,38,864	1,32,79,796	87.59%
12	StE(z)2-OE anti-H3K27me3 rep 2	1,56,06,112	1,52,58,444	85.98%
13	StE(z)2-OE anti-FLAG rep 1	1,39,84,810	1,36,68,230	89.15%
14	StE(z)2-OE anti-FLAG rep 2	1,28,18,798	1,27,76,236	86.20%

Table 4.3. Summary of peaks corresponding to different modifications Total number of identified peaks identified by MACS peak-calling software, corresponding to H3K4me3, H3K27me3, or StE(z)2 OE –FLAG, from stolons of LD vs. SD photoperiodic conditions from wild-type, and FLAG-tagged StEz2 over-expression lines.

Sr. No.	Sample	Total peaks	Peaks over the gene body	Target genes
1	Wild-type H3K4me3	20860	12650	12409
2	Wild-type H3K27me3	2309	89	88
3	StE(z)2 OE H3K4me3	10306	5234	5175
4	StE(z)2 OE H3K27me3	4682	231	226
5	StE(z)2 OE -FLAG	2035	71	67

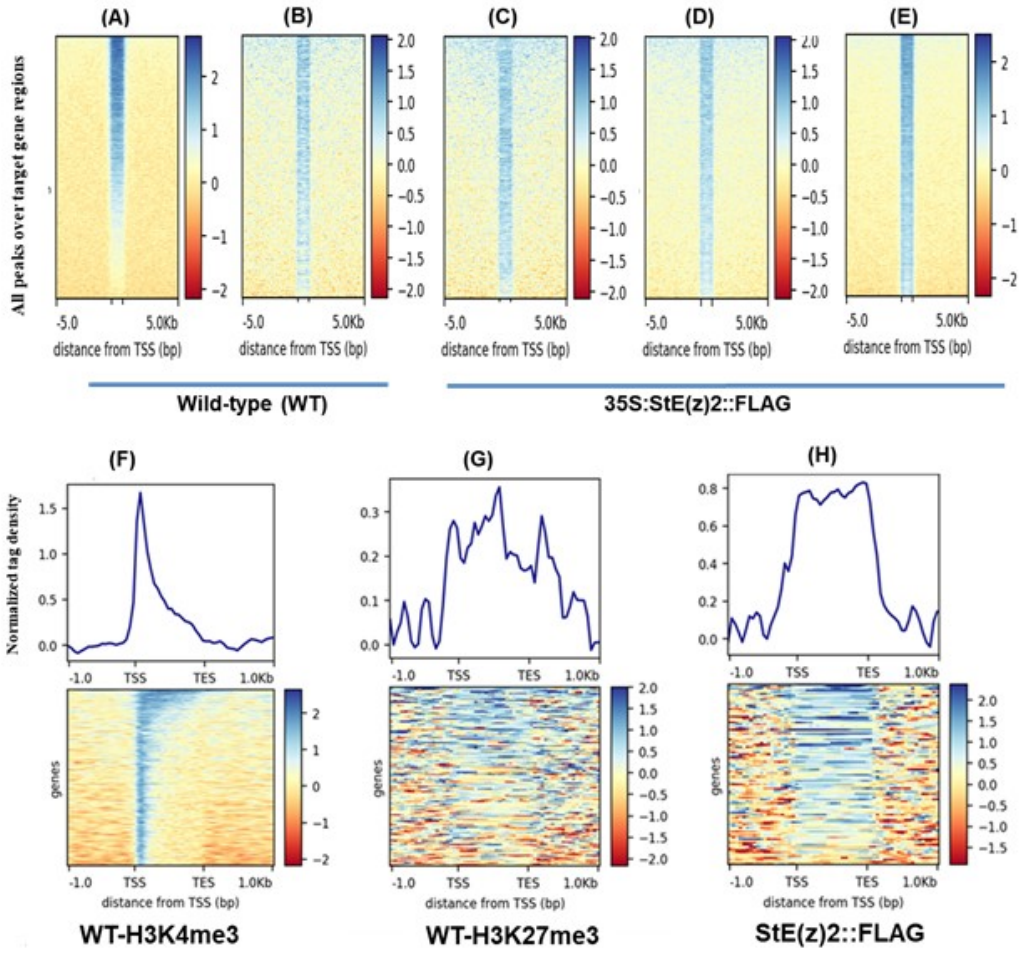

Figure 4.2. Heat maps showing the ChIP-seq read density. Read density corresponding to all the peaks associated with H3K4me3 (A and C), H3K27me3 (B and D) and StE(z)2 (E) across the genome in 15 days SD-induced stolons of WT and FLAG-tagged StE(z)2-OE plants. Distribution pattern of input normalized ChIP-seq peaks associated with H3K4me3 (F), H3K27me3 (G) and FLAG-tagged StE(z)2-OE (H) over the target gene regions drawn by deepTools plot profile function.

Using the RSAT program, we identified that the telobox motif (AAACCCTAAA) was enriched in both H3K27me3 and H3K4me3 modification sites as well as at the StE(z)2 target gene regions (Figure 4.3 A-C). Besides this, we also noticed a number of other motifs enriched at above-mentioned modification sites (Figure 4.3 A-C). GO analysis for the target genes harboring H3K4me3, H3K27me3 or StE(z)2-FLAG histone modifications showed that GO terms related to the binding and catalytic activity were most enriched in the category of molecular function, whereas GO terms related to metabolic activity were enriched in the biological process category (Figs. 4.4, 4.5 and 4.6).

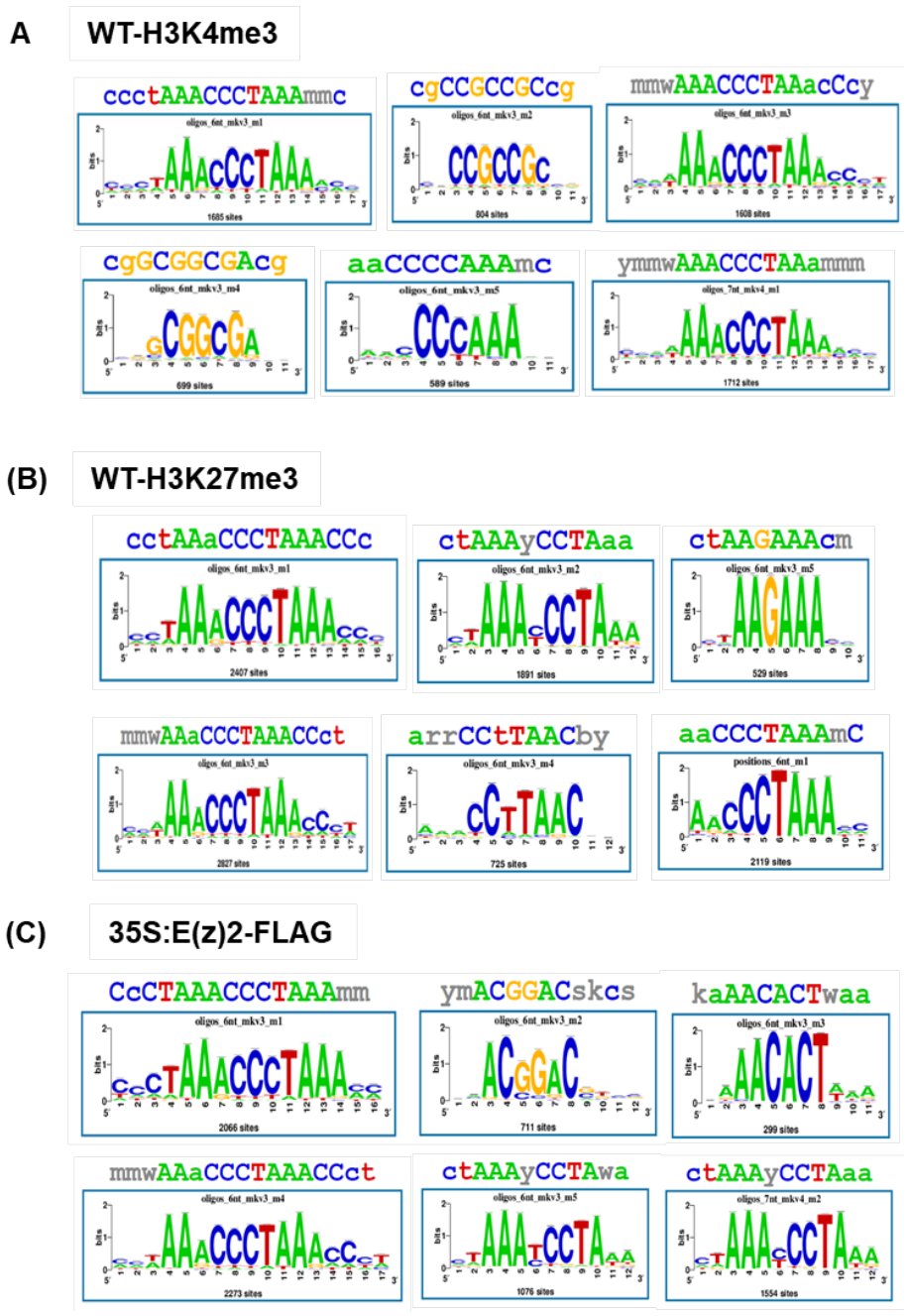

Figure 4.3. Enriched motif identification. op six enriched motifs over the target gene regions of H3K4me3 (A), H3K27me3 (B) and FLAG-tagged StE(z)2-OE (C) as identified by RSAT peak-motifs program

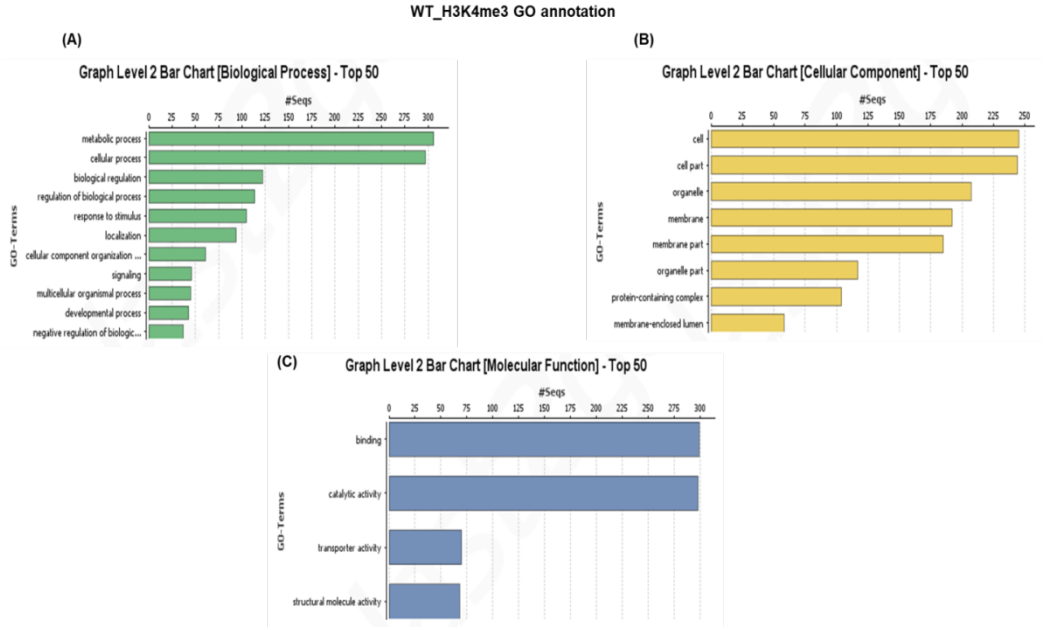

Figure 4.4. **Gene Ontology (GO) classification for H3K4me3 targets.** GO for the genes harboring H3K4me3 histone modifications in SD stolon samples of wild-type andigena plants. GO terms were categorized into biological processes, cellular components, and molecular functions. GO terms with the top 50 sequences were considered for preparing bar charts in each category.

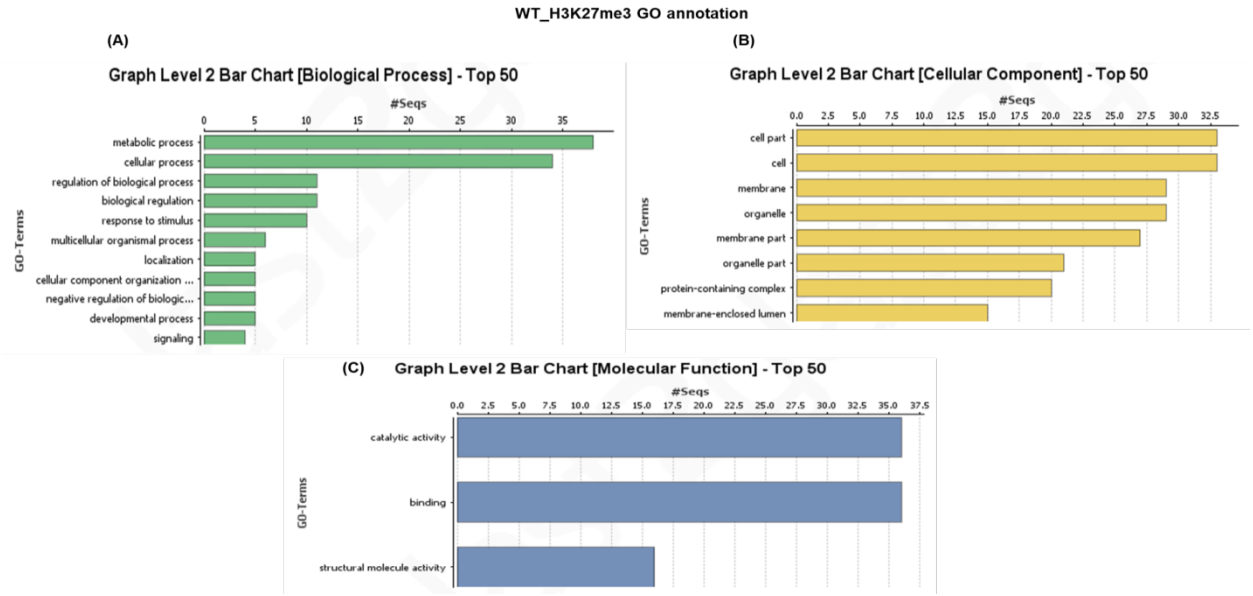

Figure 4.5. Gene Ontology (GO) classification for H3K27me3 targets. GO for the genes harboring H3K27me3 histone modifications in SD stolon samples of wild-type andigena plants. GO terms were categorized into biological processes, cellular components, and molecular functions. GO terms with the top 50 sequences were considered for preparing bar charts in each category.

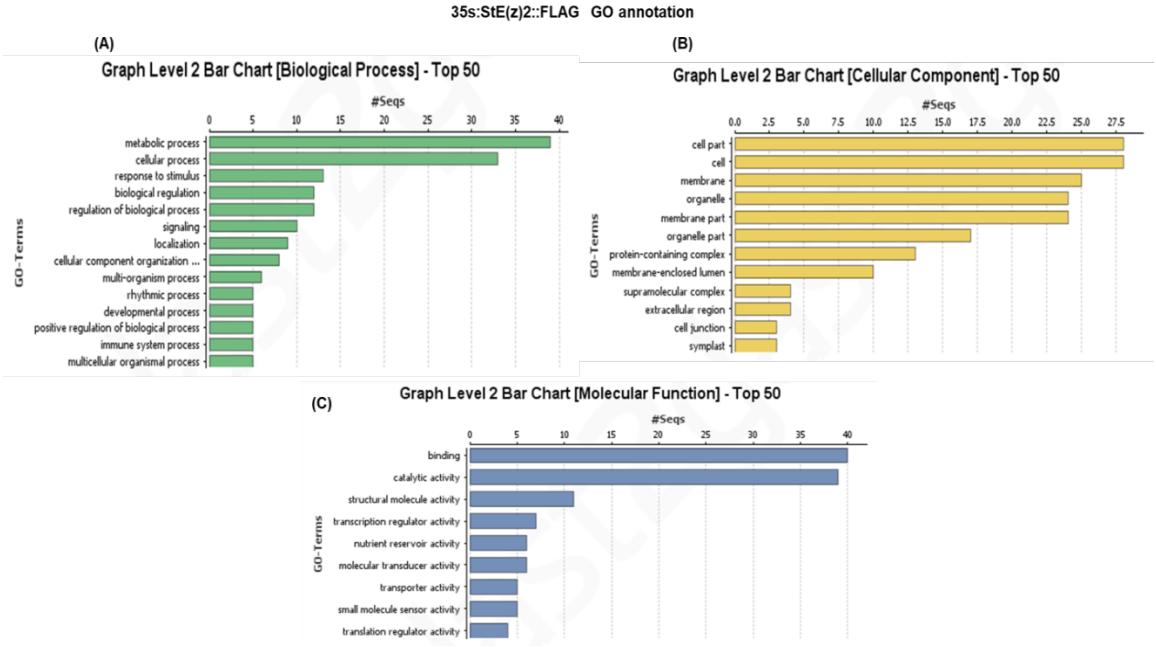

Figure 4.6. **Gene Ontology (GO) classification for *StE(z)2-FLAG* targets.** GO for genes harboring *StE(z)2-FLAG* in SD stolon samples of *StE(z)2-FLAG-OE* andigena line. GO terms were categorized into biological processes, cellular components, and molecular functions. GO terms with the top 50 sequences were considered for preparing bar charts in each category.

4.3.2 H3K27me3 and H3K4me3 modifications regulate genes associated with tuberization and metabolic pathways

ChIP-seq analysis revealed >12,000 genes are harboring active H3K4me3 modification (Supplementary Table S4). This list includes several genes involved in the tuber development pathway. For example, *BEL* and KNOX family transcription factors, *StGA2ox1*, *St14-3-3*, *StFD2*, *StMSI1*, *patatin*, *sucrose synthase,* and *transporters* (Figure 4.7 A, Supplementary Table S4). Consistently, through RT-qPCR analysis, we observed a significant upregulation of *StBEL5, St14-3-3*, *StMSI1*, *StZF2*, *StSDG4*, *purine transporter three* and *StGA2ox1* in stolon under SD compared to LD photoperiodic conditions (Figure 4.7).

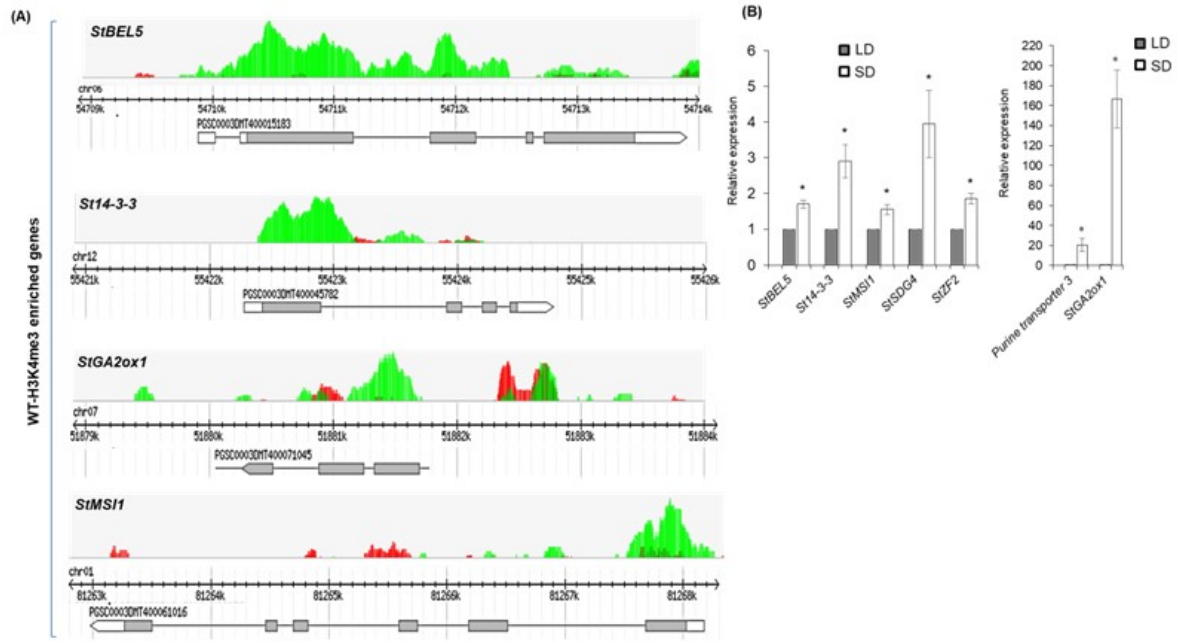

Figure 4.7. Key tuberization genes are regulated by H3K4me3 histone modifications. Visualization of chromatin occupancy of H3K4me3 (green color) and H3K27me3 (red color) modification over *StBEL5*, *StGA2ox1*, *St14-3-3,* and *StMSI1* genes through the IGB viewer (A). The lower strand below the peak regions depicts the corresponding genomic coordinates and transcript schematic as obtained from the PGSC genome browser. RT-qPCR validation of candidate genes involved in the tuberization pathway and found as the target of H3K4me3 modifications (B). The gene expression was quantified in stolons of WT andigena plants grown under LD vs. SD photoperiodic conditions. Transcript levels in LD stolons were considered as 1 to calculate the relative expression of each gene in SD stolons. Data are mean ±SD for three biological replicates. Each biological replicate had three technical replicates. *EIF3e* was used as a reference gene for expression analysis. Student's t-test was performed to check the level of significance. The asterisk (*) represents significance at $p<0.05$.

We found several other PRC members, such as *StMSI1*, *ubiquitin ligase* encoding genes as well as *histone deacetylases* as targets of H3K4me3 modifications (Supplementary Table S4). On the other hand, we observed an enrichment of H3K27me3 peaks over 2,300 sites; out of them, 89 were on the gene body (Table 4.3, Supplementary Table S5). Several genes (*glutamine synthetase*, *cytochrome P450*, *cytochrome C oxidase subunit2,* and *multidrug-resistant (MDR) ABC transporter, glutaredoxin,* and *pyruvate kinase*) related to metabolic pathways were found as targets of H3K27me3 modifications (Supplementary Table S5, Figure 4.8 A). The accumulation of the repressive H3K27me3 mark on many of these genes was associated with their reduced transcript levels in SD stolons compared to LD conditions (Figure 4.8 B). Notably,

ChIP-qPCR analysis detected a 70-80% reduction in deposition of H3K27me3 modification over the *StSP6A* locus in WT leaves under SD conditions compared to LD (Figure 4.8 C).

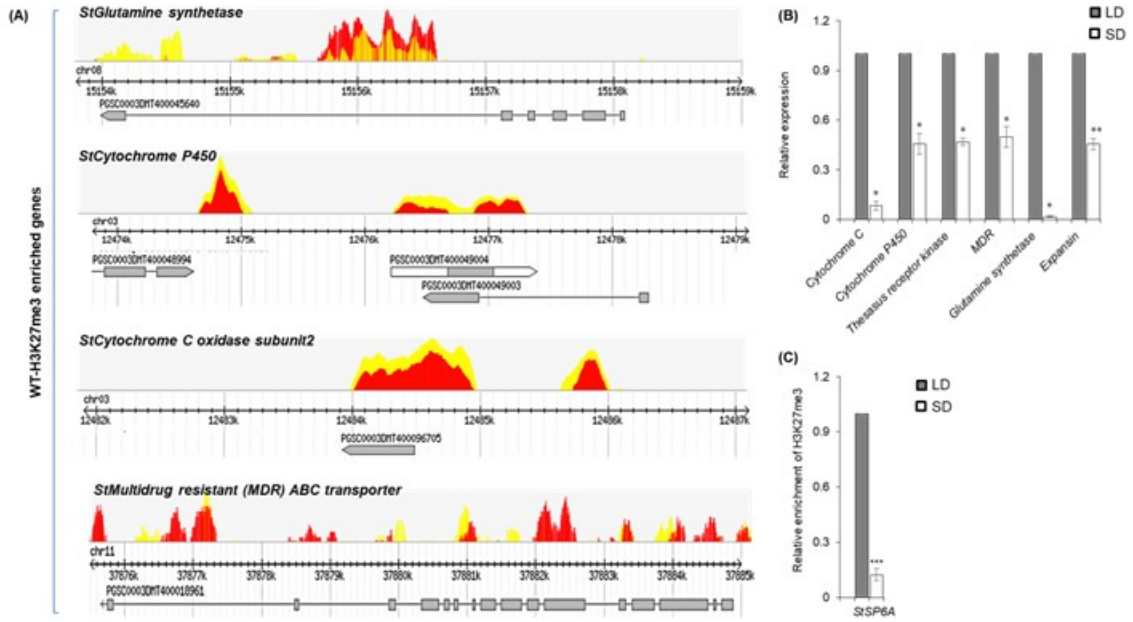

Figure 4.8. Genes that are down-regulated during tuberization harbors H3K27me3 histone modifications. Visualization of chromatin occupancy of H3K27me3 (red color) and StE(z)2:FLAG (yellow color) over the genes encoding *glutamine synthetase*, *cytochrome P450, cytochrome C oxidase subunit2* and *multidrug-resistant (MDR) ABC transporter* through the IGB viewer. The lower strand below the peak regions depicts the corresponding genomic coordinates and transcript schematic as obtained by the PGSC genome browser (A). RT-qPCR validation of metabolism-related genes that are found as targets of H3K27me3 modification (B). Transcript levels in LD stolons were considered as 1 to calculate the relative expression of each gene in SD stolon samples. Data are mean ±SD for three biological replicates. Each biological replicate had three technical replicates. *EIF3e* was used as a reference gene for expression analysis. The relative enrichment of H3K27me3 histone modification on the promoter of the *StSP6A* gene in leaves of SD vs. LD incubated WT andigena plants (C). Student's t-test was performed to check the level of significance. Asterisks (*, ** and ***) indicate significance at $p<0.05$, $p<0.01$ and $p<0.001$, respectively. ns=not significant.

4.3.3 Overexpression of FLAG-tagged StE(z)2 influenced H3K4me3 and H3K27me3 modifications over key tuberization genes

Approximately 7,600 genes lost the H3K4me3 modification mark in StE(z)2-OE lines compared to WT stolon (Supplementary Table S6). These include several auxin, brassinosteroid (BR) and cytokinin-related genes, eg. *auxin-responsive protein [ARP]*, *auxin-induced protein*, *AUX/IAA3*, *-4*, *-13*, *dormancy/auxin associated family protein*, *SAUR family proteins*, *PIN proteins*, *ARF2*, *-6*, *-8*, *-19)*, *BR receptor Theseus kinase*, *BR hydroxylase*, *isopentyl transferase*, *zeatin glucosyl transferase*, *purine transporters*, *histidine kinase* and *cytokinin receptor* (Supplementary Table S6). Several other key genes involved in tuber development, *e.g., GA2ox1*, *DOF family TF*, *POTH1, BEL1-like TF*, *patatin*, *starch synthase*, *cellulose synthase,* and *sugar transporter*, also lost active H3K4me3 modification (Supplementary Table S6). Moreover, the overexpression of FLAG-tagged StE(z)2 increased the H3K27me3 modification over 226 genes compared to 88 genes in WT condition (Supplementary Table S7). In addition to this, overexpression also resulted in the gain of H3K27me3 marks over cytokinin biosynthesis/transport genes, such as *isopentenyl transferase*, *adenylate isopentenyl transferase*, *purine transporters*, and the meristem marker gene *Clavata1* (Supplementary Table S8). Besides this, the potato storage protein gene encoding *patatin*, *HD-Zip IV gene* H3K27me3 *family member ROC5*, *F-box/kelch-repeat* (involved in light signaling), *ubiquinone oxidoreductase* (encode for the first enzyme in the respiratory electron transport chain of mitochondria) and *serine endopeptidase degp2* (involved in the photosystem protein D1 repair) also showed increased modification (Supplementary Table S8). Moreover, several stress-responsive genes, like *cold-shock protein*, *senescence-associated protein*, and *late-blight resistance protein,* were found to be targets of StE(z)2 (Supplementary Table S8).

Accessions used in this study

The list of accessions for the genes described in this study is provided as the online supplementary table (S9) as well as at the end of this Thesis.

4.4 Discussion

Short-day photoperiod triggers differential expression of numerous genes in a Spatio-temporal manner during tuber development. However, the gene regulatory network controlling their expression is not well understood in potato. In this study, we explored if chromatin modifiers have any role in the activation or repression of the tuberization associated genes. Through the ChIP-seq of FLAG-tagged StE(z)2-OE line, we have identified its direct targets in SD-induced stolons. We have also performed genome-wide ChIP-seq against H3K27me3 and H3K4me3 marks on the SD-induced stolons from WT as well as StE(z)2-OE lines. Our analysis revealed that a number of important genes influenced by the SD photoperiod during tuberization are controlled by H3K27me3 repressive and H3K4me3 activation modifications in potato.

4.4.1 H3K4me3 and H3K27me3 modifications regulate genes associated with tuber development

E(z)2 catalyzes H3K27 trimethylation that represses the target genes, whereas its effect is antagonized by TrxG members that catalyze H3K4me3 modification (Pien and Grossniklaus, 2007). ChIP-seq analysis identified > 20,000 regions associated with H3K4me3 modification and more than 2,300 regions with H3K27me3 modification (Supplementary Table S4-5). This includes several tuberization associated genes, such as *BEL1-like* and *KNOX* family transcription factors, *GA2ox1*, and StSP6A partners (*St14-3-3* and *StFD2*) (Supplementary Table S4). The regulatory mechanism that controls the expression of these genes under the SD photoperiod is not well understood. In this study, we show that the accumulation of H3K4me3 activation marks over the respective gene loci (Figure 4.7) could be the reason for their upregulation. We also observed increased H3K4me3 modification over other tuberization associated genes coding for *potato storage protein patatin*, *starch synthase,* and *sucrose transporter* (Supplementary Table S4). Several loci for miRNA156 members, as well as the *StMSI1* coding region is enriched with H3K4me3 modification (Figure 4.7A; Supplementary Table S4), possibly the cause for their high expression under SD (Figure 4.7B, Bhogale *et al.*, 2014; Kumar *et al.,* 2019). A study by Teixeira *et al.* (2006) has shown that glutamine synthetase has reduced activity in the growing tuber, while its activity increases in aerial parts of the potato plant. Our analysis revealed enrichment of H3K27me3 repressive modification over its locus in SD stolon (Figure 4.8A; Supplementary Table S5). Further, genes encoding *cytochrome P450* and *multi drug resistance*

ABC transporter were found as the targets of H3K27me3 modification (Figure 4.8B; Supplementary Table S5). The repression of cytochrome P450 affects the localization of PIN proteins and auxin-mediated patterning of cell division plane (Kawade *et al.*, 2018), whereas the multi-drug resistance ABC transporters are involved in auxin transport and elongation (Terasaka *et al.*, 2005). Additionally, we found a number of genes associated with metabolic processes, such as *pyruvate kinase* (involved in TCA cycle) and *2,4-dienoyl-CoA reductase* (involved in fatty acid β-oxidation pathway) (Allenbach and Poirier, 2000; Oliver *et al.*, 2008) as targets of StE(z)2 (Supplementary Table S5). Genes encoding for enzymes involved in cell wall decomposition and loosening, like *pectate lyase* and *polygalacturonase* (Sheehy *et al.*, 1988), were also identified as StE(z)2 targets.

We could not find *StSP6A* in the target gene list of H3K27me3 or H3K4me3 in stolon tissues. But in leaves, through ChIP-qPCR, we detected a 70-80% reduction in the enrichment of H3K27me3 repressive modification over the *StSP6A* locus under SD conditions compared to LD (Figure 4.8C), leading to its enhanced expression under SD conditions (Navarro *et al.,* 2011). Moreover, we could identify the presence of two core telobox motifs (ACCCTA) over the 3 kb *StSP6A* promoter (Supplementary Table S10) involved in the recruitment of E(z)2 homologs (Xiao *et al.*, 2017), suggesting that *StSP6A* could be regulated through H3K27me3-mediated modification laid by StE(z)2.

4.4.2 Overexpression of StE(z)2 affects tuberization by shuffling H3K27me3 and H3K4me3 modifications

ChIP-seq analysis revealed that overexpression of StE(z)2 results in 2- to 3-folds increase in genes having H3K27me3 repressive marks, whereas the number of genes with H3K4me3 modification reduced by ~60% compared to respective marks in WT stolon (Supplementary Tables S4-7). This is consistent with the H3K27 trimethylation activity of E(z)2 and competitive inhibition between H3K27me3 and H3K4me3 marks over the target recruitment **(**Shafiq *et al.*, 2014; Roy *et al.*, 2019) In the StE(z)2-OE background, several key genes related to tuberization (*StGA2ox1*, *POTH1*, *St14-3-3*, *starch synthase* and *sugar transporters*) lost the H3K4me3 modification (Supplementary Table S6). Besides this, the active H3K4me3 mark over genes involved in cytokinin and auxin metabolism was replaced by repressive H3K27me3 modification (Supplementary Table S4-S7). These changes in histone modification would perturb the

threshold hormonal levels and could have affected the belowground tuber yield. We also found that another PRC2 member *StMSI1* lost the H3K4me3 modification in the StE(z)2-OE background (Supplementary Table S6), whereas *StE(z)2* gained the repressive H3K27me3 modification over its own locus in the OE background (Supplementary Table S7). This indicates the intrinsic mechanism of the plant to control the expression of different histone modifiers through their crosstalk (Merini *et al.*, 2017; Kumar *et al.,* 2019).

Two recent reports in Arabidopsis demonstrated that the telobox and GAGA motifs in target genes facilitate binding of zinc finger (Xiao *et al.*, 2017) and TRB proteins (Zhou *et al.*, 2015; 2018), which enable the recruitment of PRC and TrxG proteins over the target sites. Similarly, we noticed that the regions associated with H3K4me3 and H3K27me3 modifications had an over-representation of telobox motif (AAACCCTAAA) (Figure 4.3 A-B), suggesting their role in the recruitment of PRC2 and TrxG proteins in potato as well. Besides this, our STRING analysis predicted that in potato, TRB protein could interact with different BEL1-like members (Supplementary Table S3), including StBEL5 (Banerjee *et al.* 2006a) and StBEL29 (Ghate *et al.*, 2017) that act as an inducer and repressor of tuberization, respectively. We hypothesize that binding of StBEL5 or -29 with TRB protein might be recruiting TrxG or PRC2 complex over tuberization associated genes, resulting in their activation or repression. It would be interesting in the future to experimentally validate this hypothesis.

In summary, we show that PRC2-mediated H3K27me3 and TrxG-mediated H3K4me3 modifications could govern potato tuber development in a photoperiod-dependent pathway.

4.5 Availability of supplementary information and raw sequencing data

All the supplementary tables (S1 – S10) mentioned in this chapter are available online and can be accessed using the following link –

https://drive.google.com/drive/u/0/folders/1UbVk8Y0W3DsLfgU90FNGF0gw_tVm6V2V

The raw sequencing data were deposited in the NCBI Short Read Archive (SRA) database (http://www.ncbi.nlm.nih.gov/sra/) and can be retrieved using the accession number SUB6395260

Findings of this chapter have been communicated as research article that is under review in Journal of Experimental Botany.

Kumar, A., Kondhare, K. R & Banerjee, A. K. Polycomb and trithorax group proteins regulate potato tuberization in a photoperiod-dependent pathway (2019).

Summary

Environmental signals influence plants to alter epigenetic modifications and trigger gene expression responses that enable the plant to adapt in a dynamic environment. Although the function of different histone modifiers, such as Polycomb group (PcG) and Trithorax group (TrxG) proteins have been characterized in the model plant Arabidopsis, yet their role in several other important crops remains under-explored. *Solanum tuberosum* ssp. andigena is a photoperiod sensitive variety of potato. Potato tuber is a specialized stem that arises from the underground organ known as the stolon. The long day conditions inhibit potato development (tuberization), whereas short-day conditions promote stolon to tuber transition. This system, thus, provides researchers a unique opportunity to understand how environmental signals, such as light, temperature, and photoperiod affect potato development. Chailakhyan et al. (1981) observed that heterografting between flowering tobacco and non-induced potato plant leads to initiation of tuber development from non-induced potato, indicating that the flowering and tuberization signals are quite similar and can be interchanged. Several studies revealed a number of common factors involved in flowering and tuberization. These include StSP6A (a close homolog of key florigen FT), CONSTANS (CO), hormones like gibberellic acid as well as microRNAs such as miR156 and miR172. Based on the close similarity between flowering and tuberization pathway and regulation of flowering related genes by PcG and TrxG members, we hypothesized that PcG proteins might be playing important role in governing the photoperiod dependent tuber development as well. To test the involvement of histone modifiers in the regulation of photoperiod dependent tuberization, the following objectives were undertaken.

1. To carry out a thorough literature survey on the role of PcG proteins in diverse plant developmental events.
2. To investigate the role of StMSI1 (a PRC2 member) and StBMI1-1 (a PRC1 member) in potato and identify their target genes.
3. Functional characterization of StE(z)2 (a H3K27 methyltransferase) in potential epigenetic regulation in potato.
4. Identification of the direct targets of StE(z)2 and the genome-wide occupancy of histone modifications during stolon-to-tuber development in potato.

Summary

Chapter 1: Introduction

In this chapter, we have carried out a thorough literature survey regarding the role of Polycomb group (PcG) proteins in diverse developmental processes in plants. The different types of PRC2 complexes and their role in phase transition in the model plant Arabidopsis is described in detail. Further, we have elaborated on the analogy between the flowering and tuberization networks. This chapter further describes the role of various factors such the CDF1, CO, and FT in flowering as well as in tuber development. Besides this, the role of microRNAs, homeobox transcription factors, and various plant growth hormones like Auxin, gibberellin, cytokinin, etc. in tuberization are also described. We have also discussed the role of PcG proteins in regulating the microRNAs, homeobox transcription factors, and plant growth hormones in the model plant Arabidopsis. Although there is plenty of literature available regarding the role of PcG proteins in Arabidopsis, but there is no information, if PcG proteins could play any role in potato development, our literature review suggests. The challenges and open questions in plant epigenetics studies are also pointed out. Finally, we proposed several objectives to study the role of PcG proteins in tuber development using *Solanum tuberosum ssp. andigena* as a model system.

Chapter 2: Investigating the role of StMSI1 (a PRC2 member) and StBMI1-1 (a PRC1 member) in potato and target genes identification

PcG proteins are important regulators of growth and development across eukaryotic lineages. They were first identified in Drosophila as multiprotein complexes, termed as Polycomb Repressive Complex 1 (PRC1) and PRC2. The PRC2 complex represses the target genes through H3K27me3 modification, whereas, the PRC1 complex regulates the genes by H2A and H2B modification. BMI1, a PRC member, represses the target genes through H2A mono-ubiquitination. A recent study in Arabidopsis has shown that BMI1 regulates meristem maintenance and cell differentiation by repressing *PLETHORA (PLT)* and *WUS homeobox-containing* (*WOX*) genes (Merini et al., 2017). Further, BMI1 knockout results in downregulation of important flowering genes, like *SQUAMOSA PROMOTER BINDING PROTEIN-LIKE* (*SPL*) and *FT*, indicating an important role in the flowering response. To avoid precocious flowering, *SPLs* are suppressed by miR156 during the juvenile phase of plants. However, during adult and

reproductive phases, miR156 expression is suppressed by BMI1 to allow the expression of *SPLs* (Merini et al., 2017).

Arabidopsis has five p55 homologs named MSI1-5 (Henning et al., 2005); out of them, MSI1 has been shown as a core member of the PRC2 complex. It belongs to the WD-40 repeat-containing protein family and has seven Tryptophan Aspartate (WD) repeats that assist in its interaction with other proteins. Previous reports on MSI1 in Arabidopsis showed that it regulates overall plant architecture as well as photoperiod dependent flowering (Henning et al., 2003; Steinbach et al., 2014).

In an experiment, we observed that overexpression of *StMSI1* produced aerial stolons and tubers under SD photoperiodic conditions from axillary nodes, a phenotype that was demonstrated earlier for miR156 over-expression in potato (Bhogale et al., 2014). This raised several interesting questions concerning the function of PcG proteins in potato, such as (i) what is the cause of aerial stolon and tuber development from axillary nodes? (ii) Do PcG proteins have any role in photoperiod-mediated control of tuberization, and (iii) is miR156 directly regulated by StMSI1, or there are other epigenetic modifiers that could regulate miR156? In this study, using several approaches, such as overexpression or knockdown of two PcG proteins StMSI1 and StBMI1-1, RNA-seq of axillary nodes of *StMSI1* overexpression and *StBMI1-1* knockdown lines, analysis of differentially expressed genes common between two lines, and ChIP-qPCR method, we could establish that StMSI1 and StBMI1-1 function upstream of miR156 to regulate aerial tubers in potato under short-day photoperiodic conditions.

Following are the important findings from this study:

1. Although the *StMSI1* and *StBMI1* express in diverse plant parts, they exhibit differential expression patterns in stolon tissues under the SD vs. LD photoperiod in potato.
2. The expression of *StMSI1* increases in stolon under short-day conditions, whereas, *StBMI1* decreases. However, during later stages of tuber development, the expression of *StMSI1* decreases, and that of *StBMI1* increases.
3. miR156 expression in stolon increases upon a perception of the SD photoperiod, indicating the opposite trend of expression between miR156 and StBMI1.

Summary

4. StMSI1 overexpression leads to the downregulation of StBMI1 and upregulation of miRNA 156.
5. Overexpression or knockdown of StMSI1 reduces belowground tuber yield accompanied by altered expression of tuber marker genes. Knockdown of StBMI1 reduces the belowground tuber yield, but its overexpression enhances the yield.
6. Overexpression lines of StMSI1 or knockdown lines of StBMI1 had a higher accumulation of miR156, and they developed aerial stolons/tubers like miR156 overexpression lines (previously reported, Bhogale et al. 2014).
7. RNA seq. data analysis of StMSI OE or StBMI-AS lines revealed that both proteins repress auxin and GA signaling related genes whereas, they promote cytokinin signaling related genes.
8. Based on this, we proposed that down-regulation of auxin and up-regulation cytokinin signaling related genes is the cause for the development of stolons/tubers from axillary nodes of these transgenic lines.
9. Also, the reduction in the expression of key tuberization inducing genes such as StSP6A explains the basis for reduced belowground tuber yield in *StMSI1* OE and *StBM1-1*-knockdown lines.

Chapter 3: Functional characterization of StE(z)2 (a H3K27 methyltransferase) in potential epigenetic regulation in potato

The core PRC2 complex in Drosophila consists of four subunits, namely Enhancer of Zeste [E(z)], Suppressor of Zeste 12 [Su(z)12], Extra sex combs (Esc), and p55. The [E(z)] protein represses target genes by catalyzing the H3K27me3 modification of these genes (Müller et al., 2002). E(z) is the main catalytic subunit of PRC2 that adds H3K27me3 repressive modification on the target chromatin through the SET domain (Su(var)3-9, E(z), Trx) (Müller *et al.,* 2002). Previous studies demonstrated that PRC2 proteins are involved in diverse processes in plants, including regulation of hormonal pathways (Lafos *et al.*, 2011; Teotia and Tang, 2015), meristematic activity and organ differentiation (Goodrich *et al.*, 1997). Arabidopsis has three homologs of E(z) named as CURLY LEAF (CLF), SWINGER (SWN), and MEDEA (MEA). They play role during different transition stages of plant development. E(z) like proteins in Arabidopsis are the part of three PRC2 complexes, known as FERTILIZATION

INDEPENDENT SEED (FIS) complex that regulates seed development (Kohler et al., 2003), EMBRYONIC FLOWER (EMF) complex that suppresses flowering during juvenile stage (Yoshida et al., 2001), and VERNALIZATION (VRN) complex, which is essential for the onset of flowering after vernalization (De Lucia et al., 2008) In this study, we have characterized the role of *StE(z)2* in potato development using overexpression and VIGS mediated knockdown approaches.

Following are the important findings from this study:

1. Potato has three *E(z)* homologs, namely *StE(z)1*, *StE(z)2,* and *PhCLF*. The *StE(z)2* shows the highest similarity to the CLF protein of Arabidopsis. All of them consist of the SET domain involved in H3K27 trimethylation over target genes.
2. Expression of *StE(z)1* and *StE(z)2* decreases in stolon under short-day photoperiod conditions.
3. Overexpression of *StE(z)2* alters overall plant architecture, including smaller leaves with reduced vascular bundles.
4. Moreover, *StE(z)2* overexpression results in reduced belowground tuber yield, however, these plants had a higher accumulation of miR156, and they also developed aerial tubers.
5. We found that important tuberization related genes, such as *StBEL5* and *StSP6A,* are repressed in *StE(z)2* OE lines whereas, their expression increases in *StE(z)2* VIGS lines.

Chapter 4: Identification of the direct targets of StE(z)2 and the genome-wide occupancy of histone modifications during stolon-to-tuber development in potato

Chromatin-remodeling through histone modification leads to Spatio-temporal regulation of genes that regulate developmental programs in response to environmental signals (Pikaard and Scheid, 2014). Polycomb Repressive Complex (PRC) and Trithorax Group (TrxG) proteins are important chromatin modifiers that antagonistically regulate target genes to ensure developmental transitions in plants (Pien and Grossniklaus, 2007). Several PRC and TrxG proteins are shown to regulate flowering and hormonal pathways in Arabidopsis (Goodrich *et al.,* 1997; Jiang *et al.,* 2008; Shafiq *et al.,* 2014; Steinbach and Hennig, 2014; Gu *et al.,* 2014). PcG mediated H3K27me3 modification represses the target genes. TrxG proteins perform H3K4me3

and H3K36me3 activation modifications through the SET domain and thereby counteract the activity of PRC proteins.

Short-day photoperiod triggers differential expression of numerous genes in potato development. However, the gene regulatory network that controls the expression of these genes in a Spatio-temporal manner during tuber development is not well understood. To identify the direct targets of StE(z)2 as well as genes associated with H3K4me3 and H3K27me3 modifications during tuberization, we have performed chromatin immunoprecipitation sequencing (ChIP-seq) on SD-induced stolons from wild-type and FLAG-tagged StE(z)2-OE line. This investigation showed that PRC2-mediated H3K27me3 and TrxG-mediated H3K4me3 modifications regulate key tuberization genes (such as *StBEL5, POTH1, StGA2ox1,* and *StSP6A*) in a photoperiod-dependent pathway in potato.

Following are the important findings from this study:

1. Through ChIP-seq analysis, we could identify 20,860 peaks of H3K4me3 and 2,309 peaks of H3K27me3 modification from WT short day induced stolon.
2. However, in FLAG-tagged StE(z)2-OE line, we could identify 2,035 peaks of E(z)2, 10,306 of H3K4me3, and 4,682 of H3K27me3 modifications from SD-induced stolon.
3. Our analysis revealed that overexpression of StE(z)2 increases the number of genes with H3K27me3 modification, whereas it reduced the number of genes with H3K4me3 modification.
4. The expressions of important genes involved in tuberization are found to be regulated through H3K4me3 and H3K27me3 modifications during stolon to tuber transition.
5. We could also identify that target site of both types of modifications were enriched in telobox motif (AAACCCTAAA) suggesting their role in the recruitment of PcG and TrxG proteins over target regions in the potato genome.
6. Through bioinformatics analysis, we also identified that E(z)2 protein interact with zinc finger protein that recognizes telobox motifs, suggesting that they might be playing an important role in targeting the PRC complex.

Future directions:

Overall, our study has established that Polycomb Group proteins regulate stolon to tuber transition as well as overall plant architecture in potato. Besides this, we have also identified the genes are regulated by PRC proteins StMSI1 as well as StBMI1. Through ChIP-seq analysis, we have identified direct targets of StE(z)2 as well as genome-wide occupancy of H3K4me3 and H3K27me3 modifications. Our study has generated a large amount of data that can be used in the future for a better understanding of potato development.

Following future directions can be taken to enhance the knowledge about photoperiod dependent tuberization in Solanum tuberosum ssp. andigena.

1. Our study has shown that more than12000 genes are regulated by the Trithorax group (TrxG) proteins mediated H3K4me3 modification. It would be interesting in the future to characterize the role of candidate TrxG proteins in potato development.
2. In this study, we have characterized the role of Three PRC proteins, however the role of other proteins in potato development cannot be ignored. Recently a PRC1 member EMF1 has been shown to regulate photoperiod dependent flowering in Arabidopsis. It would be interesting to investigate the role of StEMF1 and other PRC proteins in potato.
3. Although MSI1 is part of several other Histone modifier complexes such as histone deacetylases, In this study, we have focused only on its role associated with PRC2 complex. It would be equally interesting to see if histone acetylation/deacetylation is also contributing to regulate the downstream genes that are differentially in StMSI-OE lines.
4. Through ChiP-seq analysis, we have also identified the DNA motifs that are over-represented in target sites of H3K4me3 and H3K27me3 modifications. Future studies can figure about the role of these motifs in the recruitment of PcG and TrxG proteins to their targets.

List of gene accessions and primers used in this study

Gene accessions

Sr. No.	Gene/protein name	PGSC ID
1	MSI1	PGSC0003DMT400061016
2	BMI1-1	PGSC0003DMT400038984
3	SDG4	PGSC0003DMT400028984
4	SET7/9	PGSC0003DMT400004624
5	LHP1	PGSC0003DMT400079885
6	HDA19	PGSC0003DMT400076252
7	E3 ubiquitin-protein ligase	PGSC0003DMT400025575
8	PYL4	PGSC0003DMT400028658
9	SAUR	PGSC0003DMT400008365
10	ARF16	PGSC0003DMT400055522
11	Epidermal patterning factor (EPF)	PGSC0003DMT400043275
12	Cyclin A2 (CycA2)	PGSC0003DMT400067117
13	CLAVATA1 (CLV)	PGSC0003DMT400043020
14	ERECTA (ERC)	PGSC0003DMT400048435
15	TCP transcription factor	PGSC0003DMT400014572
16	Pseudo-response regulator	PGSC0003DMT400050251
17	Protease	PGSC0003DMT400039852
18	Chalcone synthase	PGSC0003DMT400043447
19	HD-ZIP TF	PGSC0003DMT400074934
20	Sugar transporter	PGSC0003DMT400013217
21	Longifolia	PGSC0003DMT400003717
22	Glabra	PGSC0003DMT400051268
23	SP6A	PGSC0003DMT400060057
24	14-3-3	PGSC0003DMT400045782
25	PHYB2	PGSC0003DMT400069974
26	CONSTANS (CO1)	PGSC0003DMT400075520
27	CO2	PGSC0003DMT400070680
28	Auxin efflux 1	PGSC0003DMT400072460
29	Auxin efflux 2	PGSC0003DMT400015267
30	ARP	PGSC0003DMT400015610
31	Expansin	PGSC0003DMT400003608
32	AUX/IAA	PGSC0003DMT400041976
33	AUX-IAA3	PGSC0003DMT400050101
34	CytoP450	PGSC0003DMT400044731
35	BR kinase	PGSC0003DMT400060442
36	Thesasus	PGSC0003DMT400060204
37	Phi-1 protein	PGSC0003DMT400079157
38	Sigma factor sigb regulation protein rsbq	PGSC0003DMT400092427
39	STL responsive gene	PGSC0003DMT400043632
40	GIP1	PGSC0003DMT400050285
41	GAST1	PGSC0003DMT400009367
42	ER33	PGSC0003DMT400037898
43	Purine transporter 2	PGSC0003DMT400045772
44	Purine transporter 3	PGSC0003DMT400025116
45	Zeatin riboside	PGSC0003DMT400070218
46	SPL8	PGSC0003DMT400074976
47	SPL9	PGSC0003DMT400082788
48	SPL13	PGSC0003DMT400056373

List of gene accessions and primers used in this study

49	StE(z)1	PGSC0003DMP400015912
50	StE(z)2	PGSC0003DMP400056358
51	StPHCLF2	PGSC0003DMP400007142
52	ARP	PGSC0003DMG400006093
53	Auxin induced protein	PGSC0003DMG400027717 PGSC0003DMG402004120
54	AUX/IAA 13	PGSC0003DMG400000375
55	AUX/IAA3	PGSC0003DMG402019457
56	AUX/IAA4	PGSC0003DMG400001498 PGSC0003DMG400000375
57	Dormancy/auxin associated family protein	PGSC0003DMG400004897
58	SAUR family proteins	PGSC0003DMG400030234
59	PIN proteins	PGSC0003DMG400019182 PGSC0003DMG400009927
60	ARF19	PGSC0003DMG400013686
61	ARF2	PGSC0003DMG400031888
62	ARF6	PGSC0003DMG400028826
63	ARF8	PGSC0003DMG401018664
64	DOF family growth repressor	PGSC0003DMG400030406
65	Brassinosteroid receptor Thesaus kinase	PGSC0003DMG400023419 PGSC0003DMG400021993
66	Brassinonosteroid hydroxylase	PGSC0003DMG400001060
67	Cytokinin signaling genes Isopentyl transferase	PGSC0003DMG400036656 PGSC0003DMG400014561 PGSC0003DMG400014563
68	Zeatin glucosyl transferase	PGSC0003DMG400029825 PGSC0003DMG400027291 PGSC0003DMG400028331
69	Purine transporters	PGSC0003DMG400017751 PGSC0003DMG400021023 PGSC0003DMG400009707
70	Histidine kinase	PGSC0003DMG400004643 PGSC0003DMG400029514
71	Cytokinin receptor	PGSC0003DMG400029463
72	Tuber storage proteins patatins	PGSC0003DMG402017090 PGSC0003DMG400029247
73	Starch synthases	PGSC0003DMG401013540 PGSC0003DMG402013540 PGSC0003DMG400008322
74	Cellulose synthase	PGSC0003DMG403022167 PGSC0003DMG402022167 PGSC0003DMG400003822
75	Sugar transporters	PGSC0003DM28G400027425 PGSC0003DM30G400013562 PGSC0003DMG400007865 PGSC0003DMG400000367 PGSC0003DMG400017789 PGSC0003DMG400015460 PGSC0003DMG400014898 PGSC0003DMG400012680
76	GA2ox1	PGSC0003DMG400021095
77	CLF antagonist and meristamatic zone regulator ultrapetala	PGSC0003DMG400018322
78	Trithorax	PGSC0003DMG400018162

List of gene accessions and primers used in this study

79	CLAVATA1	PGSC0003DMG400009380 PGSC0003DMG400029146
80	POTH1	PGSC0003DMG400013493
81	BEL1-LIKE	PGSC0003DMG400003751 PGSC0003DMG400019142 PGSC0003DMG400021323 PGSC0003DMG400030961
82	Adenylate isopentenyltransferase	PGSC0003DMG400038521 PGSC0003DMG400038422
83	Purine transporters	PGSC0003DMG400017751
84	Meristem marker Clavata1	PGSC0003DMG400011833
85	Patatin	PGSC0003DMG400008749 PGSC0003DMG400014104
86	HD-Zip IV gene family member ROC5	PGSC0003DMG40001087
87	F-box/kelch-repeat protein	PGSC0003DMG400023430
88	Ubiquinone oxidoreductase	PGSC0003DMG400034811
89	Serine endopeptidase degp2	PGSC0003DMG401024031

List of gene accessions and primers used in this study

List of primers used in this study

Sr.No.	Primer name	Sequence (5'→3')
1	MSI1 qFP	GATGCTGAGAATGATGCCCG
2	MSI1 qRP	TGATAAATGGGTTTTGGGGCA
3	MSI1-CDS-BamH1 FP	AACGGATCCAATGGGGAAAGACGAAGATGAG
4	MSI1-CDS-SacI RP	AAAGAGCTCAGAGGGGCAAATGGAACAAC
5	MSI1-AS SacI FP	TTAATAGAGCTCCTCACCGTCGAATGGTTACCG
6	MSI1-AS BamH1 RP	TCAATGGGATCCTGCCTCAGATGCCAAGCTACA
7	promMSI1 HindIII FP	TGGCATAAGCTTGGAAATTCTAGTTTGTGGTGGC
8	promMSI1 BamHI RP	TAGTTTGGATCCTCTTCTTCTGTTTTGAGTGTGTG
9	StBMI1-1 qFP	GTTGAGATTAGATGTATGGGAC
10	StBMI1-1 qRP	TTAAGAAGCTGGAACGCCTGG
11	BMI1_3 qFP	GGTTGATGTATGCGGAATTC
12	BMI1_3 qRP	GATATTTCCATTTACGGAAGTG
13	BMI1_4 qFP	AGGACGACAATGATGATGAAG
14	BMI1_4 qRP	TTACTATGACTACTTGATGGTGCT
15	BMI1-1 CDS XbaI FP1	AGTGTCTAGAATGACGAATCAATTGGTGAAGG
16	BMI1-1 CDS SacI RP1	CGATGAGCTCTTAAGAAGCTGGAACGCCTGG
17	BMI1-1AS SacI FP1	ACTGGAGCTCGCTGATAATAGAGAGGTGGATAG
18	BMI1-1 AS XbaI RP1	GACTTCTAGACTCTCCTTTCTCCTCACTGG
19	BMI1-1 CDSscr FP	GTTGAGATTAGATGTATGGGAC
20	BMI1-1 ASscr RP	TCTCTAAAGGAACACAGCC
21	NOST RPscr	GCAACAGGATTCAATCTTAAG
22	ElF3e qFP	GGAGCACAGGAGAAGATGAAGGAG
23	ElF3e qRP	CGTTGGTGAATGCGGCAGTAGG
24	Clavata (CLV) 3020 qFP	GCAAGACTCGGGAACATC
25	Clavata (CLV) 3020 qRP	CTAACAGAACCACACCAAAG
26	ERECTA (ERC) 8435 qFP	CACTGGAAGGAAAGCTGTAG
27	ERECTA (ERC) 8435 qRP	GTACTCTTGCCACTTCATGC
28	CyclinA2 7117 qFP	CATACAATAATCCATCCTTCC
29	CyclinA2 7117 qRP	CTTAGTGCATCCGCTTCAT
30	PHYB2 9974 qFP	GCGAGTGTGATAGATGCTGT
31	PHYB2 9974 qRP	GGACTTCTACCCACCCTTG
32	CONSTANS (CO1) 5520 qFP	GCGTTTCATCATCATCTATTG
33	CONSTANS (CO1) 5520 qRP	CTATTCTTCCTCTTCTCTCTGTAC
34	CONSTANS (CO2) 0680 qFP	CTGGGTTTAGATAGAGAAGCAAG
35	CONSTANS (CO2) 0680 qRP	GTCAACGTCATCAAACTCGC
36	TCP 4572 qFP	CTAATAATACTCACAAGCAACAG
37	TCP 4572 qRP	TCTTTCCCTTGCCCTTG
38	SPL13 6373 FP	GCAGCAGGAATTTCTAGCAG
39	SPL13 6373 RPo	GACTGGGAACGTGGGATAG
40	SPL13 6373 RPi	GCTCAAACCAATCTCCCTAG
41	SPL9 2789 qFP	CGTCGTCATCGTCTTCATCA
42	SPL9 2789 qRP	GGGATGGTATGTGAATGATGA
43	BR Kinase qFP	ATAATCATTTACGAGTACATGGAG
44	BR Kinase qRP	TGAGAACCAGTATGCAGATAGTG
45	Thesasus qFP	AATCAATCCTTCACTCCCACGA
46	Thesasus qRP	ATTTCCTGAGTGAATCAATGCTC
47	Cyto P450 qFP	GGAGAGTGATGAGCAAATAAGC
48	Cyto P450 qRP	TTGTTCTCCTTCTTCTACCTCC
49	HD-ZIP TF qFP	TTCAGAGGGTTGCTTTGGCTC

List of gene accessions and primers used in this study

50	HD-ZIP TF qRP	ACGCCTAAGAAGTACCTATAAC
51	GLABRA qFP	GCACCCATAAAGTTACCAACGG
52	GLABRA qRP	AAGTCACTGTCAAAATTGAACCA
53	Longifolia3717 qFP	ACAGCAACTCCAGAAGGAACTG
54	Longifolia3717 qRP	GAATTTCACTGTCACCGTTTGTC
55	Protease39852 qFP	CATCCCAACAGATAAAAGCCATC
56	Protease39852 qRP	TATCCGACTTGCTGCTGTTCCT
57	Epidermal pattern forming (EPF) 26067 qFP1	TCAAGTACCGAGCCTACCGAG
58	Epidermal pattern forming (EPF) 6067 qRP1	ACCTGCTACCTCCCGCACG
59	SET7/9 4624 qFP	TGCTGGGGAATGGTGTAATG
60	SET7/9 4624 qRP	TTGACACCCCACTTAAACTCC
61	14.3.3 qFP	ACTGAACTTGCCCCAACACATC
62	14.3.3 qRP	AAGCACGGTCAGGAGAGTTCA
63	Zeatin riboside qFP	GAATCTTGGAGCTTCTCAGAGT
64	Zeatin riboside qRP	CATTGTTTCTTCTCCTGTTTACTT
65	SP6A qFP	GACGATCTTCGCAACTTTTACA
66	SP6A qRP	CCTCAAGTTAGGGTCGCTTG
67	BEL5 qFP	AGGGATACTCTTATATTGTGTGAG
68	BEL5 qRP	GTCTCCACTTCTTTTCTCCTATG
69	Purine transporter 2 qFP	TCATGTTAAAGCTGGAGTTGTTG
70	Purine transporter 2 qRP	CTTCAGCTTCTCTAGTGATGGC
73	Chalcone synthase qFP	GGATCAAATTGAATTAAAGTTGGGC
74	Chalcone synthase qRP	ACCTGTAGTACCCAATCCTGC
75	Pseudo-response regulator qFP	CTTAGTATATCATTGTTTGCTGC
76	Pseudo-response regulator qRP	AAGGCAAGAGGCTCCAACTAC
77	Aux/IAA3 qFP	TGAAAGTTAGTGTTGACGGTGC
78	Aux/IAA3 qRP	GAAATCCTTAAATCCTTGAGTCC
79	Auxin Response Protein (ARP) qFP	TGCCAACCTATGAAGATAAAGATG
80	Auxin Response Protein (ARP) qRP	GCTTCTGATCCTTTCATTATGCG
81	Expansin qFP	GCAGAAGAAGTGGAGGAATTAGA
82	Expansin qRP	ATTGAGTTCTTGAACCCTTGATG
83	Aux/IAA qFP	TGGATGTCCTCAATAGTTCTGAC
84	Aux/IAA qRP	CAAGTCCAATGGCTTCTGATC
85	Auxin efflux carrier 1 qFP	TCAACCGAAGATAATAGCATGTG
86	Auxin efflux carrier 1 qRP	CTTGTGGCAATGCAGCCTGG
87	Auxin efflux carrier 2 qFP	CTGCTGCTAGTGTGATGACC
88	Auxin efflux carrier 2 qRP	AAGGCATCTGAATGTTCCACC
89	Sugar transporter qFP	TAACAGTAAATTAGGGGATGAGG
90	Sugar transporter qRP	CACCTAGAGTTTTGCTTCCGTT
91	Chromo domain-containing protein (LHP1) qFP	GGAGACGGCAAATACATGGG
92	Chromo domain-containing protein (LHP1) qRP	TTTCTTGGGTTGAGTCTGTGT
95	Small auxin up RNA (SAUR) qFP	CGAGAGGATGCGTTACGGTGTTG
96	Small auxin up RNA (SAUR) qRP	GATGATGGTGGTGGTGATGAACG
97	LOG1 qFP	GTGTTGATTCATTTTTGTCCA
98	LOG1 qRP	TACCAAACAATCATATACAGACAG
99	SDG4 FP	TAAAGATTGGGTTGAGAGGAAG

List of gene accessions and primers used in this study

100	SDG4 RP	AATCCTTGGCAAACAGAGCACTC
103	ChIP miR156b qFP	GGAGGTCATTTGGTCATTTTCT
104	ChIP miR156b qRP	GAGATTATTATACACCTTAATAGATA
105	ChIP miR156e qFP	ATAAAGGTCAAGGCTTGGAAGAC
106	ChIP miR156e qRP	GTCTTACTCATTATGAATCTCAAC
107	ChIP miR156f qFP	ATACTACTACTATTTGACAATTCAG
108	ChIP miR156f qRP	TTCTGTCAGTCCCTCTCTTCC
109	ChIP miR156g qFP	GACTCTCTATCATTCCTCACAC
110	ChIP miR156g qRP	CCTAGCTTGATGTGGCTATTGTT
111	ChIP BMI1.1 qFP	TGCCTGTGTTTTGTGCGGAAG
112	ChIP BMI1.1 qRP	AGATGCTTCACACAATATACACC
113	ChIP BMI1.3 qFP	ATGGTTCCTGTGATTAGTAGATA
114	ChIP BMI1.3 qRP	TAATACTTGCTAAAGGCTAGATG
115	U6 STP	GTCGTATCCAGTGCAGGGTCCGAGGTATTCGCACTGGATACG ACTTGGAC
116	U6 FP	GACACGCACAAATCGAGAAATG
117	Universal RP	AGTGCAGGGTCCGAGGT
118	miR156a/b/c STP	GTCGTATCCAGTGCAGGGTCCGAGGTATTCGCACTGGATACG ACGTGCTC
119	miR156a/b/c FP	GCGGCGGTGACAGAAGAGAGT
120	miR156e STP	GTCGTATCCAGTGCAGGGTCCGAGGTATTCGCACTGGATACG AGTGCTC
121	miR156e FP	GGATGTGTGACAGAAGAGAGT
122	miR156f-5p STP	GTCGTATCCAGTGCAGGGTCCGAGGTATTCGCACTGGATACG ACTGCTCA
123	miR156f-5p FP	GTTGCGTGCTGACAGAAGAGAG
124	miR172 STP	GTCGTATCCAGTGCAGGGTCCGAGGTATTCGCACTGGATACG ACATGAG
125	miR172 FP	CGGCGGTAGAATCTTGATGATG
126	Pri-miR156a FP	GTCTTATCTACAAAACTCAACTAT
127	Pri-miR156a RP	GCACAAAGGAGTAAGGTGCAG
128	Pre-miR156c FP2	GCACGAATAATGGAAGCTGCAT
129	Pri-miR156c RP	TAATAAATTAAAGGTAGAGACTAG
130	PromStE(z)2 - HindIII-FP	TCTTAAGCTTGTTGTGGGTGAGGACGATTG
131	PromStE(z)2 - BamHI-RP	GGTTGGATCCGTTTGAGAATCCGACAGGGAG
132	StE(z)2-FL - BamHI-FP	GACAGAGGATCCTTGACACCGGCAATGTCT
133	StE(z)2-FL - SacI-RP	ATAAGAGCTCCACTCAATTATGTATGCTTCCTA
134	StE(z)2-FL-FLAG - BamHI-FP	GACAGAGGATCCATGGACTACAAAGACGATGACGACAAGTT GACACCGGCAATGTCT
135	StE(z)2-AS-VIGS - SalI-FP	CGAGTCGACGGTGAAGGTGCTCCAAATGC
136	StE(z)2-AS-VIGS - ClaI-RP	TGTATCGATCATCACCATTGGAACCACC
137	StPDS-VIGS-AS - SalI-FP	GATGTCGACGGAAAGATGATGATGGAGATTG
138	StPDS -VIGS-AS - ClaI-RP	TCTATCGATGTGAGTTCAATCTGACTTGGC
139	NOST RPscr	GCAACAGGATTCAATCTTAAG
142	StE(z)1 qFP	CCTTACTGCTGCTTTAGATTCTTTTG
143	StE(z)1 qRP	GAATATTTAGTCTGGTTTGCCACAC
144	StE(z)2 qFP	TGTTTGCAGAGTCCGAAGATTATATG
145	StE(z)2 qRP	TAGATTATCAAAAGAATCCAGAGCAG
148	St Thesasus qFP	AATCAATCCTTCACTCCCACGA
149	St Thesasus qRP	ATTTCCTGAGTGAATCAATGCTC
150	St 14.3.3 qFP	ACTGAACTTGCCCCAACACATC
151	St 14.3.3 qRP	AAGCACGGTCAGGAGAGTTCA
152	StSP6A qFP	GACGATCTTCGCAACTTTTACA
153	StSP6A qRP	CCTCAAGTTAGGGTCGCTTG

List of gene accessions and primers used in this study

154	StBEL5 qFP	AGGGATACTCTTATATTGTGTGAG
155	StBEL5 qRP	GTCTCCACTTCTTTTCTCCTATG
156	St Purine transporter 3 qFP	ATAGAAATGTCAACTTATCAGTCG
157	St Purine transporter 3 qRP	ATTCATATTCATTCATTTCTTTCAC
158	St Expansin qFP	GCAGAAGAAGTGGAGGAATTAGA
159	St Expansin qRP	ATTGAGTTCTTGAACCCTTGATG
160	StSDG4 FP	TAAAGATTGGGTTGAGAGGAAG
161	StSDG4 RP	AATCCTTGGCAAACAGAGCACTC
162	StATXR3-7285 qFP	GTTCTGGCGACTGTGGTGCG
163	StATXR3-7285 qRP	CCCGCTTTGCTTTCATCTTACC
164	StATXR7-9059 qFP	GTGCTTGTCGCTTGGTTAATGG
165	StATXR7-9059 qRP	ACTGATGTGAAGATTGGTGAAGAA
166	StGA2ox1-4348 qFP	GCTTGGTGATAATAGGTTGTCC
167	StGA2ox1-4348 qRP	CACCTGGTCCGAGTCATTAAC
168	St MDR transporter qF	AGAATACCTAGTGAAGAATCTG
169	St MDR transporter qR	AACCTTGAAGAACTAATGGAGC
170	St Glutamine Synth qF	ACAACAACTTCGGTGCCTCCT
171	St Glutamine Synth qR	CTGGTTTTGAAATAGTTGCTGG
172	St Cytochrome C oxi qF	TACCACAATCGAGGAGACGG
173	St Cytochrome C oxi qR	TATTCTGGAGAAGCGTCCTC
174	St Cytochrome p450 qF	TTCACCTTGGAGACCTGATG
175	St Cytochrome p450 qR	GCACGTCGCGTGGTGTCC
176	Stu U6 STP	GTCGTATCCAGTGCAGGGTCCGAGGTATTCGCACTGGATACG ACTTGGAC
177	Stu miR156a/b/c STP	GTCGTATCCAGTGCAGGGTCCGAGGTATTCGCACTGGATACG ACGTGCTC
178	Stu miR166 STP	GTCGTATCCAGTGCAGGGTCCGAGGTATTCGCACTGGATACG ACGGGAAT
179	Stu U6 FP	GACACGCACAAATCGAGAAATG
180	Stu miR156a/b/c FP	GCGGCGGTGACAGAAGAGAGT
181	Stu miR166 FP	TGGAGGTTCGGACCAGGCTTC
182	Universal RP	AGTGCAGGGTCCGAGGT
183	StSP6A-ChIP FP	TATTTGGAGGGGTAGAGGGGT
184	StSP6A-ChIP RP	ATAATGGATGATAGTTAATCGTTC

List of gene accessions and primers used in this study

References

A.V. Probst, M. Fagard, F. Proux, P. Mourrain, S. Boutet, K. Earley, R.J. Lawrence,C.S. Pikaard, J. Murfett, I. Furner, H. Vaucheret, O.M. Scheid, (2004) Arabidopsis histone deacetylase HDA6 is required for maintenance of transcriptional gene silencing and determines nuclear organization of rDNA repeats, Plant Cell 16 1021–1034.

Abdala, G., Castro, G., Miersch, O., and Pearce, D. (2002) Changes in Jasmonate and Gibberellin Levels during Development of Potato Plants (*Solanum tuberosum*), *Plant Growth Regul.*, vol. 36, pp. 121–126.

Abelenda JA, Bergonzi S, Oortwijn M, Sonnewald S, Du M, Visser RGF, Sonnewald U, Bachem CWB. (2019) Source-sink regulation is mediated by interaction of an FT homolog with a sweet protein in potato. Current Biology **29**, 1178-1186.

Ach, R.A., Taranto, P., Gruissem, W. (1997) A conserved family of WD-40 proteins binds to the retinoblastoma protein in both plants and animals. Plant Cell 9: 1595–1606.

Aichinger E, Villar CB, Di Mambro R, Sabatini S, Kohler C. (2011) The CHD3 chromatin remodeler PICKLE and polycomb group proteins antagonistically regulate meristem activity in the Arabidopsis root. The Plant Cell **23**, 1047-1060.

Aksenova NP, Konstantinova TN, Golyanovskaya SA, Sergeeva LI, Romanov GA. 2012. Hormonal Regulation of Tuber Formation in Potato Plants. Russian Journal of Plant Physiology **59**, 451-466.

Allenbach L, Poirier Y (2000) Analysis of the Alternative Pathways for the β-Oxidation of Unsaturated Fatty Acids Using Transgenic Plants Synthesizing Polyhydroxyalkanoates in Peroxisomes. Plant Physiology **124**, 1159-1168.

Alvarez-Venegas R, Pien S, Sadder M, Witmer X, Grossniklaus U, Avramova Z (2003) ATX-1, an Arabidopsis homolog of trithorax, activatesflower homeotic genes. Curr Biol 13: 627–637.

Ausin I, Alonso-Blanco C, Jarillo JA, Ruiz-Garcia L, Martinez-Zapater JM (2004) Regulation of flowering time by FVE, a retinoblastoma-associated protein. Nat Genet 36:162–166.

Banerjee AK, Chatterjee M, Yu YY, Suh SG, Miller WA, Hannapel DJ. (2006a) Dynamics of a mobile RNA of potato involved in a long-distance signaling pathway. The Plant Cell **18**, 3443-3457.

Banerjee AK, Prat S, Hannapel DJ. (2006b) Efficient production of transgenic potato (S. tuberosum L. ssp. andigena) plants via Agrobacterium tumefaciens-mediated transformation. Plant Science **170**, 732-738.

Benhamed M, Martin-Magniette ML, Taconnat L, et al. (2008) Genome-scale Arabidopsis promoter array identifies targets of the histone acetyltransferase GCN5. Plant Journal 56, 493–504

Berger SL, Kouzarides T, Shiekhattar R, Shilatifard A. (2009) An operational definition of epigenetics. Genes and Development 23, 781–783.

Berr A, Xu L, Gao J, Cognat V, Steinmetz A, Dong A, Shen W-H. (2009) SET DOMAIN GROUP25 encodes a histone methyltransferase and is involved in FLOWERING LOCUS C activation and repression of flowering. Plant Physiology **151**, 1476-1485.

Bertrand C, Benhamed M, Li YF, Ayadi M, Lemonnier G, Renou JP, Delarue M, Zhou DX (2005) Arabidopsis HAF2 gene encoding TATA-binding protein (TBP)-associated factor TAF1, is required to integrate light signals to regulate gene expression and growth. J Biol Chem 280:1465–1473

Bhogale S, Mahajan A. S, Natarajan B, Rajabhoj M, Thulasiram H V., Banerjee A. K. 2013. MicroRNA156: A Potential Graft-Transmissible MicroRNA That Modulates Plant Architecture and Tuberization in Solanum tuberosum ssp. andigena. Plant Physiology 164, 1011–1027.

Bouveret R, Schönrock N, Gruissem W, Hennig L. (2006) Regulation of flowering time by Arabidopsis MSI1. Development **133**, 1693-1702.

Bouyer D, Roudier F, Heese M, et al. (2011) Polycomb repressive complex 2 controls the embryo-to-seedling phase transition. PLoS Genetics 7

H. Waddington, Endeavour 1, 18 (1942)

C. Wang, F. Gao, J. Wu, J. Dai, C. Wei, Y. Li (2010) Arabidopsis putative deacetylase AtSRT2 regulates basal defense by suppressing PAD4, EDS5 and SID2 expression, Plant Cell Physiol. 51, 1291–1299

C.M. Pickart (2001) Mechanisms underlying ubiquitination, Annu. Rev. Biochem. 70 503–533.

Cai S, Lashbrook CC. (2006) Laser capture microdissection of plant cells from tape-transferred paraffin sections promotes recovery of structurally intact RNA for global gene profiling. The Plant Journal **48**, 628-637.

Calonje, M. (2014). PRC1 marks the difference in plant PcG repression. Mol. Plant 7: 459-471.

Cao X., Jacobsen S.E. (2002) Locus-specific control of asymmetric and CpNpG methylation by the DRM and CMT3 methyltransferase genes. Proc. Natl. Acad. Sci. USA. 99:16491–16498. doi: 10.1073/pnas.162371599.

Cao, R., Tsukada, Y., and Zhang, Y. (2005). Role of Bmi-1 and Ring1A in H2A ubiquitylation and Hox gene silencing. Mol. Cell 20: 845-854.

Cao, X., He, Z., Guo, L., and Liu, X. (2015). Epigenetic mechanisms are critical for the regulation of WUSCHEL expression in floral meristems: figure 1. Plant Physiol. 168, 1189–1196

Carles CC, Fletcher JC (2009) The SAND domain protein ULTRAPETALA1 acts as a trithorax group factor to regulate cell fate in plants. Genes Dev 23: 2723–2728

Carrera, E., Jackson, S.D., and Prat, S. (1999) Feedback Control and Diurnal Regulation of Gibberellin 20_ Oxidase Transcript Levels in Potato, *Plant Physiol.*, vol. 119, pp. 765–773.

Cartagena, J.A., Matsunaga, S., Seki, M., Kurihara, D., Yokoyama, M., Shinozaki, K., Fujimoto, S., Azumi, Y., Uchiyama, S., and Fukui, K. (2008). The Arabidopsis SDG4 contributes to the regulation of pollen tube growth by methylation of histone H3 lysines 4 and 36 in mature pollen. Dev. Biol. 315: 355-368.

Castro, G., Abdala, G., Aguero, C., and Tizio, R. (2000), Interaction between Jasmonic and Gibberellic Acids on *In Vitro* Tuberization of Potato Plants, *Potato Res.*,2000, vol. 43, pp. 83–88.

Chanvivattana, Y. et al. (2004) Interaction of Polycomb-group proteins controlling flowering in Arabidopsis. Development 131, 5263–5276

Chapman HW (1958) Tuberization in the potato plant. Physiol Plant 11: 215–224

Chaudhury, Peacock WJ. 1997. Fertilization-independent seed development in Arabidopsis thaliana. 94, 4223–4228.

Chen H, Banerjee AK, Hannapel DJ. (2004) The tandem complex of BEL and KNOX partners is required for transcriptional repression of ga20ox1. Plant Journal 38, 276–284.

Cheng, L., Shafiq, S., Xu, W. et al. (2018) EARLY FLOWERING IN SHORT DAYS (EFS) regulates the seed size in Arabidopsis Sci. China Life Sci. 61: 214.

Chincinska IA, Liesche J, Krügel U, Michalska J, Geigenberger P, Grimm B, Kühn C. (2008) Sucrose transporter StSUT4 from potato affects flowering, tuberization, and shade avoidance response. Plant Physiology **146**, 515-528.

Choi SC, Lee S, Kim S-R, Lee Y-S, Liu C, Cao X, An G. (2014) Trithorax Group Protein Oryza sativa Trithorax1 Controls Flowering Time in Rice via Interaction with Early heading date3. Plant Physiology **164**, 1326-1337.

Clara L. van Emmerik, Hugo van Ingen (2019) Unspinning chromatin: Revealing the dynamic nucleosome landscape by NMR Elsevier Volume 110, Pages 1-19

Cloos PAC, Christensen J, Agger K, Helin K. (2008) Erasing the methyl mark: Histone demethylases at the center of cellular differentiation and disease. Genes and Development 22, 1115–1140.

Conesa A, Götz S, Garcia-Gomez JM, Terol J, Talon M, Robles M. (2005) Blast2GO: a universal tool for annotation, visualization and analysis in functional genomics research. Bioinformatics **21**, 3674-3676.

Dai, X., and Zhao, P.X. (2011). psRNATarget: a plant small RNA target analysis server. Nucleic Acids Res. 39: W155-9.

De Lucia F, Crevillen P, Jones AM, Greb T, Dean C. (2008). A PHD-polycomb repressive complex 2 triggers the epigenetic silencing of FLC during vernalization. Proceedings of the National Academy of Sciences of the United States of America **105**, 16831-16836.

De Lucia, F., Crevillen, P., Jones, A.M., Greb, T., and Dean, C. (2008). A PHD-polycomb repressive complex 2 triggers the epigenetic silencing of FLC during vernalization. Proc. Natl. Acad. Sci. USA 105: 16831-16836.

Deal RB, Henikoff S. (2011). Histone variants and modifications in plantgene regulation. Curr Opin Plant Biol 14: 116–122

Deng, W., Liu, C., Pei, Y., Deng, X., Niu, L., & Cao, X. (2007). Involvement of the histone acetyltransferase AtHAC1 in the regulation of flowering time via repression of FLOWERING LOCUS C in Arabidopsis. *Plant physiology*, *143*(4), 1660–1668. doi:10.1104/pp.106.095521

Dereeper A, Guignon V, Blanc G, Audic S, Buffet S, *et al.* (2008) Phylogeny.fr: robust phylogenetic analysis for the non-specialist. Nucleic Acids Research **36**, W465-469.

Dereeper, A., Guignon, V., Blanc, G., Audic, S., Buffet, S., Chevenet, F., Dufayard, J.F., Guindon, S., Lefort, V., Lescot, M., Claverie, J.M., Gascuel, O. (2008). Phylogeny.fr: robust phylogenetic analysis for the non-specialist. Nucl. Acids Res. 36: W465-469.

Derkacheva, M., Steinbach, Y., Wildhaber, T., Mozgova, I., Mahrez, W., Nanni, P., Bischof, S., Gruissem, W., and Hennig, L. (2013). Arabidopsis MSI1 connects LHP1 to PRC2 complexes. EMBO J. 32: 2073-2085.

Dhonukshe P, Weits DA, Cruz-Ramirez A, Deinum EE, Tindemans SH, Kakar K, et al. (2012) A PLETHORA auxin transcription module controls cell division plane rotation through MAP65 and CLASP. Cell; 149:383-96.

Dobin, A., Davis, C.A., Schlesinger, F., Drenkow, J., Zaleski, C., Jha, S., Batut, P., Chaisson, M., Gingeras, T.R. (2013). STAR: Ultrafast universal RNA-seq aligner. Bioinformatics 29: 15-21.

Dodsworth, S. (2009). A diverse and intricate signalling network regulates stem cell fate in the shoot apical meristem. Dev. Biol. 336, 1–9.

Domagalska, M.A., and Leyser, O. (2011). Signal integration in the control of shoot branching. Nature Rev. Mol. Cell Biol. 12: 211-221.

Du J, Rietman H, Vleeshouwers VG. (2014) Agroinfiltration and PVX Agroinfection in Potato and Nicotiana benthamiana. Journal of Visualized Experiments **83**, e50971, doi:10.3791/50971.

Ebbs, M. L., and Bender, J. (2006). Locus-specific control of DNA methylation by the Arabidopsis SUVH5 histone methyltransferase. Plant Cell 18, 1166–1176. doi: 10.1105/tpc.106.041400

Eviatar-Ribak T, Shalit-Kaneh A, Chappell-Maor L, Amsellem Z, Eshed Y, Lifschitz E (2013) A cytokinin-activating enzyme promotes tuber formation in tomato. Curr Biol 23: 1057–1064

Ewing EE, Struik PC. (1992) Tuber formation in potato: induction, initiation and growth. Horticultural Reviews **14**, 89-197.

Ewing, E.E., The Role of Hormones in Potato (*Solanum tuberosum* L.) Tuberization, Plant Hormone pp 698-724.

Exner, V., Taranto, P., Schonrock, N., Gruissem, W., and Hennig, L. (2006). Chromatin assembly factor CAF-1 is required for cellular differentiation during plant development. Development 133, 4163-4172.

F. Agius, A. Kapoor, J. K. Zhu (2006) Role of the Arabidopsis DNA glycosylase/lyase ROS1 in active DNA demethylation. Proc. Natl. Acad. Sci. U.S.A. 103, 11796–11801.

Faivre-Rampant O, Cardle L, Marshall D, Viola R, Taylor MA. (2004) Changes in gene expression during meristem activation processes in *Solanum tuberosum* with a focus on the regulation of an auxin response factor gene. J Exp Bot; 55:613-22.

Falong Lu, Xia Cui, Shuaibin Zhang, Chunyan Liu & Xiaofeng Cao (2010) JMJ14 is an H3K4 demethylase regulating flowering time in Arabidopsis Cell Research ,volume20, pages387–390

Falong Lu, Xia Cui, Shuaibin Zhang, Thomas Jenuwein & Xiaofeng Cao (2011) Arabidopsis REF6 is a histone H3 lysine 27 demethylase , Nature Genetics volume 43, pages715–719

Fan D., Dai Y., Wang X., Wang Z., He H., Yang H., Cao Y., Deng X. W. and Ma L. (2012). IBM1, a JmjC domain-containing histone demethylase, is involved in the regulation of RNA-directed DNA methylation through the epigenetic control of RDR2 and DCL3 expression in Arabidopsis. Nucleic Acids Res. 40, 8905-8916.

Franco-Zorrilla, J.M., Valli, A., Todesco, M., Mateos, I., Puga, M.I., Rubio-Somoza, I., Leyva, A., Weigel, D., García, J.A., and Paz-Ares, J. (2007). Target mimicry provides a new mechanism for regulation of microRNA activity. Nat. Genet. 39: 1033-1037.

Furner, I.J., Sheikh, M.A., and Collett, C.E. (1998). Gene silencing and homology-dependent gene silencing in Arabidopsis: Genetic modifiers and DNA methylation. Genetics 149, 651–662

Gao R, Wang Y, Gruber MY, Hannoufa A. 2018. MiR156/SPL10 modulates lateral root development, branching and leaf morphology in Arabidopsis by silencing AGAMOUS-LIKE Frontiers in Plant Science **8**, 2226.

Garner WW, Allard HA (1920) Effect of length of day and other factors of the environment on growth and reproduction in plants. J Agric Res 18: 553–578

Gendall, A.R. et al. (2001) The VERNALIZATION 2 gene mediates the epigenetic regulation of vernalization in Arabidopsis. Cell 107, 525–535

Ghate, T.H., Sharma, P., Kondhare, K.R., Hannapel, D.J., and Banerjee, A.K. (2017). The mobile RNAs, StBEL11 and StBEL29, suppress growth of tubers in potato. Plant Mol. Bio. 93(6): 563-578.

Goodrich J, Puangsomlee P, Martin M, Long D, Meyerowitz EM, Coupland G. 1997. A Polycomb-group gene regulates homeotic gene expression in Arabidopsis. Nature 386, 44-51.

Götz S, García-Gómez JM, Terol J, Williams TD, Nagaraj SH, Nueda MJ, Robles M, Talón M, Dopazo J, Conesa A. 2008. High-throughput functional annotation and data mining with the Blast2GO suite. Nucleic Acids Research **36**, 3420-3435.

Greb, T. et al. (2007) The PHD finger protein VRN5 functions in the epigenetic silencing of Arabidopsis FLC. Curr. Biol. 17, 73–78 Sanchez-Pulido, L. et al. (2008) RAWUL: A new Ubiquitin-like domain in PRC1 Ring finger proteins that unveils putative plant and worm PRC1 orthologs. BMC Genomics 9, 308

Gregory LE (1956) Some factors for tuberization in the potato plant. Am J Bot 43: 281–288

Grossniklaus U, Paro R. 2014. Transcriptional silencing by Polycomb group proteins. Cold Spring Harb Perspect Biol 6: a019331.

Grossniklaus, U. et al. (1998) Maternal control of embryogenesis by MEDEA, a Polycomb group gene in Arabidopsis. Science 280, 446–450

Gu X, Xu T, He Y. 2014. A Histone H3 Lysine-27 Methyltransferase Complex Represses Lateral Root Formation in Arabidopsis thaliana. Molecular Plant **7**, 977-988.

Gu, X., Jiang, D., Yang, W., Jacob, Y., Michaels, S. D., & He, Y. (2011). Arabidopsis homologs of retinoblastoma-associated protein 46/48 associate with a histone deacetylase to act redundantly in chromatin silencing. *PLoS genetics*, *7*(11), e1002366. doi:10.1371/journal.pgen.1002366

Hake S, Smith HMS, Holtan H, Magnani E, Mele G, Ramirez J. 2004. The role of knox genes in plant development. Annual review of cell and developmental biology 20, 125–151.

Harashima H, Sugimoto K (2016) Integration of developmental and environmental signals into cell proliferation and differentiation through RETINOBLASTOMA-RELATED 1. Curr Opin Plant Biol 29: 95–103

Hay A, Tsiantis M. 2010. KNOX genes: Versatile regulators of plant development and diversity. Development 137: 3153–3165.

He, G., Elling, A. A., & Deng, X. W. (2011). The Epigenome and Plant Development. doi:10.1146/annurev-arplant 042110-103806.

He, Y., and Amasino, R. M. (2005). Role of chromatin modification in flowering-time control. *Trends Plant Sci.* 10, 30–35. doi: 10.1016/j.tplants.2004.11.003

Hedden, P. and Phillips, A.L., Gibberellin Metabolism: New Insight Revealed by Genes, *Trends PlantSci.,* 2000, vol. 5, pp. 523–530.

Henderson IR, Jacobsen SE. 2007. Epigenetic inheritance in plants. Nature 447, 418–24.

Hennig L, Bouveret R, Gruissem W. 2005. MSI1-like proteins: An escort service for chromatin assembly and remodeling complexes. Trends in Cell Biology 15, 295–302.

Hennig L, Derkacheva M. 2009. Diversity of Polycomb group complexes in plants: same rules, different players? Trends in Genetics 25, 414–423.

Hennig L, Taranto P, Walser M, Schönrock N, Gruissem W. 2003. Arabidopsis MSI1 is required for epigenetic maintenance of reproductive development. Development **130**, 2555-2565.

Hennig, L. et al. (2003) Arabidopsis MSI1 is required for epigenetic maintenance of reproductive development. Development 130, 2555–2565

Holec, Sarah, and Frédéric Berger. 2012. "Polycomb Group Complexes Mediate Developmental Transitions in Plants." Plant Physiology 158 (1): 35–43. doi:10.1104/pp.111.186445

Hsieh, L.C., Lin, S.I., Shih, A.C., Chen, J.W., Lin, W.Y., Tseng, C.Y., Li, W.H., and Chiou, T.J. (2009). Uncovering small RNA-mediated responses to phosphate deficiency in Arabidopsis by deep sequencing. Plant Physiol. 151: 2120-2132.

Ido Keren, Vitaly Citovsky (2016), The Arabidopsis thaliana histone deubiquitinase OTLD1 represses the transcription of growth regulators and promotes plant growth. SCIENCE SIGNALING 20 DEC:2016 RA125

Ikeuchi, M., Iwase, A., Rymen, B., Harashima, H., Shibata, M., Ohnuma, M., et al. (2015). PRC2 represses dedifferentiation of mature somatic cells in Arabidopsis. Nat. Plants 1:15089.

J. Smalle, R.D. Vierstra, The ubiquitin 26s proteasome proteolytic pathway, Annu. Rev. Plant Biol. 55 (2004) 555–590.

J. Xiao, H. Zhang, L. Xing, S. Xu, H. Liu, K. Chong, Y. Xu Requirement of histone acetyltransferases HAM1 and HAM2 for epigenetic modification of FLC in regulating flowering in Arabidopsis

Jackson SD (1999) Multiple signaling pathways control tuber induction in potato. Plant Physiol 119: 1–8

Jackson, S. and Prat, S., (1996) Control of Tuberization in Potato by Gibberellins and Phytochrome B, *Physiol. Plant.*, , vol. 98, pp. 407–412

Jackson, S.D., Heyer, A., Dietze, J., Prat, S. (1996). Phytochrome B mediates the photoperiodic control of tuber formation in potato. Plant J. 9: 159-166

Jackson, S.D., James, P.E., Carrera, E., Prat, S., and Thomas, B., 2000Regulation of Transcript Levels of a Potato Gibberellin 20_Oxidase Gene by Light and Phytochrome B, *Plant Physiol.*, , vol. 124, pp. 423–430

Jacob, Y., Feng, S., LeBlanc, C. A., Bernatavichute, Y. V., Stroud, H., Cokus, S., … Michaels, S. D. (2009). ATXR5 and ATXR6 are H3K27 monomethyltransferases

required for chromatin structure and gene silencing. *Nature structural & molecular biology*, *16*(7), 763–768. doi:10.1038/nsmb.1611

Jae-Young Yun, Yosuke Tamada, Ye Eun Kang, Richard M. Amasino, (2012) ARABIDOPSIS TRITHORAX-RELATED3/SET DOMAIN GROUP2 is Required for the Winter-Annual Habit of Arabidopsis thaliana, Plant and Cell Physiology, Volume 53, Issue 5, May, Pages 834–846

Jefferson RA. (1987). Assaying chimeric genes in plants: The GUS gene fusion system. Plant Molecular Biology Reporter **5**, 387-405.

Jeong J-H, Song H-R, Ko J-H, Jeong Y-M, Kwon YE, Seol JH, et al. (2009) Repression of FLOWERING LOCUS T Chromatin by Functionally Redundant Histone H3 Lysine 4 Demethylases in Arabidopsis. PLoS ONE 4(11): e8033.

Jian Zheng Fengying Chen Zhi Wang Hong Cao Xiaoying Li Xin Deng Wim J. J. Soppe Yong Li Yongxiu Liu (2011) A novel role for histone methyltransferase KYP/SUVH4 in the control of Arabidopsis primary seed dormancy https://doi.org/10.1111/j.1469-8137.2011.03969.x

Jiang D, Wang Y, Wang Y, He Y. 2008. Repression of FLOWERING LOCUS C and FLOWERING LOCUS T by the Arabidopsis polycomb repressive complex 2 components. PLoS One **3**, e3404.

Jiang D, Yang W, He Y, Amasino RM (2007) Arabidopsis relatives of the human lysine-specific Demethylase1 repress the expression of FWA and FLOWERING LOCUS C and thus promote the floral transition. Plant Cell 19: 2975–2987

K.K. Lee, J.L. Workman, (2007) Histone acetyltransferase complexes: one size doesn't fit all, Nat. Rev. Mol. Cell Biol. 8 284–295.

Kankel M.W., Ramsey D.E., Stokes T.L., Flowers S.K., Haag J.R., Jeddeloh J.A., Riddle N.C., Verbsky M.L., Richards E.J. (2003)Arabidopsis MET1 Cytosine Methyltransferase Mutants. Genetics.;163:1109–1122.

Kawade K, Li Y, Koga H, Sawada Y, Okamoto M, Kuwahara A, Tsukaya H, Hirai MY. (2018) The cytochrome P450 CYP77A4 is involved in auxin-mediated patterning of the Arabidopsis thaliana embryo. Development **145**, dev168369

Kerstetter, R., Vollbrecht, E., Lowe, B., Veit, B., Yamaguchi, J., and Hake, S. (1994). Sequence analysis and expression patterns divide the maize knotted1-like homeobox genes into two classes. Plant Cell 6, 1877–1887

Kim GT, Tsukaya H, Uchimiya H. 1998. The CURLY LEAF gene controls both division and elongation of cells during the expansion of the leaf blade in Arabidopsis thaliana. Planta **206**, 175-183.

Kim SY, Zhu T, Sung ZR. Epigenetic regulation of gene programs by EMF1 and EMF2 in Arabidopsis, Plant Physiol. , 2010, vol. 152 (pg. 516-528)

Kim SY, He Y, Jacob Y, Noh Y-S, Michaels S, Amasino R. 2005. Establishment of the vernalization-responsive, win- ter-annual habit in Arabidopsis requires a putative histone H3 methyl transferase. The Plant Cell. **17**, 3301-3310

Kinoshita T, Harada JJ, Goldberg RB, Fischer RL. 2001. Polycomb repression of flowering during early plant development.

Kloosterman B, Abelenda J a, Gomez MDMC, et al. 2013. Naturally occurring allele diversity allows potato cultivation in northern latitudes. Nature 495, 246–50.

Kloosterman B, Vorst O, Hall RD, Visser RG, Bachem CW. Tuber on a chip: differential gene expression during potato tuber development. Plant Biotechnol J. 2005;3:505–19.

Köhler C., Hennig,L., Spillane,C., Pien,S., Gruissem,W. and Grossniklaus,U. (2003) The Polycomb-group protein MEDEA regulates seed development by controlling expression of the MADS-box gene *PHERES1*. Genes Dev., 17, 1540–1553.

Köhler, C., Hennig, L., Bouveret, R., Gheyselinck, J., Grossniklaus, U., and Gruissem, W. (2003). Arabidopsis MSI1 is a component of the MEA/FIE polycomb group complex and required for seed development. EMBO J. 22, 4804-4814.

Kolomiets, M.V., Hannapel, D.J., Chen, H., Tymeson, M., and Glodon, R.J., (2001) Lipoxygenase Is Involved in the Control of Potato Tuber Development, *Plant Cell*, , vol. 13, pp. 613–626.

Kumar A, Kondhare KR, Vetal PV, Banerjee AK. (2019). Polycomb group proteins StMSI1 and StBMI1-1 function upstream of miRNA156 to regulate aerial tuber formation in potato (S. tuberosum ssp. andigena) under short-day photoperiod. Plant Physiology. DOI:10.1104/pp.19.00416

Kumar D,Wareing PF (1973) Studies on tuberization in Solanum andigena. I. Evidence for the existence and movement of a specific tuberization stimulus. New Phytol 72: 283–287

L. Hicke, (2001) Protein regulation by monoubiquitin, Nat. Rev. Mol. Cell Biol. 2 195–201.

Lafos M, Kroll P, Hohenstatt ML, Thorpe FL, Clarenz O, Schubert D. (2011). Dynamic regulation of H3K27 trimethylation during Arabidopsis differentiation. PLoS Genetics **7**, e1002040

Langmead B, Trapnell C, Pop M, Salzberg SL. 2009. Ultrafast and memory-efficient alignment of short DNA sequences to the human genome. Genome Biology **10**, R25.

Law JA, Jacobsen SE. (2010) Establishing, maintaining and modifying DNA methylation patterns in plants and animals. Nature Reviews Genetics.;11(3):204–220. pmid:20142834

Lee J, Shim D, Moon S, Kim H, Bae W, Kim K, Kim Y-H, Rhee S-K, Hong CP, Hong S-Y. 2018. Genome-wide transcriptomic analysis of BR-deficient Micro-Tom reveals correlations between drought stress tolerance and brassinosteroid signaling in tomato. Plant Physiology and Biochemistry **127**, 553-560.

Lee, H., Yoo, S.J., Lee, J.H., Kim, W., Yoo, S.K., Fitzgerald, H., Carrington, J.C., Ahn, J.H. (2010). Genetic framework for flowering-time regulation by ambient temperature-responsive miRNAs in Arabidopsis. Nucleic Acids Res. 38: 3081-3093.

Leroy, O. et al. (2007) Polycomb group proteins function in the female gametophyte to determine seed development in plants. Development 134, 3639–3648

Lescot, M., Dehais, P., Thijs, G., Marchal, K., Moreau, Y., van de Peer, Y., Rouze, P., and Rombauts, S. (2002). PlantCARE, a database of plant cis-acting regulatory elements and a portal to tools for in silico analysis of promoter sequences. Nucleic Acids Res. 30: 325-327.

Li H., Luan S. (2011) The cyclophilin AtCYP71 interacts with CAF-1 and LHP1 and functions in multiple chromatin remodeling processesMol. Plant, 4, pp. 748-758

Li, H., Torres-Garcia, J., Latrasse, D., Benhamed, M., Schilderink, S., Zhou, W., Bisseling, T. (2017). Plant-Specific Histone Deacetylases HDT1/2 Regulate *GIBBERELLIN 2-OXIDASE2* Expression to Control Arabidopsis Root Meristem Cell Number. *The Plant cell*, *29*(9), 2183–2196. doi:10.1105/tpc.17.00366

Li, J., Wang, Z., Hu, Y., Cao, Y., & Ma, L. (2017). Polycomb Group Proteins RING1A and RING1B Regulate the Vegetative Phase Transition in *Arabidopsis*. *Frontiers in plant science*, *8*, 867. doi:10.3389/fpls.2017.00867

Liu X, Zhou C, Zhao Y, Zhou S, Wang W, Zhou D. 2014. The rice enhancer of zeste [E(z)] genes SDG711 and SDG718 are respectively involved in long day and short day signaling to mediate the accurate photoperiod control of flowering time. Frontiers in Plant Science **5**, 591.

Liu Y, Koornneef M, Soppe WJJ. (2007) The absence of histone H2B monoubiquitination in the Arabidopsis hub1 (rdo4) mutant reveals a role for chromatin remodeling in seed dormancy. Plant Cell; 19:433 – 44.

Liu, D.D., Zhou, L.J., Fang, M.J., Dong, Q.L., An, X.H., You, C-X., and Haoa, Y-J. (2016). Polycomb-group protein SlMSI1 represses the expression of fruit-ripening genes to prolong shelf life in tomato. Sci. Rep. 6: 31806.

Liu, H., Zhang, H., Dong, Y. X., Hao, Y. J., and Zhang, X. S. (2018). DNA METHYLTRANSFERASE1 -mediated shoot regeneration is regulated by cytokinin-induced cell cycle in Arabidopsis. N. Phytol. 217, 219–232.

Liu, X.,Wei, X., Sheng, Z., Jiao, G., Tang, S., Luo, J., et al. (2016). Polycomb protein OsFIE2 affects plant height and grain yield in rice. PLoS ONE 11:e0164748.

Livak KJ, Schmittgen TD. 2001. Analysis of relative gene expression data using real-time quantitative PCR and the 2(-Delta Delta C (T)) Method. Methods **25**, 402-408.

Locascio A, Blázquez M a, Alabadí D. 2013. Dynamic regulation of cortical microtubule organization through prefoldin-DELLA interaction. Current biology : CB 23, 804–9.

Lodha M, Marco CF, Timmermans MC. 2008. Genetic and epigenetic regulation of stem cell homeostasis in plants. Cold Spring Harbor Symposia on Quantitative Biology **73**, 243-251.

Lodha M, Marco CF, Timmermans MCP. (2013a) The ASYMMETRIC LEAVES complex maintains repression of KNOX homeobox genes via direct recruitment of Polycomb-repressive complex2. Genes and Development 27, 596–601.

Luo, M. et al. (1999) Genes controlling fertilization-independent seed development in Arabidopsis thaliana. Proc. Natl. Acad. Sci. U. S. A. 96, 296–301

Luo, M. et al. (2009) Expression, imprinting, and evolution of rice homologs of the Polycomb Group genes. Mol. Plant 2, 711–723

Luo, M., Wang, Y.Y., Liu, X., Yang, S., Lu, Q., Cui, Y., Wu, K. (2012). HD2C interacts with HDA6 and is involved in ABA and salt stress response in Arabidopsis. J. Exp. Bot. 63: 3297–3306

Luo, M., Yu, C. W., Chen, F. F., Zhao, L., Tian, G., Liu, X., Wu, K. (2012). Histone deacetylase HDA6 is functionally associated with AS1 in repression of KNOX genes in arabidopsis. *PLoS genetics*, *8*(12), e1003114. doi:10.1371/journal.pgen.1003114

M. Luo, M.-Z. Luo, D. Buzas, J. Finnegan, C. Helliwell, E.S. Dennis, W.J. Peacock, A.Chaudhury,(2008) UBIQUITIN-SPECIFIC PROTEASE 26 is required for seed development and the repression of PHERES1 in Arabidopsis, Genetics 180 229–236.

Machá ková, I., Konstantinova, T.N., Sergeeva, L.I., Lozhnikova, V.N., Golyanovskaya, S.A., Dudko, N.D., Eder, J., and Aksenova, N.P., (1998) Photoperiodic Control of Growth, Development and Phytohormone Balance in *Solanum tuberosum, Physiol. Plant.*, , vol. 102, pp. 272–278.

Mahajan A, Bhogale S, Kang IH, Hannapel DJ, Banerjee AK. (2012) The mRNA of a Knotted1-like transcription factor of potato is phloem mobile. Plant Molecular Biology **79**, 595-608.

Mahajan AS, Kondhare KR, Rajabhoj MP, Kumar A, Ghate T, Ravindran N, Habib F, Siddappa S, Banerjee AK. 2016. Regulation, over-expression and target gene identification of Potato Homeobox 15 (POTH15) - a class-I KNOX gene in potato. Journal of Experimental Botany **67**, 4255-4272.

Mallory, A.C., Bartel, D.P., and Bartel, B. (2005). MicroRNA-directed regulation of Arabidopsis AUXIN RESPONSE FACTOR17 is essential for proper development and modulates expression of early auxin response genes. Plant Cell 17: 1360-1375.

Martin A, Adam H, Díaz-Mendoza M, Zurczak M, González-Schain ND, Suárez-López P. 2009. Graft-transmissible induction of potato tuberization by the microRNA miR172. Development **136**, 2873-2881.

Martinez-Balbas, M.A., Tsukiyama, T., Gdula, D., and Wu, C. (1998). Drosophila NURF-55, a WD repeat protein involved in histone metabolism. Proc. Natl. Acad. Sci. USA 95, 132-137.

Martinez-Garcia JF, Virgos-Soler A, Prat S. 2002. Control of photoperiod-regulated tuberization in potato by the Arabidopsis flowering-time gene CONSTANS. Proceedings of the National Academy of Sciences of the United States of America **99**, 15211-15216.

Martínez-Macías, M.I., Qian, W., Miki, D., Pontes, O., Liu, Y., Tang, K., Liu, R., Morales-Ruiz, T., Ariza, R.R., Roldán-Arjona, T., Zhu, J.K. (2012). A DNA 3′ phosphatase functions in active DNA demethylation in Arabidopsis. Mol. Cell 45: 357–370

Matsuki, T., Tazaki, H., Fujimori, T., and Hogetsu, T., (1992) The Influences of Jasmonic Acid Methyl Ester on Microtubules in Potato Cells Formation of Potato Tubers, *Biol. Biotechnol. Biochem.*, vol. 56, pp. 1329–1333.

Mattsson J, Sung ZR, Berleth T. 1999. Responses of plant vascular systems to auxin transport inhibition. Development **126**, 2979-2991.

Mehdi, S., Derkacheva, M., Ramström, M., Kralemann, L., Bergquist, J., and Hennig, L. (2016). The WD40 domain protein MSI1 functions in a histone deacetylase complex to fine-tune abscisic acid signaling. Plant Cell Adv. 28(1): 42-54.

Merini W, Romero-Campero FJ, Gomez-Zambrano A, Zhou Y, Turck F, Calonje M. 2017. The Arabidopsis Polycomb Repressive Complex 1 (PRC1) components AtBMI1A, B and C impact gene networks throughout all stages of plant development. Plant Physiology **173**, 627-641.

Mokronosov, A.T., Chailakhyan, M.Kh. and Mokronosov, (1990) Tuberization and Sink–Source Relations in Potato, *Regulyatsiya rosta i razvitiya ukartofelya* (Regulation of Potato Growth and Development), A.T., Eds., Moscow: Nauka, , pp. 6–12.

Mosquna, A. et al. (2009) Regulation of stem cell maintenance by the Polycomb protein FIE has been conserved during land plant evolution. Development 136, 2433–2444

Mozgová, I., Mu-oz-Viana, R., and Hennig, L. (2017). PRC2 represses hormone-induced somatic embryogenesis in vegetative tissue of Arabidopsis thaliana. PLoS Genet. 13:e1006562.

Müller J, Hart CM, Francis NJ, Vargas ML, Sengupta A, *et al.* 2002. Histone methyltransferase activity of a Drosophila Polycomb group repressor complex. Cell **111**, 197-208.

Müller-Xing R, Clarenz O, Pokorny L, Goodrich J, Schubert D. 2014. Polycomb-Group Proteins and FLOWERING LOCUS T Maintain Commitment to Flowering in Arabidopsis thaliana. The Plant cell 26, 2457–2471.

Murashige T, Skoog F. 1962. A revised medium for rapid growth and bioassays with tobacco tissue cultures. Physiologia Plantarum **15**, 473-479.

Navarro C, Abelenda JA, Cruz-Oró E, Cuéllar CA, Tamaki S, Silva J, Shimamoto K, Prat S. 2011. Control of flowering and storage organ formation in potato by FLOWERING LOCUS T. Nature **478**, 119-122.

Nazarian-Firouzabadi F, Visser RGF. 2017. Potato starch synthases: functions and relationships. Biochemistry and Biophysics Reports **10**, 7-16.

Nguyen, N.T.T., Contreras-Moreira, B., Castro-Mondragon, J.A., Santana-Garcia, W., Ossio, R., Robles-Espinoza, C.D., Bahin, M., Collombet, S., Vincens, P., Thieffry, D., van Helden, J., Medina-Rivera, A., and Thomas-Chollier, M. (2018). RSAT: regulatory sequence analysis tools 20th anniversary. Nucleic Acids Res.: gky317.

Oh, S., Park, S., and van Nocker, S. (2008). Genic and global functions for Paf1C in chromatin modification and gene expression in Arabidopsis. PLoS Genet. 4:e1000077. doi: 10.1371/journal.pgen.1000077

Ohad, N. et al. (1999) Mutations in FIE, a WD Polycomb group gene, allow endosperm development without fertilization. Plant Cell 11, 407– 416

Okano Y, Aono N, Hiwatashi Y, Murata T, Nishiyama T, Ishikawa T, Kubo M, Hasebe M. 2009. A polycomb repressive complex 2 gene regulates apogamy and gives evolutionary insights into early land plant evolution. Proceedings of the National Academy of Sciences of the United States of America 106, 16321–6.

Oliver SN, Lunn JE, Urbanczyk-wochniak E, *et al.* 2008. Decreased expression of cytosolic ppyruvate kinase in potato tubers leads to a decline in pyruvate resulting in an in vivo repression of the alternative oxidase. Plant Physiology **148**, 1640-1654.

Onodera Y, Pikaard CS, Pontes O, Haag JR, Nunes PC, Ream T. (2005). Plant Nuclear RNA Polymerase IV Mediates siRNA and DNA Methylation-Dependent Heterochromatin Formation. Cell 120, 613–622.

Ortega-Galisteo, A.P., Morales-Ruiz, T., Ariza, R.R. et al. (2008) Arabidopsis DEMETER-LIKE proteins DML2 and DML3 are required for appropriate distribution of DNA methylation marksPlant Mol Biol 67: 671.

Pagnussat GC, Yu HJ, Ngo QA, Rajani S, Mayalagu S, et al. (2005). Genetic and molecular identification of genes required for female gametophyte development and function in Arabidopsis. Development 132:603–14

Palmer CE, Smith OE. (1969) Cytokinins and tuber induction in the potato plant. Nature **221**, 279-280.

Pandey R, Muller A, Napoli C, Selinger D, Pikaard C, Richards E, Bender J, Mount D, Jorgensen R (2002) Analysis of histone acetyltransferase and histone deacetylase families of Arabidopsis thaliana suggests functional diversification of chromatin modification among multicellular eukaryotes. Nucleic Acid Research., 30 (23): 5036-5055. 10.1093/nar/gkf660.

Pasare, S.A. et al. (2013) The role of the potato (Solanum tuberosum) CCD8 gene in stolon and tuber development. New Phytol. 198, 1108–1120

Paszkowski J, Grossniklaus U (2011). Selected aspects of transgenerational epigenetic inheritance and resetting in plants. Curr Opin Plant Biol 14: 195–203.

Pavlopoulou, S. Kossida Plant cytosine-5 DNA methyltransferases (2007): structure, function, and molecular evolution Genomics, 90 pp. 530-541

Pazhouhandeh, M., Molinier, J., Berr, A., & Genschik, P. (2011). MSI4/FVE interacts with CUL4-DDB1 and a PRC2-like complex to control epigenetic regulation of flowering time in Arabidopsis. *Proceedings of the National Academy of Sciences of the United States of America*, *108*(8), 3430–3435. doi:10.1073/pnas.1018242108

Pelacho, A.M. and Mingo_Castel, A.M., (1991) Jasmonic Acid Induces Tuberization of Potato Stolons *In Vitro*, *Plant Physiol.,* , vol. 97, pp. 1253–1255.

Peterson, A.J., Mallin, D.R., Francis, N.J., Ketel, C.S., Stamm, J., Voeller, R.K., Kingston, R.E., and Simon, J.A. (2004). Requirement for sex comb onmidleg protein interactions in Drosophila polycomb group repression. Genetics 167: 1225-1239.

Picó, S., Ortiz-Marchena, M.I., Merini, W., and Calonje, M. (2015). Deciphering the role of POLYCOMB REPRESSIVE COMPLEX1 variants in regulating the acquisition of flowering competence in Arabidopsis. Plant Physiol. 168: 1286-1297.

Pien S, Grossniklaus U. 2007. Polycomb group and trithorax group proteins in Arabidopsis. Biochimica et Biophysica Acta (BBA) - Gene Structure and Expression **1769**, 375-382.

Pikaard CS, Scheid OM. 2014. Epigenetic regulation in plants. Cold Spring Harbor Perspectives in Biology 6, a019315.

Prematilake, D.P., and Mendis, M.H. (1999). Microtubers of potato (Solanum tuberosum L.): In vitro conservation and tissue culture. J. Natl. Sci. Found. Sri Lanka 27: 17-28.

Probst AV, Fagard M, Proux F, Mourrain P, Boutet S, et al. (2004) Arabidopsis histone deacetylase HDA6 is required for maintenance of transcriptional gene silencing and determines nuclear organization of rDNA repeats. Plant Cell. ;16:1021–1034.

Quarrie, S.A., *Droopy* (1982) A Wilty Mutant of Potato Deficient in Abscisic Acid, *Plant Cell Environ.*, vol. 5, pp. 23–26.

Quinlan AR, Hall IM. (2010). Bedtools: a flexible suite of utilities for comparing genomic features. Bioinformatics **26**, 841-842.

Pandey R, Müller A, Napoli CA, et al. (2002) Analysis of histone acetyltransferase and histone deacetylase families of Arabidopsis thaliana suggests functional diversification of chromatin modification among multicellular eukaryotes. Nucleic Acids Res.;30(23):5036–5055.

Ramirez F, Dundar F, Diehl S, Gruning BA, Manke T. (2014) deepTools: a flexible platform for exploring deep-sequencing data. Nucleic Acids Research **42**, W187-W191.

Ren J, Wen L, Gao X, Jin C, Xue Y, Yao X. (2009) DOG 1.0: Illustrator of protein domain structures. Cell Research **19**, 271.

Robinson JT, Thorvaldsdóttir H, Winckler W, Guttman M, *et al.* (2011) Integrative Genomics Viewer. Nature Biotechnology **29**, 24-26.

Rodriguez Falcon, M., Bou, J., and Prat, S., (2006) Seasonal Control of Tuberization in Potato: Conserved Elements with the Flowering Response, *Annu. Rev. Plant Biol.*, vol. 57, pp. 151–180.

Roth, S.Y.; Denu, J.M.; Allis, C.D. (2001) Histone acetyltransferases. Annu. Rev. Biochem., 70, 81–120.

Roumeliotis E, Visser RG, Bachem CW. 2012. A crosstalk of auxin and GA during tuber development. Plant Signaling and Behavior **7**, 1360-1363.

Roumeliotis, E. et al. (2012) The effects of auxin and strigolactones on tuber initiation and stolon architecture in potato. J. Exp. Bot. 63, 4539–4547 80

Roy D, Chakrabarty J, Mallik R, Chaudhuri S. 2019. Rice Trithorax factor ULTRAPETALA 1 (OsULT1) specifically binds to "GAGAG" sequence motif present in Polycomb response elements. Biochimica et Biophysica Acta: Gene Regulatory Mechanisms **1862**, 582-597.

Rubio-Somoza, I., Zhou, C.M., Confraria, A., Martinho, C., von Born, P., Baena-Gonzalez, E., Wang, J.W., and Weigel, D. (2014). Temporal control of leaf complexity by miRNA-regulated licensing of protein complexes. Curr. Biol. 24: 2714-2719.

Sarkar, D., Pandey, S.K., and Sharma, S., (2006) Cytokinins Antagonize the Jasmonates Action on the Regulation of Potato (*Solanum tuberosum* L.) Tuber Formation *InVitro*, *Plant Cell, Tissue Organ Cult.*, , vol. 87,pp. 285–295.

Schroeder DF, Gahrtz M, Maxwell BB, Cook RK, Kan JM, Alonso JM, Ecker JR, Chory J (2002) De-etiolated 1 and damaged DNA binding protein 1 interact to regulate Arabidopsis photomorphogenesis. Curr Biol ; 12:1462-72

Schubert D, Primavesi L, Bishopp A, Roberts G, Doonan J, Jenuwein T, Goodrich J. (2006) Silencing by plant Polycomb-group genes requires dispersed trimethylation of histone H3 at lysine 27. EMBO J 25: 4638–4649.

Schuettengruber B, Cavalli G. (2009) Recruitment of polycomb group complexes and their role in the dynamic regulation of cell fate choice. Development 136: 3531–3542.

Scofield S, Dewitte W, Murray J a H, Arabidopsis T, Knat BP (2008) A model for Arabidopsis class - 1 KNOX gene function. Plant Journal, The, 257–259.

Seo, E., Kim, T., Park, J.H., Yeom, S-I., Kim, S., Seo, M-K., Shin, C., and Choi, D. (2018) Genome-wide comparative analysis in Solanaceous species reveals evolution of microRNAs targeting defense genes in Capsicum spp. DNA Res. 25(6): 561-575.

Servet C, e Silva NC, Zhou DX (2010) Histone acetyltransferase AtGCN5/HAG1 is a versatile regulator of developmental and inducible gene expression in Arabidopsis. Mol Plant 3:670–677

Shafiq S, Berr A, Shen WH. 2014. Combinatorial functions of diverse histone methylations in Arabidopsis thaliana flowering time regulation. New Phytologist **201**, 312-322.

Shao, Z., Raible, F., Mollaaghababa, R., Guyon, J.R., Wu, C.T., Bender, W., Kingston, R.E. (1999). Stabilization of chromatin structure by PRC1, a Polycomb complex. Cell 98: 37-46.

Sharma P, Lin T, Hannapel DJ. 2016. Targets of the StBEL5 transcription factor include the FT ortholog StSP6A. Plant Physiology **170**, 310-324.

Shaver S., Casas-Mollano J. A., Cerny R. L., Cerutti H. (2010). Origin of the polycomb repressive complex 2 and gene silencing by an E(z) homolog in the unicellular alga *Chlamydomonas*. *Epigenetics* 5 301–312. 10.4161/epi.5.4.11608

Sheehy RE, Kramer M, Hiatt WR. (1988) Reduction of polygalacturonase activity in tomato fruit by antisense RNA. Proceedings of the National Academy of Sciences of the United States of America **85**, 8805-8809.

Shi YG, Tsukada Y. (2013) The discovery of histone demethylases. Cold Spring Harb Perspect Biol 5: 017947.

Sieburth LE. 1999. Auxin is required for leaf vein pattern in Arabidopsis. Plant Physiology 121, 1179-1190.

Sievers F, Wilm A, Dineen D, Gibson TJ, *et al.* 2011. Fast, scalable generation of high-quality protein multiple sequence alignments using Clustal Omega. Molecular Systems Biology **7**, 539.

Simko, I., (1994) Sucrose Application Causes Hormonal Changes Associated with Potato Tuberization, *J. Plant Growth Regul.,* , vol. 13, pp. 73–77.

Singh A, Roy S, Singh S, Das SS, Gautam V, Yadav S, *et al.* 2017. Phytohormonal crosstalk modulates the expression of miR166/165s, target class III HD-ZIPs, and KANADI genes during root growth in Arabidopsis thaliana. Scientific Reports **7**, 3408.

Sonnewald U, Studer D, Rocha-Sosa M, Willmitzer L. (1989) Immunocytochemical localization of patatin, the major glyco protein in potato (Solanum tuberosum L.) tubers. Planta **178**, 176-183.

Springer NM, Danilevskaya ON, Hermon P, Helentjaris TG, Phillips RL, Kaeppler HF, Kaeppler SM, Wisconsin NMS. (2002) Sequence Relationships , Conserved Domains , and Expression Patterns for Maize Homologs of the Polycomb Group Genes E (z) , esc , and E (Pc) 1. Plant Physiol. Apr; 128(4): 1332–1345.

Steinbach Y, Hennig L. (2014) Arabidopsis MSI1 functions in photoperiodic flowering time control. Frontiers in plant science 5, 77

Sun, Q., and Zhou, D.X. (2008). Rice jmjC domain-containing gene JMJ706 encodes H3K9 demethylase required for floral organ development. Proc. Natl. Acad. Sci. USA 105: 13679-84.

Sung, S. and Amasino, R.M. (2004) Vernalization in Arabidopsis thaliana is mediated by the PHD finger protein VIN3. Nature 427, 159–164

Sung, S. et al. (2006) A PHD finger protein involved in both the vernalization and photoperiod pathways in Arabidopsis. Genes Dev. 20, 3244–3248

Szklarczyk D, Morris JH, Cook H, Kuhn M, *et al.* (2017) The STRING database in 2017: quality-controlled protein-protein association networks, made broadly accessible. Nucleic Acids Research **45**, D362-368.

T. F. Hsieh (2016) Epigenetics: A tug of war for DNA methylation. Nat. Plants 2, 16171

Tamada Y, Yun J-Y, Woo SC, Amasino R. (2009) ARABIDOPSIS TRITHORAX-RELATED7 is required for methyla- tion of lysine 4 of histone H3 and for transcriptional activation of FLOWERING LOCUS C. The Plant Cell **21**, 3257-3269.

Teixeira J, Pereira S, Queiro F. (2006) Specific roles of potato glutamine synthetase isoenzymes in callus tissue grown under salinity: molecular and biochemical responses. Plant Cell, Tissue and Organ Culture **87**, 1-7.

Teo CJ, Takahashi K, Shimizu K, Shimamoto K, Taoka KI. (2017) Potato tuber induction is regulated by interactions between components of a tuberigen complex. Plant and Cell Physiology **58**, 365-374.

Teotia S, Tang G. (2015) To bloom or not to bloom: role of microRNAs in plant flowering. Molecular Plant **8**, 359-377.

Terasaka K, Blakeslee JJ, Titapiwatanakun B, *et al.* (2005) PGP4, an ATP binding cassette P-glycoprotein, catalyzes auxin transport in Arabidopsis thaliana roots. The Plant Cell **17**, 2922-2939.

Thomas-Chollier M, Herrmann C, Defrance M, Sand O, Thieffry D, van Helden J. (2012) RSAT peak-motifs: motif analysis in full-size ChIP-seq datasets. Nucleic Acids Research **40**, e31

Trapnell, C., Hendrickson, D.G., Sauvageau, M., Goff, L., Rinn, J.L., and Pachter, L. (2013). Differential analysis of gene regulation at transcript resolution with RNA-seq. Nat. Biotechnol. 31: 46-53.

Turck F, Roudier F, Farrona S, Martin-Magniette M-L, Guillaume E, Buisine N, Gagnot S, Martienssen RA, Coupland G, Colot V (2007) Arabidopsis TFL2/LHP1 specifically associates with genes marked by trimethylation of histone H3 lysine 27. PLoS Genet 3: e86

Uchida, N., Townsley, B., Chung, K.H., and Sinha, N. (2007). Regulation of SHOOT MERISTEMLESS genes via an upstream-conserved noncoding sequence coordinates leaf development. Proc. Natl. Acad. Sci. USA 104: 15953-15958.

Vaillant I, Paszkowski J. (2007) Role of histone and DNA methylation in gene regulation. Current Opinion in Plant Biology 10, 528–533.

Van den Berg, J.H., Simko, J., Davies, P.J., Ewing, E.E., and Halinska, A., (1995) Morphology and Gibberellin A12 Metabolism in WildType and Dwarf Solanum

tuberosum ssp. Andigena Grown under Long and Short Photoperiods Volume 146, Issue 4, July, Pages 467-473.

Van Helden, J. (2003). Regulatory sequence analysis tools. Nucleic Acids Res. 31(13): 3593-3596.

Vaniyambadi V. Sridhar, Avnish Kapoor, Kangling Zhang, Jianjun Zhu, Tao Zhou, Paul M. Hasegawa, Ray A. Bressan & Jian-Kang Zhu (2007) Control of DNA methylation and heterochromatic silencing by histone H2B deubiquitination Nature volume 447, pages735–738

Vreugdenhil, D. and Struik, P.C., (1989), An Integrated View of the Hormonal Regulation of Tuber Formation in Potato (*Solanum tuberosum*), *Physiol. Plant.,* vol. 75, pp. 525–531.

Vreugdenhil, D. and van Dijk, W., (1989) Effects of Ethylene on the Tuberization of Potato (*Solanum tuberosum*) Cuttings, *Plant Growth Regul.*, , vol. 8, pp. 31–39.

Wang S, Cao L, Wang H. (2016) Arabidopsis ubiquitin-conjugating enzyme UBC22 is required for female gametophyte development and likely involved in Lys11-linked ubiquitination. J Exp Bot.;67(11):3277–3288.

Wang, J.W., Wang, L.J., Mao, Y.B., Cai, W.J., Xue, H.W., and Chen, X.Y. (2005). Control of root cap formation by microRNA-targeted auxin response factors in Arabidopsis. Plant Cell 17: 2204-2216.

Wion D, Casadesús J. (2006) N6-methyl-adenine: an epigenetic signal for DNA-protein interactions. Nature reviews. Microbiology 4, 183–92.

Woo, H. R., Pontes, O., Pikaard, C. S., & Richards, E. J. (2007). VIM1, a methylcytosine-binding protein required for centromeric heterochromatinization. Genes & development, 21(3), 267–277. doi:10.1101/gad.1512007

Wood, C.C. et al. (2006) The Arabidopsis thaliana vernalization response requires a Polycomb-like protein complex that also includes VERNALIZATION INSENSITIVE 3. Proc. Natl. Acad. Sci. U. S. A. 103, 14631–14636

Wu, G., Park, M.Y., Conway, S.R., Wang, J.W., Weigel, D., and Poethig, R.S. (2009). The sequential action of miR156 and miR172 regulates developmental timing in Arabidopsis. Cell 138: 750-759.

Wu, X-H., Wang, Y., Zhuo, Z., Jiang, F., and Wu, Y-D. (2012). Identifying the hotspots on the top faces of WD40-repeat proteins from their primary sequences by β-bulges and DHSW tetrads. PLoS ONE 7: e43005.

Xiang C, Han P, Lutziger I, Wang K, Oliver D. (1999) A mini binary vector series for plant transformation. Plant Molecular Biology **40**, 711-718.

Xiao J, Jin R, Yu X, Shen M, Wagner JD, *et al.* (2017) Cis and trans determinants of epigenetic silencing by Polycomb repressive complex 2 in Arabidopsis. Nature Genetics 49, 1546-1552.

Xing, S., Salinas, M., Höhmann, S., Berndtgen, R., and Huijser, P. (2010). miR156-targeted and nontargeted SBP-box transcription factors act in concert to secure male fertility in Arabidopsis. Plant Cell 22: 3935-3950.

Xu L, Shen W-H (2008) Polycomb silencing of KNOX genes confines shoot stem cell niches in Arabidopsis. Curr Biol 18: 1966–1971

Xu X, Pan S, Cheng S, Zhang B, Mu D, *et al.* 2011. Genome sequence and analysis of the tuber crop potato. Nature **475**, 189-195.

Xu X, van Lammeren AAM, Vermeer E, Vreugdenhil D. 1998b. The role of gibberellin, abscisic acid, and sucrose in the regulation of potato tuber formation in vitro. Plant Physiology **117**, 575-584

Xu X, Vreugdenhil D, van Lammeren AAM (1998b) Cell division and cell enlargement during potato tuber formation. J Exp Bot 49: 573–582

Y. Liu, F. Wang, H. Zhang, H. He, L. Ma, X.W. Deng, (2008) Functional characterization of the Arabidopsis ubiquitin-specific protease gene family reveals specific role and redundancy of individual members in development, Plant J. 55 844–856.

Y. Zhang, (2003) Transcriptional regulation by histone ubiquitination and deubiquitination, Genes Dev. 17 2733–2740

Y. Choi et al. (2002) DEMETER, a DNA glycosylase domain protein, is required for endosperm gene imprinting and seed viability in Arabidopsis. Cell 110, 33–42 .

Yang, C., Bratzel, F., Hohmann, N., Koch, M., Turck, F., and Calonje, M. (2013). VAL- and AtBMI1-mediated H2Aub initiate the switch from embryonic to post-germinative growth in Arabidopsis. Curr. Biol. 23: 1324-1329

Yang, S., Li, C., Zhao, L., Gao, S., Lu, J., Zhao, M., et al. (2015). The Arabidopsis SWI2/SNF2 chromatin remodeling ATPase BRAHMA targets directly to PINs and is required for root stem cell niche maintenance. Plant Cell 27, 1670–1680.

Yoshida, N. et al. (2001) EMBRYONIC FLOWER2, a novel Polycomb group protein homolog, mediates shoot development and flowering in Arabidopsis. Plant Cell 13, 2471–2481

Yu Zhang, Suhua Feng, Fangfang Chen, Haodong Chen, Jia Wang, Chad McCall, Yue Xiong, Xing Wang Deng (2008) Arabidopsis DDB1-CUL4 ASSOCIATED FACTOR1 Forms a Nuclear E3 Ubiquitin Ligase with DDB1 and CUL4 That Is Involved in Multiple Plant Developmental Processes Plant Cell 2008

Yu, S., Cao, L., Zhou, C.M., Zhang, T.Q., Lian, H., Sun, Y. Wu, J.Q., Huang, J.R., Wang, G.D., and Wang, J.W. (2013). Sugar is an endogenous cue for juvenile-to-adult phase transition in plants. elife 2: e00269.

Yu, S., Galvao, V.C., Zhang, Y.C., Horrer, D., Zhang, T.Q., Hao, Y.H., Feng, Y.Q., Wang, S., Schmid, M., and Wang, J.W. (2012). Gibberellin regulates the Arabidopsis floral transition through miR156-targeted SQUAMOSA PROMOTER BINDING-LIKE transcription factors. Plant Cell 24: 3320-3332.

Zeng Z, Zhang W, Marand AP, Zhu B, Buell CR, Jiang J. 2019. Cold stress induces enhanced chromatin accessibility and bivalent histone modifications H3K4me3 and H3K27me3 of active genes in potato. Genome Biology **20**, 123.

Zhang X, Clarenz O, Cokus S, Bernatavichute YV, Pellegrini M, Goodrich J, Jacobsen SE. 2007a. Whole-genome analysis of histone H3 Lysine 27 trimethylation in Arabidopsis. PLoS Biol 5: e129. Ach R a, Taranto P, Gruissem W. 1997. A conserved family of WD-40 proteins binds to the retinoblastoma protein in both plants and animals. The Plant cell 9, 1595–1606.

Zhang Y, Liu T, Meyer CA, Eeckhoute J, Johnson DS, *et al.* 2008. Model-based analysis of ChIP-Seq (MACS). Genome Biology **9**, R137.

Zhang, X. et al. (2007) Whole-genome analysis of Histone H3 Lysine 27 trimethylation in Arabidopsis. PLoS Biol. 5, 1026–1035

Zhang-Wei Liu, Chang-Rong Shao, Cui-Jun Zhang, Jin-Xing Zhou, Su-Wei Zhang, Lin Li, She Chen,Huan-Wei Huang,Tao Cai,Xin-Jian He (2014) The SET Domain Proteins SUVH2 and SUVH9 Are Required for Pol V Occupancy at RNA-Directed DNA Methylation Loci PLOS GENETICS

Zhao Z, Yu Y, Meyer D, Wu C, Shen W-H. 2005. Prevention of early flowering by expression of FLOWERING LOCUS C requires methylation of histone H3 K36. Nature Cell Biology **7**, 1256-1260.

Zhou D. (2009). Regulatory mechanism of histone epigenetic modifications in plants Journal Epigenetics 4, 15-18

Zhou Y, Hartwig B, Velikkakam JG, Schneeberger K, Turck F. (2015) Complementary activities of TELOMERE REPEAT BINDING proteins and Polycomb Group complexes in transcriptional regulation of target genes. The Plant Cell **28**, 87-101.

Zhou Y, Wang Y, Krause K, Yang T, Dongus JA, Zhang Y, Turck F. (2018) Telobox motifs recruit CLF/SWN-PRC2 for H3K27me3 deposition via TRB factors in Arabidopsis. Nature Genetics **50**, 638-644.

Zheng X1, Pontes O, Zhu J, Miki D, Zhang F, Li WX, Iida K, Kapoor A, Pikaard CS, Zhu JK. (2008) ROS3 is an RNA-binding protein required for DNA demethylation in Arabidopsis. Nature. 455(7217):1259-62.

References

Amit Kumar

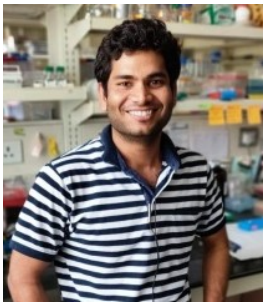

Molecular Plant Biology Lab (Prof. Anjan K. Banerjee)
Indian Institute of Science Education and Research (IISER Pune),
Dr. Homi Bhabha road, Pashan,
Pune- 411008, Maharashtra, India
E-mail: amit.kumar@students.iiserpune.ac.in
Date of Birth – 1st April 1990

Education

Ph.D. (Plant Molecular Biology) 2013-2019 Indian Institute of Science Education and Research, Pune, India.

Ph.D. Dissertation – Understanding the role of Polycomb group (PcG) proteins in potato development.

This work aimed towards understanding the epigenetic mechanisms controlling the stolon to tuber transition in Potato under different photoperiodic conditions. I characterised the candidate PRC2 and PRC1 members' role in potato development. Additionally, I used RNA seq. and ChIP seq. approaches to find out their downstream targets.

M.Sc. (Botany) 2010-2012 Jai Narain Vyas University Jodhpur, India
B.Sc. (Biology) 2007-2010 Jai Narain Vyas University Jodhpur, India

Research Interest

Plant developmental biology, molecular biology, epigenetic regulation, non-coding RNAs, long-distance signaling and bioinformatics analysis.

Publications

- **Kumar, A.,** Kondhare, K. R., Vetal, P. V. & Banerjee, A. K.(**2019**) Polycomb group proteins StMSI1 and StBMI1 regulate microRNA156 during aerial tuber formation in potato under short-day photoperiod **(Plant Physiology,** DOI:10.1104/pp.19.00416).

- **Kumar, A.,** Kondhare, K. R & Banerjee, A. K. Polycomb and trithorax group proteins regulate potato tuberization in a photoperiod-dependent pathway **2019** (**Under review, Journal of Exp. Bot.**).

- Kondhare, K. R., **Kumar, A.,** Hannapel, D. J. & Banerjee, A. K. (**2018**) Conservation of polypyrimidine tract binding proteins and their putative target RNAs in several storage root crops. ***BMC Genomics*** 19, 124.

- Mahajan, A. S., Kondhare, K. R., Rajabhoj, M. P., **Kumar, A.,** Ghate, T., Ravindran, N., Habib, F., Siddappa, S. & Banerjee, A. K. **(2016)** Regulation, over-expression and target gene identification of Potato Homeobox 15 (POTH15) - a class-I KNOX gene in potato. ***J. Exp. Bot***. 67 (14), 4255-4272.

Book chapter

- Kondhare, K. R., **Kumar, A.** & Banerjee, A. K (**2018**) Photoperiod-mediated regulation of tuberization in potato (*S. tuberosum* spp. *andigena*). ***Trends in Frontal Areas of Plant Science Research***. ISBN: 978-81-8487-605-5. Narosa Publishing Group.

Research skills & expertise

Plant transformation and maintenance Plant tissue culture: Hands-on experience in routine plant tissue culturing, generation of transgenic plants, Potato/Tobacco leaf transformation via *Agrobacterium* infections, agro-infiltration in Potato/Tobacco, floral-dip transformation in Arabidopsis.

Molecular & Biochemical techniques Recombinant DNA techniques: Routine cloning methods, transformations in *E. Coli* and *Agrobacterium* strains; PCR, RT-PCR, Quantitative RT-PCR, CRISPR-Cas9 mediated genome editing; Virus Induced Gene Silencing (VIGS), ChIP-qPCR, small RNA detection, 5' RLM-RACE for miRNA cleavage site mapping; Protein expression and purification; Yeast one-hybrid assay; Basic understanding of LC-MS for metabolite analysis.

Bioinformatics & Computation expertise in RNA-Sequencing. and ChIP-Sequencing analysis using different tools such as Tuxedo suite, Bowtie, PePr, MACS, deepTools etc.

Microscopy & Histology scanning electron microscope, confocal microscope, stereo and compound microscope, Microtome and vibrotome sectioning of plant tissues

Oral and poster presentation

June 2019 – Poster presentation Polycomb group proteins StMSI1 and StBMI1 regulate microRNA156 during aerial tuber formation in potato under short day photoperiod, 6th European workshop on plant chromatin (**EWPC-2019, MPIPZ Cologne, Germany**)
January 2019 – Poster presentation, Polycomb group proteins StMSI1 and StBMI1 regulate tuber development in potato under short-day photoperiod, 7th International Conference on Molecular Signalling, (**ICMS-2019, NCCS-Pune, India**)
August 2018 – Oral presentation Polycomb group protein StMSI1 regulates potato development via photoperiod dependent pathway, 12th Congress of the International Plant Molecular Biology (**IPMB -2018, Montpellier, France**).
December 2017 – Poster presentation Polycomb group protein StMSI1 regulates potato development via photoperiod dependent pathway, International Conference on Plant Developmental Biology (**ICPDB-2017, NISER-Bhubaneswar, India**)
June 2017 – Poster presentation Functional characterization of Polycomb group proteins in potato development, Indian Society for Developmental Biology meeting (**InSDB-2017, IISER-Pune, India**)
August 2016 – Poster presentation Investigating the role of polycomb group proteins in potato development, (**Bio-annual talks 2016, IISER- Pune, India**)

Awards, scholarships, and achievements

Travel grant, 2019, by Council of Scientific and Industrial Research (CSIR), Govt. of India, to attend 6th European workshop on plant chromatin (EWPC-2019, MPIPZ Cologne, Germany)
Best Poster Award, Jan. 2019, 7th International Conference on Molecular Signalling, ICMS-2019 (NCCS-Pune, India)
Travel grant, 2018 by Department of Biotechnology (DBT), Government of India and Infosys foundation, to attend 12th Congress of the International Plant Molecular Biology (IPMB -2018, Montpellier, France).
Senior Research Fellowship, 2015–2018, by Council of Scientific & Industrial Research (*CSIR*), Government of India.
Junior Research Fellowship, 2014–2015, by Council of Scientific & Industrial Research (*CSIR*), Government of India.
Junior Research Fellowship, 2013 – 2014 by University Grant Commission (UGC), Government of India.
National Eligibility Test (NET) University/College teaching eligibility test conducted By CSIR and UGC, All India rank 44

Co-mentored projects –

BS-MS Dissertation, IISER Pune (2019)
Mr. Akshay Wagh
Functional characterization of Polycomb Repressor Complex1 member protein StEMF1 in potato.

M.Sc. Dissertation, Fergusson College Pune (2019)
Ms. Sayali Khedkar
Functional characterization of StE(z)2 in potato using VIGS mediated knockdown strategy

BS-MS Dissertation, Institute of Bioinformatics & Biotechnology, Pune University (2018)
Mr. Maruf Shaikh,
Cloning and expression analysis of *StEMF1* promoter in potato under different photoperiods

Project Trainee, IISER-Pune (2017-2018)
Ms. Pallavi V. Vetal
Cloning and functional characterization of a ubiquitin ligase coding gene *StBMI1*in potato

Semester Project, IISER Pune (2015)
Mr. Rutwik Bardapurkar
Identification and cloning of Trithorax family homolog genes in potato

Additional experiences

Lab reagents purchase actively involved in the process of purchasing and managing the reagents for our lab at IISER Pune.

Teaching Assistance conducted theory classes in a plant biology course, and worked as a teaching assistant for introductory biology course at IISER-Pune.

Conference Organization participated in the organization of 35th Annual Plant Tissue Culture Association (PTCA) meeting -2014 held at IISER, Pune

Next Generation Sequencing club member the NGS discussion group headed by Dr. Krishanpal at IISER Pune frequently organizes talks related to NGS methodologies and advancements in NGS technology.

References

- **Prof. Anjan K. Banerjee**
  Biology Division
  Indian Institute of Science Education and Research (IISER) Pune, India
  Phone: +91-20-25908181
  E-mail: akb@iiserpune.ac.in
  Website: http://www.iiserpune.ac.in/~akb/

- **Dr. Krishanpal Karmodiya**
  Assistant Professor**,** Biology Division
  Indian Institute of Science Education and Research (IISER) Pune, India
  Phone: +91-20-25908195
  E-mail: krish@iiserpune.ac.in
  Website: http://krishanpalk.wixsite.com/krish

E-licenses from publishers to reproduce figures in this thesis

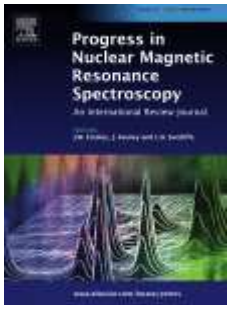

Title: Unspinning chromatin: Revealing the dynamic nucleosome landscape by NMR

Author: Clara L. van Emmerik,Hugo van Ingen

Publication: Progress in Nuclear Magnetic Resonance Spectroscopy

Publisher: Elsevier

Date: February 2019

Creative Commons Attribution-NonCommercial-No Derivatives License (CC BY NC ND)

Copyright Clearance Center

Confirmation Number: 11859097
Order Date: 10/13/2019

Customer Information

Customer: AMIT KUMAR
Account Number: 3001534944
Organization: AMIT KUMAR
Email: amit.kumar@students.iiserpune.ac.in
Phone: +91 2025908057
Payment Method: Invoice

This is not an invoice

Order Details

Special Orders

Annual review of plant biology

Billing Status: **Not Billed**

Order detail ID: 72042578
ISSN: 1545-2123
Publication Type: e-Journal
Volume:
Issue:
Start page:
Publisher: ANNUAL REVIEWS
Author/Editor: Annual Reviews, Inc

Permission Status: **Special Order**
Special Order Update: Checking availability

Permission type: Republish or display content
Type of use: Thesis/Dissertation
Job Ticket: 501520539

Requestor type	Author of requested content
Format	Print, Electronic
Portion	chart/graph/table/figure
Number of charts/graphs/tables/figures	1
The requesting person/organization	Amit Kumar
Title or numeric reference of the portion(s)	Figure-3
Title of the article or chapter the portion is from	The Epigenome and Plant Development
Editor of portion(s)	Sabeeha S. Merchant
Author of portion(s)	Guangming He
Volume of serial or monograph	62
Page range of portion	419
Publication date of portion	March 23, 2011
Rights for	Main product
Duration of use	Life of current edition
Creation of copies for the disabled	no
With minor editing privileges	no

For distribution to	Worldwide
In the following language(s)	Original language of publication
With incidental promotional use	no
Lifetime unit quantity of new product	Up to 499
Title	Investigating the Role of Polycomb Group Proteins in Potato Development
Institution name	INDIAN INSTITUTE OF SCIENCE EDUCATION AND RESEARCH PUNE, INDIA
Expected presentation date	Oct 2019

Note: This item will be managed through CCC'S **RightsLink service.** More info **TBD**

Total order items: 1

Order Total: TBD
(Excludes TBD items)

Copyright Clearance Center

Confirmation Number: 11859093
Order Date: 10/13/2019

Customer Information

Customer: AMIT KUMAR
Account Number: 3001534944
Organization: AMIT KUMAR
Email: amit.kumar@students.iiserpune.ac.in
Phone: +91 2025908057
Payment Method: Invoice

This is not an invoice

Order Details

Plant physiology

Billing Status: **N/A**

Order detail ID:	72042573
ISSN:	1532-2548
Publication Type:	e-Journal
Volume:	
Issue:	
Start page:	
Publisher:	AMERICAN SOCIETY OF PLANT BIOLOGISTS
Author/Editor:	American Society of Plant Biologists ; American Society of Plant Physiologists

Permission Status: Granted

Permission type: Republish or display content
Type of use: Republish in a thesis/dissertation
Order License Id: 4687191390270

Requestor type	Author of requested content
Format	Print, Electronic
Portion	chart/graph/table/figure
Number of charts/graphs/tables/figures	1
The requesting person/organization	AMIT KUMAR
Title or numeric reference of the portion(s)	FIGURE-2
Title of the article or chapter the portion is from	Polycomb Group Complexes Mediate Developmental Transitions in Plants
Editor of portion(s)	Michael R. Blatt
Author of portion(s)	Sarah Holec and Frederic Berger
Volume of serial or monograph	158
Page range of portion	37
Publication date of portion	January 2012
Rights for	Main product
Duration of use	Life of current edition
Creation of copies for the disabled	no
With minor editing privileges	no
For distribution to	Worldwide

In the following language(s)	Original language of publication
With incidental promotional use	no
Lifetime unit quantity of new product	Up to 499
Title	Investigating the Role of Polycomb Group Proteins in Potato Development
Institution name	INDIAN INSTITUTE OF SCIENCE EDUCATION AND RESEARCH PUNE, INDIA
Expected presentation date	Oct 2019

Note: This item was invoiced separately through our **RightsLink service.** More info **$ 0.00**

Total order items: 1 **Order Total: $0.00**

Title:	Diversity of Polycomb group complexes in plants: same rules, different players?
Author:	Lars Hennig,Maria Derkacheva
Publication:	Trends in Genetics
Publisher:	Elsevier
Date:	September 2009

Order Completed

Thank you for your order.

This Agreement between AMIT KUMAR ("You") and Elsevier ("Elsevier") consists of your license details and the terms and conditions provided by Elsevier and Copyright Clearance Center.

Your confirmation email will contain your order number for future reference.

printable details

License Number	4687220675046
License date	Oct 13, 2019
Licensed Content Publisher	Elsevier
Licensed Content Publication	Trends in Genetics
Licensed Content Title	Diversity of Polycomb group complexes in plants: same rules, different players?
Licensed Content Author	Lars Hennig,Maria Derkacheva
Licensed Content Date	Sep 1, 2009
Licensed Content Volume	25
Licensed Content Issue	9
Licensed Content Pages	10
Type of Use	reuse in a thesis/dissertation
Portion	figures/tables/illustrations
Number of figures/tables/illustrations	1
Format	both print and electronic
Are you the author of this Elsevier article?	No
Will you be translating?	No
Original figure numbers	Figure-2
Title of your thesis/dissertation	Investigating the Role of Polycomb Group Proteins in Potato Development
Publisher of new work	INDIAN INSTITUTE OF SCIENCE EDUCATION AND RESEARCH PUNE, INDIA
Expected completion date	Oct 2019
Estimated size (number of pages)	1
Requestor Location	AMIT KUMAR IISER PUNE INDIA Pune, other 411008 India Attn:

Publisher Tax ID	GB 494 6272 12
Total	0.00 USD

ORDER MORE CLOSE WINDOW

SPRINGER NATURE

Title:	The genetic basis of flowering responses to seasonal cues
Author:	Fernando Andrés et al
Publication:	Nature Reviews Genetics
Publisher:	Springer Nature
Date:	Aug 17, 2012

Order Completed

Thank you for your order.

This Agreement between AMIT KUMAR ("You") and Springer Nature ("Springer Nature") consists of your license details and the terms and conditions provided by Springer Nature and Copyright Clearance Center.

Your confirmation email will contain your order number for future reference.

printable details

License Number	4687230026371
License date	Oct 13, 2019
Licensed Content Publisher	Springer Nature
Licensed Content Publication	Nature Reviews Genetics
Licensed Content Title	The genetic basis of flowering responses to seasonal cues
Licensed Content Author	Fernando Andrés et al
Licensed Content Date	Aug 17, 2012
Type of Use	Thesis/Dissertation
Requestor type	academic/university or research institute
Format	print and electronic
Portion	figures/tables/illustrations
Number of figures/tables/illustrations	1
High-res required	no
Will you be translating?	no
Circulation/distribution	1 - 29
Author of this Springer Nature content	no
Title	Investigating the Role of Polycomb Group Proteins in Potato Development
Institution name	INDIAN INSTITUTE OF SCIENCE EDUCATION AND RESEARCH PUNE, INDIA
Expected presentation date	Oct 2019
Portions	Figure-1
Requestor Location	AMIT KUMAR IISER PUNE INDIA Pune, other 411008 India Attn:
Total	0.00 USD

ORDER MORE CLOSE WINDOW

Title:	Flowering and tuberization: a tale of two nightshades
Author:	José A. Abelenda,Cristina Navarro,Salomé Prat
Publication:	Trends in Plant Science
Publisher:	Elsevier
Date:	February 2014

Order Completed

Thank you for your order.

This Agreement between AMIT KUMAR ("You") and Elsevier ("Elsevier") consists of your license details and the terms and conditions provided by Elsevier and Copyright Clearance Center.

Your confirmation email will contain your order number for future reference.

printable details

License Number	4687230582091
License date	Oct 13, 2019
Licensed Content Publisher	Elsevier
Licensed Content Publication	Trends in Plant Science
Licensed Content Title	Flowering and tuberization: a tale of two nightshades
Licensed Content Author	José A. Abelenda,Cristina Navarro,Salomé Prat
Licensed Content Date	Feb 1, 2014
Licensed Content Volume	19
Licensed Content Issue	2
Licensed Content Pages	8
Type of Use	reuse in a thesis/dissertation
Portion	figures/tables/illustrations
Number of figures/tables/illustrations	1
Format	both print and electronic
Are you the author of this Elsevier article?	No
Will you be translating?	No
Original figure numbers	Figure-1
Title of your thesis/dissertation	Investigating the Role of Polycomb Group Proteins in Potato Development
Publisher of new work	INDIAN INSTITUTE OF SCIENCE EDUCATION AND RESEARCH PUNE, INDIA
Expected completion date	Oct 2019
Estimated size (number of pages)	1
Requestor Location	AMIT KUMAR IISER PUNE INDIA Pune, other 411008 India Attn:

Publisher Tax ID	GB 494 6272 12
Total	0.00 USD

ORDER MORE CLOSE WINDOW

SPRINGER NATURE

Title:	The essential role of microRNAs in potato tuber development: a mini review
Author:	Bhavani Natarajan, Sneha Bhogale, Anjan K. Banerjee
Publication:	Indian Journal of Plant Physiology
Publisher:	Springer Nature
Date:	Jan 1, 2017

Order Completed

Thank you for your order.

This Agreement between AMIT KUMAR ("You") and Springer Nature ("Springer Nature") consists of your license details and the terms and conditions provided by Springer Nature and Copyright Clearance Center.

Your confirmation email will contain your order number for future reference.

printable details

License Number	4687231282785
License date	Oct 13, 2019
Licensed Content Publisher	Springer Nature
Licensed Content Publication	Indian Journal of Plant Physiology
Licensed Content Title	The essential role of microRNAs in potato tuber development: a mini review
Licensed Content Author	Bhavani Natarajan, Sneha Bhogale, Anjan K. Banerjee
Licensed Content Date	Jan 1, 2017
Licensed Content Volume	22
Licensed Content Issue	4
Type of Use	Thesis/Dissertation
Requestor type	academic/university or research institute
Format	print and electronic
Portion	figures/tables/illustrations
Number of figures/tables/illustrations	1
Will you be translating?	no
Circulation/distribution	1 - 29
Author of this Springer Nature content	no
Title	Investigating the Role of Polycomb Group Proteins in Potato Development
Institution name	INDIAN INSTITUTE OF SCIENCE EDUCATION AND RESEARCH PUNE, INDIA
Expected presentation date	Oct 2019
Portions	Figure-3
Requestor Location	AMIT KUMAR IISER PUNE INDIA Pune, other 411008

India
Attn:

Total 0.00 USD

ORDER MORE CLOSE WINDOW

Copyright Clearance Center

Confirmation Number: 11859094
Order Date: 10/13/2019

Customer Information

Customer: AMIT KUMAR
Account Number: 3001534944
Organization: AMIT KUMAR
Email: amit.kumar@students.iiserpune.ac.in
Phone: +91 2025908057
Payment Method: Invoice

This is not an invoice

Order Details

Plant physiology

Billing Status: **N/A**

Order detail ID:	72042574
ISSN:	1532-2548
Publication Type:	e-Journal
Volume:	
Issue:	
Start page:	
Publisher:	AMERICAN SOCIETY OF PLANT BIOLOGISTS
Author/Editor:	American Society of Plant Biologists ; American Society of Plant Physiologists

Permission Status: Granted

Permission type: Republish or display content
Type of use: Republish in a thesis/dissertation
Order License Id: 4687200651902

Requestor type	Author of requested content
Format	Print, Electronic
Portion	chart/graph/table/figure
Number of charts/graphs/tables/figures	1
The requesting person/organization	Amit Kumar
Title or numeric reference of the portion(s)	Figure-7
Title of the article or chapter the portion is from	Deciphering the Role of POLYCOMB REPRESSIVE COMPLEX1 Variants in Regulating the Acquisition of Flowering Competence in Arabidopsis
Editor of portion(s)	Michael R. Blatt
Author of portion(s)	Sara Picó
Volume of serial or monograph	168
Page range of portion	1294
Publication date of portion	August 2015
Rights for	Main product
Duration of use	Life of current edition
Creation of copies for the disabled	no
With minor editing privileges	no

For distribution to	Worldwide
In the following language(s)	Original language of publication
With incidental promotional use	no
Lifetime unit quantity of new product	Up to 499
Title	Investigating the Role of Polycomb Group Proteins in Potato Development
Institution name	INDIAN INSTITUTE OF SCIENCE EDUCATION AND RESEARCH PUNE, INDIA
Expected presentation date	Oct 2019

Note: This item was invoiced separately through our **RightsLink service.** More info **$ 0.00**

Total order items: 1 **Order Total: $0.00**

Copyright Clearance Center

Note: Copyright.com supplies permissions but not the copyrighted content itself.

1 PAYMENT 2 REVIEW 3 CONFIRMATION

Step 3: Order Confirmation

Thank you for your order! A confirmation for your order will be sent to your account email address. If you have questions about your order, you can call us 24 hrs/day, M-F at +1.855.239.3415 Toll Free, or write to us at info@copyright.com. This is not an invoice.

Confirmation Number: 11859101
Order Date: 10/13/2019

If you paid by credit card, your order will be finalized and your card will be charged within 24 hours. If you choose to be invoiced, you can change or cancel your order until the invoice is generated.

Payment Information

AMIT KUMAR
amit.kumar@students.iiserpune.ac.in
+91 2025908057
Payment Method: invoice

Billing address:

IISER PUNE INDIA
Pune, 411008
IN

Order Details

Special Orders

Annual review of plant biology

Order detail ID: 72042585
Job Ticket: 501520546

ISSN: 1545-2123
Publication Type: e-Journal
Volume:
Issue:
Start page:
Publisher: ANNUAL REVIEWS
Author/Editor: Annual Reviews, Inc

Permission Status: **Special Order**
Special Order Update: Checking availability

Permission type:
Republish or display content
Type of use:
Thesis/Dissertation

Requestor type	Author of requested content
Format	Print, Electronic
Portion	chart/graph/table/figure
Number of charts/graphs/tables/figures	1
The requesting person/organization	Amit Kumar
Title or numeric reference of the portion(s)	Figure-1

Title of the article or chapter the portion is from	Seasonal Control of Tuberization in Potato: Conserved Elements with the Flowering Response
Editor of portion(s)	Sabeeha S. Merchant
Author of portion(s)	Mariana Rodriguez-Falcon and Salome Prat
Volume of serial or monograph	57
Page range of portion	154
Publication date of portion	2 June 2006
Rights for	Main product
Duration of use	Life of current edition
Creation of copies for the disabled	no
With minor editing privileges	yes
For distribution to	Worldwide
In the following language(s)	Original language of publication
With incidental promotional use	no
Lifetime unit quantity of new product	Up to 499
Title	Investigating the Role of Polycomb Group Proteins in Potato Development
Institution name	INDIAN INSTITUTE OF SCIENCE EDUCATION AND RESEARCH PUNE, INDIA
Expected presentation date	Oct 2019

Note: This item will be managed through CCC's **RightsLink service.**More info **TBD**

This is not an invoice.

Total order items: 1

Order Total: TBD

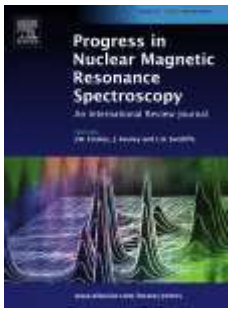

Title:	Unspinning chromatin: Revealing the dynamic nucleosome landscape by NMR
Author:	Clara L. van Emmerik,Hugo van Ingen
Publication:	Progress in Nuclear Magnetic Resonance Spectroscopy
Publisher:	Elsevier
Date:	February 2019

Creative Commons Attribution-NonCommercial-No Derivatives License (CC BY NC ND)

Copyright Clearance Center

Confirmation Number: 11859097
Order Date: 10/13/2019

Customer Information

Customer: AMIT KUMAR
Account Number: 3001534944
Organization: AMIT KUMAR
Email: amit.kumar@students.iiserpune.ac.in
Phone: +91 2025908057
Payment Method: Invoice

This is not an invoice

Order Details

Special Orders

Annual review of plant biology

Billing Status: **Not Billed**

Order detail ID: 72042578
ISSN: 1545-2123
Publication Type: e-Journal
Volume:
Issue:
Start page:
Publisher: ANNUAL REVIEWS
Author/Editor: Annual Reviews, Inc

Permission Status: **Special Order**
Special Order Update: Checking availability

Permission type: Republish or display content
Type of use: Thesis/Dissertation
Job Ticket: 501520539

Requestor type	Author of requested content
Format	Print, Electronic
Portion	chart/graph/table/figure
Number of charts/graphs/tables/figures	1
The requesting person/organization	Amit Kumar
Title or numeric reference of the portion(s)	Figure-3
Title of the article or chapter the portion is from	The Epigenome and Plant Development
Editor of portion(s)	Sabeeha S. Merchant
Author of portion(s)	Guangming He
Volume of serial or monograph	62
Page range of portion	419
Publication date of portion	March 23, 2011
Rights for	Main product
Duration of use	Life of current edition
Creation of copies for the disabled	no
With minor editing privileges	no

For distribution to	Worldwide
In the following language(s)	Original language of publication
With incidental promotional use	no
Lifetime unit quantity of new product	Up to 499
Title	Investigating the Role of Polycomb Group Proteins in Potato Development
Institution name	INDIAN INSTITUTE OF SCIENCE EDUCATION AND RESEARCH PUNE, INDIA
Expected presentation date	Oct 2019

Note: This item will be managed through CCC'S **RightsLink service.** More info **TBD**

Total order items: 1

Order Total: TBD
(Excludes TBD items)

Copyright Clearance Center

Confirmation Number: 11859093
Order Date: 10/13/2019

Customer Information

Customer: AMIT KUMAR
Account Number: 3001534944
Organization: AMIT KUMAR
Email: amit.kumar@students.iiserpune.ac.in
Phone: +91 2025908057
Payment Method: Invoice

This is not an invoice

Order Details

Plant physiology

Billing Status: **N/A**

Order detail ID:	72042573
ISSN:	1532-2548
Publication Type:	e-Journal
Volume:	
Issue:	
Start page:	
Publisher:	AMERICAN SOCIETY OF PLANT BIOLOGISTS
Author/Editor:	American Society of Plant Biologists ; American Society of Plant Physiologists

Permission Status: Granted

Permission type: Republish or display content
Type of use: Republish in a thesis/dissertation
Order License Id: 4687191390270

Requestor type	Author of requested content
Format	Print, Electronic
Portion	chart/graph/table/figure
Number of charts/graphs/tables/figures	1
The requesting person/organization	AMIT KUMAR
Title or numeric reference of the portion(s)	FIGURE-2
Title of the article or chapter the portion is from	Polycomb Group Complexes Mediate Developmental Transitions in Plants
Editor of portion(s)	Michael R. Blatt
Author of portion(s)	Sarah Holec and Frederic Berger
Volume of serial or monograph	158
Page range of portion	37
Publication date of portion	January 2012
Rights for	Main product
Duration of use	Life of current edition
Creation of copies for the disabled	no
With minor editing privileges	no
For distribution to	Worldwide

In the following language(s)	Original language of publication
With incidental promotional use	no
Lifetime unit quantity of new product	Up to 499
Title	Investigating the Role of Polycomb Group Proteins in Potato Development
Institution name	INDIAN INSTITUTE OF SCIENCE EDUCATION AND RESEARCH PUNE, INDIA
Expected presentation date	Oct 2019

Note: This item was invoiced separately through our **RightsLink service.** More info **$ 0.00**

Total order items: 1 **Order Total: $0.00**

Title:	Diversity of Polycomb group complexes in plants: same rules, different players?
Author:	Lars Hennig,Maria Derkacheva
Publication:	Trends in Genetics
Publisher:	Elsevier
Date:	September 2009

Order Completed

Thank you for your order.

This Agreement between AMIT KUMAR ("You") and Elsevier ("Elsevier") consists of your license details and the terms and conditions provided by Elsevier and Copyright Clearance Center.

Your confirmation email will contain your order number for future reference.

printable details

License Number	4687220675046
License date	Oct 13, 2019
Licensed Content Publisher	Elsevier
Licensed Content Publication	Trends in Genetics
Licensed Content Title	Diversity of Polycomb group complexes in plants: same rules, different players?
Licensed Content Author	Lars Hennig,Maria Derkacheva
Licensed Content Date	Sep 1, 2009
Licensed Content Volume	25
Licensed Content Issue	9
Licensed Content Pages	10
Type of Use	reuse in a thesis/dissertation
Portion	figures/tables/illustrations
Number of figures/tables/illustrations	1
Format	both print and electronic
Are you the author of this Elsevier article?	No
Will you be translating?	No
Original figure numbers	Figure-2
Title of your thesis/dissertation	Investigating the Role of Polycomb Group Proteins in Potato Development
Publisher of new work	INDIAN INSTITUTE OF SCIENCE EDUCATION AND RESEARCH PUNE, INDIA
Expected completion date	Oct 2019
Estimated size (number of pages)	1
Requestor Location	AMIT KUMAR IISER PUNE INDIA Pune, other 411008 India Attn:

Publisher Tax ID	GB 494 6272 12
Total	0.00 USD

ORDER MORE CLOSE WINDOW

SPRINGER NATURE

Title: The genetic basis of flowering responses to seasonal cues
Author: Fernando Andrés et al
Publication: Nature Reviews Genetics
Publisher: Springer Nature
Date: Aug 17, 2012

Order Completed

Thank you for your order.

This Agreement between AMIT KUMAR ("You") and Springer Nature ("Springer Nature") consists of your license details and the terms and conditions provided by Springer Nature and Copyright Clearance Center.

Your confirmation email will contain your order number for future reference.

printable details

License Number	4687230026371
License date	Oct 13, 2019
Licensed Content Publisher	Springer Nature
Licensed Content Publication	Nature Reviews Genetics
Licensed Content Title	The genetic basis of flowering responses to seasonal cues
Licensed Content Author	Fernando Andrés et al
Licensed Content Date	Aug 17, 2012
Type of Use	Thesis/Dissertation
Requestor type	academic/university or research institute
Format	print and electronic
Portion	figures/tables/illustrations
Number of figures/tables/illustrations	1
High-res required	no
Will you be translating?	no
Circulation/distribution	1 - 29
Author of this Springer Nature content	no
Title	Investigating the Role of Polycomb Group Proteins in Potato Development
Institution name	INDIAN INSTITUTE OF SCIENCE EDUCATION AND RESEARCH PUNE, INDIA
Expected presentation date	Oct 2019
Portions	Figure-1
Requestor Location	AMIT KUMAR IISER PUNE INDIA Pune, other 411008 India Attn:
Total	0.00 USD

ORDER MORE CLOSE WINDOW

Title:	Flowering and tuberization: a tale of two nightshades
Author:	José A. Abelenda,Cristina Navarro,Salomé Prat
Publication:	Trends in Plant Science
Publisher:	Elsevier
Date:	February 2014

Order Completed

Thank you for your order.

This Agreement between AMIT KUMAR ("You") and Elsevier ("Elsevier") consists of your license details and the terms and conditions provided by Elsevier and Copyright Clearance Center.

Your confirmation email will contain your order number for future reference.

printable details

License Number	4687230582091
License date	Oct 13, 2019
Licensed Content Publisher	Elsevier
Licensed Content Publication	Trends in Plant Science
Licensed Content Title	Flowering and tuberization: a tale of two nightshades
Licensed Content Author	José A. Abelenda,Cristina Navarro,Salomé Prat
Licensed Content Date	Feb 1, 2014
Licensed Content Volume	19
Licensed Content Issue	2
Licensed Content Pages	8
Type of Use	reuse in a thesis/dissertation
Portion	figures/tables/illustrations
Number of figures/tables/illustrations	1
Format	both print and electronic
Are you the author of this Elsevier article?	No
Will you be translating?	No
Original figure numbers	Figure-1
Title of your thesis/dissertation	Investigating the Role of Polycomb Group Proteins in Potato Development
Publisher of new work	INDIAN INSTITUTE OF SCIENCE EDUCATION AND RESEARCH PUNE, INDIA
Expected completion date	Oct 2019
Estimated size (number of pages)	1
Requestor Location	AMIT KUMAR IISER PUNE INDIA Pune, other 411008 India Attn:

Publisher Tax ID	GB 494 6272 12
Total	0.00 USD

ORDER MORE CLOSE WINDOW

SPRINGER NATURE

Title:	The essential role of microRNAs in potato tuber development: a mini review
Author:	Bhavani Natarajan, Sneha Bhogale, Anjan K. Banerjee
Publication:	Indian Journal of Plant Physiology
Publisher:	Springer Nature
Date:	Jan 1, 2017

Order Completed

Thank you for your order.

This Agreement between AMIT KUMAR ("You") and Springer Nature ("Springer Nature") consists of your license details and the terms and conditions provided by Springer Nature and Copyright Clearance Center.

Your confirmation email will contain your order number for future reference.

printable details

License Number	4687231282785
License date	Oct 13, 2019
Licensed Content Publisher	Springer Nature
Licensed Content Publication	Indian Journal of Plant Physiology
Licensed Content Title	The essential role of microRNAs in potato tuber development: a mini review
Licensed Content Author	Bhavani Natarajan, Sneha Bhogale, Anjan K. Banerjee
Licensed Content Date	Jan 1, 2017
Licensed Content Volume	22
Licensed Content Issue	4
Type of Use	Thesis/Dissertation
Requestor type	academic/university or research institute
Format	print and electronic
Portion	figures/tables/illustrations
Number of figures/tables/illustrations	1
Will you be translating?	no
Circulation/distribution	1 - 29
Author of this Springer Nature content	no
Title	Investigating the Role of Polycomb Group Proteins in Potato Development
Institution name	INDIAN INSTITUTE OF SCIENCE EDUCATION AND RESEARCH PUNE, INDIA
Expected presentation date	Oct 2019
Portions	Figure-3
Requestor Location	AMIT KUMAR IISER PUNE INDIA Pune, other 411008

India
Attn:

Total 0.00 USD

ORDER MORE CLOSE WINDOW

Copyright Clearance Center

Confirmation Number: 11859094
Order Date: 10/13/2019

Customer Information

Customer: AMIT KUMAR
Account Number: 3001534944
Organization: AMIT KUMAR
Email: amit.kumar@students.iiserpune.ac.in
Phone: +91 2025908057
Payment Method: Invoice

This is not an invoice

Order Details

Plant physiology

Billing Status: **N/A**

Order detail ID:	72042574
ISSN:	1532-2548
Publication Type:	e-Journal
Volume:	
Issue:	
Start page:	
Publisher:	AMERICAN SOCIETY OF PLANT BIOLOGISTS
Author/Editor:	American Society of Plant Biologists ; American Society of Plant Physiologists

Permission Status: Granted

Permission type: Republish or display content
Type of use: Republish in a thesis/dissertation
Order License Id: 4687200651902

Requestor type	Author of requested content
Format	Print, Electronic
Portion	chart/graph/table/figure
Number of charts/graphs/tables/figures	1
The requesting person/organization	Amit Kumar
Title or numeric reference of the portion(s)	Figure-7
Title of the article or chapter the portion is from	Deciphering the Role of POLYCOMB REPRESSIVE COMPLEX1 Variants in Regulating the Acquisition of Flowering Competence in Arabidopsis
Editor of portion(s)	Michael R. Blatt
Author of portion(s)	Sara Picó
Volume of serial or monograph	168
Page range of portion	1294
Publication date of portion	August 2015
Rights for	Main product
Duration of use	Life of current edition
Creation of copies for the disabled	no
With minor editing privileges	no

For distribution to	Worldwide
In the following language(s)	Original language of publication
With incidental promotional use	no
Lifetime unit quantity of new product	Up to 499
Title	Investigating the Role of Polycomb Group Proteins in Potato Development
Institution name	INDIAN INSTITUTE OF SCIENCE EDUCATION AND RESEARCH PUNE, INDIA
Expected presentation date	Oct 2019

Note: This item was invoiced separately through our **RightsLink service.** More info **$ 0.00**

Total order items: 1 **Order Total: $0.00**

Copyright Clearance Center

Note: Copyright.com supplies permissions but not the copyrighted content itself.

1 PAYMENT 2 REVIEW 3 CONFIRMATION

Step 3: Order Confirmation

Thank you for your order! A confirmation for your order will be sent to your account email address. If you have questions about your order, you can call us 24 hrs/day, M-F at +1.855.239.3415 Toll Free, or write to us at info@copyright.com. This is not an invoice.

Confirmation Number: 11859101
Order Date: 10/13/2019

If you paid by credit card, your order will be finalized and your card will be charged within 24 hours. If you choose to be invoiced, you can change or cancel your order until the invoice is generated.

Payment Information

AMIT KUMAR
amit.kumar@students.iiserpune.ac.in
+91 2025908057
Payment Method: invoice

Billing address:

IISER PUNE INDIA
Pune, 411008
IN

Order Details

Special Orders

Annual review of plant biology

Order detail ID: 72042585
Job Ticket: 501520546

ISSN: 1545-2123
Publication Type: e-Journal
Volume:
Issue:
Start page:
Publisher: ANNUAL REVIEWS
Author/Editor: Annual Reviews, Inc

Permission Status: **Special Order**
Special Order Update: Checking availability

Permission type:
Republish or display content
Type of use:
Thesis/Dissertation

Requestor type	Author of requested content
Format	Print, Electronic
Portion	chart/graph/table/figure
Number of charts/graphs/tables/figures	1
The requesting person/organization	Amit Kumar
Title or numeric reference of the portion(s)	Figure-1

Title of the article or chapter the portion is from	Seasonal Control of Tuberization in Potato: Conserved Elements with the Flowering Response
Editor of portion(s)	Sabeeha S. Merchant
Author of portion(s)	Mariana Rodríguez-Falcón and Salome Prat
Volume of serial or monograph	57
Page range of portion	154
Publication date of portion	2 June 2006
Rights for	Main product
Duration of use	Life of current edition
Creation of copies for the disabled	no
With minor editing privileges	yes
For distribution to	Worldwide
In the following language(s)	Original language of publication
With incidental promotional use	no
Lifetime unit quantity of new product	Up to 499
Title	Investigating the Role of Polycomb Group Proteins in Potato Development
Institution name	INDIAN INSTITUTE OF SCIENCE EDUCATION AND RESEARCH PUNE, INDIA
Expected presentation date	Oct 2019

Note: This item will be managed through CCC's **RightsLink service.**More info **TBD**

This is not an invoice.

Total order items: 1

Order Total: TBD